

Addis Ababa University  
Addis Ababa Institute of Technology



School of Graduate Students  
School of Mechanical and Industrial Engineering  
Department of Mechanical Engineering

Structural Design and Simulation of Lightweight Formula SAE  
Racing Car

A Thesis Research Paper Submitted for the Partial Fulfillment of Degree of Masters of  
Science in Mechanical Engineering (Design)

By

Nikodmose Moges Gebre

Advisor: Ermias G. Koricho (Ph.D.)

Co-advisor: Mr. Hairedin Ismal (Ph.D. Candidate)

Addis Ababa, Ethiopia

October 2018

## **Declaration**

This is to certify that the thesis presented by Nikodmose Moges Gebre, titled as “Structural Design and Simulation of Lightweight Formula SAE Racing Car” and submitted to the School of Mechanical and Industrial Engineering in the partial fulfillment of the requirements for the award of the degree of masters of science in Mechanical Design Engineering with the regulations of the university, and meet accepted standards with respect to originality and quality.

Nikodmose Moges Gebre \_\_\_\_\_

Name

Signature

Date

This thesis has been submitted for examination with approval as a university advisor.

Ermias G. Koricho (Ph.D.) \_\_\_\_\_

Advisor

Signature

Date

Hairedin Ismal (Ph.D. Candidate) \_\_\_\_\_

Co-advisor

Signature

Date

Addis Ababa University  
Addis Ababa Institute of Technology  
School of Graduates Students  
Structural Design and Simulation of Lightweight Formula SAE Racing Car  
By  
Nikodmose Moges Gebre  
Addis Ababa Institute of Technology  
Approved by Board of Examiners

Ermias G. Koricho (Ph.D.)

Advisor

\_\_\_\_\_  
Signature

\_\_\_\_\_  
Date

Hairedin Ismal  
(Ph.D. Candidate)

Co-advisor

\_\_\_\_\_  
Signature

\_\_\_\_\_  
Date

Mulugeta Habtemariam  
(Ph.D. Candidate)

Internal Examiner

\_\_\_\_\_  
Signature

\_\_\_\_\_  
Date

Samuel Tesfaye (Ph.D.)

External Examiner

\_\_\_\_\_  
Signature

\_\_\_\_\_  
Date

Yilma Tadesse (Ph.D.)

Chairman

\_\_\_\_\_  
Signature

\_\_\_\_\_  
Date

Ermias Tesfaye (Ph.D.)

Director of Post-graduate

\_\_\_\_\_  
Signature

\_\_\_\_\_  
Date

## Tables of Content

TABLES OF CONTENT.....	II
LIST OF TABLES.....	VI
LIST OF FIGURES .....	VII
NOMENCLATURE .....	XI
ACKNOWLEDGMENT.....	XV
ABSTRACT.....	XVI
CHAPTER 1 .....	1
INTRODUCTION .....	1
<b>1.1 Introduction.....</b>	<b>1</b>
<b>1.2 Background.....</b>	<b>4</b>
1.2.1 Terminology, Overview of Vehicle Chassis Structure Types and Lodes.....	4
1.2.1.1 Terminology .....	4
1.2.2 Overview of Vehicle Chassis Structure Types (Modern Structure Types) .....	6
1.2.3 Overview of Vehicle Chassis Load Types .....	8
1.2.3.1 Vertical Symmetric or Vertical Bending (‘pure bending’) Load Case .....	9
1.2.3.2 Vertical Asymmetric or Longitudinal Torsion (Pure Torsion Analysis Case) .....	10
1.2.3.3 Longitudinal loads (Braking).....	10
1.2.3.4 Lateral Bending Load (Cornering).....	10
1.2.3.5 Crash or Impact cases (Front, Side and Rollover Crash) .....	11
1.2.3.6 Horizontal Lozengeing.....	13
1.2.3.7 Combinations of Load Cases .....	13
1.2.4 Overview of Vehicle Crash Box or Impact Attenuator Types .....	14
1.2.5 Overview of Vehicle Crash Box or Impact Attenuator Load Types.....	14
<b>1.3 Motivation.....</b>	<b>15</b>
<b>1.4 Problem Statement .....</b>	<b>15</b>
<b>1.5 Objectives.....</b>	<b>16</b>
1.5.1 General Objectives .....	16
1.5.2 Specific Objectives.....	16
<b>1.6 The scope of the Research .....</b>	<b>16</b>
<b>1.7 Methodology .....</b>	<b>16</b>
<b>1.8 Layout of the Thesis.....</b>	<b>19</b>

CHAPTER 2 .....	20
LITERATURE REVIEW .....	20
<b>2.1 Previous Works.....</b>	<b>20</b>
2.1.1 Previous Works of Formula SAE Chassis .....	20
2.1.2 Previous Works of Crash Box or Impact Attenuator .....	24
<b>2.2 Summary of the Prevised Works on the Frame Structure and Crash Box .....</b>	<b>25</b>
CHAPTER 3 .....	27
MATERIALS SELECTION, CONDITIONS, AND METHODS .....	27
<b>3.1 Materials Selection.....</b>	<b>27</b>
3.1.1 Material Selection for Formula SAE Chassis .....	27
3.1.2 Material Selection for Crash Box or Impact Attenuator.....	33
<b>3.2 Modeling .....</b>	<b>37</b>
3.2.1 Geometrical Modeling .....	37
3.2.1.1 Geometrical Modeling for Formula SAE Chassis .....	37
3.2.1.1.1 Selection of Chassis and Pipe Cross-sectional Area.....	37
3.2.1.1.2 Driver Ergonomics.....	37
3.2.1.1.3 General Design Requirements .....	38
3.2.1.1.4 Basic Structural Members Requirement .....	40
3.2.1.2 Geometrical Modeling for Crash Box or Impact Attenuator .....	46
3.2.1.2.1 Formula SAE M1 Crash Box Model.....	46
3.2.1.2.2 Formula SAE M2 Crash Box with Holes.....	48
3.2.1.2.3 Formula SAE M3 Crash Box or Impact Attenuator with Caterpillar Model .....	49
<b>3.3 Mathematical Modeling.....</b>	<b>52</b>
3.3.1 Mathematical Modeling of Chassis .....	52
3.3.2 Mathematical Modeling of Crash Box or Impact Attenuator .....	61
<b>3.4 Finite Element Modeling and analysis .....</b>	<b>62</b>
3.4.1 Finite Element Modeling and analysis for Formula SAE Chassis .....	62
3.4.1.1 Formula SAE M1 with Old Boundary Condition.....	65
3.4.1.1.1 Vertical Symmetric or Vertical Bending ('pure bending') Load Analysis .....	65
3.4.1.1.2 Vertical Asymmetric or Longitudinal Torsion (Pure Torsion Analysis Case).....	65
3.4.1.1.3 Longitudinal loads (Braking) Analysis .....	65
3.4.1.1.4 Lateral Bending (Cornering) Analysis.....	66
3.4.1.1.5 Crash or Impact cases (Front, Side and Rollover Crash) Analysis .....	67
3.4.1.1.6 Combinations of Load Analysis .....	67
3.4.1.1.7 Horizontal Lozengeing Analysis .....	67
3.4.1.2 Formula SAE M1 and M2 with New Boundary Condition .....	68
3.4.1.2.1 Vertical Symmetric or Vertical Bending ('pure bending') Load Analysis .....	68
3.4.1.2.2 Vertical Asymmetric or Longitudinal Torsion (Pure Torsion Analysis Case).....	70
3.4.1.2.3 Longitudinal loads (Braking) Analysis .....	73
3.4.1.2.4 Lateral Bending (Cornering) Analysis .....	73
3.4.1.2.5 Crash or Impact cases (Front, Side and Rollover Crash) Analysis .....	75
3.4.1.2.6 Horizontal Lozengeing Analysis .....	78

3.4.1.2.7	Combinations of Load Analysis .....	79
3.4.1.3	Topological optimization of Formula SAE M1 Chassis .....	80
3.4.2	Finite Element Modeling and Analysis for Crash Box or Impact Attenuator .....	81
CHAPTER 4 .....		85
RESULTS AND DISCUSSION .....		85
<b>4.1</b>	<b>Results .....</b>	<b>85</b>
4.1.1	Formula SAE M1 with Old Boundary Condition Result (Quai-Static Simulation) .....	85
4.1.1.1	Vertical Symmetric or Vertical Bending ('pure bending') Load Analysis .....	85
4.1.1.2	Vertical Asymmetric or Longitudinal Torsion (Pure Torsion Analysis Case).....	87
4.1.1.3	Longitudinal loads (Braking) Analysis .....	87
4.1.1.4	Lateral Bending (Cornering) Analysis.....	89
4.1.1.5	Crash or Impact cases (Front, Side and Rollover Crash) Analysis .....	91
4.1.1.6	Horizontal Lozenging Analysis .....	91
4.1.1.7	Combinations of Load Analysis .....	93
4.1.2	Formula SAE M1 with New Boundary Condition Result (Quai-Static Simulation) .....	95
4.1.2.1	Vertical Symmetric or Vertical Bending ('pure bending') Load Analysis .....	95
4.1.2.2	Vertical Asymmetric or Longitudinal Torsion (Pure Torsion Analysis Case).....	97
4.1.2.3	Longitudinal loads (Braking) Analysis .....	99
4.1.2.4	Lateral Bending (Cornering) Analysis.....	101
4.1.2.5	Crash or Impact cases (Front, Side and Rollover Crash) Analysis .....	103
4.1.2.6	Horizontal Lozenging Analysis .....	109
4.1.2.7	Combinations of Load Analysis .....	111
4.1.3	Formula SAE M1 Topological Optimization with New Boundary Condition Result .....	113
4.1.4	Formula SAE M2 with New Boundary Condition Result (Quai-Static Simulation) .....	115
4.1.4.1	Vertical Symmetric or Vertical Bending ('pure bending') Load Analysis .....	115
4.1.4.2	Vertical Asymmetric or Longitudinal Torsion (Pure Torsion Analysis Case).....	117
4.1.4.3	Longitudinal loads (Braking) Analysis .....	119
4.1.4.4	Lateral Bending (Cornering) Analysis.....	121
4.1.4.5	Crash or Impact cases (Front, Side and Rollover Crash) Analysis .....	123
4.1.4.6	Horizontal Lozenging Analysis .....	129
4.1.4.7	Combinations of Load Analysis .....	131
4.1.5	Formula SAE Crash Box results (Dynamic Simulation).....	133
4.1.5.1	Formula SAE Crash Box M1 or Impact Attenuator .....	133
4.1.5.2	Formula SAE Crash Box M2 or Impact Attenuator with Holes .....	134
4.1.5.3	Formula SAE Crash Box M3 or Impact Attenuator with Caterpillar Model.....	135
<b>4.2</b>	<b>Discussion.....</b>	<b>136</b>
4.2.1	Discussion on Formula SAE M1, M2 with Old and New Boundary Condition Results .....	136
4.2.2	Discussion on Formula SAE M1, M2 and M3 Crash Box or Impact Attenuator Results .....	140
CHAPTER 5 .....		146
CONCLUSION AND RECOMMENDATION .....		146
<b>5.1</b>	<b>Conclusion.....</b>	<b>146</b>
5.1.1	Conclusion on Formula SAE Chassis.....	146
5.1.2	Conclusion on Crash Box or Impact Attenuator .....	146

<b>5.2</b>	<b>Recommendation .....</b>	<b>148</b>
5.2.1	Recommendation on Formula SAE Chassis .....	148
5.2.2	Recommendation on Crash Box or Impact Attenuator .....	148
<b>5.3</b>	<b>Future Work on Formula SAE Chassis and Crash Box or Impact Attenuator .....</b>	<b>148</b>
	<b>REFERENCE.....</b>	<b>150</b>

## List of Tables

Table 1 Evaluation of Positive Decisions for Formula SAE Chassis .....	28
Table 2 Evaluation of weighting factor for Formula SAE Chassis .....	28
Table 3 Properties of candidate materials for Formula SAE Chassis [20], [28], [29] , [30].....	29
Table 4 Scaled property of candidate materials for Formula SAE Chassis.....	30
Table 5 Performance index ( $\gamma$ ) of candidate materials for Formula SAE Chassis .....	30
Table 6 FOM of candidate materials for Formula SAE Chassis .....	31
Table 7 Ranking of candidate material for Formula SAE Chassis .....	32
Table 8 Revision of property of SAE 1018 Steel [29] .....	32
Table 9 Aluminum 7075-T651 reports for Formula SAE Crash Box material by using Johnson-Cook model Parameters [26] .....	36
Table 10 Minimum dimension specification [2].....	39
Table 11 Frame outside diameter Vs thickness for Formula SAE Chassis [2].....	45
Table 12 Approximate masses of main components for Formula SAE M1 Chassis [2], [7], [12], [17].....	68
Table 13 Approximate masses of main components for Formula SAE M2 Chassis [2], [7], [12], [17].....	69
Table 14 Optimization constrained and non-constrained region.....	81
Table 15 Mesh property used for the Formula SAE Crash Box Models.....	84
Table 16 Overall result of Formula SAE M1 and M2 Chassis according to the different boundary condition .....	138
Table 17 Summary results of Formula SAE Crash Box models .....	141

## List of Figures

Figure 1.1 Space-frame primary structural components of Formula SAE .....	2
Figure 1.2 Illustration of Formula 1 racing car front structure components [5]. .....	3
Figure 1.3 General geometry of proposed crash tubes based on FSAE rules [8] .....	4
Figure 1.4 Sheet steel backbone Chassis (courtesy Lotus Car Ltd) [3].....	6
Figure 1.5 Triangulated sports car structure (courtesy of Cater ham Cars Ltd) [3].....	7
Figure 1.6 Monocoque structure [3] and Formula 1 racing car.....	7
Figure 1.7 Modern integral body-in-white (courtesy General Motors Corporation) [3] .....	8
Figure 1.8 SAE Vehicle axis system [3] and Formula SAE M2 Model.....	9
Figure 1.9 Vertical symmetric load case for Formula SAE M1 Chassis.....	9
Figure 1.10 Vertical asymmetric load case (courtesy of National Motor Museum, Beaulieu) [3] and free body diagram of longitudinal Torsion deformation mode [13].....	10
Figure 1.11 Braking load.....	10
Figure 1.12 Lateral bending [13] .....	11
Figure 1.13 Finite element model of Formula SAE M1 Chassis for front impact.....	11
Figure 1.14 Side impact model of Formula SAE M1 .....	12
Figure 1.15 Rollover impact model of Formula SAE M1 .....	12
Figure 1.16 Horizontal Lozenging deformation mode [13]. .....	13
Figure 0.17 Combination load case of Formula SAE M2 Chassis.....	13
Figure 1.18 Formula SAE Crash Box or Impact Attenuator [2] .....	14
Figure 1.19 Description of load and boundary condition for Crash Box or Impact Attenuator .....	15
Figure 1.20 Structural design and simulation of lightweight Formula SAE Chassis and Crash Box flow chart .....	18
Figure 3.1 Figure of merit (FOM) for the selected material .....	31
Figure 3.2 Schematic of the problem of the normal impact of a circular plate by a cylindrical punch with a hemispherical nose [26].....	34
Figure 3.3 A 95 <sup>th</sup> percent male profile [2] .....	38
Figure 3.4 FSAE Keep Out Zones [2] .....	38
Figure 3.5 Properly triangulated structure [2].....	39
Figure 3.6 Helmet clearance when rollover take place by the main and role hoops [2].....	40
Figure 3.7 Basic components of Formula SAE M2 Chassis model .....	40
Figure 3.8 Side view of structural members requirement seat by FSAE [2] .....	42
Figure 3.9 Formula SAE M2 structural members.....	43
Figure 3.10 Cockpit opening from the top view and internal cross-section from the side view.....	43

Figure 3.11 Cockpit opening from the top view and internal cross-section from the side view of Formula SAE M2 Chassis .....44

Figure 3.12 Steps used to model Formula SAE Chassis .....44

Figure 3.13 Formula SAE M1 Chassis Model with a 95th percentile male template (all units in mm) .....45

Figure 3.14 Formula SAE M2 Chassis Model (all units in mm).....46

Figure 3.15 3D Model for FSAE M1 Crash Box or Impact Attenuator based on FSAE rule .....47

Figure 3.16 FSAE M1 Crash Box or Impact Attenuator Model with 2mm thickness (mm) .....47

Figure 3.17 FSAE M2 Crash Box or Impact Attenuator with internal support and hole .....49

Figure 3.18 Caterpillars body part .....49

Figure 3.19 Formula SAE caterpillar Crash Box model generation .....50

Figure 3.20 FSAE Crash Box or Impact Attenuator with caterpillar Model with 2mm thickness .....51

Figure 3.21 Order of degrees of freedom (12 DOFs) for three-dimensional frame members [38].....55

Figure 3.22 Coordinate transformation for a frame element in space [38] .....57

Figure 3.23 Vectors for defining the location and three-dimensional orientation of the frame element in space [38].....58

Figure 3.24 Mesh size and contact between members .....63

Figure 3.25 Static analysis for Formula SAE Chassis .....64

Figure 3.26 Pure bending load applied on the Formula SAE M1 Chassis .....65

Figure 3.27 Longitudinal load (braking) applied to the Formula SAE M1 Chassis .....66

Figure 3.28 Lateral bending (cornering) load applied on the Formula SAE M1 Chassis.....66

Figure 3.29 Combination of the load applied on the Formula SAE M1 Chassis.....67

Figure 3.30 Horizontal lozenging load applied on the Formula SAE M1 Chassis .....68

Figure 3.31 Pure bending load applied on the Formula SAE M1 Chassis (front, side, and isometric view) .....69

Figure 3.32 Pure bending load applied on the Formula SAE M2 Chassis (front, side, and isometric view) .....70

Figure 3.33 Pure torsional load applied on the Formula SAE M1 Chassis (front, side, and isometric view)....71

Figure 3.34 Pure torsional load applied on the Formula SAE M2 Chassis (front, side, and isometric view)....72

Figure 3.35 Torsional load applied on Formula SAE Chassis .....72

Figure 3.36 Longitudinal (braking) load applied on the Formula SAE M1 Chassis (front, side, and isometric view) .....73

Figure 3.37 Lateral bending (cornering) load applied on the Formula SAE M1 Chassis (front, side, and isometric view).....74

Figure 3.38 Lateral bending (cornering) load applied on the Formula SAE M2 Chassis (front, side, and isometric view).....74

Figure 3.39 Front impact load applied on the Formula SAE M1 Chassis (front, side, and isometric view).....75

Figure 3.40 Front impact load applied on the Formula SAE M2 Chassis (front, side, and isometric view).....75

Figure 3.41 Side impact load applied on the Formula SAE M1 Chassis (front, side, and isometric view) .....76

Figure 3.42 Side impact load applied on the Formula SAE M2 Chassis (front, side, and isometric view) .....76

Figure 3.43 Rollover load applied on the Formula SAE M1 Chassis (front, side, and isometric view).....77

Figure 3.44 Rollover impact load applied on the Formula SAE M2 Chassis (front, side, and isometric view) 78

Figure 3.45 Horizontal lozenging load applied on the Formula SAE M1 Chassis (front, side, and isometric view) .....79

Figure 3.46 Horizontal lozenging load applied on the Formula SAE M2 Chassis (front, side, and isometric view) .....79

Figure 3.47 Combination of the load applied on the Formula SAE M1 Chassis (Isometric view) .....80

Figure 3.48 Combination of the load applied on the Formula SAE M2 Chassis (front, side, and isometric view) .....80

Figure 3.49 ANSYS Explicit Dynamics system for Crash Box .....82

Figure 3.50 Description of load and boundary condition for Crash Box or Impact Attenuator .....83

Figure 3.51 Boundary condition on Crash Box or Impact Attenuator in ANSYS Explicit Dynamics for M1, M2, and M3.....84

Figure 4.1 Formula SAE M1 Chassis pure bending results .....86

Figure 4.2 Formula SAE M1 Chassis longitudinal load results .....88

Figure 4.3 Formula SAE M1 Chassis lateral bending results .....90

Figure 4.4 Formula SAE M1 Chassis lateral bending results .....92

Figure 4.5 Formula SAE M1 Chassis combined load results.....94

Figure 4.6 Formula SAE M1 Chassis pure bending results .....96

Figure 4.7 Formula SAE M1 Chassis pure torsional load results .....98

Figure 4.8 Formula SAE M1 Chassis longitudinal load results .....100

Figure 4.9 Formula SAE M1 Chassis lateral bending results .....102

Figure 4.10 Formula SAE M1 Chassis lateral bending results .....104

Figure 4.11 Formula SAE M1 Chassis lateral bending results .....106

Figure 4.12 Formula SAE M1 Chassis lateral bending results .....108

Figure 4.13 Formula SAE M1 Chassis lateral bending results .....110

Figure 4.14 Formula SAE M1 Chassis combined load results.....112

Figure 4.15 Optimization 1 base on the following loading types.....113

Figure 4.16 Optimization 2 based on Pure Torsion analysis.....114

Figure 4.17 Optimization results from the impact analysis .....114

Figure 4.18 Formula SAE M1 Chassis pure bending results .....116

Figure 4.19 Formula SAE M1 Chassis pure torsion results .....118

Figure 4.20 Formula SAE M1 Chassis longitudinal load results .....120

Figure 4.21 Formula SAE M2 Chassis lateral bending results ..... 122

Figure 4.22 Formula SAE M2 Chassis front impact results ..... 124

Figure 4.23 Formula SAE M2 Chassis side impact results ..... 126

Figure 4.24 Formula SAE M2 Chassis rollover impact results ..... 128

Figure 4.25 Formula SAE M1 Chassis lateral bending results ..... 130

Figure 4.26 Formula SAE M1 Chassis combined load results ..... 132

Figure 4.27 Total deformation of FSAE Crash Box (Side and Top View) ..... 133

Figure 4.28 Total deformation of FSAE Crash Box M2 model ..... 134

Figure 4.29 Total deformation of internal Caterpillar model Crash Box (different view) ..... 136

Figure 4.30 Mass of the Formula SAE Chassis vs Chassis type ..... 139

Figure 4.31 Torsional stiffness vs Chassis type ..... 139

Figure 4.32 Maximum Von-Miss Stress vs Formula SAE Chassis type ..... 140

Figure 4.33 Maximum total deformation vs Formula SAE Chassis type ..... 140

Figure 4.34 Total deformation Vs Time for Formula SAE Crash Box's ..... 142

Figure 4.35 Mean Reaction Force Vs Time for Formula SAE Crash Box's ..... 143

Figure 4.36 Acceleration Vs time of Formula SAE Crash Box's ..... 144

Figure 4.37 Formula SAE Crash Box maximum peak and average acceleration results ..... 144

Figure 4.38 Crash force vs displacement for Formula SAE Crash Box's ..... 145

Figure 4.39 Different energy forms vs Crash Box type ..... 145

## Nomenclature

$\sigma_u$	Ultimate Tensile strength
$\sigma_y$	Yield Strength or Yield Tensile Strength
E	Young's Modulus or Modulus of Elasticity
$\sigma$	Normal Stress
$\varepsilon$	Normal Strain
C's	Material-dependent elastic constants
$\varepsilon_i$	Strain $i=x,y,z$
$\gamma_{ij}$	Shear Strain $i=x,y,z$ $j=x,y,z$
G or $\mu$	Share Modulus
K	Bulk Modulus or Modulus of Rigidity
$\nu$	Poisson's Ratio
$\rho$	Density
$L_f$	Length of the test section at the fracture
$L_G$	Gauge length
N	Number of possible decisions
$\alpha$	Weighting Factor
$\gamma$	Performance index
$\alpha_i$	Weighting Factor
$\beta_i$	Scaled property
Ct	The total cost of the material/unit weight
$\dot{\varepsilon}_e^p$	Reference strain rate
A	Elastic limit or Initial yield stress
B	Modulus of strain hardening or hardening constant,
C	Strain rate sensitivity index/constant
n	Exponent of strain hardening

$m$	Exponent of thermal weakening
$\dot{\varepsilon}$	Non-dimensional speed of plastic strain
$\varepsilon$	Equivalent plastic strain
$\bar{T}$	Homological temperature
$T$	Current temperature
$T_r$	Reference (usual room temperature)
$T_m$	Melting temperature
$\beta$	Represents the fraction of plastic work that is converted into heat
$C_p$	Heat capacity of the material
$U$	Strain energy (internal work)
$V$	External work
$\delta$	Virtual operator
$\delta U_1$	Virtual strain energy
$[B]$	Strain-displacement matrices
$[D]$	Elastic matrix
$\{u\}$	Nodal displacement vector
$\{\varepsilon\}$	Strain vector
$\{\sigma\}$	Stress vector
$vol$	Volume of element
$area_f$	Area of the distributed resistance
$\{w_n\}$	Motion normal to the surface
$[N_n]$	matrices of shape function for normal motions at the surface
$\{w\}$	The vector of displacements of general point
$\{F^a\}$	Acceleration (D'Alembert) force vector
$t$	Time
$\{p\}$	Applied pressure vector

$area_p$	The area over which pressure acts
$\{F_e^{nd}\}$	The nodal force applied to the element
$[K_e]$	Element stiffness matrix
$[K_e^f]$	Element foundation stiffness matrix
$\{F_e^{th}\}$	Element thermal load vector
$[M_e]$	Element mass matrix
$\{\ddot{u}\}$	Acceleration vector (such as the gravitational effect)
$\{F_e^{Pr}\}$	Element pressure load vector
$[K]$	Total stiffness matrix
$\{u\}$	Nodal displacement vector
$N$	Number of elements
$[K_e]$	Element stiffness matrix
$\{F^r\}$	Reaction load vector
$\{F^a\}$	Total applied load vector
$I_x, I_y, \text{ and } I_z$	Second moments of area/inertia of the cross-section of the beam with respect to the x, y, and z-axes respectively
$J$	Polar moment of inertia of the cross-section of the bar
$T$	Transformation matrices
$D_e$	Global coordinate system
$d_e$	Local coordinate system
$V_1, V_2, \text{ and } V_3$	Position vectors
$V$	Computed volume
$M$	Number of constraints
$U_c^j$	Computed compliance of load case j
$\underline{U_c^j}$	Lower bound for compliance of load case j
$\overline{U_c^j}$	Upper bound for compliance of load case j

$F$	Computed weighted compliance function
$\underline{F}$	Lower bound for the weighted compliance function
$\overline{F}$	Upper bound for the weighted compliance function
$[m]$	Mass matrix
$\{\ddot{x}\}$	Acceleration
$[C]$	Damping matrix
$\{\dot{x}\}$	Velocity
$[K]$	Stiffness matrix
$\{x\}$	Nodal displacement vector
$\{F\}$	Nodal external force vector
$g$	Gravitational acceleration
DLM	Digital logic method
PD	Positive decisions
FOM	Figure of Merit
FSAE	Formula Society of Automotive Engineering
BC	Boundary Condition
PCF	Peak Crash Force
MCF	Mean Crash Force
EA	Energy Absorption
SEA	Specific Energy Absorption

## Acknowledgment

The authors wish to acknowledge individuals and sources that contributed to this research: (1) the almighty God, (2) my advisers Dr. Ermias G. Koricho, my co-adviser Mr. Hairedin Ismal (Ph.D. Candidate) and Mr. Araya Abera (Ph.D. Candidate) who give me unlimited advice, instructions, and encouragement at every step of this research. Sincerely I thank all the Staff members of Addis Ababa University, AAiT, SMiE design stream staffs, Vehicle Research Center Staffs and my big thanks to everyone those who stood beside me to finish this research.

Finally, I must express my very profound gratitude to my parents (Moges Gebre G/Mariam and Zenebework Bekele Teklewold) and family members (Daniel, Emebet, Alemtshay, Aster, Sisay, Behalu, Issac, Kidus, Napolyon, Lisanework, Kebede, Henok, Yonas, Abel, Dawit, Firehiwot and Jerusalem) for providing me with unfailing support and continuous encouragement throughout my years of study and through the process of researching and writing this thesis. This accomplishment would not have been possible without them.

Thank you.

Nikodmose Moges Gebre

## Abstract

Currently, car racing takes place in Ethiopia. But still, there is a big question ‘How it has been designed?’, ‘What kind of cars?’, and ‘How the safety of driver seems?’. This research focused on the structural design and simulation of Formula SAE lightweight racing car: it is based on the Formula Society of Automotive Engineering that demands with intention to introduced the Formula SAE Chassis and Crash Box in Ethiopia, without compromising the structural safety and performance, according to geometry improvement, improving boundary condition used, weight reduction, material selection and crashworthiness of the vehicle.

The structural design of Formula SAE Chassis and Crash Box were performed by using SOLIDWORK2018, and their simulation was done using ANSYS 19.1 FEA simulation software. The design and analysis of Formula SAE racing car Chassis consider seven types of loading conditions, such as static (pure bending, pure torsion, braking, lateral cornering, horizontal lozenging and combination) and crash (front, side, and rollover) loading. According to the result of Von-Mess stress and failure criterion, the material shows the resistance to the applied stress because the Von-Misses stress from a different type of loading is below the yield strength of SAE 1018 steel material. All the deformation result from different loading conditions are less than 25 mm. In addition to that, the torsional stiffness shows an increment by 19.53% and weight reduction by 20.81% from Formula SAE Chassis M1 model (old model).

The main reasons of the adding the crash box in any vehicle is to absorb more energy especially for racing cars and three types model considered according to Formula SAE rule, using Aluminum 7075-T651 plate by applying Johnson-Cook strength and material models because of impact simulation complicity. Then FEA simulation result shows adding holes and caterpillar geometry increase the total deformation (70.606mm to 141.49mm), reduce the peak crash force (110.82KN to 53.21KN), average acceleration (31.6g to 11.78g), peak acceleration (37.08g to 17.86g) and increase energy absorption (7388.82J to 7488.18J) comparing the Crash Box models. Finally, the Formula SAE M3 Crash Box model is selected for the Formula SAE racing car because of less peak crash force with a larger time to rich it, beneficial energy absorption, higher velocity generation, satisfactory average acceleration, satisfactory peak acceleration, smooth, steady and large total deformation due to the adding of the caterpillar geometry in the Formula SAE Crash Box from bioinspired idea caterpillar insect.

**Keywords:** Finite Element Analysis (FEA), Model, Simulation, Topological optimization, Formula SAE Chassis, and Crash Box.

# CHAPTER 1

## INTRODUCTION

### 1.1 Introduction

The first Formula 1 racing takes place in 1906 G.C; in the earliest days of automotive men want to race and won, by the 1915 G.C Mercedes and Ferrari build a small Formula 1 racing cars with small fuel tank and engine in front because of that the stability of the racing car with regard to speed/acceleration and cornering is not good. However, in England, engineer John Cooper builds a small Formula 1 racing cars with small engine and position behind the driver or rear engine. It revolutionized the history of racing cars by optimizing the balance of the Formula 1 racing car which gives a great level of grip around the corner [1].

Since the improvement of Formula 1 engine and position behind, the racing cars speed increase spectacularly but designers/engineers need the best Chassis structure and energy absorption devise for Formula 1 to improve load transfer and energy absorption by the structural system [1].

Chassis is a structure that used to support all loads applied by different components (engine, driver and so on) and the load created externally. Chassis frames can also consider as the structures with a carefully weighed arrangement of material that is intended to resist loads is called as structures. Formula SAE automotive space frame Chassis is a skeleton material on which most of the mechanical parts that include the tires, brakes, engines, and etc. are bolted [2] and an essential structural backbone of an automobile, especially in a racing car and need good designs allow a light and stiff Chassis to fabricated at a minimal expense and weight without compromising the safety of the driver.

In space-frame Chassis, structural design applying node-to-node triangulation arrangement for the frame members projected onto a plane, where a coplanar load applied in any direction, at any node, results in only tensile or compressive forces in the frame members as seen in Figure 1.1. This is also, what is meant by "properly triangulated" when the frame structure of Formula SAE crates to improve the load path. Also in Monocoque structure design (Figure 1.2) improving the aerodynamic effect of Formula 1 after observing the aerodynamics effect of airplanes which create a downward force to keep the racing car on the ground with a better racing tire [2].

Formula SAE space-frame structure Chassis are designed and manufactured by using mild or alloy, Steel tubing (minimum 0.1% carbon) with the recommended proper thickness and cross-sectional area (circular and rectangular) [2], nowadays by replacing the frame structure with a Carbon fiber reinforced composite material in the form of Monocoque and Semi-Monocoque structure which reduced the weight, aerodynamic drag force on the Formula 1 structure, but increase the cost of production associated with material used and manufacturing complexity [3].

In the history of racing, there is a different type of Chassis structure that the basic ones are space-frame and Monocoque [4]. Basic components of the space-frame structure of Formula SAE are shown in Figure 1.1 below with respect to their definitions [2]:

- 1. Main Hoop:** a roll bar located alongside or just behind the driver,
- 2. Front Hoop:** a roll bar located above the driver's legs, in proximity to the steering wheel,
- 3. Main Hoop bracing:** used to support the main roll hoop bracing from the back side of the Chassis,
- 4. Side impact structure or zone:** The area of the side of the car extending from the top of the floor to 350mm (13.8 inches) above the ground and from the Front Hoop back to the Main Hoop,
- 5. Front bulkhead:** A planar structure that defines the forward plane of the major structure of the Frame and functions to provide protection for the driver's feet, and
- 6. Front Crash Box or Impact Attenuator:** A deformable, energy absorbing device located forward of the Front Bulkhead.

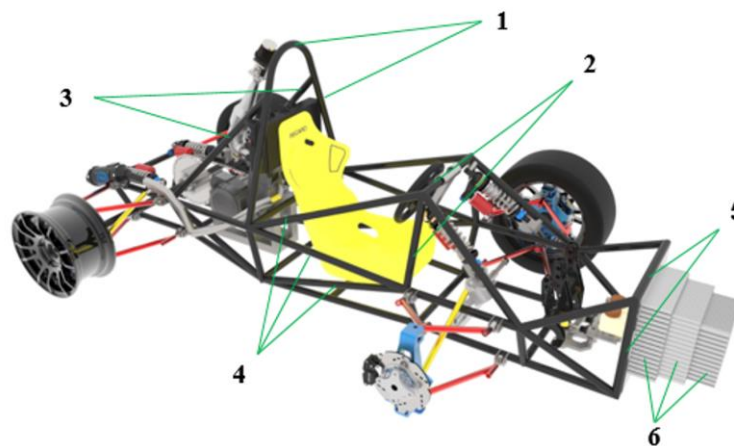


Figure 1.1 Space-frame primary structural components of Formula SAE

Basic primary components of Monocoque structure of Chassis and Crash Box or impact attenuator shown in Figure 1.2.

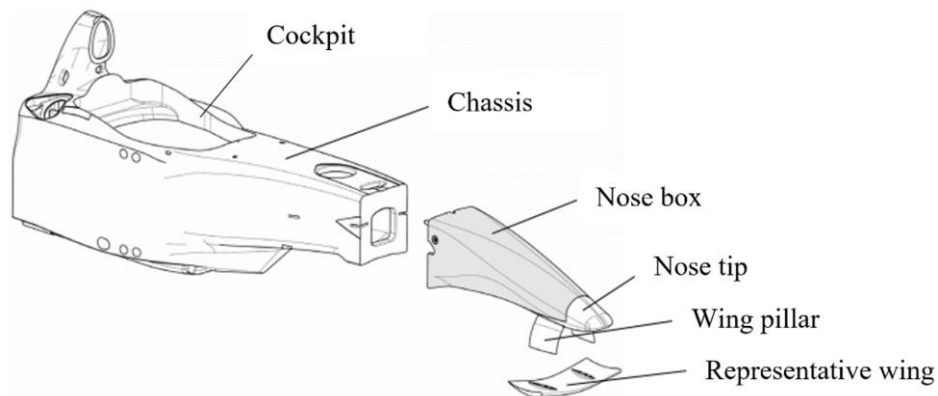


Figure 1.2 Illustration of Formula 1 racing car front structure components [5].

Nowadays speed of the ordinary and racing cars is high, therefore when accidents happen the best structural design of Crash Box or Impact Attenuator required with better energy absorption, deformation, and stiffness to guide impact forces generated. According to low-speed impact the damage to the race car minimum compare to high-speed impact, the device should guide forces generated/propagated from the impact into the car body structure in a collapsed manner to prevent injury or death on the driver's and to reduce repair costs in low-speed vehicle collision [6].

The Crash Box or impact attenuator is a thin-walled structure attached in a vehicle bumper structure or side rail for ordinary cars and Front Bulkhead for race cars. A thin-walled shell type has a high crash energy absorption or dissipation property and thus offers excellent protection to the structure, also they are cheap, efficient and reliable, they are popularly used as energy absorbing materials for the Crash Box or impact attenuator devices [7]. Since speed brings danger to the driver and structure of the vehicle when impact/crash occurs between two racing cars or rigid wall the front, back and side impact structures [6].

Formula SAE Crash Box or impact attenuator structure are designed and manufactured by using Steel frame, solid steel or aluminum plate and nowadays for Formula 1 race car they use a revolutionized ideas by using carbon fiber reinforced composite material, but it is very safe, light, stiff, bodywork with better adaptability of change in circumstances and higher cost [2] in the form of Carbon mold and inside the Carbon mold there is lightweight aluminum honeycomb core structure with a better energy absorption (Figure 1.2). Technology advancement gained from these advanced material has produced Formula 1 that are lighter, faster and safe than ever before [3].

It has been demonstrated by many researchers that thin-wall shell type of crash absorber dissipates energy under opposite effects of impact, thus offers protection to the structure and cheap, efficient, and reliable. Figure 1.3 shows the schematic diagram of the crash tubes with a height ( $H$ ), depth ( $D$ ) and thickness ( $T$ ) [2], [8] are popularly used as energy absorbing devices for Formula SAE Crash Box.

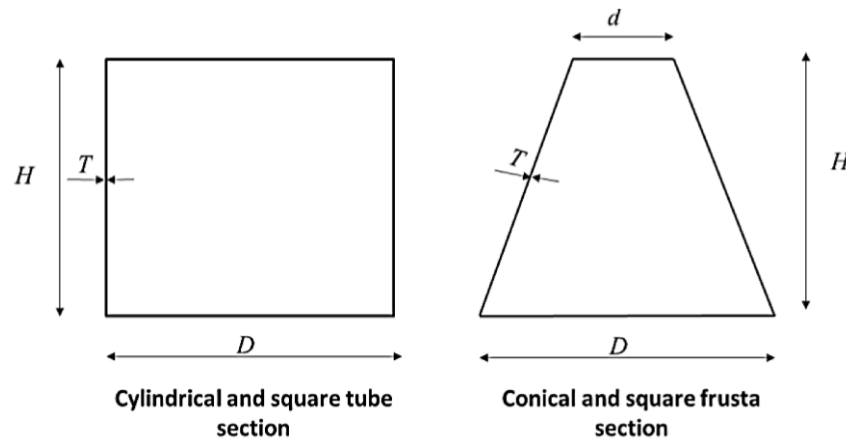


Figure 1.3 General geometry of proposed crash tubes based on FSAE rules [8]

The Formula SAE competition attracts students from different universities and different countries with objectives to design analysis and manufacture a racing car. The competition evaluation criteria divided into two main parts. The first one is a static part and another one is a dynamic part. The ideal car should be of high performance, good fuel economy and should satisfy all the design safety rules mentioned in the rulebook of FSAE international [2].

## 1.2 Background

### 1.2.1 Terminology, Overview of Vehicle Chassis Structure Types and Loads

#### 1.2.1.1 Terminology

The main purpose of the structure (Chassis and Crash Box/Impact Attenuator) is to maintain the shape of the vehicle and to support the various loads applied to it. The structure usually accounts for a large proportion of the development and manufacturing cost in a new vehicle programmed, and many different structural concepts are available to the designer. It is essential that the best one chosen to ensure acceptable structural performance within other design constraints such as cost, volume, a method of production, product application, safety, ergonomics etc. Assessments of the performance of a vehicle structure related to its strength, stiffness, vibration behavior and crashworthiness. A design aim is to achieve sufficient levels of these with as little mass as possible [2], [3].

The strength requirement implies that no part of the structure will lose its function when it subjected to road loads. Loss of function may cause by instantaneous overloads due to extreme load cases, or by material fatigue [1], [2].

**(a) Stiffness**

The vehicle body subjected to a moment applied at the axle centerlines by applying upward and downward loads at each axle in this case. These loads result in a twisting action or torsion moment about the longitudinal axis of the vehicle [1]. The two most commonly used are [3]:

(1) Bending stiffness  $K_B$ : Bending stiffness is less significant relative to the torsional stiffness of a car chassis. In static bending, the wheel loads and their distribution deviate only slightly [9], which relates the symmetrical vertical deflection of a point near the center of the wheelbase to multiples of the total static loads on the vehicle [3]. (2) Torsion stiffness  $K_T$ : The torsional rigidity is defined as the torsional response (defined as some deflection angle) of a structure to an applied torque loading [10].

These two cases apply completely different local loads cases to individual components within the vehicle. It is usually found that the torsion case is the most difficult to design and a benchmark to indicate the effectiveness of the vehicle structure [3].

**(b) Vibrational Behavior**

The global vibrational characteristics of a vehicle related to both its stiffness and mass distribution. The frequencies of the global bending and torsional vibration modes commonly used as benchmarks for vehicle structural performance. However, bending and torsion stiffness influence the vibrational behavior of the structure, particularly its first few Mode and natural frequency [3].

**(c) Crashworthiness or Impact Energy Absorption**

Crashworthiness is the ability of a structure to protect its occupants during an impact or crash. This commonly tested when investigating the safety of vehicles. Depending on the nature of the impact and the vehicle involved, different criteria used to determine the crashworthiness of the structure. Several criteria are used to assess crashworthiness prospectively, including the deformation patterns of the vehicle structure, the acceleration experienced by the vehicle during an impact, and the probability of injury predicted by human body models [1].

For many years' crashworthiness was seen by the automotive designer as something to be tolerated and necessitated only that the seat belts complied with the British Standard

[1] and for Formula SAE vehicle the impact velocity is 7 m/s with decelerates the vehicle at a rate not exceeding 20 g's average and 40 g's peak [2].

### 1.2.2 Overview of Vehicle Chassis Structure Types (Modern Structure Types)

#### a. Backbone Structure

The 'Backbone' Chassis structure is a relatively modern example of the 'large section tube' concept (although Tatra vehicles of the 1930s had backbone structures). This used on specialist sports cars such as the Lotus shown in Figure 1.4. It still amounts to a 'separate Chassis frame'. The backbone Chassis derives its stiffness from the large cross-sectional enclosed area of the 'backbone' member. Such specialist vehicles often have bodies made of glass-reinforced plastic. On many vehicles of this type, the combined torsion stiffness of the Chassis and the attached body together is greater than the sum of the stiffnesses of the individual items [3].

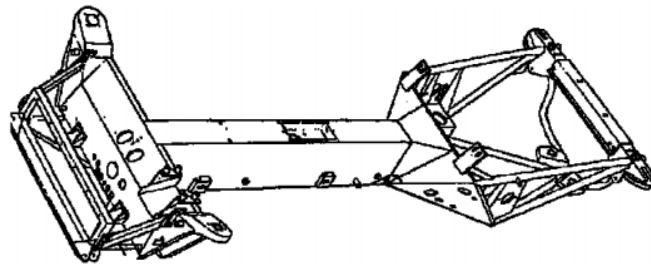


Figure 1.4 Sheet steel backbone Chassis (courtesy Lotus Car Ltd) [3]

#### b. Triangulated Tube or Space Frame Structure

The space frame is the most efficient type of Chassis, which is possible to build in limited production. Unitary construction may be superior in some instances but there are many factors again a Chassis of this type having adequate torsional rigidity without automatically having ample rigidity in bending [11]. Stiffening of the edges of the passenger compartment top opening, particularly at the corners, can also bring some improvement to the torsional performance. This method of construction is best suited to low volume production because of low tooling costs. It is not well suited to mass production due to complication and labor-intensive manufacture [3].

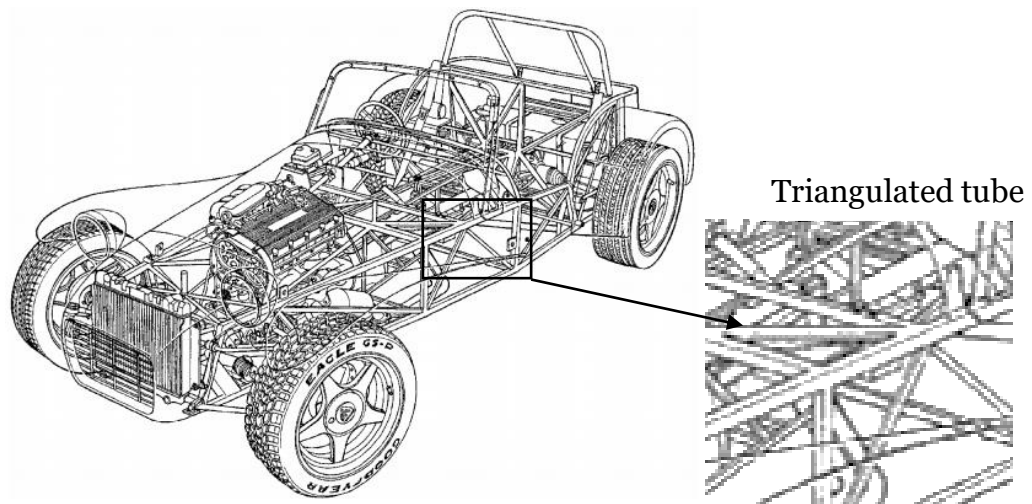


Figure 1.5 Triangulated sports car structure (courtesy of Caterham Cars Ltd) [3].

### c. Pure Monocoque

The logical conclusion of the ‘closed box’ approach is the ‘Monocoque’ (in French: ‘single shell’) with the dual role of the body surface and structure. This is the automotive version of aircraft construction, weight efficient, relatively rare and restricted to racing cars as shown in Figure 1.6. There are several reasons for this. First, for the Monocoque to work efficiently, it requires a totally closed tube. However, practical vehicles require openings for passenger entry, outward visibility, etc. This requires interruptions to the ‘single shell’, which then reduce it to an open section, with consequent lowering of torsion stiffness. Also, the shell requires reinforcement: (a) to prevent buckling, and (b) to carry out of plane loads [3].

Typical Formula 1 racing car Monocoques, usually made of carbon fiber composite sandwich material, can have torsion stiffness greater than 30,000 Nm/deg. for the composite ‘tub’ alone. In such vehicles, the engine and gearbox also act as load-bearing structures, in series with the Monocoque [3].



Figure 1.6 Monocoque structure [3] and Formula 1 racing car

#### d. Integral or Unitary Body Structure

Are the most widely used modern car structure type, the chassis, and bodywork in one unit, even though it may be made up of numerous panels formed into a structure by loading-carrying joints and made from spot welded, pressed sheet metal platform Chassis supplemented by superstructures which also provides stiffness. It is well suited to mass production methods [11].

Figure 1.7 shows a modern example of an integral ‘body-in-white’ (i.e. bare body shell). The integral body is really a mixture of the Monocoque and the ‘birdcage’ types. The body forms a ‘closed box’ torsion structure with consequent high stiffness. The walls, or ‘surfaces’ of the box, consist of the skin panels (such as the roof, floor bulkheads, etc.) where possible. Elsewhere open bay ring frames (side frame, windshield frames etc.) form the surface of the box, wherever openings are required. Beam members are also used to carry out-of-plane loads, for example in the floor [3].

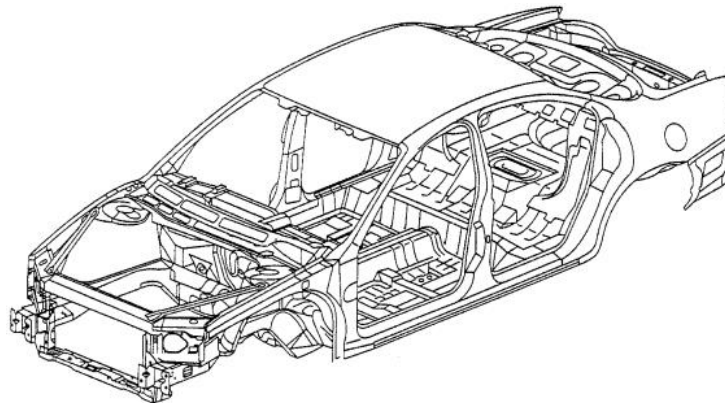


Figure 1.7 Modern integral body-in-white (courtesy General Motors Corporation) [3]

#### 1.2.3 Overview of Vehicle Chassis Load Types

There are different kind of load applied on the vehicle Chassis structure in a principal ‘normal running and worst scenario’ global road loads cases are as follows (see Figure 1.8 below with respect to axis directions) [1], [3]:

1. Vertical Symmetrical or Vertical Bending (‘pure bending case’) causes bending about the Y–Y axis,
2. Vertical Asymmetric or Longitudinal Torsion (‘pure torsion case’) causes torsion about the X–X axis and bending about the Y–Y axis,
3. Longitudinal loads (braking),
4. Lateral Bending (cornering),
5. Crash or impact cases (front, side, and rollover crash),

6. Horizontal Lozenging,
7. Combinations of load (pure bending and torsion),
8. Local load cases (e.g. door slam, etc.) [Not consider in this research paper because the Formula SAE did not have any door].

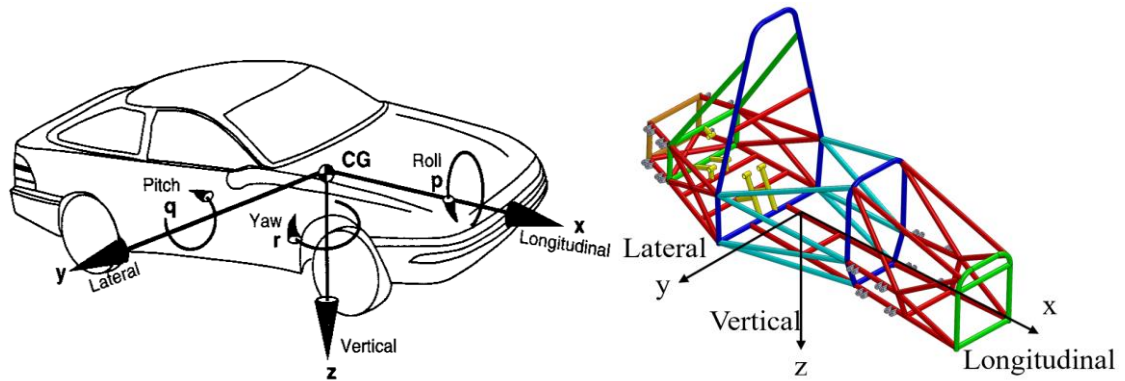


Figure 1.8 SAE Vehicle axis system [3] and Formula SAE M2 Model

### 1.2.3.1 Vertical Symmetric or Vertical Bending (‘pure bending’) Load Case

This occurs when the weight of driver, engine, drive-train, radiator, and shell etc. under an effect of gravity produce sag in the frame see Figure 1.9 [12]. This applies a bending moment to the vehicle about a vertical axis. The weight of the driver and other components mounted to the frame, such as the engine and other parts carry in bending through the car frame [13].

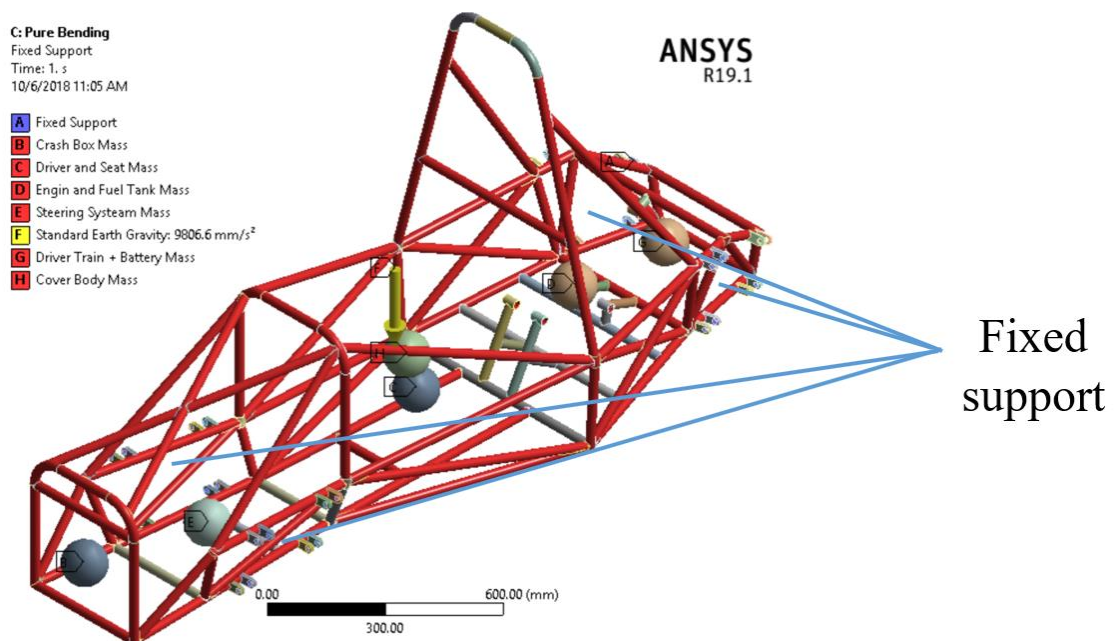


Figure 1.9 Vertical symmetric load case for Formula SAE M1 Chassis

### 1.2.3.2 Vertical Asymmetric or Longitudinal Torsion (Pure Torsion Analysis Case)

The torsion loads result from applied loads acting on one or two oppositely opposed corners of the car. The frame can think of as a torsion spring connecting the two ends where the suspension loads act. Torsional loading and the accompanying deformation of the frame and suspension parts can affect the handling and performance of the car. The resistance to torsional deformation often quoted as stiffness in foot-pounds per degree (ft-lb/deg.) or Newton-meter per degree (N-m/deg.). This is generally thought to be the primary determinant of frame performance for an FSAE race car [13].

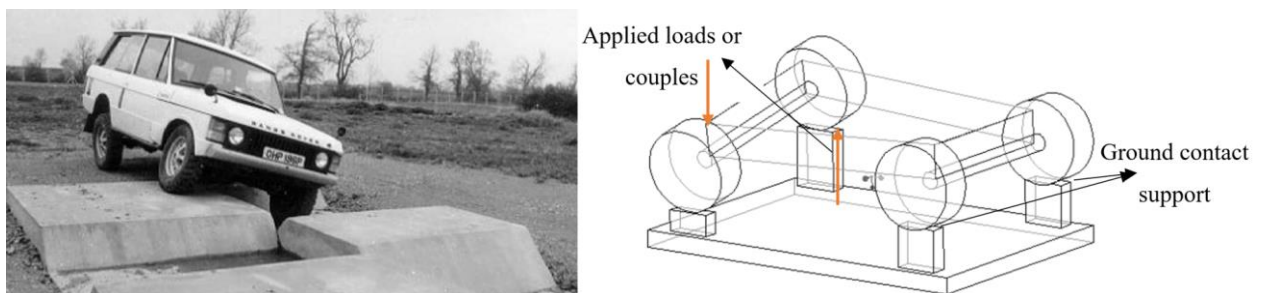


Figure 1.10 Vertical asymmetric load case (courtesy of National Motor Museum, Beaulieu)

[3] and free body diagram of longitudinal Torsion deformation mode [13]

### 1.2.3.3 Longitudinal loads (Braking)

The braking forces at the ground contact patches are offset by a vertical distance from the vehicle center of gravity, there will be weight transfer from the rear to the front wheels [3].

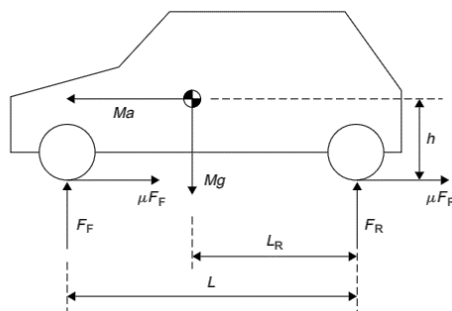


Figure 1.11 Braking load

### 1.2.3.4 Lateral Bending Load (Cornering)

Lateral bending loads are induced in the frame for various reasons, sliding of tires due to cornering (the lateral force reaches a maximum on one side of the wheel opposite the curb just lifts off but actual rollover of the car will not occur unless there is sufficient energy before impact to lift the vehicle center of gravity) such as road camber, side wind loads and

centrifugal forces caused by cornering. The sideways forces will act along the length of the car and resisted at the tires. This causes a lateral load and resultant bending [3].

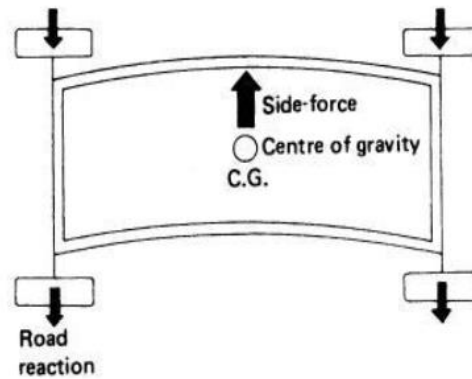


Figure 1.12 Lateral bending [13]

### 1.2.3.5 Crash or Impact cases (Front, Side and Rollover Crash)

There are different kind of crash or impact based on the car-to-car collision and car to barrier collision:

- a. **Front Impact Case:** in the front impact scenario the following load (120kN, 0kN, 0kN) applied in the actual attachment points between the impact attenuator and the front bulkhead, with a fixed displacement (x, y, z) [2].

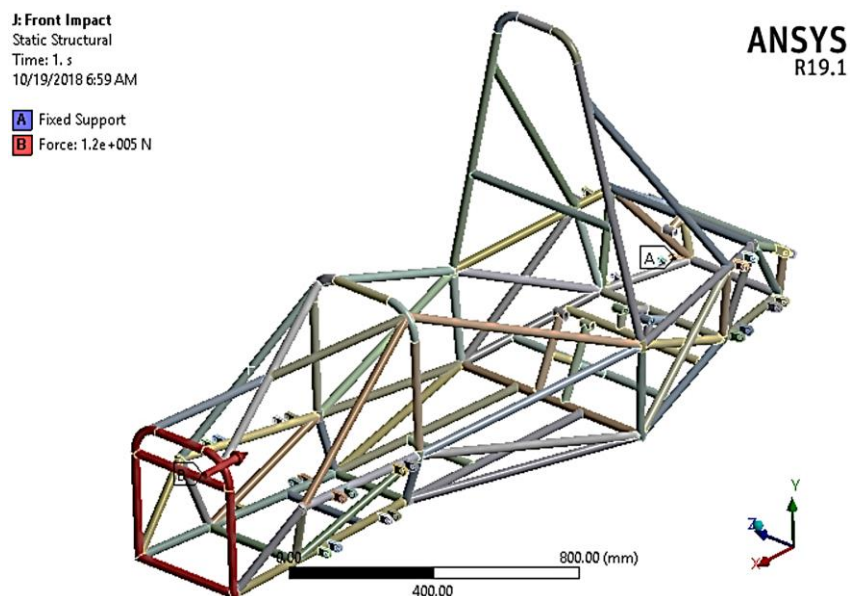


Figure 1.13 Finite element model of Formula SAE M1 Chassis for front impact

- b. **Side Impact Case,** these crashes often occur at intersections, and when two vehicles pass on a multi-lane roadway or the car bombard with side walls or barriers [1].

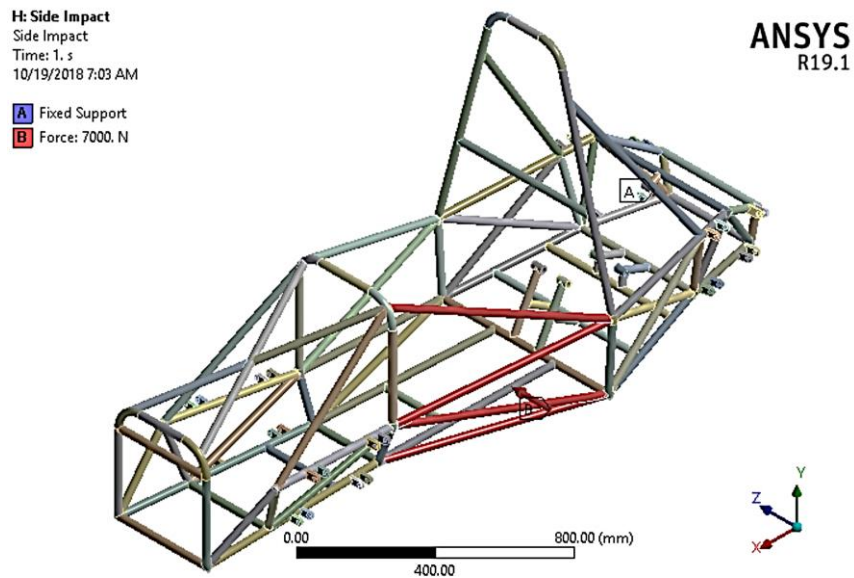


Figure 1.14 Side impact model of Formula SAE M1

**c. Rollover Case**, are directly related to a vehicle's stability in turns. The stability influenced by the relationship between the center of gravity and the track width (distance between the left and right wheels). A high center of gravity and narrow track can make a vehicle unstable in fast turns or sharp changes of direction increasing the odds that it will tip over once it begins to skid sideways. The problem is easily noticeable in sport-utility vehicles, which have higher ground clearance for off-road driving. In addition, these types of crashes have identified as a major contributor to serious spinal injuries resulting in varying degrees of long-term paralysis and disability [1].

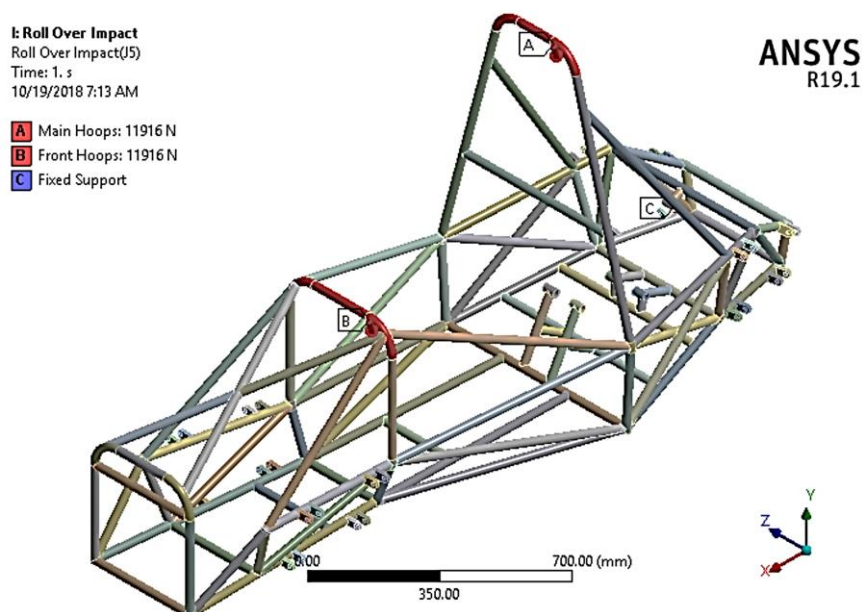


Figure 1.15 Rollover impact model of Formula SAE M1

### 1.2.3.6 Horizontal Lozenging

Forward and backward forces applied at opposite wheels cause this deformation. These forces may be caused by vertical variations in the pavement or the reaction from the road driving the car forward. These forces tend to distort the frame into a parallelogram shape as shown in Figure 1.16 [14].

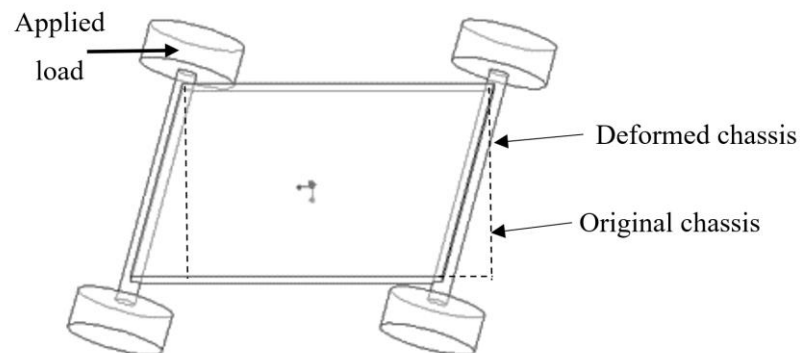


Figure 1.16 Horizontal Lozenging deformation mode [13].

### 1.2.3.7 Combinations of Load Cases

After seeing the effects of each load case separately the final one will be by combining the load case on the Chassis to predicate the output result in the worst scenario [3] and in a real situation, the torsion case cannot exist without bending as gravitational forces are always present. Therefore, the two cases must be considered together when representing a real situation [1].

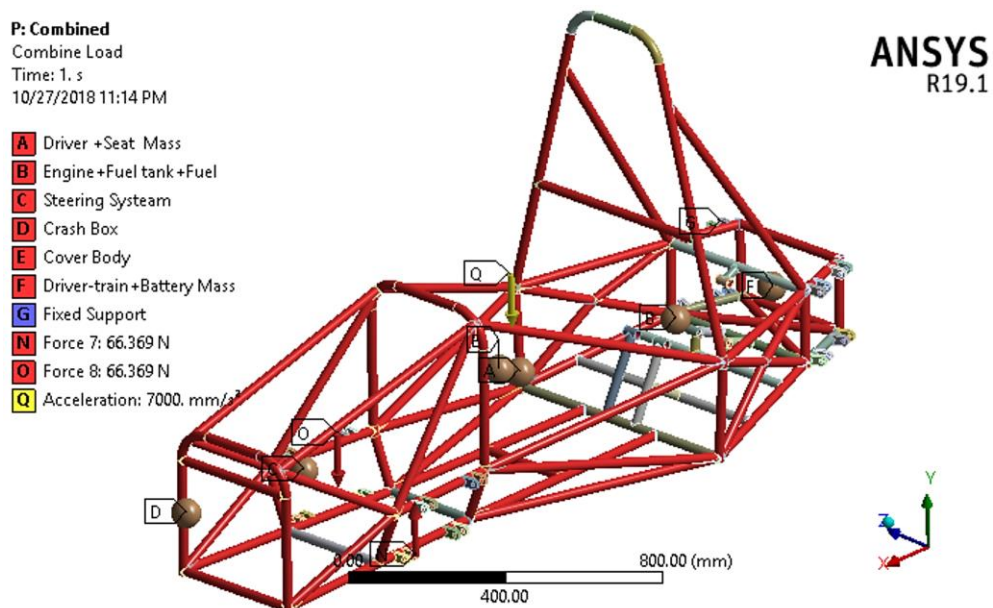


Figure 0.17 Combination load case of Formula SAE M2 Chassis

### 1.2.4 Overview of Vehicle Crash Box or Impact Attenuator Types

There are different types and cross-sectional area of Crash Box or Impact Attenuators. Depending on the type of load applied in the vehicle, these factors are the weight of the vehicle, the size of the vehicle, working condition, working area, and so many reasons. For the Formula SAE racing car, the Crash Box or impact attenuator has a basic structure as shown in Figure 1.18 based on FSAE 2017-18 rulebook [2].

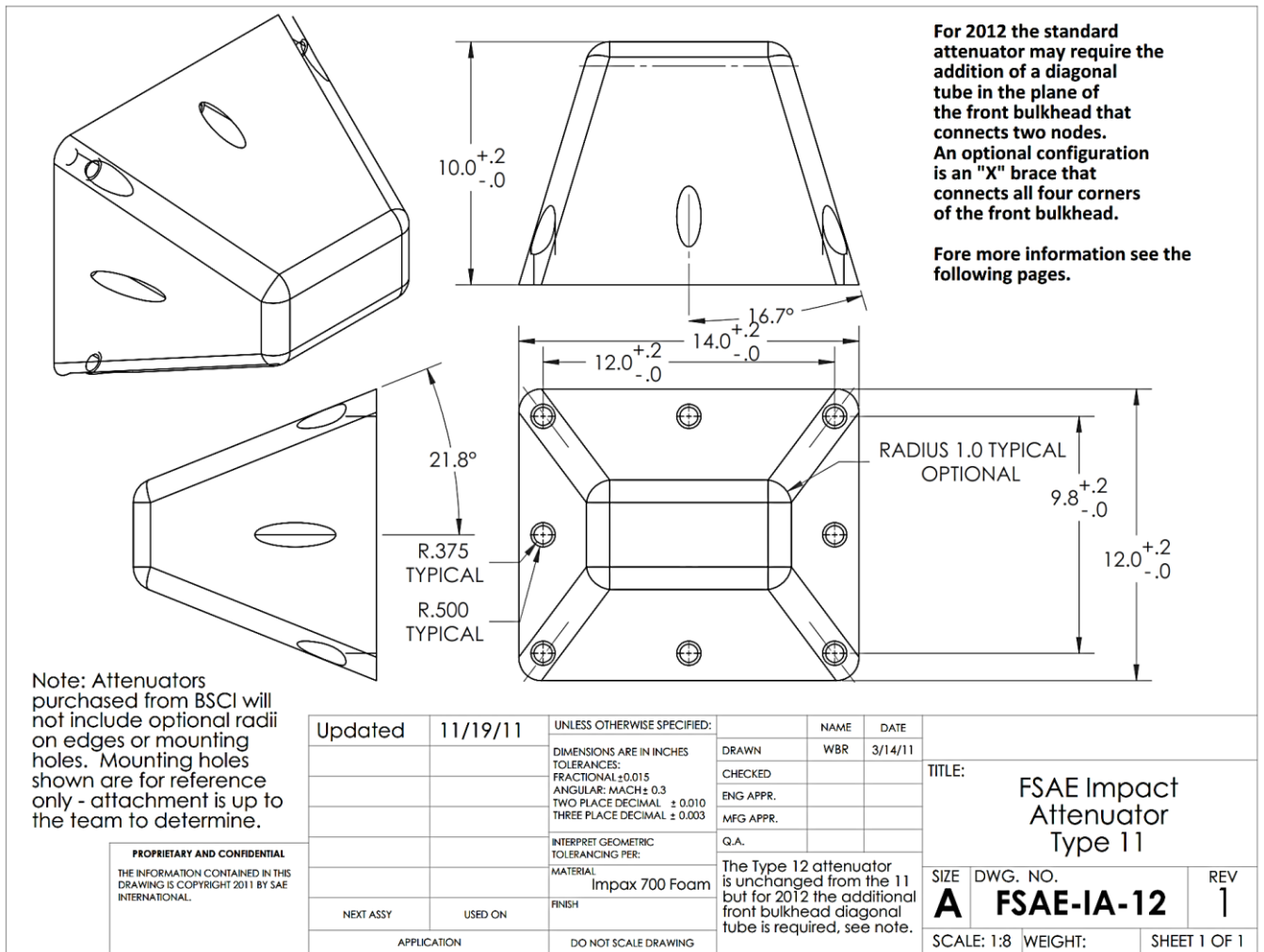


Figure 1.18 Formula SAE Crash Box or Impact Attenuator [2]

### 1.2.5 Overview of Vehicle Crash Box or Impact Attenuator Load Types

The FSAE functional demand for the Impact Attenuator or Crash Box is that: when the device mounted on the front of a vehicle Chassis that is Front Bulkhead with a total mass of 300kg. The average deceleration and peak deceleration should not exceed 20g and 40g respectively where g is the gravitational acceleration [2], [8] and that the modest requirements of an impact at 25.2km/hr. (7m/s) into a solid barrier were met [2], with a total kinetic energy of  $0.5 \times 300 \text{Kg} \times 7 \text{m/sec} = 7350 \text{J}$ .

A rigid barrier fixed in all translational and rotational directions, although the impact attenuator made to translate only in z-direction towards the rigid barrier with an initial velocity of 7m/s and a mass of 300kg attached to it.

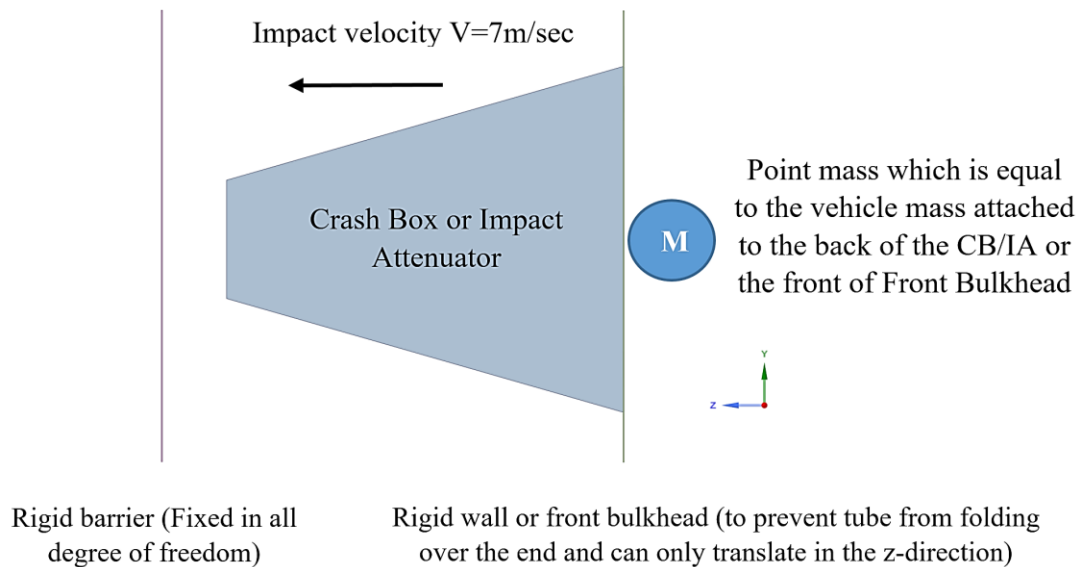


Figure 1.19 Description of load and boundary condition for Crash Box or Impact Attenuator

### 1.3 Motivation

Racing cars anticipated to perform in very high acceleration, braking, handling, aesthetics, ergonomics, manufacturing, and maintenance within minimum manufacturing cost no compromise on driver safety. The weight of the vehicle is one of the big factors, currently in Ethiopia car racing takes place but there is a big question 'How it has been designed?', 'What kind of cars?', and 'How the safety of driver seems?'.

The answer to all these questions is responded by the beneficial design of Formula SAE racing car and which have many components or system, the first and most important part of the Formula SAE vehicle are Chassis and Crash Box or Impact Attenuator, with can stand all kind of loading condition during its mobility with regarded vehicle weight, boundary condition, shape, size, dimensions, efficient energy absorption, safety and comfort to the driver by following a Formula SAE design requirements.

### 1.4 Problem Statement

In Ethiopia in different time and place car racing takes place but almost all the time they use ordinary cars for racing purpose. Because of that, the driver's safety is at risk, driving performance is different from racing car drivers and there is a big technology gap in the design, simulation, and manufacture of the racing car due to that the stiffness, torsional rigidity, and crashworthiness of racing car structure are in danger or at risk. Safety and

performance of Formula SAE Chassis and Crash Box or Impact Attenuator they all affected by the weight, geometry and boundary conditions used in the structure of the vehicle.

## **1.5 Objectives**

### **1.5.1 General Objectives**

The main objectives of this research focused on the structural design and simulation of lightweight Formula SAE racing car based on Society of Automotive Engineering structural requirement with the aim/goal to introduced the Formula SAE Chassis and Crash Box or Impact Attenuator in Ethiopia and also, to reduce the weight, improve the structural geometry and crashworthiness of lightweight Formula SAE Chassis and Crash Box with regard/respect to safety and performance.

### **1.5.2 Specific Objectives**

- ✓ Review and study the existing structure of Formula SAE racing car.
- ✓ Remodel and analyze the Chassis structure and impact attenuator of Formula SAE by using FEA.
- ✓ Check and select appropriate structure material, which is stiff enough to withstand the static (vertical bending, lateral bending, longitudinal, torsional, and horizontal Lozenging), and dynamic loads (crash or impact).
- ✓ Identify which structural members and generate the new Formula SAE Chassis structure.
- ✓ Generate the new Crash Box model from the bioinspired idea.
- ✓ Validate the result according to the Formula SAE rule and regulation.

## **1.6 The scope of the Research**

- ✓ It is only structural design and simulation of lightweight Formula SAE Chassis and Crash Box (Impact Attenuator).
- ✓ Achieve the structural (Chassis and Crash Box) prerequisites of lightweight Formula SAE.
- ✓ Improve the structural geometry of Formula SAE.
- ✓ Structure design of lightweight Formula SAE for static and dynamic loading condition (impact/energy absorption).

## **1.7 Methodology**

There is two way of modeling the space frame structure of the Chassis and Crash Box, which are physical, and software modeling of analysis. The physical model analysis of the

space frame or Crash Box is not recommended because it is not economical therefore the software modeling of the frame structure was performed by seating different approximate boundary conditions by following the SAE rules [14].

Structural design and simulation of lightweight Formula SAE Chassis and Crash Box performed by using SOLIDWORKS modeling, finite element analysis by using ANSYS Workbench and ANSYS Explicit Dynamics. Secondary data collection method which is grazing different published papers, journals, looking up general vehicles frames and visiting the existing automotive company. Finally, Formula SAE chasses and Crash Box design and simulation with appropriate structural material that would have lightweight, better stiffness, and crashworthy properties used.

### **SOLIDWORKS Modeling and Finite Element Analysis by using ANSYS Workbench and ANSYS Explicit Dynamics**

The finite element method (FEM) is a computational technique used to obtain approximate solutions for boundary value problems in engineering [15]. There are different modeling and simulation software to perform the structural design and simulation of lightweight Formula SAE Chassis and Crash Box. SOLIDWORKS software used for creating a three-dimensional model of the space-frame Chassis and Crash Box structure by complying Formula Society of Automotive Engineering rules. In addition, ANSYS Workbench and ANSYS Explicit Dynamics simulation software applied for finite element analysis of the lightweight Formula SAE structure by applying a wide range of boundary conditions.

The following procedures are used [14]:

1. Data collection (Secondary data collection method which is grazing different published papers, journals, looking up general vehicles frames and visiting existing automotive company).
2. By using SOLIDWORKS software, a three-dimensional structure of the Formula SAE Chassis and Crash Box created, by adopting the Formula Society of Automotive Engineering (FSAE) rules.
3. Model generation from SOLIDWORKS to ANSYS Workbench:
  - ✓ Simplifications, idealizations.
  - ✓ Define materials/material properties.
  - ✓ Generate a finite element model (mesh) or meshing software.
4. Solution generation stage:
  - ✓ Specify boundary conditions by following SAE rules and other standard books.
  - ✓ Obtain the solution.

5. Review the results:

- ✓ Plot/list results (stiffens of the Chassis checked (by seeing the total deformation, torsional rigidity, equivalent stress, equivalent elastic strain, and strain energy) and impact load (by examining the energy absorption of the Crash Box for the front impact case by seeing force, acceleration, total energy absorption and displacement with respect to time)).
- ✓ Check the validity comparing with SAE rules.

Note: Figure 1.20 shows how the structure design and simulation of lightweight Formula SAE Chassis and Crash Box is performed by using finite element method steps.

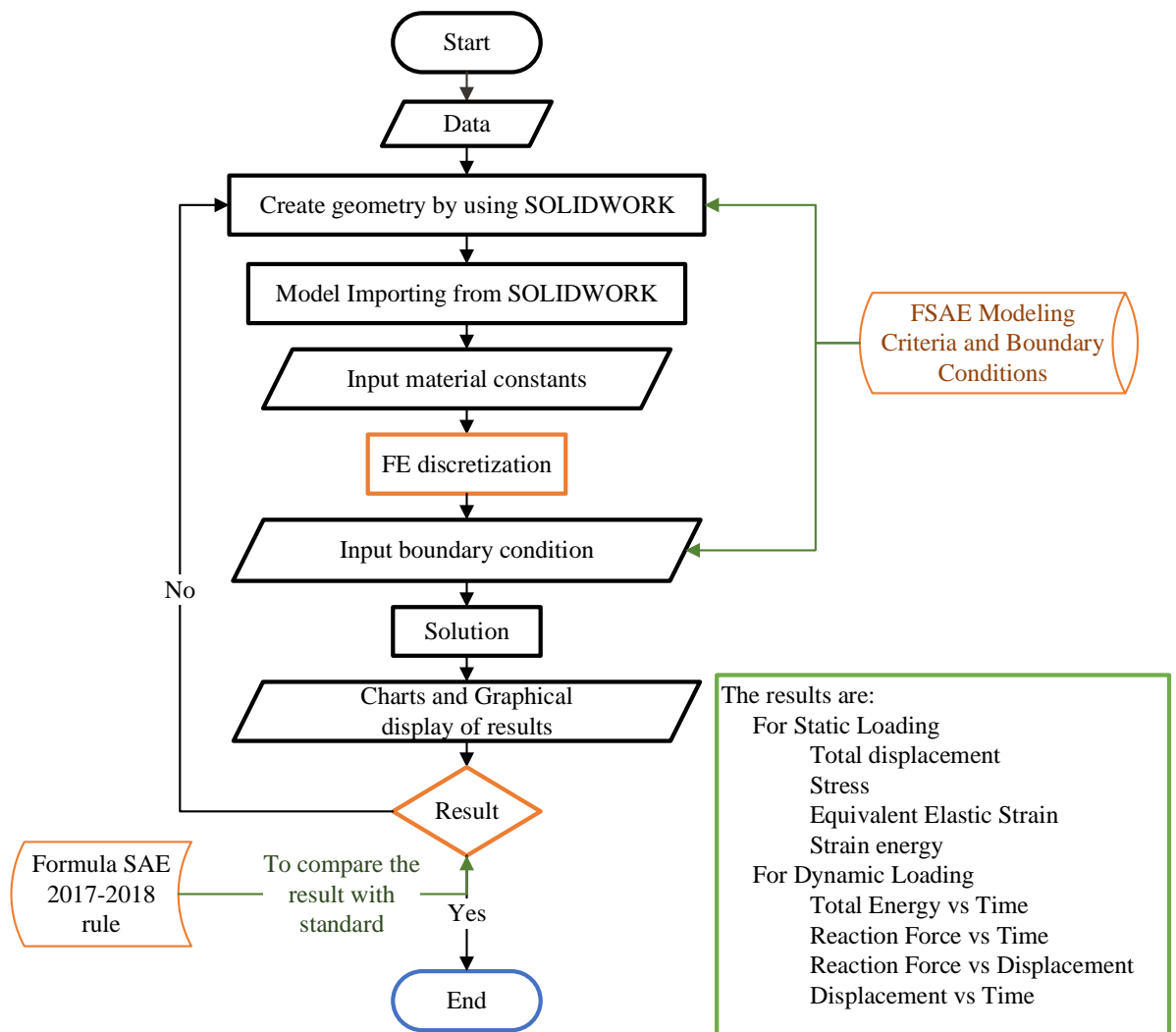


Figure 1.20 Structural design and simulation of lightweight Formula SAE Chassis and Crash Box flow chart

## 1.8 Layout of the Thesis

This “Structural Design and Simulation of Lightweight Formula SAE Racing Car” research paper organized into five chapters:

In **chapter one**, introduction background, statement of the problem, the motivation of the research, objectives, scope, and methodology discussed, other than of Formula SAE Chassis and Crash Box types, loading condition.

In **chapter two**, the survey of literature related to the research investigated, going through journals, articles, publications, and 2017-18 Formula SAE® Rules books for Formula SAE Chassis and Crash Box or impact attenuator.

In **chapter three**, material modeling for Chassis and Crash Box, geometrical modeling, mathematical modeling, finite element modeling and analysis for formula SAE Chassis and Crash Box discussed in detail.

In **chapter four**, the finite element analysis results clearly displayed and discussed in detail for the two Formula SAE Chassis and three Crash Box using different figures, charts, and table.

In **chapter five**, conclusions, recommendations, and future work for “Structural Design and Simulation of Lightweight Formula SAE Racing Car” discussed, concerning weight reduction, geometrical improvement, and another main point.

## CHAPTER 2

### LITERATURE REVIEW

#### 2.1 Previous Works

##### 2.1.1 Previous Works of Formula SAE Chassis

All competitions in the Formula SAE Series may post rule variations specific to the operation of the events in their countries and sponsor by the Society of Automotive Engineers with different collegiate/university student's. However, the vehicle design requirements and restrictions will remain unchanged [2]. Racing cars are expected to perform in very high acceleration, braking, handling, aesthetics, ergonomics, manufacturing, and maintenance within minimum manufacturing cost no compromise on driver safety and weight is one of the big factors [7].

The objectives are to develop a dynamically balanced vehicle to withstand all kind of terrain during its mobility (stresses, vibrations and noise in the different components of its structure), simulate real-world engineering design projects, their related challenges and also vehicle development by following the Formula SAE manual with respect to vehicle weight, boundary condition, shape, size, dimensions, efficient energy consumption, safety, comfort of the driver and economical vehicle frame that will abide by all the Formula SAE design requirements [16].

The Chassis should be strong enough to absorb all kind of energy, these energies created due to front, back, side, rollover in dynamic loading condition and longitudinal torsion, vertical bending, lateral bending, horizontal lozenging, combined in static loading condition be distributed progressively [2], [4], [15], [17]. The Formula SAE rule book provided the detail description of the material which is used while the design of the vehicle Chassis these has extended the structure strength and module the design [4].

During designing of Chassis for main section or components, it should be looked upon for the front roll hoop, main roll hoop, front bulkhead, rear bulkhead, ground clearance, wheel center lines, and side impact structures, by taking considerations of engine mounting points the position of main roll hoop has been fixed and position. Adequate space should give to the engine, drivetrain components, maximum space was given to cockpit area for better comfort with the help of Formula SAE rulebook, the cockpit area was settled and with tolerance to 5th percentile female to 95th percentile male [2], [15], [18].

The roll cage is a tabular or space frame design of Formula SAE Chassis consists of the rectangular and circular cross-section area of the material, with minimum welds on the frame pipes and maximum bends ensuring better strength and less cost of production of the vehicle. The roll cage must be constructed of steel tubing, with a minimum size of the steel tube should not be less than 25.4mmx2.41mm and strength requirements dictated by Formula SAE rule [2], [19]. The frame developed by using O section type pipe has strength and rigidity than any other section such as I, T and C. The theory of the bending and torsion explains that circular section is always perfect to resist the twisting and the rolling effects [16].

The material property of the Chassis plays an important role while designing and manufacturing the car Chassis but it depended on the types of Chassis and loading condition [16]. Some of the material used for the Formula SAE space frame Chassis structure is with the following mechanical material property.

AISI 1018 (Ultimate tensile strength 440MPa, Carbon content 0.18%, Modulus of Elasticity 210GPa, Brinell hardness 120, strength to weight ratio at yield 38kN-m/kg, Poisson's ratio 0.29, thermal conductivity (ambient) 42W-m/K and 19% Elongation and density 7860 Kg/m<sup>3</sup>) [4], [17], [20], [21].

Steel grade SI3074 with Young's modulus 200GPa, Poisson ratio 0.266, density 7860kg/m<sup>3</sup> and yield strength 373MPa with the internal energy, total kinetic energy, and rigid wall force Steel IS grade 3074 has better energy absorbing capabilities for tubular space frame by providing a driver safety in front and side crash) [12], [7], mild steel (Density 7800Kg/m<sup>3</sup>, UTS 400MPa, Yield strength 300MPa, Young's Modulus 207GPa, Poisson's ratio 0.3 and Plastic strain at UTS 0.35 with ) [22].

AISI 4130 steel (density 7850 kg/m<sup>3</sup>, Young's modulus 205GPa, Poisson's ratio 0.285 and yield strength 460MPa) [15], Chromoly 4130 (density 7.8g/cm<sup>3</sup>, thermal conductivity 42.7W/m-K, strength to weight ratio 72-133KN-m/Kg, Brinell Hardness 217, Elastic Modulus 190-210GPa, Yield Strength 480MPa and Ultimate Strength 590MPa with lighter weight and higher strength to weight ratio) and SAE-AISI 1018 (density 7.8g/cm<sup>3</sup>, thermal conductivity 51.9W/m-K, strength to weight ratio 55-60KN-m/Kg, Brinell Hardness 126, Elastic Modulus 205GPa, Yield Strength 370MPa and Ultimate Strength 440MPa) [16].

The materials (Steel S355, Steel S255, and Aluminum Alloy 5082T6) have the advantage of solving the overweight problem with good mechanical properties, cost-effective, anti-corrosion, good energy absorption and quite hard for bending can be created to have the same strength as stainless steel [20]. AISI 1020 Steel with the following material propriety Density 7.7 to 8.3\*1000 Kg/m<sup>3</sup>, Poisson's ratio 0.27-0.29, Elastic Modulus 190-210GPa,

Tensile Strength 394.7MPa, Yield Strength 294.8MPa, and Hardness 111HB) [23]. As known that Steel grade IS3074, Aluminum alloy 6082T6, and Steel S275 are a lightweight material, good mechanical properties, cost-effective, anti-corrosion, good energy absorption and quite hard for bending can be created to have the same strength as stainless steel [19].

After creating a three-dimensional model and choosing appropriate simulation software side by side the next step is to identify a different kind of boundary condition applied on the FSAE Chassis based on the type of loading conditions. These loading conditions are on the rule stated in FSAE and other vehicle Chassis design books with the assumption to approach the real-world consideration because of a complex of a real-world situation and to simplify the problem. These assumptions are the tires are considered as linear springs and the mass of the engine, gearbox and the other components are lumped at exactly placed at the center of gravity location of nodes [13]. The basic types of the load applied on the FSAE Chassis are static and dynamic loading type:

### **Static loading type**

To estimate the various load which are acting on the vehicle FSAE structure are estimate according to the center of gravity of the vehicle and these loads act as a manner of driver 100Kg [15] or 75Kg [17], Engine 80Kg [15] or 70Kg [17], Driver train 20Kg, Chassis 80Kg, Battery 4Kg [15] or 3Kg [17], Steering 10kg [15] or 13Kg [17] and also by consideration of various masses such as the wishbone (front & rear), radiator, petrol tank etc. then the weight of the car is considered to be approximately 285Kg [17] to 300Kg [2].

The Formula SAE vehicle frame model is a uniaxial element with tension-compression, torsion, and bending capabilities and has six degrees of freedom at two nodes: three translations in the nodal x, y, and z directions and three rotations about the nodal x, y, and z-axes is used in the pre-processing steps [16].

The basic static load applied on the Chassis are Longitudinal Torsion, Vertical Bending, Lateral Bending, and Horizontal Lozening and also was design to withstand such a load 3.5g bump, 1.5g breaking, 1.5g lateral [15], [17] and 4g load on the main hoop [17] with all the mass seat on the Formula SAE frame structure of the Chassis to see the real scenario occurred on it.

- a. Vertical bending analysis:** both wheels on the front axle of the vehicle encounter a symmetrical bump simultaneously [3] and this applies a bending moment to the vehicle about a lateral axis and all the weight are considered [17].
- b. Longitudinal torsional analysis:** (a force experienced at the wheel center is to be 1000N the load is applied on each side of the front suspension hard points in a couple

from opposite to each other in direction one in up and the other down) [17] or 2500 Nm/degree of torsional loading after fixing the two back side suspension connecting point fixed [17].

- c. Lateral bending:** are induced in the frame for various reasons, sliding of tires (cornering), Kerb nudge or overturning and the sideways forces will act along the length of the car and will be resisted at the tires with a magnitude of 1.5g, this causes a lateral load and resultant bending [3].
- d. Horizontal Lozenging:** Forward and backward forces applied at opposite wheels cause this deformation. These forces caused by vertical variations in the pavement or the reaction from the road driving the car forward. These forces tend to distort the frame into a parallelogram shape [13] with a magnitude of 3.5g [15], [17].
- e. Combined loading:** due to the combination of pure bending and pure torsional load case [2].

#### **Dynamic loading type**

In this case, there is a change in force through time and material deformation take place due to the impact energy created by Formula SAE car velocity from a different side (front, side, and rollover) of the structure. The boundary conditions applied are:

- a. Font impact:** in the front impact scenario the following load (120kN, 0kN, 0kN) applied in the actual attachment points between the impact attenuator and the front bulkhead, with a fixed displacement (x, y, z) but not rotation of the bottom nodes of both sides of the main roll hoop and both locations where the main hoop and shoulder harness tube connect a maximum allowable deflection of 25mm and no failure must occur anywhere in structure [2], [16].
- b. Side impact:** the load applied is (0N, 7.0kN, 0N) with the following application point in the actual attachment points between the front roll and main roll hoop and fixed to the bottom nodes of both sides of the main. Fixed displacement (x, y, z) but not the rotation of the bottom nodes of both sides of the front and main roll hoops with a maximum allowable deflection of 25 mm and failure must not occur anywhere in structure [2], [16].
- c. Rollover impact:** in the main roll hoop, bracing and bracing support the following load applied (6.0kN, 5.0kN, -9.0kN) on top of main roll hoop and fixed displacement (x, y, z) but not rotation of the bottom nodes of both sides of the front and main roll hoops, with maximum allowable deflection of 25mm and no failure, must occur anywhere in structure [2], [16] and in the front roll hoops, the following load applied is (6.0kN, 5.0kN, -9.0kN) on the top of front roll hoop and fixed displacement (x, y, z) but not rotation of the bottom

nodes of both sides of the front and main roll hoops, with a maximum allowable deflection of 25mm and no failure must occur anywhere in structure [2], [16].

Before the numerical, analytical simulation and manufacturing of the FSAE Chassis take place the three-dimensional modeling take place by following the FSAE rule book and standard, different type of software used such as SOLIDWORKS, Catia, Auto CAD, Space Claim in ANSYS and with appropriate thickness, weldment, cross-sectional area and so on [5], [7], [19]–[22], [24].

The Formula SAE Chassis should be strong enough to absorb the energy when dynamic loads (impact (front, roll over and side)) and static loads (see section 1.2.3) compelled therefore to predicate the future senior encountered on the frame structure and to mitigate or reduced the disaster occurred in driver there are different type of software used for numerical analysis of finite element method of the frame structure depending on the type of boundary condition applied, these are ANSYS Workbench (Static Structure and Explicit Dynamics), Hyper-mesh, Ls-Dyna, Hyper Works, Abaqus, CATIA, and SOLIDWORKS. When the frame structure imported in a different format as a beam, shell element with different thickness, cross-section area, and material property stated in FSAE rule books [5], [7], [19]–[22], [24].

### **2.1.2 Previous Works of Crash Box or Impact Attenuator**

An Impact Attenuator, which is also known as a crash cushion or crash attenuator, is a device that used to reduce the damage done to the structures, vehicles, and driver resulting from a motor vehicle collision. Crash Box designed to absorb the vehicle's kinetic energy in the form of an even manner deformation. If the uneven manner of deformation takes place, then the driver might suffer from low to high injury by experiencing spikes in g's [19].

The material property of the Crash Box plays an important role while designing and manufacturing the car Crash Box but it depended on the types of CB/IA and loading condition [16]. The material used for the Formula SAE CB/IA structure is carbon fiber/epoxy skin laminates, aluminum Nomex honeycomb core [18] and Aluminum (Aluminum alloy AA2028A [25], Aluminum 7075-T651 [26] and etc.).

Aluminum has the following property comparing to Steel, the density of Aluminum approximately less than three times of density of Steel, this means the mass of aluminum is three times lighter than Steel this will reduce the Crash Box weight by three times than Steel. Modulus of elasticity of Aluminum is three times less than that of Steel, which will improve the flexibility of the Crash Box by three times for Aluminum as the Crash Box needed, which

means the aluminum Crash Box will absorb maximum amount of energy by maximum deformation, that is why Aluminum has low stiffness, high weight-stiffness ratio and widely used in energy absorbing components [25].

Before the numerical, analytical simulation and manufacturing of the FSAE Crash Box or Impact Attenuator take place the three-dimensional modeling, take place by following the FSAE rule. The modeling software used is SOLIDWORKS, Catia, Auto CAD, Space Claim in ANSYS and with an appropriate thickness, weldment. The Formula SAE Crash Box should be strong and flexible enough to absorb the energy when impact load compelled. Therefore, to predicate the future senior encountered on the Crash Box and to mitigate or reduced the disaster occurred in the driver and reduced the maintenance cost of other parts [19], [25].

The front Crash Box of Formula SAE racing car absorbed the kinetic energy created by the speed of the car. The speed of the car affected by the area of lightweight material and the aerodynamic effect of the front Crash Box design and Therefore a nose cone geometry is used [2], [18]. There are different types FEM software such as ANSYS Workbench Explicit Dynamics, Hyper-mesh, Ls-Dyna, Hyper Works, Abaqus and imported in different format use shell element with different thickness and geometry [19], [25].

The finite element analysis (FEA) of the front Crash Box structural analysis is performed explicitly with solver FEM software with laminated composite material model with the total weight of the vehicle and dummy 300Kg, friction contact between the impact structure and rigid wall (sliding energy) and impact velocity of 7m/s (23.0 ft/sec) the velocity obviously is much lower than typical race track speed, but before a racing car frontally strikes a rigid wall its speed is usually reduced by gravel run-off area and the deformation tire barriers [2], [18] and expected to decelerate at a rate not exceeding 20 g's average and 40 g's peak [2].

After performing of the numerical simulation of FEA simulation the energy absorption of the front Crash Box structure was compared with the crash test results (displacement (mm) Vs. Deceleration (g)) and the initial kinetic energy absorbed by the Crash Box material, deformation and Force vs time [2], [18].

## **2.2 Summary of the Previses Works on the Frame Structure and Crash Box**

The performance and safety of Formula SAE affected by the design of Chassis and impact attenuator more information and research are needed on these research papers with regard to [5], [7], [19]–[22], [24]:

- ✓ Masses, centers of gravity, and inertia tensors of the engine, radiator, gearbox and other important parts or boundary conditions used.

- ✓ Appropriate structural geometry, material, and reduction of weight of the Chassis with better crash worthiness property.
- ✓ Modeling and simulation software used in the design and analysis purpose for the Chassis and Crash Box.
- ✓ When the Crash Box design it needs additional materials, holes, etc. to increase energy absorption by stabilizing the crush pattern and bettering the collapse of the tube.
- ✓ Strain rate effect ignored in the analyses which cause another structural failure in the Crash Box when impact scenario take place.
- ✓ Test like the CFD, Chassis Balancing, Thermal Heating, Heat Treatment etc. can be carried out on various manufacturing and stimulation software's that can result in a more specific, sophisticated, and detailed inquiry or analysis of the created Formulae-1 and Formula SAE Module.
- ✓ The numbers of permutations in which triangulations can do and the Chassis can design are infinite and one can try and optimize the Chassis design by further reducing the weight.

## CHAPTER 3

### MATERIALS SELECTION, CONDITIONS, AND METHODS

#### 3.1 Materials Selection

These mechanical and physical properties are very important for the selection of the material for the frame structure of the Chassis and Crash Box (Impact Attenuator): such as Ultimate tensile strength, yield tensile strength, Modules of elasticity, Bulk modulus, Shear modulus, Poisson ratio, the percentage of elongation at break and density.

##### 3.1.1 Material Selection for Formula SAE Chassis

###### Number of positive decisions for Formula SAE Chassis Material Selection

The basic methods of selection of materials are the cost per unit property and digital logic method (DLM). These properties have their own way of selecting of material, (1) DLM consider based on the following parameters, these are density, yield tensile strength, ultimate tensile strength, module of elasticity and Poisson's ratio and (2) Cost per unit property consider selection of material according to the material strength property [24], [27].

The digital logic method (DLM) used to select the material used for the Formula SAE Chassis. Based on that the DLM use multipoint of view, these are density, yield tensile strength, ultimate tensile strength, module of elasticity and Poisson's ratio to select the material used for the Chassis by following the following steps and the five positive decisions values have a great impact on the Chassis structure associated with regard to weight, strength, and safety of the driver [24], [27].

###### Number of Positive Decisions (PD)

Density, Ultimate tensile strength, yield tensile strength, Modulus of elasticity and Poisson's ratio, are a factor applied in the selection of optimal material for Formula SAE Chassis. The number of possible decisions depends upon the number of properties. The number of properties is five ( $n = 5$ ). The number of possible decisions calculated by equation 1:

$$N = \frac{n(n - 1)}{2} \quad (1)$$

Therefore; the number of possible decisions,  $N = \frac{5(5-1)}{2} = 10$

In comparing two properties, the more important properties given the number 1 and the less important given as 0. The number 1 through 10 shows that the importunateness and

rank of the material property when value 1 has a larger ranking and 10 has less rank in the material property. The properties and decision numbers listed in Table 1.

Table 1 Evaluation of Positive Decisions for Formula SAE Chassis

Material Properties	Decision Numbers										Positive Decisions (PD)
	1	2	3	4	5	6	7	8	9	10	
Density	1	0	1	0	0	0	1	0	0	0	3
Ultimate tensile strength	0	1	0	1	0	0	0	0	0	0	2
Yield tensile strength	0	0	1	0	0	1	0	0	0	0	2
Modulus of elasticity	1	0	0	1	0	0	0	0	0	0	2
Poisson's ratio	0	0	0	0	0	0	1	0	0	0	1
Total Numbers Decision (N)											10

### Weighting Factor ( $\alpha$ ) Analysis

The weighting factor obtained from the positive decision Table 1, in which each of the properties is compared to each another. A weighting factor for each property is obtained by dividing the number of positive decisions (PD) for each property into the total number of possible decisions (N) as seen in equation 2 [24], [27].

$$\text{Mathematically, } \alpha = \frac{PD}{N} \tag{2}$$

Table 2 Evaluation of weighting factor for Formula SAE Chassis

Material Properties	Positive Decisions (PD)	Weighting Factor ( $\alpha = \frac{PD}{N}$ )
Density	3	0.3
Ultimate tensile strength	2	0.2
Yield tensile strength	2	0.2
Modulus of elasticity	3	0.2
Poisson's ratio	1	0.1
Total(N)	10	1.0

### Scaled Property Value

To calculate the scaled property value (see equation 3 and equation 4) the following points are needed, beneficial (where higher value is required) and non-beneficial (where a lower value is required) attributes. For the evaluation of the scaled property, materials with

a higher module of elasticity, ultimate tensile strength and yield tensile strength are beneficial and highest value rated as 100 and yield tensile strength, Poisson's ratio, and density are not-beneficial for Formula SAE Chassis, therefore, their lowest value is considered as 100. Scaled property values are calculated using equation [24], [27]:

$$\text{For beneficial; scaled property value} = \frac{\text{Numerical value of property}}{\text{Maximum value in the list}} * 100\% \quad (3)$$

$$\text{For non-beneficial; scaled property value} = \frac{\text{Minimum value in the list}}{\text{Numerical value of the property}} * 100\% \quad (4)$$

**Note:** The following material selected from different journals, research papers, and selected as number one candidate material.

Table 3 Properties of candidate materials for Formula SAE Chassis [20], [28], [29], [30]

Material	Number of properties				
	1	2	3	4	5
	Density, Kg/m <sup>3</sup>	Ultimate tensile strength, MPa	Yield tensile strength, MPa	Modulus of elasticity, GPa	Poisson's ratio
SAE 1018 Steel	7800	420	360	210	0.29
AISI 4130 Steel	7800	440	460	205	0.285
IS 3074 Steel	7860	313.8	373	200	0.266
Steel S355	7850	470	355	195	0.3
Steel S275	7800	370	275	200	0.3

The higher value of ultimate tensile strength, yield tensile strength, and moduli of elasticity are 470MPa, 460MPa & 210GPa. The lowest value for density and Poisson's ratio is 7800Kg/m<sup>3</sup> and 0.266. After seating in the above values in the above equation 3 and equation 4 the scaled property evaluated:

Table 4 Scaled property of candidate materials for Formula SAE Chassis

Material	Number of properties				
	1	2	3	4	5
SAE 1018 Steel	100	89.4	78.3	100	88.9
AISI 4130 Steel	100	93.6	100	97.6	93.4
IS 3074 Steel	99.2	66.8	81.1	95.2	100
Steel S355	99.4	100	77.2	92.8	88.7
Steel S275	100	78.7	59.8	95.2	88.7

### Performance Index

Performance index ( $\gamma$ ) used in the ranking of the material based on their values and calculated by using equation 5. The performance index analyzed by summing up the values of the weighting factor and the scaled property values for all relevant properties. Then the performance indices become [24], [27]:

$$\gamma = \sum_i^n \alpha_i \beta_i \quad (5)$$

Table 5 Performance index ( $\gamma$ ) of candidate materials for Formula SAE Chassis

Material	Weighting Factor ( $\alpha$ ) x Scaled property ( $\beta$ )					Performance Index, $\gamma = \sum_i^n \alpha_i \beta_i$
	1	2	3	4	5	
SAE 1018 Steel	30	17.88	15.66	20	8.89	92.43
AISI 4130 Steel	30	17.72	20	19.52	9.34	97.58
IS 3074 Steel	29.76	13.36	16.22	19.04	10	88.38
Steel S355	29.82	20	15.44	18.56	8.87	92.69
Steel S275	30	15.7	11.96	19.04	8.87	85.61

### A Figure of Merit (FOM)

The performance index evaluated in the above indicates that the material selection by considering the material strength property without considering the material cost. It is important to consider the cost of material before making any final decision. However, if there are so many mechanical properties to be considered, the cost of material considered separately to modify the material performance index ( $\gamma$ ). Therefore, by considering the

market price of the material other than the density and, the figure of merit (FOM) become by using equation 6 [24], [27],

$$\text{FOM} = \frac{\gamma}{C_t \rho} \quad (6)$$

Where:  $\gamma$  - Performance index,

$C_t$  is Total cost of the material/unit weight,

$\rho$  - Density of the material

Table 6 FOM of candidate materials for Formula SAE Chassis

Material	$C_t$ (US \$/Kg)	$\rho$ (Kg/m <sup>3</sup> )	$\gamma$	$\text{FOM} = \frac{\gamma}{C_t \rho}$
SAE 1018 Steel	0.57	7800	92.43	0.020789474
AISI 4130 Steel	0.88	7800	97.58	0.0142162
IS 3074 Steel	1.26	7860	88.38	0.008924028
Steel S355	0.6	7850	92.69	0.019679406
Steel S275	0.55	7800	85.61	0.019955711

## Ranking

Different mechanical and physical properties with respect to the cost of the material combined to select the suitable material for the Formula SAE Chassis. Therefore, the material that was having higher numerical value will have more influence than lower value by its weighting factor. The ranking of the material with respect to figure of merit (FOM) evaluated from the performance indices ( $\gamma$ ), total cost of the material per unit weight ( $C_t$ ) and density of the material ( $\rho$ ) values and the ranking take place based on the material FOM descending order as seen in Figure 3.1 [24], [27].

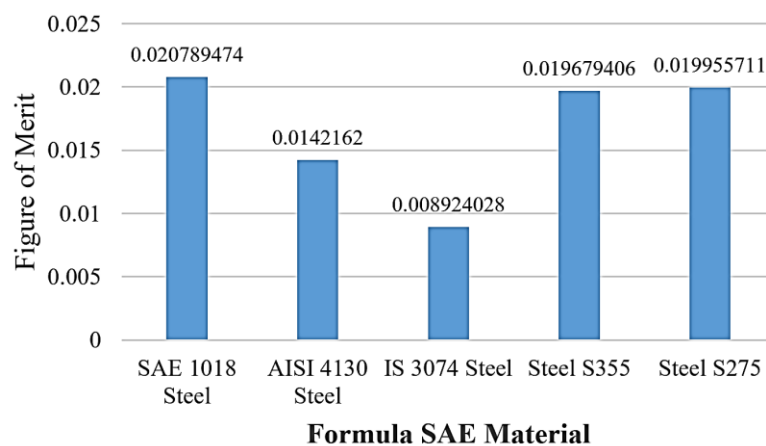


Figure 3.1 Figure of merit (FOM) for the selected material

Table 7 Ranking of candidate material for Formula SAE Chassis

Material	Ct (US \$/Kg)	$\rho$ (Kg/m <sup>3</sup> )	$\gamma$	FOM = $\frac{\gamma}{C_t \rho}$	Ranking
SAE 1018 Steel	0.62	7800	92.43	0.020789474	1
AISI 4130 Steel	0.88	7800	97.58	0.0142162	5
IS 3074 Steel	1.26	7860	88.38	0.008924028	4
Steel S355	0.6	7850	92.69	0.019679406	3
Steel S275	0.55	7800	85.61	0.019955711	2

From the above Table 7 and Figure 3.1 shows that SAE 1018 Steel has the higher value of the figure of merit, which indicated it has a less total cost of the material per unit weight, approximately have less material density and third performance index value. Therefore SAE 1018 Steel has a larger figure of merit and used for the Formula SAE Chassis structure with the following mechanical property as shown in Table 8.

Table 8 Revision of property of SAE 1018 Steel [29]

Material Property	SAE 1018 Steel
Density, Kg/m <sup>3</sup>	7800
Ultimate tensile strength, MPa	420
Yield tensile strength, MPa	360
Modulus of elasticity, GPa	210
Bulk modulus, GPa	166.7
Shear modulus, GPa	81.395
Poisson's ratio	0.29
Elongation at break	19 %
Cost (US \$/Kg)	0.57
Brinell hardness	120
Carbone content	18%
Strength to weight ratio at yield, kN-m/kg	38
Thermal conductivity (ambient), W-m/K	42

### 3.1.1 Material Selection for Crash Box or Impact Attenuator

Aluminum used for the Crash Box because, the density of Aluminum approximately less than three times of density of Steel, this means the mass of aluminum is three times lighter than Steel, it will reduce the Crash Box weight by three times than Steel. Modulus of elasticity of Aluminum is three times less than that of Steel, this directly affects the flexibility of the Crash Box by three times for Aluminum as the Crash Box needed and it can absorb maximum amount of energy by maximum deformation, that is why Aluminum has low stiffness so it has high weight- stiffness ratio [25].

And comparing to carbon fiber reinforced composite material to Aluminum both are safe, light, stiff and bodywork with better adaptability of change in circumstances, but in carbon fiber reinforced composite material has a high cost of production and need advanced manufacturing technology [2], [3].

There are different criteria to describe the material property when crash or impact scenario take place. According to these criteria's the material property when impact scenario take place is beyond the elastic limit, different and have a high amount of kinetic energy will be generated, therefore the energy will be converted to another form of Energy's (deformation, sound, heat, and friction energy). According to Johnson-Cook strength and failure model that predict/anticipate more accurate result focusing on these energies created [26], [31], [32].

#### Johnson-Cook strength and failure models

Aluminum 7075-T651 plate used for the Crash Box or Impact Attenuate. According to Johnson-Cook strength and failure models, the material must satisfy the criteria to absorb the energy that will be generated due to impact velocity, therefore the kinetic energy generated due to impact will be converted to deformation, sound, heat, and friction energy. Plasticity and failure model Johnson and Cook (1985) proposed that the material is loaded with shock and impact the environment in the plastic range the following factors include large strains, large strain rates, high pressures and high temperatures [26].

According to Johnson-Cook strength and failure models, there are different constants which predicate the energy absorption propriety of the material. Therefore, to fined theses constants the following procedure followed. A schematic experimental set up of the Aluminum 7075-T651 plate considered is shown in Figure 3.2 and the plate clamped around its periphery and a cylindrical punch with spherical nose and attached to a relatively mass, impact velocity of the mass,  $V_0$  with the plate. The prediction of the velocity threshold

between impact with penetration and without penetration of the plate. The tests specimen dimensions are  $D=171.45\text{mm}$  and  $t=12.7\text{mm}$ , while the punch had a diameter  $d=12.7\text{mm}$  and mass was  $138.8\text{Kg}$  as seen in Figure 3.2 [26].

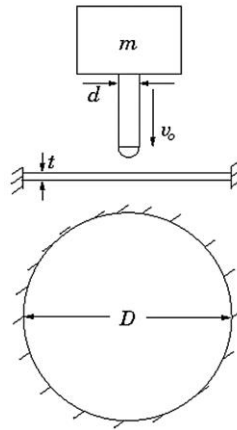


Figure 3.2 Schematic of the problem of the normal impact of a circular plate by a cylindrical punch with a hemispherical nose [26]

### Basics of the Johnson-Cook Strength Model

The expression for the equivalent stress-plastic strain ( $\sigma_e - \varepsilon_e^p$ ) the curve of the material depends on the current plastic strain rate and the temperature. Therefore these parameters are decomposed in a multiplicative manner as seen in equation 7 [26]:

$$\sigma_e = [A + B(\varepsilon_e^p)^n] \left[ 1 + C \ln \left( \frac{\dot{\varepsilon}_e^p}{\dot{\varepsilon}_{e0}^p} \right) \right] [1 - \check{T}^m] \quad (7)$$

$$\check{T} = \frac{T - T_r}{T_m - T_r} \quad (8)$$

Here,  $\dot{\varepsilon}_e^p$  = Reference strain rate,

A - Elastic limit or Initial yield stress,

B – Modulus of strain hardening or hardening constant,

C – Strain rate sensitivity index/constant,

n – Exponent of strain hardening,

m – Exponent of thermal weakening,

$\dot{\varepsilon}$  - The non-dimensional speed of plastic strain,

$\varepsilon$  - Equivalent plastic strain,

$\check{T}$  - Homological temperature,

T - Current temperature,

$T_r$  - Reference (usual room temperature),

$T_m$  - Melting temperature.

Finally, the five parameters A, B, C, n, m are approximated to match material test data obtained from experiment (quasi-static, dynamic conditions and as well as at temperature are needed to fit this model) [26].

### Failure Models

The failure model is also constructed using a multiplicative decomposition of the effect of triaxiality, which is the ratio of the mean hydrostatic stress to the equivalent stress ( $\eta = \sigma_m / \epsilon_e$ ), strain rate and temperature on the equivalent plastic strain at failure as seen in equation 9 [26]:

$$\epsilon_{ef}^p = [d_1 + d_2 e^{d_3 \eta}] \left[ 1 + d_4 \ln \left( \frac{\dot{\epsilon}_e^p}{\dot{\epsilon}_{e0}^p} \right) \right] [1 - d_5 \hat{T}] \quad (9)$$

Here  $d_1 - d_5$  adjusted to best represent the experimentally obtained material failure data on dependent of the equivalent plastic strain at failure on triaxiality has an exponential form, as suggested by Rice and Tracey (1969) for the enlargement of spherical voids. Since the triaxiality, strain rate and temperature at a material point can change during the loading history, a cumulative damage variable is defined as [26]:

$$\bar{D} = \int \frac{d\hat{\epsilon}_e^p}{\hat{\epsilon}_e^p \left( \frac{\eta, \dot{\epsilon}_e^p}{\dot{\epsilon}_e^p, \hat{T}} \right)} \quad (10)$$

With failure occurring when  $\bar{D} = 1$

To calculate the temperature, rise in the material generated in response to plastic deformation and calculated on the assumption of adiabatic heating. It assumed that the impact event is so fast that enough time is not available to conduct heat away from the regions with large plastic deformation. Under these conditions, the rise of temperature  $\Delta T = T - T_r$  is directly related to the plastic work done at a material point by using equation 11 [33]:

$$\Delta T = \frac{\beta W^p}{\rho C_p} \quad (11)$$

Where  $\beta$  - Represents the fraction of plastic work that is converted into heat,

$\rho$  - Density of the material and

$C_p$  - Heat capacity of the material.

The parameter  $\beta$  is generally taken to be a constant in the order of 0.90 to 0.95, but it can depend on strain and strain rate and assuming constant values in the order of 0.90 to 0.95 is a good approximation, especially as the strains become larger [33].

### Calibration of the Johnson-Cook model Parameters

The data presented provides information that allows the determination of the parameters of the Johnson-Cook model for the Al 7075-T651 material of the plate specimens used in the impact tests. The material used for the Crash Box have the following property  $\rho = 2810 \text{ kg/m}^3$ ,  $CP = 960 \text{ J/(kg K)}$ ,  $T_m = 750\text{K}$  (1350OR),  $T_r = 293 \text{ K}$  (527OR) and  $\dot{\epsilon}_e^p = 0.00016 \text{ 1/s}$  from the Aerospace Specification Metal website [26].

(asm.matweb.com/search/SpecificMaterial.asp?bassnum=MA7075T6).

From the quasi-static uniaxial tension test at room temperature to evaluate the coefficient of  $A=517\text{MPa}$ ,  $B=405\text{MPa}$  and  $n=0.41$  from the stress-strain curve, by using high temperature test the value of  $m$  was determined and picked to match the experimental result by considering the temperature generated at the time interval and the stress induced in the material, Therefore  $m=1.1$ . And finally, to calibrate the constant  $C$  in the strength model, a first estimate made based on the ratio of the flow stresses in the quasi-static and dynamic tests. Therefore it becomes  $C=0.0075$  from the stress-strain curves of the predictions and test results [26].

A summary of all the parameters that including the material model is shown in Table 9:

Table 9 Aluminum 7075-T651 reports for Formula SAE Crash Box material by using Johnson-Cook model Parameters [26]

Strength Model Parameters		Failure Model Parameters	
Elastic limit or Initial yield stress, A	517MPa	D1	0.025
Modulus of strain hardening or hardening constant, B	405MPa	D2	0.15
Strain rate sensitivity index/constant, C	0.0075	D3	-1.5
Exponent of strain hardening, n	0.41	D4	-0.039
Exponent of thermal weakening, m	1.1	D5	8.0
Other Parameters		Thermal parameters	
Density, $\rho$	2810 Kg/m <sup>3</sup>	Heat capacity of the material, $C_p$	960 J/(Kg-K)
Reference strain rate, $\dot{\epsilon}_e^p$	0.00016/s	Melting temperature, $T_m$	750K
Young's Modulus, E	71.7GPa	Reference (usual room temperature), $T_r$	293K
Poisson's ratio, $\nu$	0.33	$\beta$	0.95

## 3.2 Modeling

### 3.2.1 Geometrical Modeling

#### 3.2.1.1 Geometrical Modeling for Formula SAE Chassis

##### 3.2.1.1.1 Selection of Chassis and Pipe Cross-sectional Area

As stated in the above (section 1.2.2) there are different type of Chassis structure but, the **triangulated tube** or **space frame Chassis** was selected because of many high-end sports cars have been designed with a space frame Chassis structure due to the following major advantages and as Formula SAE rule stated [2], [11], [21]:

- ✓ It gives in weight reduction while maintaining its rigidity.
- ✓ Avoid long unsupported and no-load carrying members, members which have an excessively high length/cross-section ratio.
- ✓ The only forces acting on the Chassis joints are tension and compression comparing to the bending load crated in the Chassis structure with proper triangulation of the space frame structure.
- ✓ Less cost of production and maintenances.
- ✓ Easy to reaper or maintenances.
- ✓ The frame developed by using O section type pipe, which has high strength and rigidity than any other section such as I, T and C.
- ✓ The theory of the bending and torsion explains that circular section is always perfect to resist the twisting and the rolling effects.

##### 3.2.1.1.2 Driver Ergonomics

The vehicle must accommodate drivers whose height ranges from 5th percentile female to 95th percentile male and must satisfy the requirements of the Formula SAE Rules. Detailed anthropometric data for the 5th percentile female and 95th percentile male in the following Figure 3.3 from a side view with the following dimensions [2]:

- ✓ A circle of diameter 200 mm will represent the hips and buttocks.
- ✓ A circle of diameter 200 mm will represent the shoulder/cervical region.
- ✓ A circle of diameter 300 mm will represent the head (with helmet).
- ✓ A straight line measuring 490 mm will connect the centers of the two 200 mm circles.

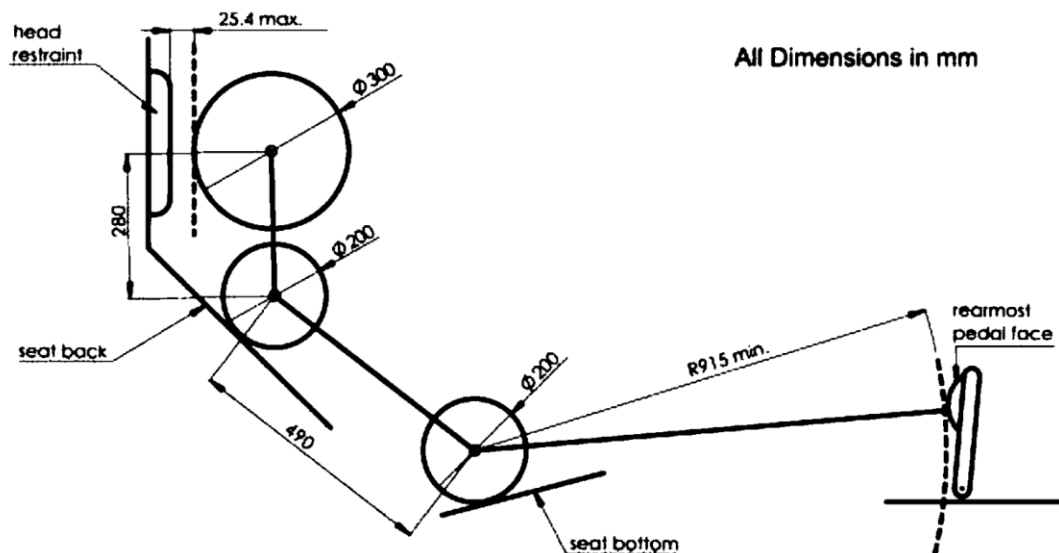


Figure 3.3 A 95<sup>th</sup> percent male profile [2]

### 3.2.1.1.3 General Design Requirements

The vehicle must be open-wheeled and open-cockpit with four wheels that are not in a straight line in an "Open Wheel" format. No part of the vehicle may enter a keep-out-zone defined by two lines extending vertically from positions 75mm in front of and 75mm behind, the outer diameter of the front and rear tires in the side view elevation of the vehicle, with tires, steered straight ahead. This keep-out zone will extend laterally from the outside plane of the wheel/tire to the inboard plane of the wheel/tire. See Figure 3.4 "Keep Out Zones" below and must also comply with the dimension's requirements of aerodynamic devices as seen in Figure 3.4.

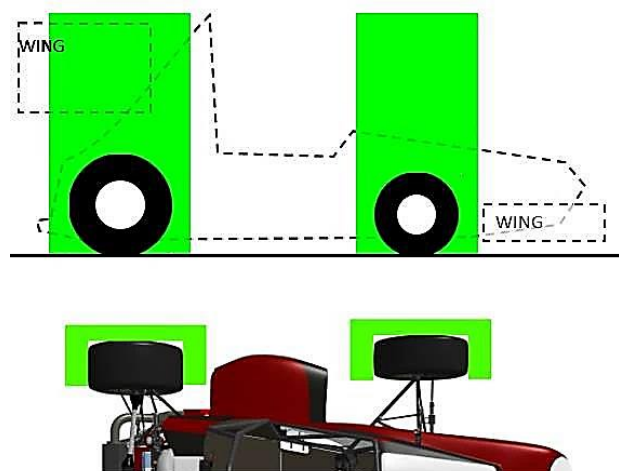


Figure 3.4 FSAE Keep Out Zones [2]

There must be no openings through the bodywork into the driver compartment from the front of the vehicle back to the roll bar main hoop other than that required for the cockpit opening. Minimal openings around the front suspension components allowed. Vehicle Track

(the smaller track of the vehicle (front or rear) must be no less than 75% of the larger track) and visible access (all items on the Inspection Form must be clearly visible to the technical inspectors without using instruments such as endoscopes or mirrors. Visible access may be provided by removing body panels or by providing removable access panels) [2].

### Driver's Cell

Among other requirements, the vehicle's structure must include main hoops, front hoops, roll hoops bracing and supports, side impact structure, front bulkhead, front bulkhead support system and Impact Attenuator with a proper node-to-node triangulation as seen in Figure 3.5 [2].

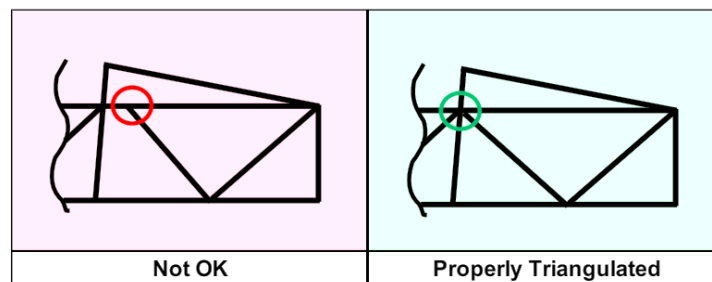


Figure 3.5 Properly triangulated structure [2]

The Primary baseline steel material structure of the car must be constructed of Either: mild or alloy, steel tubing (minimum 0.1% carbon) of the minimum dimensions specified in the following Table 10 [2].

Table 10 Minimum dimension specification [2]

Application	Outside dimension x Wall thickness
Main & Front Hoops, Shoulder Harness Mounting Bar	Round 1.0-inch (25.4 mm) x 0.095 inch (2.4 mm) or Round 25.0 mm x 2.50 mm metric
Side Impact Structure, Front Bulkhead, Roll Hoop Bracing, Drives Restraint Harness Attachment (except as noted above) EV: Accumulator Protection Structure	Round 1.0-inch (25.4 mm) x 0.065 inch (1.65 mm) or Round 25.0 mm x 1.75 mm metric or Round 25.4 mm x 1.60 mm metric or Square 1.00-inch x 1.00-inch x 0.047 inch or Square 25.0 mm x 25.0 mm x 1.20 mm metric
Front Bulkhead Support, Main Hoop Bracing Supports EV: Tractive System Components Protection	Round 1.0-inch (25.4 mm) x 0.047 inch (1.20 mm) or Round 25.0 mm x 1.5 mm metric or Round 26.0 mm x 1.2 mm metric
Bent Upper Side-Impact Member (T3.24.3a)	Round 1.375-inch (35.0mm) x 0.047-inch (1.20mm)

The driver's head and hands must not contact the ground in any rollover attitude. The Frame must include both the Main Hoop and a Front Hoop as shown in Figure 3.6 [2].

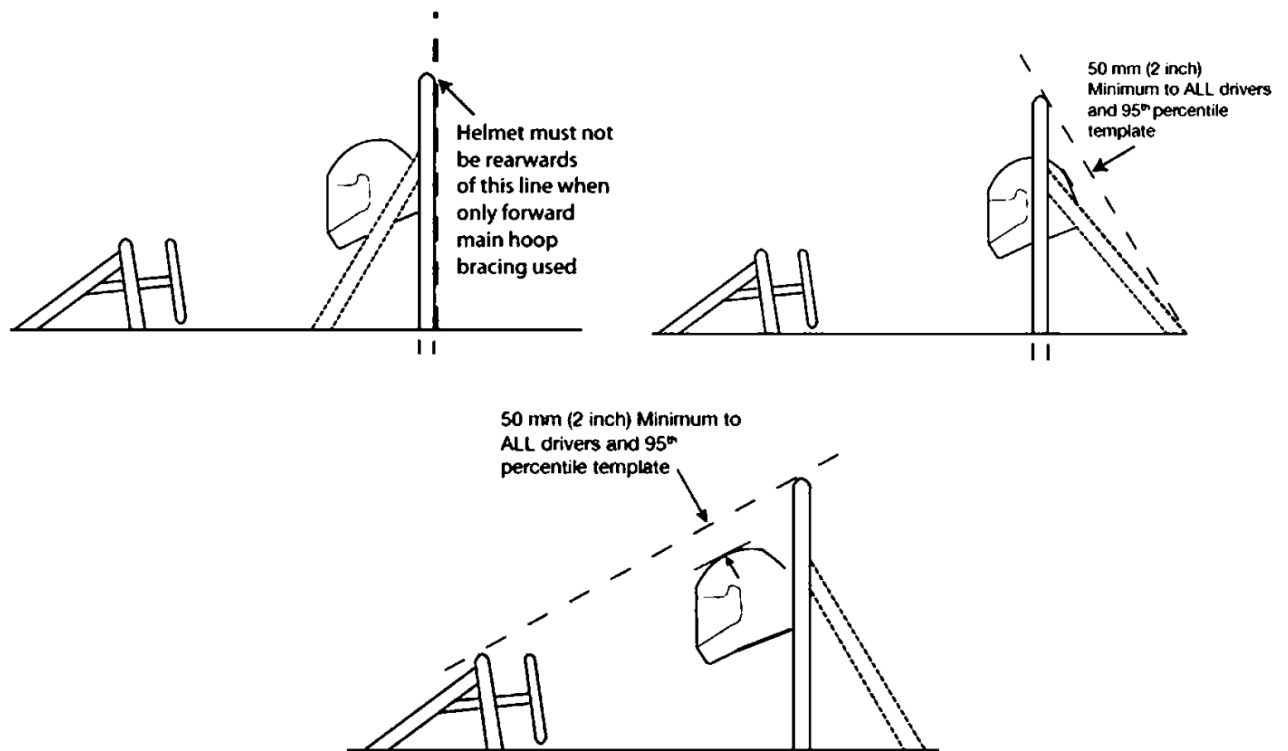


Figure 3.6 Helmet clearance when rollover take place by the main and role hoops [2]

#### 3.2.1.1.4 Basic Structural Members Requirement

Basic components of Formula SAE Chassis structures:

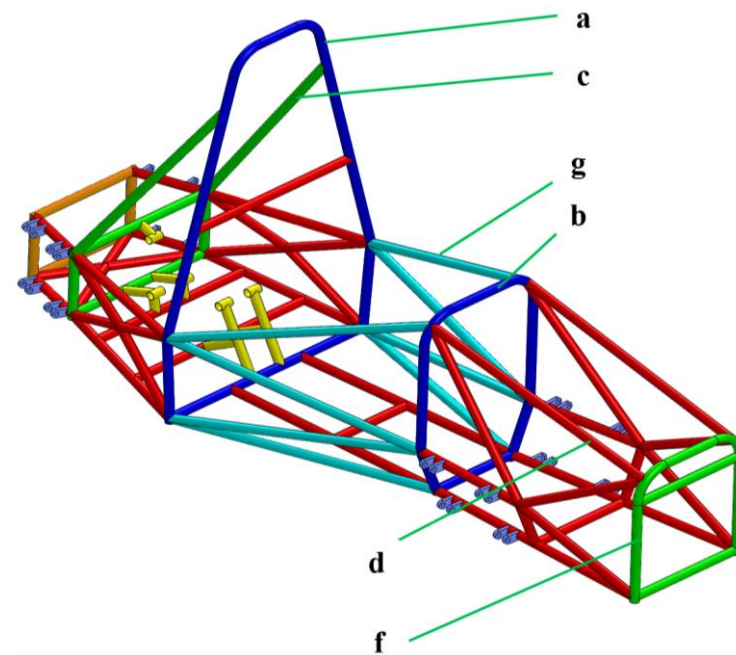


Figure 3.7 Basic components of Formula SAE M2 Chassis model

**a. Main Hoop**

The use of aluminum alloys, titanium alloys or composite materials for the Main Hoop is prohibited and must extend from the lowest frame member on one side of the frame, up, over, and down the lowest frame member on the other side of the frame. In the side view of the vehicle, the portion of the Main Roll Hoop that lies above its attachment point to the upper Side Impact tube, must be within ten degrees ( $10^\circ$ ) of the vertical and the main hoop bracing must be within the requirement angle and spacing from the top of main hoops see Figure 3.6 and Figure 3.7. Figure 3.7 Basic components of Formula SAE M2 Chassis model. And also, the front view of the vehicle, the vertical members of the Main Hoop must be at least 380 mm apart (inside dimension) at the location where the Main Hoop is attached to the bottom tubes of the Major Structure of the Frame [2].

**b. Front Hoop**

The Front Hoop must construct of closed section metal tubing and extend from the lowest Frame Member on one side of the Frame, up, over, and down to the lowest Frame member on the other side of the Frame with proper triangulation, it is permissible to fabricate the Front Hoop from more than one piece of tubing. The top-most surface of the Front Hoop must be no lower than the top of the steering wheel in any angular position. The Front Hoop must be no more than 250 mm (9.8 inches) forward of the steering wheel. Inside view, no part of the Front Hoop can be inclined at more than twenty degrees ( $20^\circ$ ) from the vertical [2].

**c. Main Hoop Bracing**

The Main Hoop must support by two braces extending in the forward or rearward direction on both the left and right sides of the Main Hoop and attached as near as possible to the top of the Main Hoop but not more than 160 mm below the top-most surface of the Main Hoop. The included angle formed by the Main Hoop and the Main Hoop braces must be at least thirty degrees ( $30^\circ$ ). Also, must be straight, i.e. without any bends [2].

**d. Front Hoop Bracing**

The Front Hoop must be supported by two braces extending in the forward direction on both the left and right sides of the Front Hoop, constructed such that they protect the driver's legs and should extend to the structure in front of the driver's feet attached as near as possible to the top of the Front Hoop but not more than 50.8 mm (2 in) below the top-most surface of the Front Hoop. If the Front Hoop leans rearwards by more than ten degrees ( $10^\circ$ ) from the vertical, it must support by additional bracing to the rear. This bracing must be constructed of material rules [2].

### e. Other Bracing Requirements

Where the braces are not welded to steel Frame Members, the braces must securely attach to the Frame using 8 mm Metric Grade 8.8 (5/16 in SAE Grade 5), or stronger bolts. Mounting plates welded to the Roll Hoop braces must be at least 2.0 mm thick steel [2].

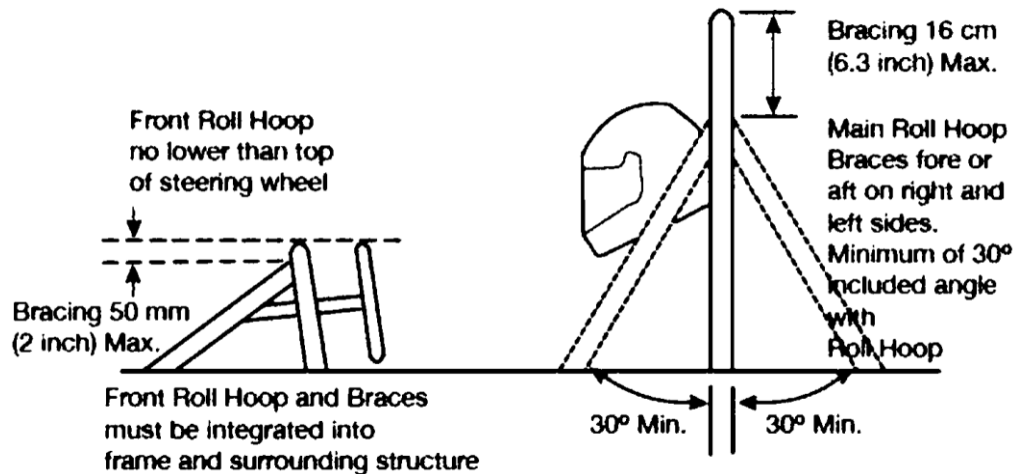


Figure 3.8 Side view of structural members requirement seat by FSAE [2]

### f. Bulkhead

The Front Bulkhead must be constructed of closed section tubing which is located forward of all non-crushable objects, e.g. batteries, master cylinders, hydraulic reservoirs and must be supported back to the Front Roll Hoop by a minimum of three Frame Members on each side of the vehicle; an upper member; lower member and diagonal brace to provide triangulation see Figure 3.9 [2].

### g. Side Impact Structure for Tube Frame

At least three tubular structures members must be used for side impact structure located on each side of the driver while seated in the normal driving position, with proper triangulation and allowable to fabricate the Side Impact structural members from more than one piece of tubing as seen in Figure 3.9 [2].

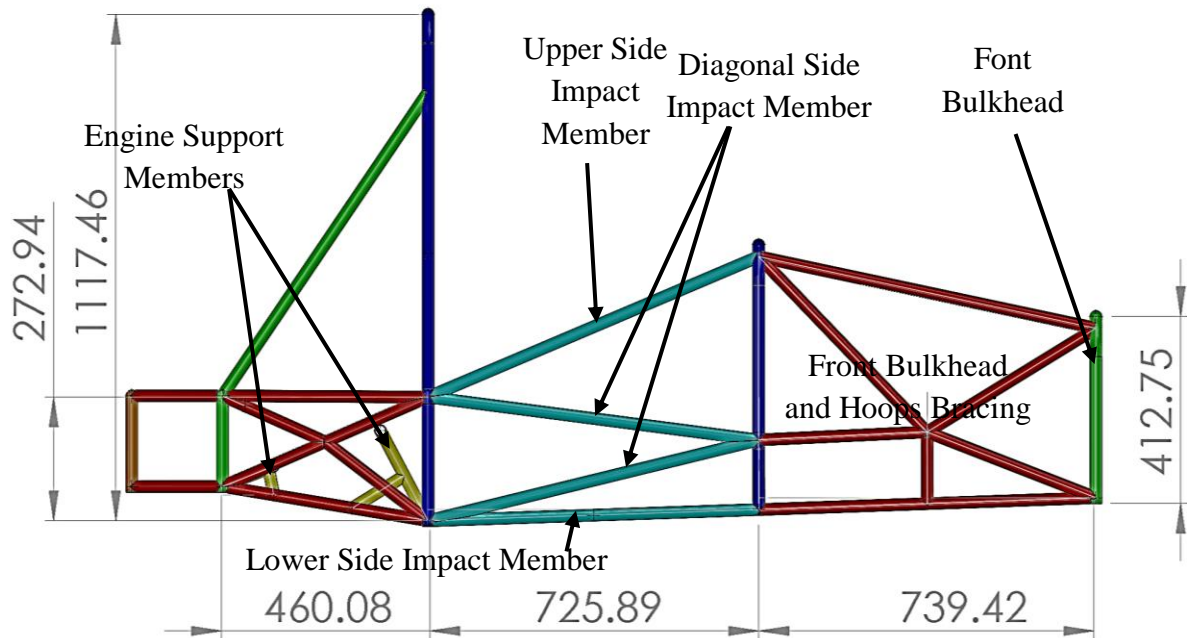


Figure 3.9 Formula SAE M2 structural members

**h. Cockpit Opening**

To ensure that the opening giving access to the driver inside of the cockpit with adequate/proper size as shown in Figure 3.10 and Figure 3.11 inserted into the cockpit opening and driver's leg. It will be held horizontally and inserted vertically until it has passed below the top bar of the Side Impact (or until it is 350 mm (13.8 inches) above the ground for monocoque cars) [2].

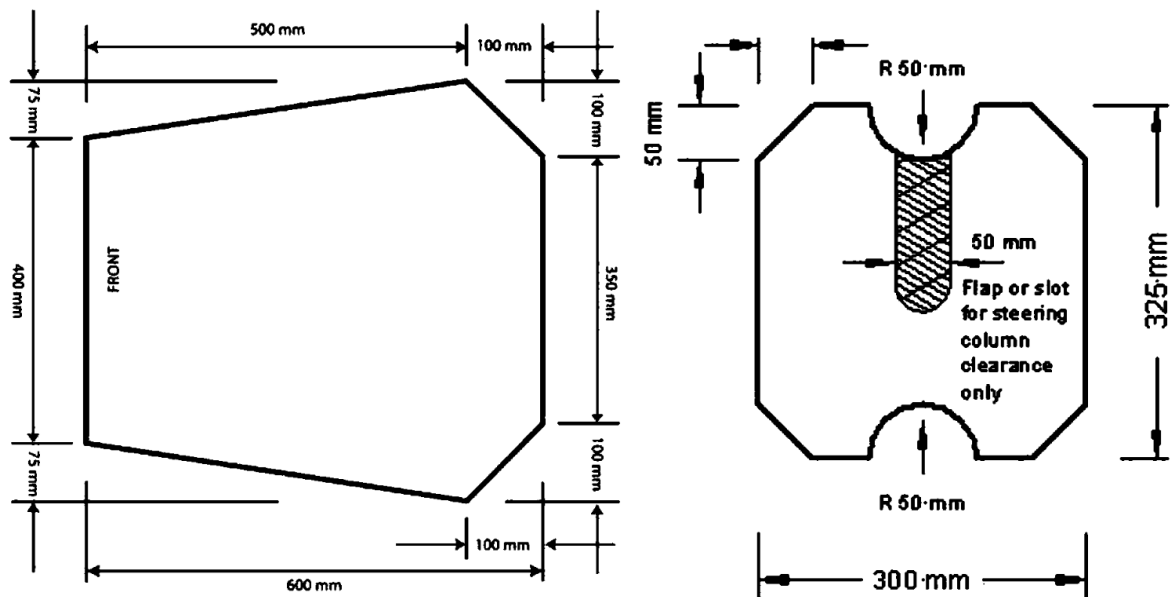


Figure 3.10 Cockpit opening from the top view and internal cross-section from the side view

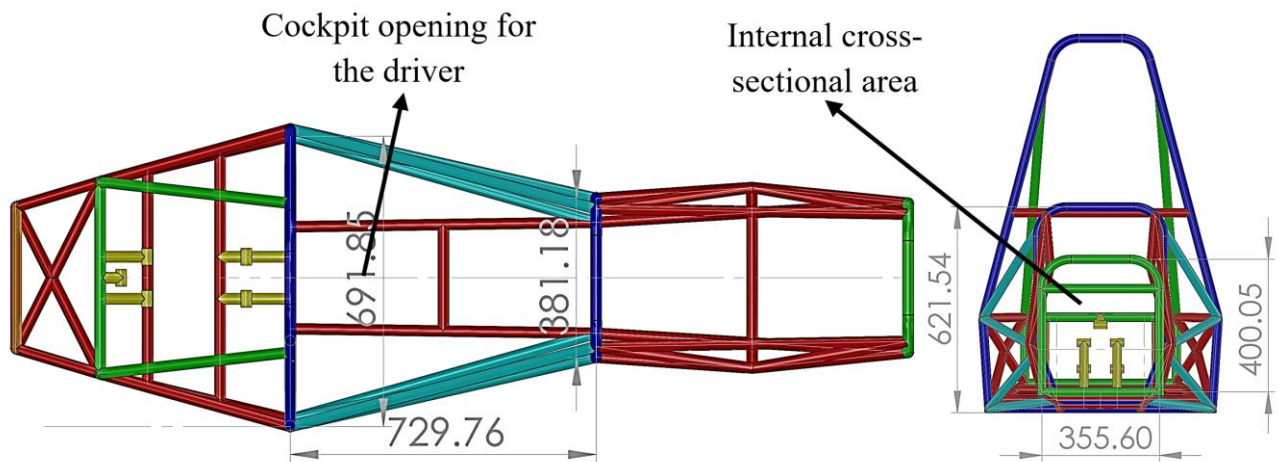


Figure 3.11 Cockpit opening from the top view and internal cross-section from the side view of Formula SAE M2 Chassis

From Figure 3.12 the following steps take place when the Formula SAE Chassis modeled:

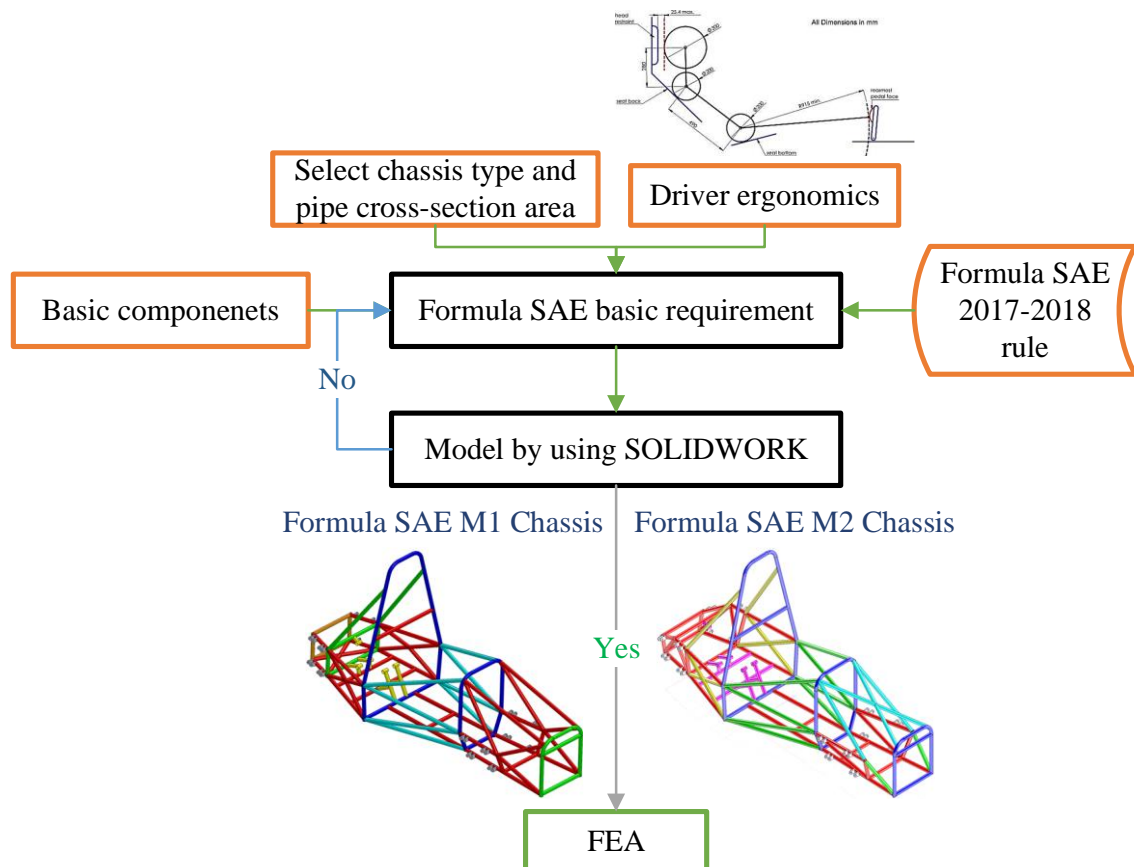


Figure 3.12 Steps used to model Formula SAE Chassis

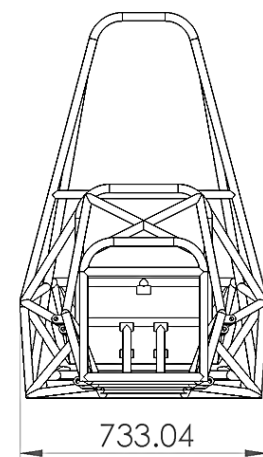
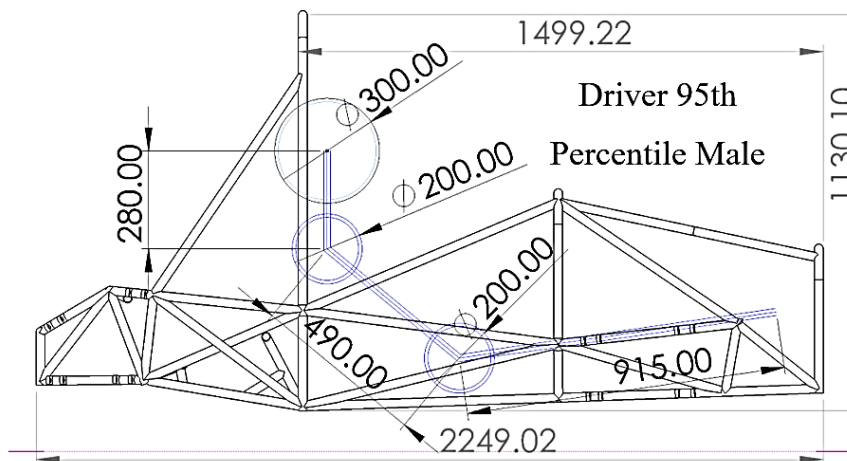
Finally, the Chassis designed in SOLIDWORKS 2018 software. The SOLIDWORKS CAD model then exported into the FEA software. The finite element model created using ANSYS 19.1. The Chassis modeled as frame elements with circular hollow sections with outside diameter and thickness relation.

Table 11 Frame outside diameter Vs thickness for Formula SAE Chassis [2]

Part Name	Formula SAE M1		Formula SAE M2	
	Thickness, mm	Outside Diameter, mm	Thickness, mm	Outside Diameter, mm
Main & Front Hoops, Shoulder Harness Mounting Bar	2.5	Round 25.0	2.4	Round 25.4
Side Impact Structure, Front Bulkhead, Roll Hoop Bracing, Driver's Restraint Harness Attachment	1.75	Round 25.0	1.6	Round 25.4
Front Bulkhead Support, Main Hoop Bracing Supports	1.5	Round 25.0	1.2	Round 25.4

Side View with the driver on it

Front View



Top View

Isometric View

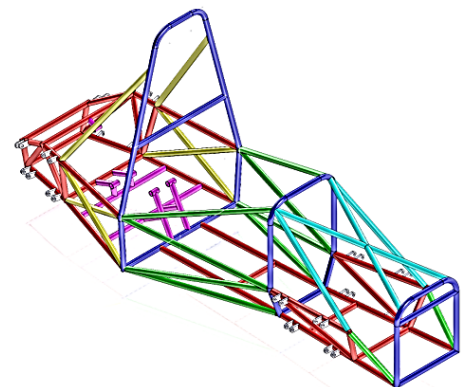
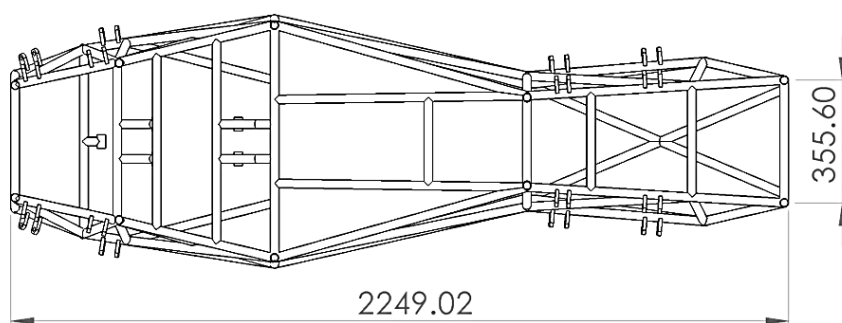


Figure 3.13 Formula SAE M1 Chassis Model with a 95th percentile male template (all units in mm)

After performing the topological optimization on ANSYS 19.1 Workbench the final frame structure base on the maximum stress created on the frame from different loading condition, with a hollow circular cross-section and the following outside diameter and thickness as seen Figure 3.13.

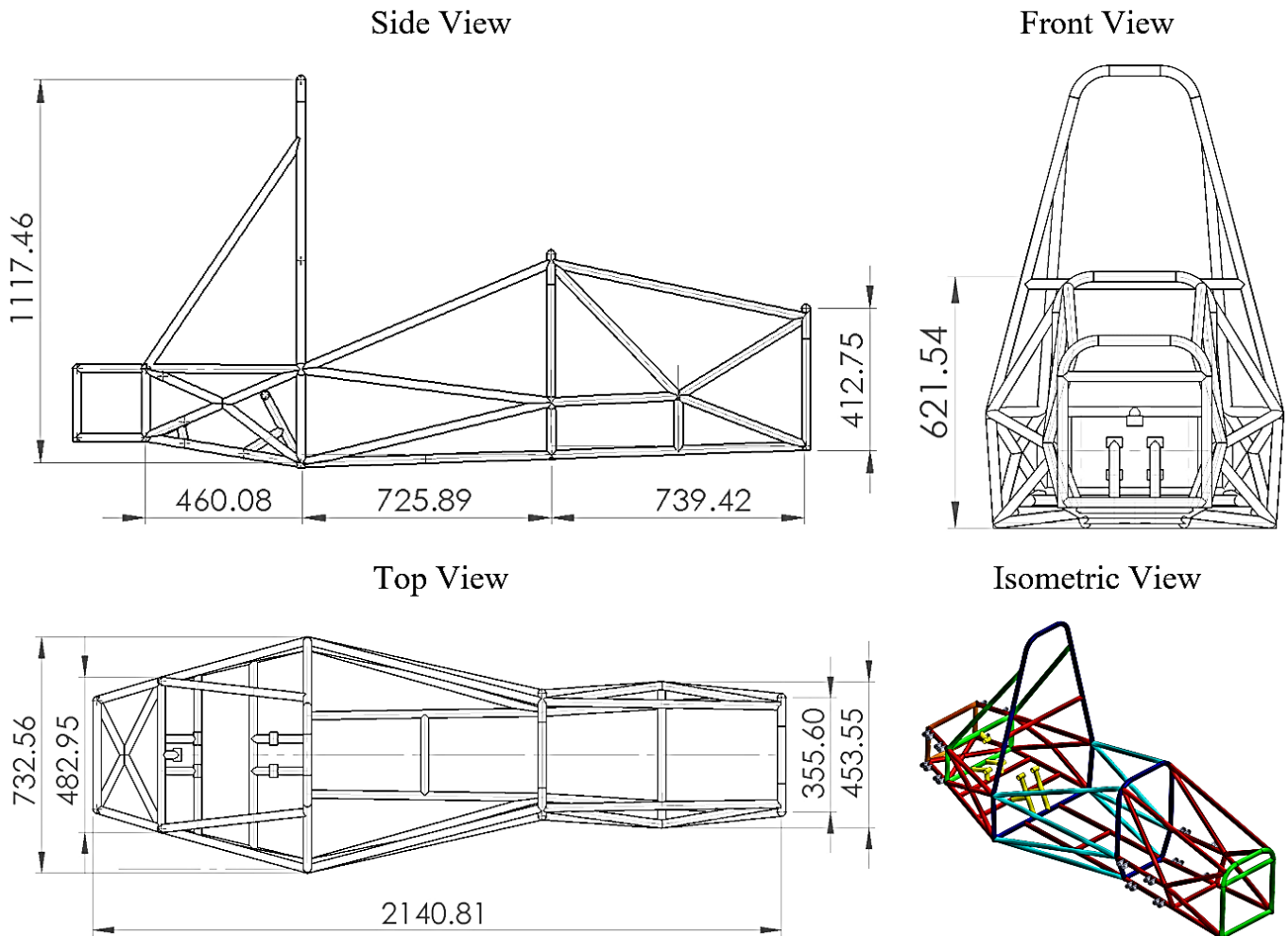


Figure 3.14 Formula SAE M2 Chassis Model (all units in mm)

### 3.2.1.2 Geometrical Modeling for Crash Box or Impact Attenuator

#### 3.2.1.2.1 Formula SAE M1 Crash Box Model

A thin-wall shell type of Crash Box has a high crash absorption base on FSAE and many researches, because kinetic energy in the form of an even manner deformation [19] and offers protection to the structure being considered and since they are cheap, efficient and reliable, are popularly used as energy absorbing devices [8]. The minimum size of Crash Box base on FSAE book, at least 200 mm (7.8 in) long (with its length oriented along the fore/aft axis of the Frame), 100 mm (3.9 in) high, 200 mm (7.8 in) wide [2].

The Crash Box geometry depends on the geometry of Front Bulkhead and the front area of the Front Bulkhead is 12in (304.8mm) high, 14in (355.6mm) width. Therefore the Crash Box was designed in SOLIDWORKS 2018 software and assembled in the front of the bulkhead with 12in (304.8mm) high, 14in (355.6mm) width with a minimum distance of 10in (254mm) forward of the bulkhead with 2mm thickness as seen in Figure 3.15 and Figure 3.16 [2], [34].

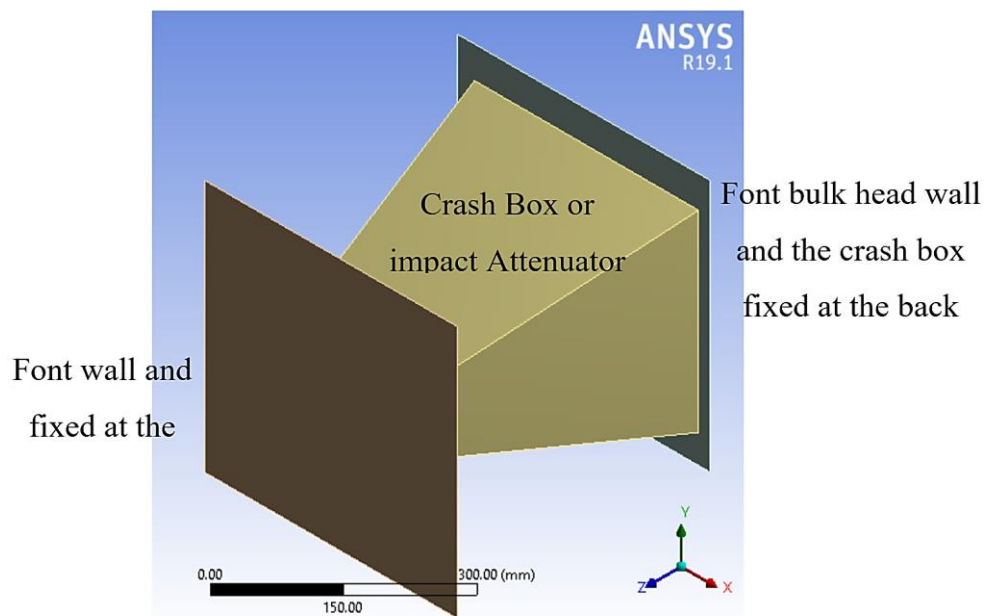
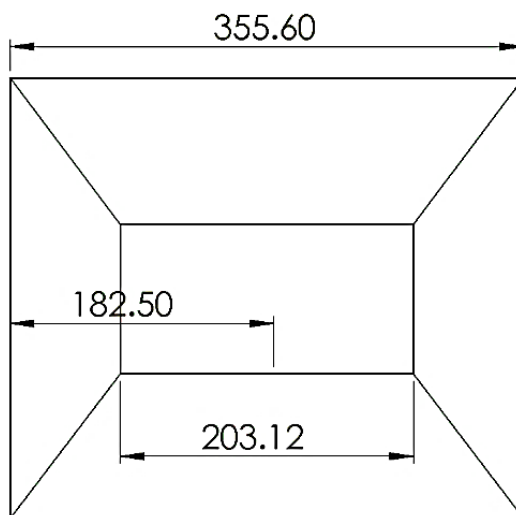


Figure 3.15 3D Model for FSAE M1 Crash Box or Impact Attenuator based on FSAE rule

Front view



Side view

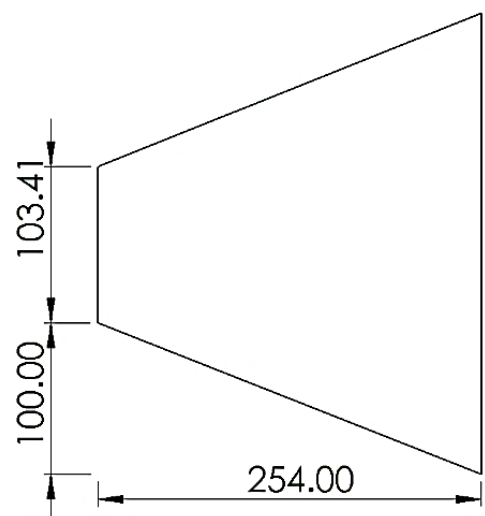
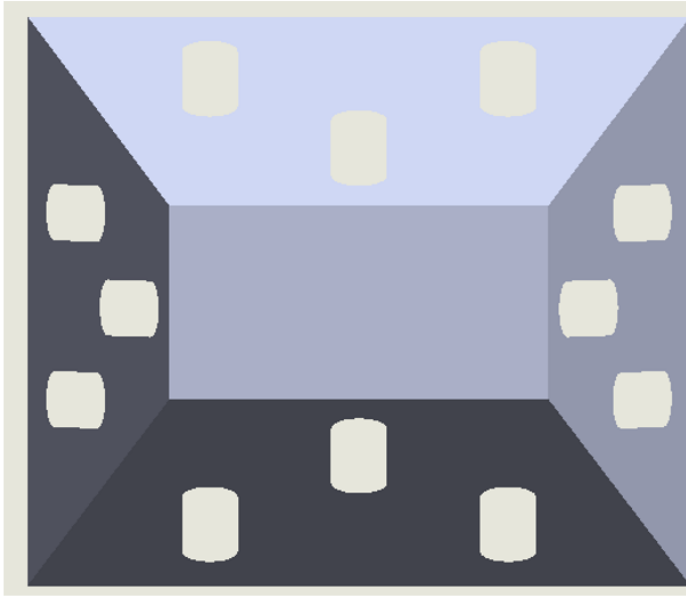


Figure 3.16 FSAE M1 Crash Box or Impact Attenuator Model with 2mm thickness (mm)

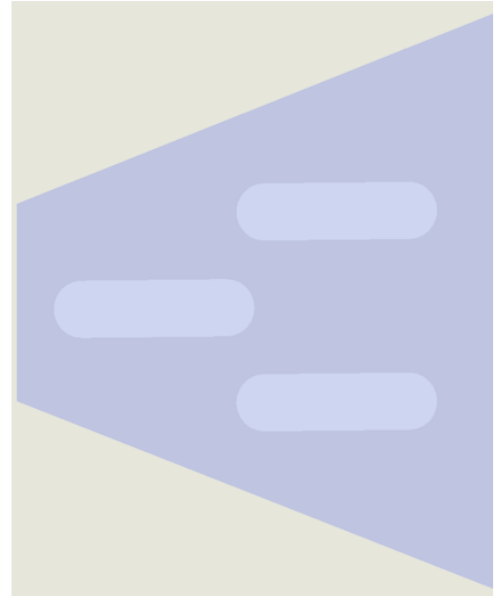
### 3.2.1.2.2 Formula SAE M2 Crash Box with Holes

Adding holes and the x-shape material in the Crash Box structure add a batter energy absorption and deformation for the sheet metal structure [6]. The following model with holes and additional energy absorbing geometry added to the Formula SAE Crash Box model as seen in Figure 3.17.

Front view



Side view

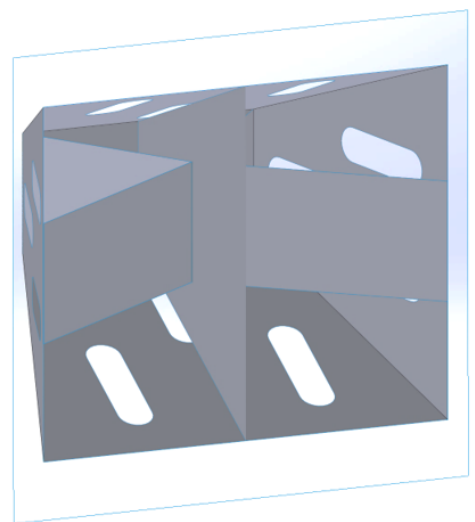


Top view

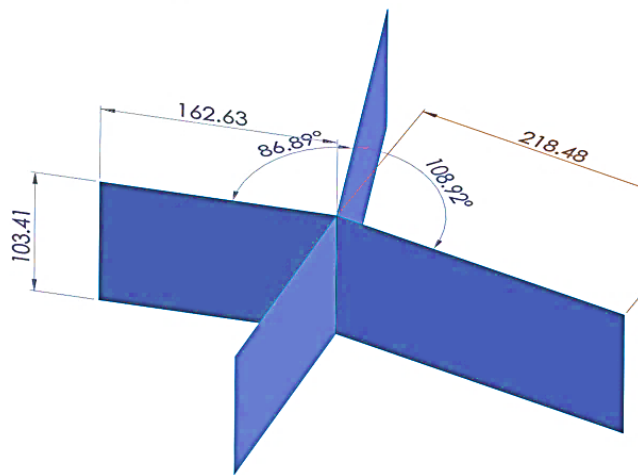


3D Model of M2 Crash Box

backside



Internal energy ansorber part isomtric view



Top view

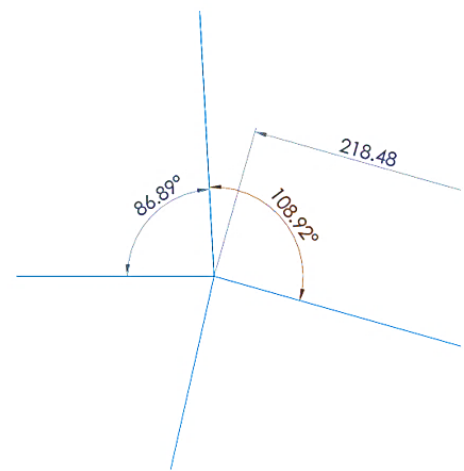


Figure 3.17 FSAE M2 Crash Box or Impact Attenuator with internal support and hole

### 3.2.1.2.3 Formula SAE M3 Crash Box or Impact Attenuator with Caterpillar Model

Biological structural or Bio-inspired materials are especially of interest to engineers and material scientists because of their hierarchical structures as well as mechanical properties superior to man-made counterpart materials and with a good energy absorption ability this makes them important to the Crash Box structure of the vehicle [35].

There are different insects in our world, when we see the caterpillar insect it have its own type of anatomy with the advantage of protecting its self from another insects and fall from the top of a tree [36]. Some caterpillars are quite hairy, while others are smooth. Despite these differences, all caterpillars share certain morphological features. These common features are labeled and described in the caterpillar diagram as seen in Figure 3.18.

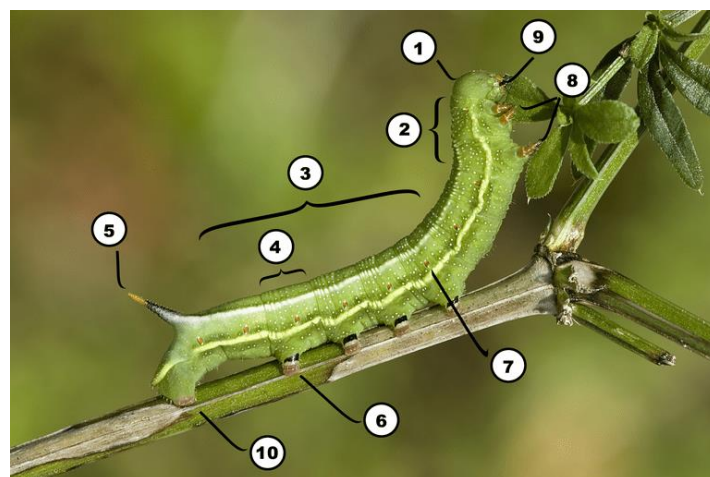


Figure 3.18 Caterpillars body part

The caterpillar anatomy as seen in Figure 3.18 have the following parts Head (part 1), Thorax (part 2), Abdomen (part 3), Segment (part 4), Horn (part 5), Prolegs (part 6), Spiracle (part 7), True Legs (part 8), Mandibles (part 9) and Anal Prolegs (part 10). When the Caterpillar Crash Box model creates by using the basic part of the Caterpillar insect is Abdomen (part 3) and separated into segments (part 4).

Figure 3.19 shows the creation of the Caterpillar geometry and assembled inside the Formula SAE Crash Box model with a detail discription of the contact created in the caterpillar geometry. The static and dynamic coefficient of friction tack place between the Crash Box, the caterpillar geometry is 0.3 and 0.2 respectively because the material used is Aluminum 7075-T651.

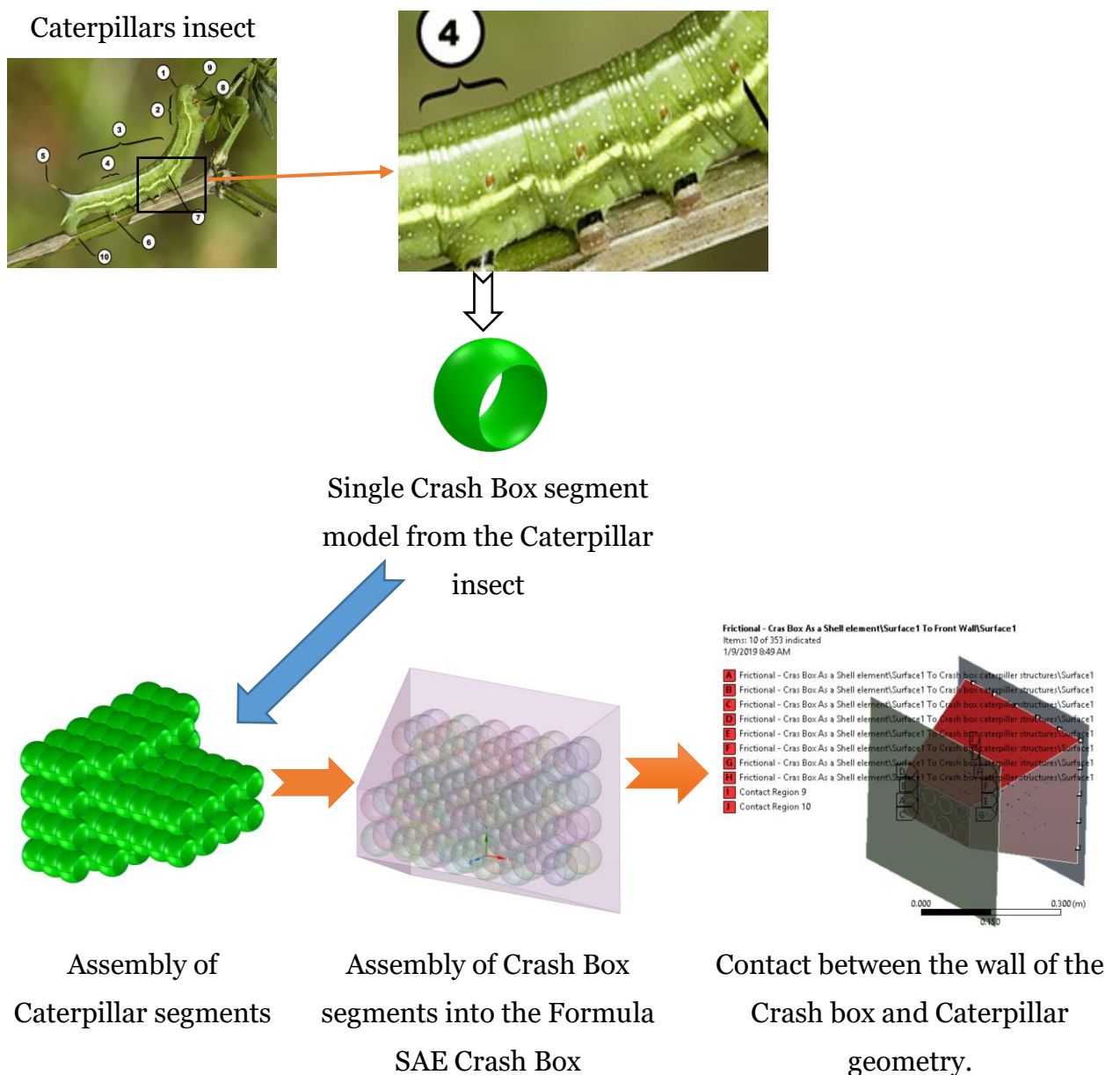
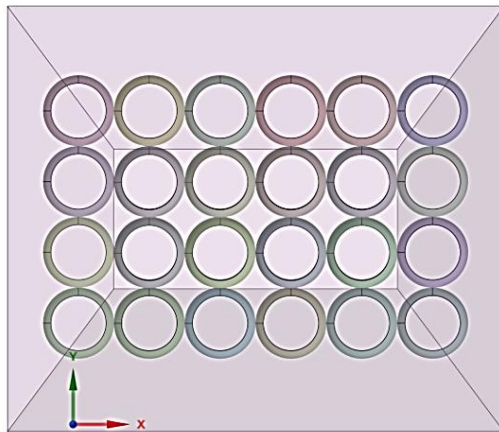
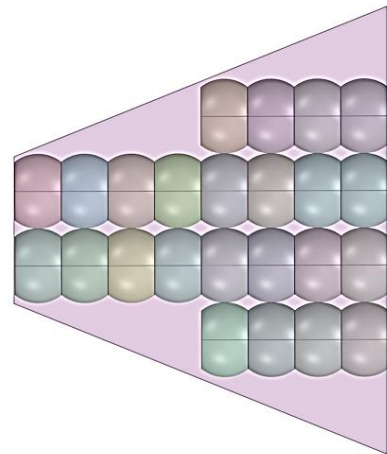


Figure 3.19 Formula SAE caterpillar Crash Box model generation

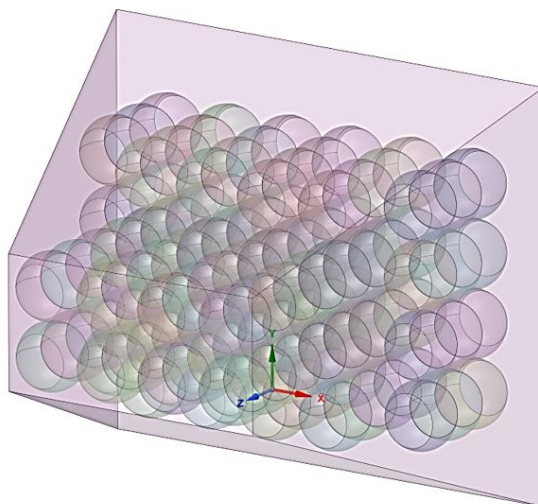
Front view



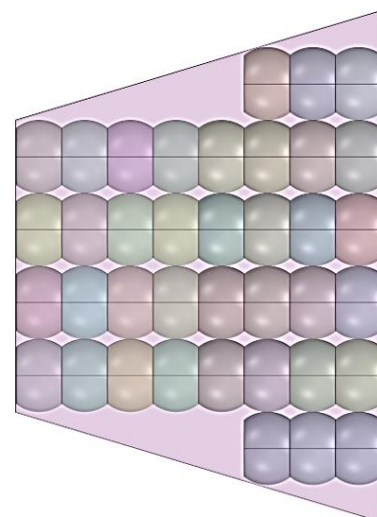
Side view



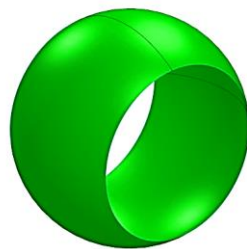
3D Model of caterpillar Crash Box



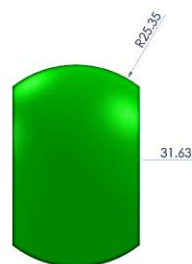
Top view



Inside the shell element



Front view



Side view

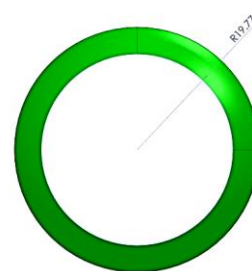


Figure 3.20 FSAE Crash Box or Impact Attenuator with caterpillar Model with 2mm thickness

### 3.3 Mathematical Modeling

#### 3.3.1 Mathematical Modeling of Chassis

The principle of virtual work states that a virtual (very small) change of the internal strain energy must be offset by an identical change in externally applied load [37]:

$$\delta U = \delta V \quad (12)$$

Where  $U$  = Strain energy (internal work) =  $U_1 + U_2$

$V$  = External work =  $V_1 + V_2 + V_3$

$\delta$  = Virtual operator

$$\text{The virtual strain energy is: } \delta U_1 = \int_{\text{vol}} \{\delta \varepsilon\} \{\sigma\} d(\text{vol})^T \quad (13)$$

Where  $\{\varepsilon\}$  = Strain vector,  $\{\sigma\}$  Stress vector,  $\text{vol}$  = Volume of element and  $(\text{vol})^T$  = Volume of element.

The material used for the frame structure is SAE 1018 Steel with uniform material and geometry property then the virtual strain energy becomes [37]:

$$\delta U_1 = \int_{\text{vol}} (\{\delta \varepsilon\}^T [D] \{\varepsilon\} - \{\delta \varepsilon\}^T [D] \{\varepsilon^{\text{th}}\}) d(\text{vol})^T \quad (14)$$

The strain related to the nodal displacement by:  $\{\varepsilon\} = [B] \{u\}$

Where  $[B]$  = Strain-displacement matrices, based on the element shape function

$\{u\}$  = Nodal displacement vector

$[D]$  = Elastic matrix

All effects are considered in the global coordinate system and noting that  $\{u\}$  does not vary over the volume the virtual strain energy become [37]:

$$\delta U_1 = \{\delta u\}^T \int_{\text{vol}} \{B\}^T [D] [B] d(\text{vol}) \{u\} - \{\delta u\}^T \int_{\text{vol}} \{B\}^T [D] \{\varepsilon^{\text{th}}\} d(\text{vol}) \quad (15)$$

Another form of virtual strain energy is when a surface against a distributed resistance, as foundation stiffness. The may be written as [37]:

$$\delta U_2 = \int_{\text{area}_f} \{\delta w_n\}^T \{\sigma\} d(\text{area}_f) \quad (16)$$

Where  $\{w_n\}$  = motion normal to the surface,  $\{\sigma\}$  = Stress carried by the surface and  $\text{area}_f$  = area of the distributed resistance, both  $\{w_n\}$  and  $\{\sigma\}$  have only one nonzero component.

The point-wise normal displacement is related to the nodal displacement by:  $\{w_n\} = [N_n] \{u\}$ , where  $[N_n]$  is matrices of shape function for normal motions at the surface.

The stress,  $\{\sigma\} = k\{w_n\}$ ,  $k$  is the foundation stiffness in units of force per unit area and constant across the area of the frame. Then another form virtual strain energy becomes [37]:

$$\delta U_2 = \{\delta w_n\}^T k \int_{\text{area}_f} \{N_n\}^T [N_n] d(\text{area}_f) \{u\} \quad (17)$$

Next, the external virtual work considered. The inertial effect will be studied first [37]:

$$\delta V_1 = \int_{\text{vol}} \{\delta w\}^T \frac{\{F^a\}}{\text{vol}} d(\text{vol}) \quad (18)$$

where  $\{w\}$  = Vector of displacements of general point and  $\{F^a\}$  = Acceleration (D'Alembert) force vector

$$\text{According to Newton's second law: } \frac{\{F^a\}}{\text{vol}} = \rho \frac{\partial^2}{\partial t^2} \{w\} \quad (19)$$

Where  $\rho$ ,  $t$  are density and time respectively.

The displacement within the element is related to the nodal displacement by:

$$\{w\} = [N] \{u\} \quad (20)$$

Where  $[N]$  is the matrix of shape function and it is also the density of the frame structure is constant throughout the surface then [37]:

$$\delta V_1 = -\{\delta u\}^T \rho \int_{\text{vol}} [N]^T [N] d(\text{vol}) \frac{\delta^2}{\delta t^2} \{u\} \quad (21)$$

the pressure force vector formulation starts with [37]:

$$\delta V_2 = \int_{\text{area}_p} \{\delta w_n\}^T \{P\} d(\text{area}_p) \quad (22)$$

Where  $\{p\}$  and  $\text{area}_p$  the applied pressure vector (normal constants only one non-zero component) and area over which pressure acts. Then it becomes [37]:

$$\delta V_2 = \{\delta w_n\}^T \int_{\text{area}_p} [N_n] \{P\} d(\text{area}_p) \quad (23)$$

Unless otherwise noted, pressures applied to the outside surface of each element and area normal to the curved surface, if applicable. The nodal force applied to the element can be accounted for by [37]:

$$\delta V_2 = \{\delta u_n\}^T \{F_e^{nd}\} \quad (24)$$

where  $\{F_e^{nd}\}$  is a nodal force applied to the element.

Finally, combine the above equations

$$\begin{aligned}
 & \{\delta u\}^T \int_{vol} [B]^T [D] d(vol) \{u\} - \{\delta u\}^T \int_{vol} [B]^T [D] \{\varepsilon^{th}\} d(vol) + \{\delta u\}^T k \{u\} \\
 & + \{\delta u\}^T \int_{area_f} [N]^T [N] d(area_f) \{u\} \\
 & = -\{\delta u\}^T \rho \int_{vol} [N]^T [N] d(vol) \frac{\delta^2}{\delta t^2} \{u\} \\
 & + \{\delta u\}^T \int_{area_p} [N]^T \{p\} d(area_p) + \{\delta u\}^T \{F_e^{nd}\}
 \end{aligned} \tag{25}$$

Nothing that  $\{\delta u\}^T$  vector is a set of arbitrary virtual displacement common in all of the above terms, the condition required to satisfy the equation above and reduced to [37]:

$$([K_e] + [K_e^f]) \{u\} - \{F_e^{th}\} = [M_e] \{\ddot{u}\} + \{F_e^{pr}\} + \{F_e^{nd}\} \tag{26}$$

This equation represents the equilibrium equation on a one element basics.

Where

$$[K_e] = \int_{vol} [B]^T [D] d(vol) = \text{Element stiffness matrix}$$

$$[K_e^f] = \int_{area_f} [N]^T [N] d(area_f) = \text{Element foundation stiffness matrix}$$

$$\{F_e^{th}\} = \int_{vol} [B]^T [D] \{\varepsilon^{th}\} d(vol) = \text{Element thermal load vector}$$

$$[M_e] = \rho \int_{vol} [N]^T [N] d(vol) \frac{\delta^2}{\delta t^2} \{u\} = \text{Element mass matrix}$$

$$\{\ddot{u}\} = \frac{\delta^2}{\delta t^2} \{u\} = \text{Acceleration vector (such as gravitational effect)}$$

$$\{F_e^{pr}\} = \int_{area_p} [N]^T \{p\} d(area_p) = \text{Element pressure load vector}$$

A frame element formulated to model a straight bar of an arbitrary cross-section, which can deform not only in the axial direction but also in the directions perpendicular to the axis of the bar. The bar capable of carrying both axial and transverse forces, as well as moments. Therefore, a frame element is seen to possess the properties of both truss and beam elements [38].

A typical three-dimensional frame structure is shown in Figure 3.21. Frame members in a frame structure are joined together by welding so that both forces and moments can be transmitted between members [37]. The static analysis solution method is valid for all degrees of freedom (DOF) except inertial and damping effects neglected, exclude for static acceleration fields. Description of structural systems the overall equilibrium equations for linear structural static analysis are [37]:

$$\{F\} = [K]\{U\} \text{ or } \{F^a\} + \{F^r\} = [K]\{U\} \tag{27}$$

Where  $[K]$  = total stiffness matrix

$\{u\}$  = Nodal displacement vector

$N$  = Number of elements

$\{F^r\}$  = Reaction load vector

$\{F^a\}$ , the total applied load vector, defined by:

$$\{F^a\} = \{F^{nd}\} + \{F^{ac}\} + \sum_{m=1}^N [F]_e^{th} + \{F_e^{pr}\} \quad (28)$$

Where  $\{F^{nd}\}$  = Applied nodal load vector

$\{F^{ac}\} = -[M]\{ac\}$  = Acceleration load vector

$\{M\}$  = Total mass matrix =  $\sum_{e=1}^N M_e$

$[M_e]$  = Element mass matrix

$\{a_e^{th}\}$  = Total acceleration vector

$\{F_e^{th}\}$  = Element thermal load vector

$\{F_e^{pr}\}$  = Element pressure load vector

The finite element equations for space frames in the local coordinate have six DOFs at a single node, which are three translational displacements in the  $x$ ,  $y$  and  $z$  directions, and three rotations with respect to the  $x$ ,  $y$ , and  $z$ -axes. Therefore, a single element with two nodes has twelve DOFs, as shown in Figure 3.21 below.

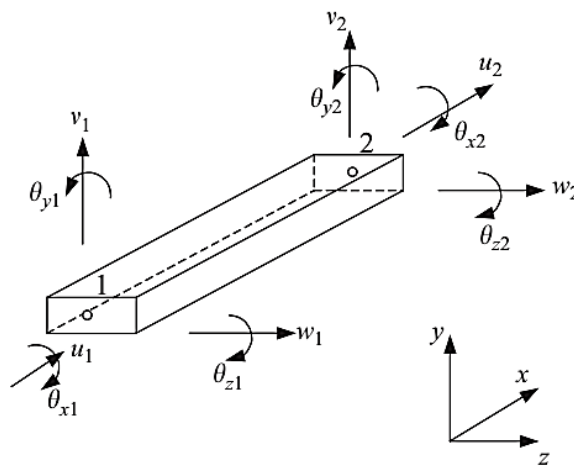


Figure 3.21 Order of degrees of freedom (12 DOFs) for three-dimensional frame members [38].

The element displacement vector for a frame element in space can be written as displacement at node 1 and 2.



$$[M_e] = \frac{\rho A a}{105} \begin{bmatrix} 70 & & & & & & & & & & & & \\ 0 & 78 & & & & & & & & & & & \\ 0 & 0 & 78 & & & & & & & & & & \\ 0 & 0 & 0 & 70r_x^2 & & & & & & & & & \\ 0 & 0 & -22a & 0 & 8a^2 & & & & & & & & \\ 0 & -22a & 0 & 0 & 0 & 8a^2 & & & & & & & \\ 35 & 0 & 0 & 0 & 0 & 0 & 70 & & & & & & \\ 0 & 27 & 0 & 0 & 0 & 0 & 0 & 78 & & & & & \\ 0 & 0 & 27 & 0 & 13a & 0 & 0 & 0 & 78 & & & & \\ 0 & 0 & 0 & 35r_x^2 & 0 & 0 & 0 & 0 & 0 & 70r_x^2 & & & \\ 0 & 0 & 13a & 0 & -6a^2 & 0 & 0 & 0 & 22a & 0 & 8a^2 & & \\ 0 & -13a & 0 & 0 & 0 & -6a^2 & 0 & -22a & 0 & 0 & 0 & 8a^2 \end{bmatrix} \quad (31)$$

Where,  $r_x^2 = \frac{I_x}{A}$  in which  $I_x$  is the second moment of area/inertia of the cross-section of the beam with respect to the x-axis.

To transform the local coordinate system to the global coordinate system, take the two local nodes 1 and 2 corresponded to global nodes i and j respectively, the displacement on each node have three translational, three rotational according to x, y, z-axes and sequentially by  $d_1$  to  $d_{12}$  corresponding to the physical deformations. The transformation matrices T gives the relation between the local coordinate system  $d_e$  and the global coordinate system  $D_e$ , for the same element based on the global coordinate system [38].

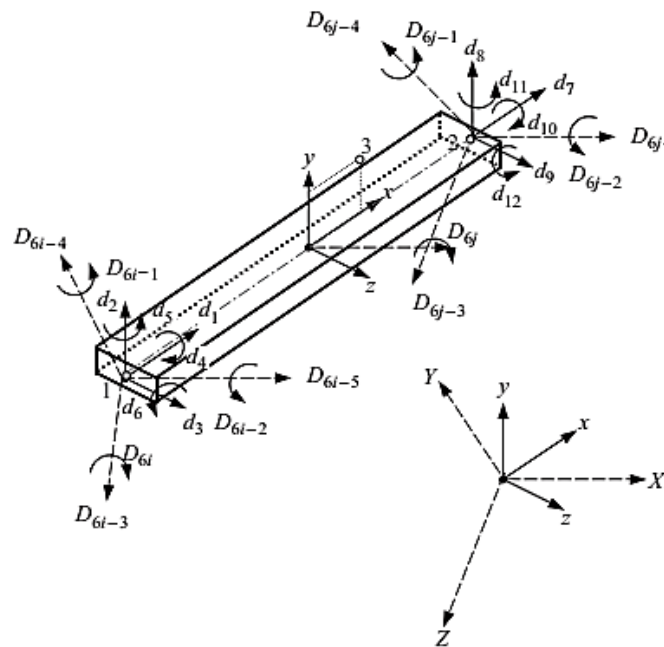


Figure 3.22 Coordinate transformation for a frame element in space [38]

$$d_e = TD_e \quad (32)$$

Where

$$d_e = \begin{Bmatrix} D_{6i-5} \\ D_{6i-4} \\ D_{6i-3} \\ D_{6i-2} \\ D_{6i-1} \\ D_{6i} \\ D_{6j-5} \\ D_{6j-4} \\ D_{6j-3} \\ D_{6j-2} \\ D_{6j-1} \\ D_{6j} \end{Bmatrix}, T = \begin{bmatrix} T_3 & 0 & 0 & 0 \\ 0 & T_3 & 0 & 0 \\ 0 & 0 & T_3 & 0 \\ 0 & 0 & 0 & T_3 \end{bmatrix} \text{ and } T_3 = \begin{bmatrix} l_x & m_x & n_x \\ l_y & m_y & n_y \\ l_z & m_z & n_z \end{bmatrix} \quad (33)$$

Where  $l_k, m_k,$  and  $n_k$  ( $k= x, y, z$ ) are directional cosines defined by

$$\begin{aligned} l_x &= \cos(x, X), m_x = \cos(x, Y), n_x = \cos(x, Z) \\ l_y &= \cos(y, X), m_y = \cos(y, Y), n_y = \cos(y, Z) \\ l_z &= \cos(z, X), m_z = \cos(z, Y), \text{ and } n_z = \cos(z, Z) \end{aligned} \quad (34)$$

To define these direction cosines, the position, and the three-dimensional orientation of the frame element must define first. With nodes 1 and 2, the location of the element fixed on the local coordinate frame, and the orientation of the element has also been fixed in the x-direction. However, the local coordinate frame can still rotate about the axis of the beam. One more additional point in the local coordinate must be defined. This point can be chosen anywhere in the local x–y plane, but not on the x-axis. Therefore, node 3 is chosen, as shown in Figure 3.23 [38].

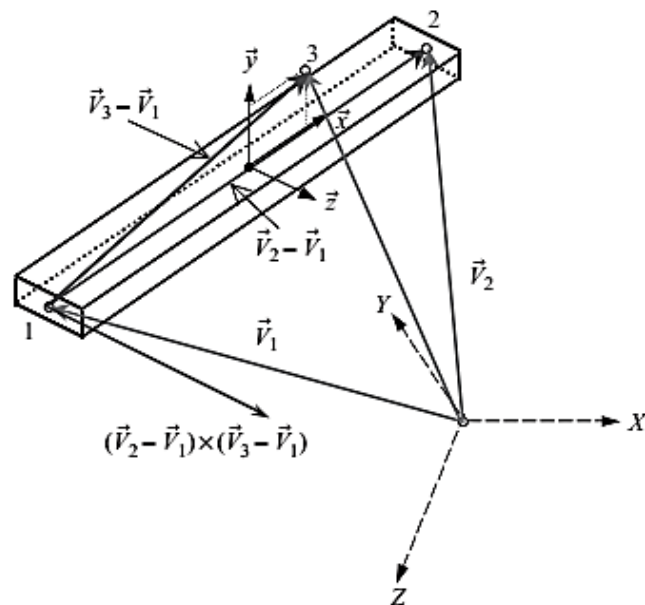


Figure 3.23 Vectors for defining the location and three-dimensional orientation of the frame element in space [38]

The position vectors  $V_1$ ,  $V_2$ , and  $V_3$  can be expressed as [38]:

$$\vec{V}_1 = X_1\vec{X} + Y_1\vec{Y} + Z_1\vec{Z}, \vec{V}_2 = X_2\vec{X} + Y_2\vec{Y} + Z_2\vec{Z} \text{ and } \vec{V}_3 = X_3\vec{X} + Y_3\vec{Y} + Z_3\vec{Z} \quad (35)$$

Vectors  $(V_2 - V_1)$  and  $(V_3 - V_1)$  can thus be obtained using the above equation as follows:

$$\text{And } \vec{V}_2 - \vec{V}_1 = X_{21}\vec{X} + Y_{21}\vec{Y} + Z_{21}\vec{Z}, \vec{V}_3 - \vec{V}_1 = X_{31}\vec{X} + Y_{31}\vec{Y} + Z_{31}\vec{Z} \quad (36)$$

The length of the frame element:

$$l_e = |\vec{V}_1 - \vec{V}_2| = \sqrt{X_{21}^2 + Y_{21}^2 + Z_{21}^2} \quad (37)$$

The unit vector along the x-axis:

$$\vec{x} = \frac{(\vec{V}_1 - \vec{V}_2)}{|\vec{V}_1 - \vec{V}_2|} = \frac{X_{21}}{2a}\vec{X} + \frac{Y_{21}}{2a}\vec{Y} + \frac{Z_{21}}{2a}\vec{Z} \quad (38)$$

Therefore, the direction cosines in the x-direction are:

$$l_x = \cos(x, X) = \vec{x} \cdot \vec{X} = \frac{X_{21}}{2a}, m_x = \cos(x, Y) = \vec{x} \cdot \vec{Y} = \frac{Y_{21}}{2a}, n_x = \cos(x, Z) = \vec{x} \cdot \vec{Z} = \frac{Z_{21}}{2a} \quad (39)$$

From Figure 3.23, the direction of the z-axis can be defined by the cross product of vectors  $(V_2 - V_1)$  and  $(V_3 - V_1)$ . Hence, the unit vector along the z-axis can be expressed as [38]:

$$\vec{z} = \frac{(\vec{V}_2 - \vec{V}_1) \times (\vec{V}_3 - \vec{V}_1)}{|(\vec{V}_2 - \vec{V}_1) \times (\vec{V}_3 - \vec{V}_1)|} \quad (40)$$

$$\vec{z} = \frac{1}{2A_{123}} \{(Y_{21}Z_{31} - Y_{31}Z_{21})\vec{X} + (Z_{21}X_{31} - X_{31}Z_{21})\vec{Y} + (X_{21}Y_{31} - Y_{31}X_{21})\vec{Z}\} \quad (41)$$

$$\text{Where } A_{123} = \sqrt{(Y_{21}Z_{31} - Y_{31}Z_{21})^2 + (Z_{21}X_{31} - X_{31}Z_{21})^2 + (X_{21}Y_{31} - Y_{31}X_{21})^2}$$

Becomes

$$\begin{aligned} l_z &= \vec{z} \cdot \vec{X} = \frac{1}{2A_{123}} (Y_{21}Z_{31} - Y_{31}Z_{21}) \\ m_z &= \vec{z} \cdot \vec{Y} = \frac{1}{2A_{123}} (Z_{21}X_{31} - X_{31}Z_{21}) \\ n_z &= \vec{z} \cdot \vec{Z} = \frac{1}{2A_{123}} (X_{21}Y_{31} - Y_{31}X_{21}) \end{aligned} \quad (42)$$

Since the y-axis is perpendicular to both the x-axis and the z-axis, the unit vector along the y-axis can be obtained by cross product [38],

$$\vec{y} = \vec{y} \times \vec{x}$$

Which gives  $l_y = m_z n_x - n_z m_x$ ,  $m_y = n_z l_x - l_z n_x$ ,  $n_y = l_z m_x - m_z l_x$

Using the transformation matrix, T, the matrices for space frame elements in the global the coordinate system can be obtained as [38]:

$$\begin{aligned}
\mathbf{K}_e &= \mathbf{T}^T \mathbf{k}_e \mathbf{T} \\
\mathbf{M}_e &= \mathbf{T}^T \mathbf{m}_e \mathbf{T} \\
\mathbf{F}_e &= \mathbf{T}^T \mathbf{f}_e
\end{aligned} \tag{43}$$

After finding the total deformation, equivalent stress, equivalent strain, and strain energy on the Formula SAE M1 Chassis with the new boundary condition, the next step is to find the best design regarding Formula SAE rule. To do that the structural optimization of the frame structure take place, a kind of optimization used to improve structures, where responses come from finite element results and the design variables correspond to parameters that describe the structure [39].

Topological optimization is a special form of shape optimization, with a goal of finding suited amount of material used for the body with respect to criterion (i.e. global stiffness, stress, deformation etc.) takes out a maximum or minimum value subject to given constraints (i.e. volume reduction) and the material distribution function over a body serves as optimization parameter by defining necessary input variables (material properties, FE model, loads, etc.) for the structural problem [37].

The objective function (i.e. the function to be minimized, which are volume) and the state variables (i.e. constrained dependent variables, which are equivalent stress and total deformation) selected among a set of predefined criteria of Formula SAE M1 Chassis with new boundary condition [37].

By applying the topological optimization design with to minimum volume objectives function ( $V$ ) subject to the constraints ( $U_c^j$ ) defined. The design variables ( $\eta_i$ ) are internal, expected densities that assigned to each finite element “ $i$ ” in the topological Formula SAE M1 Chassis. The expected densities for each element vary from 0 to 1; where  $\eta_i \approx 0$  represent material to remove;  $\eta_i \approx 1$  represents material that should keep. Stated simple mathematical terms, the optimization problem is formulated as [37]:

$$V = \text{a minimum with respect to } \eta_i \tag{44}$$

Subjected to  $0 < \eta_i \leq 1$  ( $i=1, 2, 3, \dots, N$ ) and  $\underline{U}_c^j < U_c^j \leq \overline{U}_c^j$  ( $i=1, 2, 3, \dots, m$ )

Where  $V$  = Computed volume

$M$  = Number of constraints

$U_c^j$  = Computed compliance of load case  $j$

$\underline{U}_c^j$  = lower bound for compliance of load case  $j$

$\overline{U}_c^j$  = upper bound for compliance of load case  $j$

Additionally, it can constrain the weight compliance function (F) in this case the k constants are subjected by only one constraint of the form [37]:

$$\underline{F} \leq F \leq \bar{F} \quad (45)$$

Where:  $t_i$  = computed weighted compliance function

$\underline{F}$  = lower bound for the weighted compliance function

$\bar{F}$  = upper bound for the weighted compliance function

### 3.3.2 Mathematical Modeling of Crash Box or Impact Attenuator

Generally, dealing with multiple-degree of freedom systems the foregoing concepts may be extended for general cases and the Crash Box is subjected to a low impact velocity 7m/s, and acceleration with integration time step. The basic equation of motion solved by an implicit transient dynamic analysis by using equation 46 [2], [40]:

$$[m]\{\ddot{x}\} + [C]\{\dot{x}\} + [K]\{x\} = \{F\} \quad (46)$$

Where  $\{x\}$  is the nodal displacement vector,  $\{F\}$  is the nodal external force vector,  $[m]$  is called mass matrix,  $[C]$  is called the damping matrix,  $[K]$  is the stiffness matrix. Represent the governing equation of a transient structural simulation viewed as force equilibrium relation. The term  $[m]\{\ddot{x}\}$  is an inertial force,  $[C]\{\dot{x}\}$  is a damping force and  $[K]\{x\}$  is a static force and all of them resisted by external force  $\{F\}$  [40]. The Crash Box act as energy damping mechanisms, material stiffness and with a mass of the vehicle added and material stiffens.

Energy conservation is a measure of the quality of an explicit dynamic simulation. Bad energy conservation usually implies a less than optimal model definition. This parameter allows to automatically to see the solution of conservation of energy. The global energy is accounted as follows in equation 47 [40]:

Reference Energy = [Internal Energy + Kinetic Energy + Hourglass Energy]  
at the reference cycle

Current Energy = [Internal Energy + Kinetic Energy + Hourglass Energy] at  
the current cycle

Work Done = Work done by constraints + Work done by loads + Work done (47)  
by body forces + Energy removed from the system by element erosion +  
Work done by contact penalty forces

$$\text{Energy Error} = \frac{|\text{Current Energy} - \text{Reference Energy} - \text{Work Done}|}{\max(|\text{Current Energy}|, |\text{Reference Energy}|, |\text{Kinetic Energy}|)}$$

### **Crashworthiness indicator in the Formula SAE Crash Box**

To evaluate the performance of the Formula SAE crash Box thin-wall structures, several crashworthiness indicators are discussed in this section as follow which help to select the best Crash Box structure.

- a. Specific Energy Absorption (SEA): energy absorbed per unit mass, which evaluates the efficiency of Energy Absorption (EA) and is as follows:

$$SEA = \frac{EA}{m} \quad (48)$$

Where  $m$  is the mass of the structure,  $EA$  represents the total absorption during effective crash distance. The effective crash distance is set to be 10mm in this research paper.

- b. Mean Crashing Force (MCF): evaluates the crush strength of a Crash Box structure and described as the total energy absorption divided by the deformation length  $d$ .

$$MCF = \frac{EA}{d} \quad (49)$$

- c. Pick Crash Force (PCF): an indicator often considered critical to the survival rate of the driver or occupants in the vehicle safety.
- d. Total deformation or deformation length ( $d$ ): shows when the conservation of energy from kinetic energy to deformation to reduce the damage done to structures, vehicles, and driver resulting from a motor vehicle collision.

## **3.4 Finite Element Modeling and analysis**

### **3.4.1 Finite Element Modeling and analysis for Formula SAE Chassis**

The frame element also known in many commercial software packages as the general beam element, or even simply the beam element. Commercial software packages usually offer both pure beam and frame elements, but frame structures used in actual engineering applications. A three-dimensional spatial frame structure can practically take forces and moments of all directions. Hence, it can be considered to be the most general form of an element with a one-dimensional geometry and applicable for the analysis of skeletal type systems of both planar frames (two-dimensional frames) and space frames (three-dimensional frames) structures [38].

Selecting realistic boundary conditions for Formula SAE Chassis Model is one of the most important and challenging parts of before setting up a simulation. Thus, the first part is to understand what the expected real-world behavior. Secondly, understanding how such behavior is modeled in the software. This raises the question: what is the right boundary

condition, how to find them? what is the basic component of the basic component of vehicle and location?

The basic component of Formula SAE vehicle is a seat, Engine, fuel tank, driver train, Battery, Steering, FSAE Crash Box, Body cover including an airfoil, Formula SAE Chassis and adding the driver and fuel mass, these are attached to the vehicle chassis and cause a different kind of loading condition. Their respect center of mass found when the geometry development of the FSAE Chassis in section 3.2.1.1. and basic component geometry size, attachment, and arrangement with respect to their location.

Formula SAE Chassis subjected to different kinds of loading in real-world conditions due to the boundary condition subjected and they can vary the result found in the simulation, based on that in this research paper classified the boundary condition used in two parts:

- a. **Old boundary condition:** applied on the Formula SAE M1 Chassis the following assumption take place from the preceding researches and journal papers and is the result of all mass (278.248Kg) of the component including the Chassis weight applied at the center of the vehicle case different kind of loading.
- b. **New boundary condition:** applied on the Formula SAE M1 and M2 Chassis in their perspective center of mass such as driver + seat 75Kg, Engine 70Kg, fuel + fuel tank 9.62Kg, driver train 20Kg, Battery 4Kg, Steering 10kg, FSAE Crash Box M1 3Kg, Body cover including airfoil 35Kg, [2], [15], [17] Formula SAE M1 and M2 Chassis mass case different kind of loading.

The static analysis solution method is applicable to all degrees of freedom space frame structure without considering the Inertial and damping effects, except for static acceleration fields [37]. The Chassis designed in SOLIDWORKS 2018 software and exported into the FEA software ANSYS 19.1, with a circular hollow cross-sections area pipe.

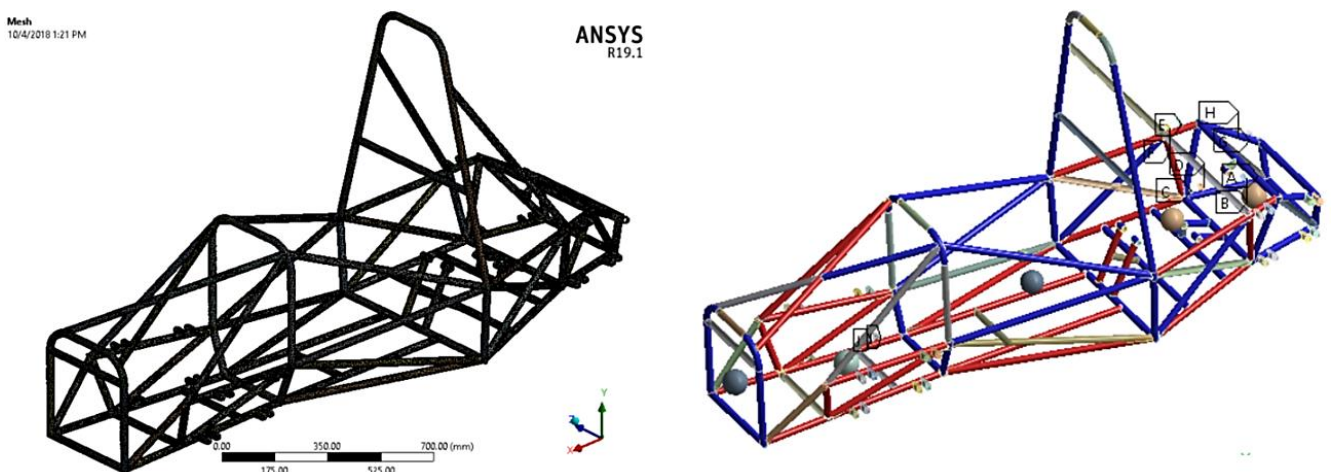


Figure 3.24 Mesh size and contact between members

The mesh size for each element length of 10mm with a Tetrahedrons of the order of quadratic, with element number 173448 and node number 355898 for Formula SAE M1 Chassis and element number 197785 and node number 406022 for Formula SAE M2 Chassis considered as a beam element. The finite element modeling and illustrate using Figure 3.25:

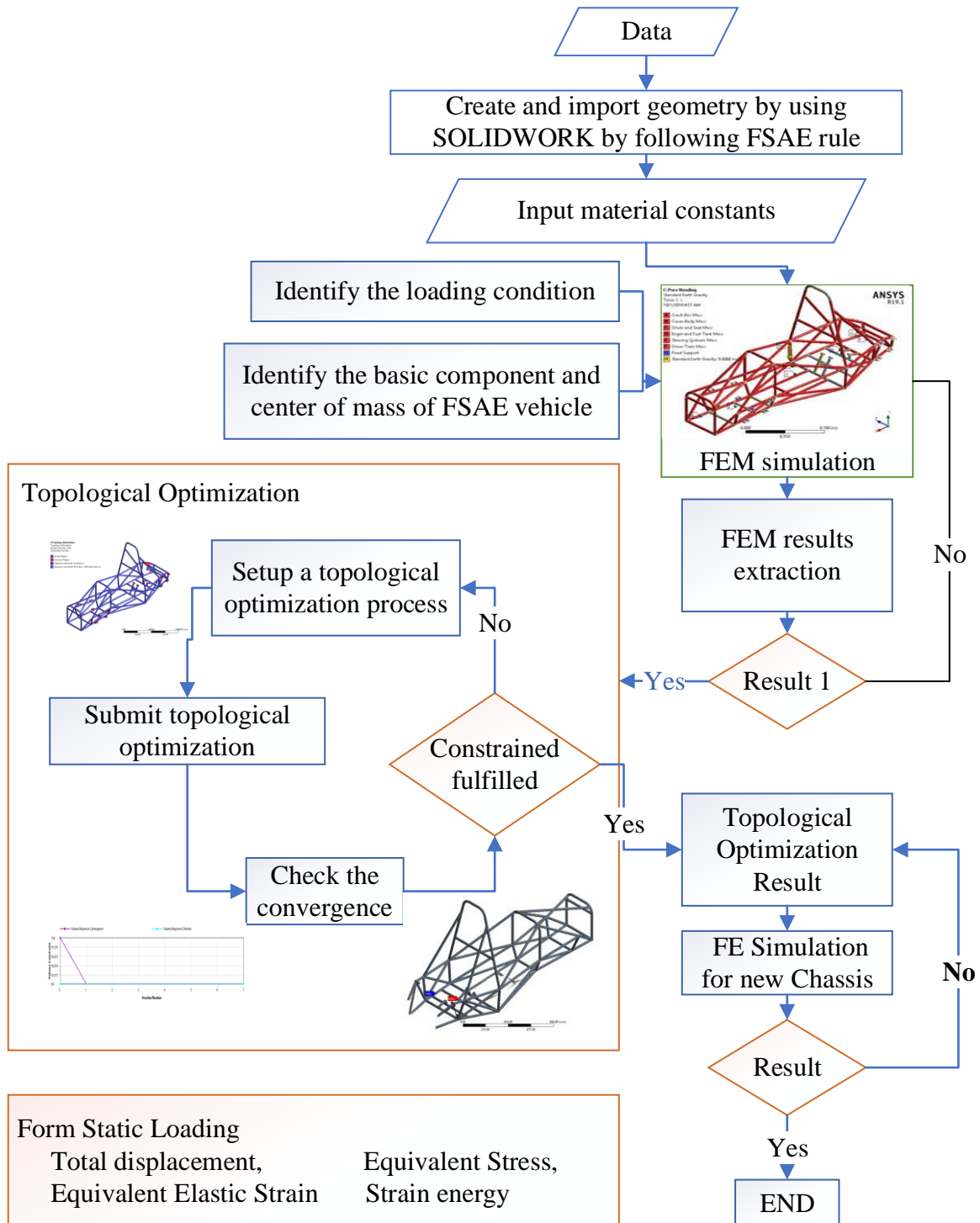


Figure 3.25 Static analysis for Formula SAE Chassis

### 3.4.1.1 Formula SAE M1 with Old Boundary Condition

#### 3.4.1.1.1 Vertical Symmetric or Vertical Bending ('pure bending') Load Analysis

To estimate the various load which are acting on the vehicle FSAE structure are estimate according to the center of gravity of the vehicle and these loads act as a manner of driver 75Kg [17], Engine 70Kg [17], fuel + fuel tank 9.62Kg [12], driver train 20Kg, Chassis 36.628Kg, Battery 4Kg [12], Steering 10kg [12], FSAE Crash Box M1 3Kg and Body cover including airfoil 35Kg, then the weight of the car become 278.248Kg and fixed in the steering system joint place as see in Figure 3.26.

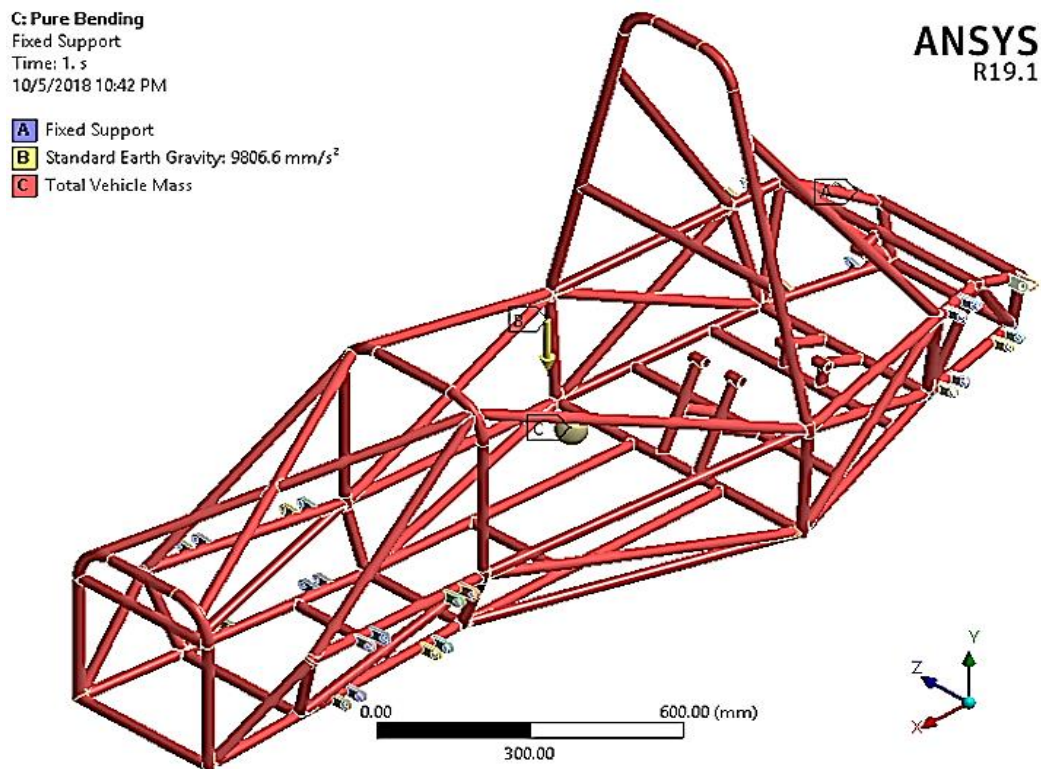


Figure 3.26 Pure bending load applied on the Formula SAE M1 Chassis

#### 3.4.1.1.2 Vertical Asymmetric or Longitudinal Torsion (Pure Torsion Analysis Case)

The same as section 3.4.1.2.2 because, the total mass of the vehicle distributed equally to four points on the steering system hinge, based on that 68.3625Kg ( $278.248\text{Kg}/4$ ) applied to each point, each steering system hinge have four hinges used to connect the steering system to the Formula SAE M1 Chassis.

#### 3.4.1.1.3 Longitudinal loads (Braking) Analysis

The total mass of the Formula SAE is 278.243Kg, the position at the center of the vehicle with a gravity acceleration of  $9.81\text{m/s}^2$  and a braking load of  $1.5g$  ( $14.715\text{m/s}^2$ ) induced in the frame structure due to stop. The firm-fixed in four sides of the steering points.

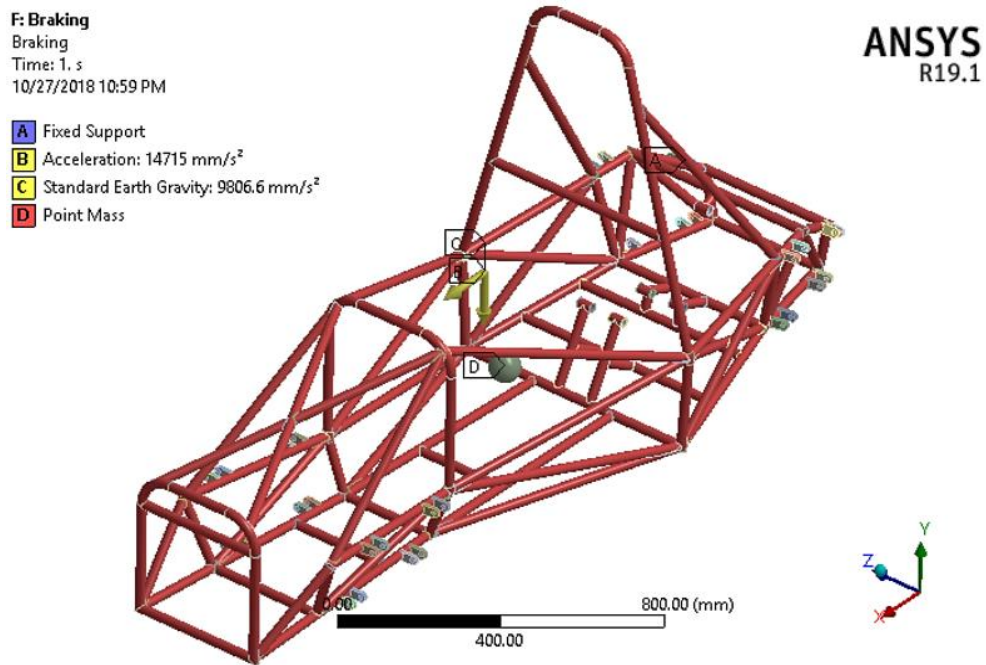


Figure 3.27 Longitudinal load (braking) applied to the Formula SAE M1 Chassis

#### 3.4.1.1.4 Lateral Bending (Cornering) Analysis

The total mass of the Formula SAE is 278.243Kg, the position at the center of the vehicle with a gravity acceleration of  $9.81\text{m/s}^2$ . Induced in the frame structure due to sliding of tires (cornering) and the sideways forces will act along the length of the car Chassis, will be resisted at the tires with a magnitude of  $1.5g$  ( $14.715\text{m/s}^2$ ), this causes a lateral load and resultant bending [3].

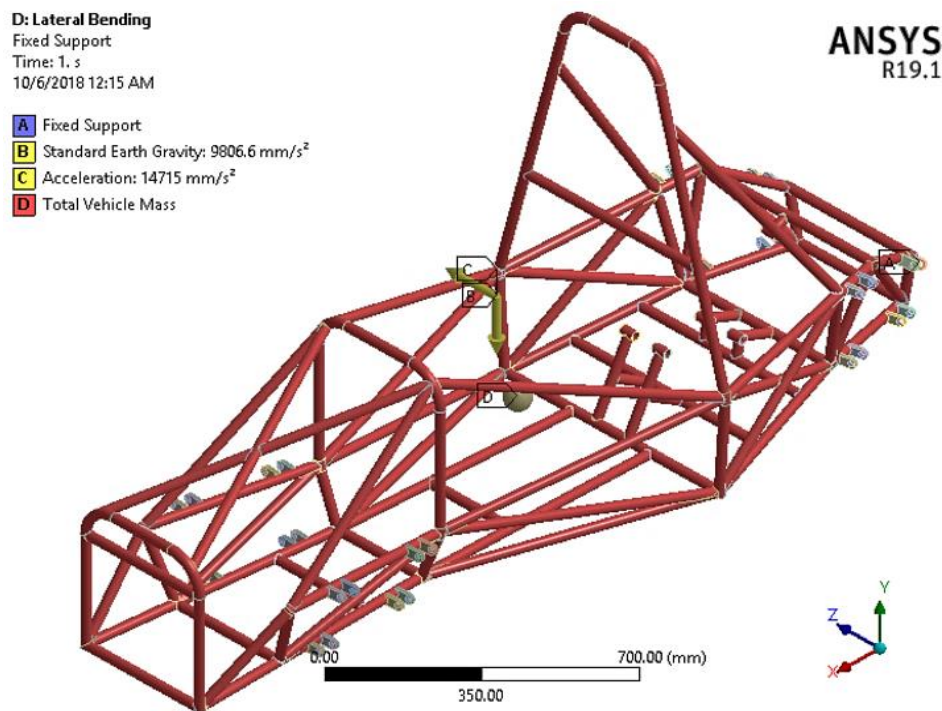


Figure 3.28 Lateral bending (cornering) load applied on the Formula SAE M1 Chassis

### 3.4.1.1.5 Crash or Impact cases (Front, Side and Rollover Crash) Analysis

The same as section 3.4.1.2.5 because, the same amount of load applied in the main hoops, front hoops, and front bulkhead in Formula SAE M1 Chassis.

### 3.4.1.1.6 Combinations of Load Analysis

This occurred due to the combination of pure bending and pure torsional load case [2].

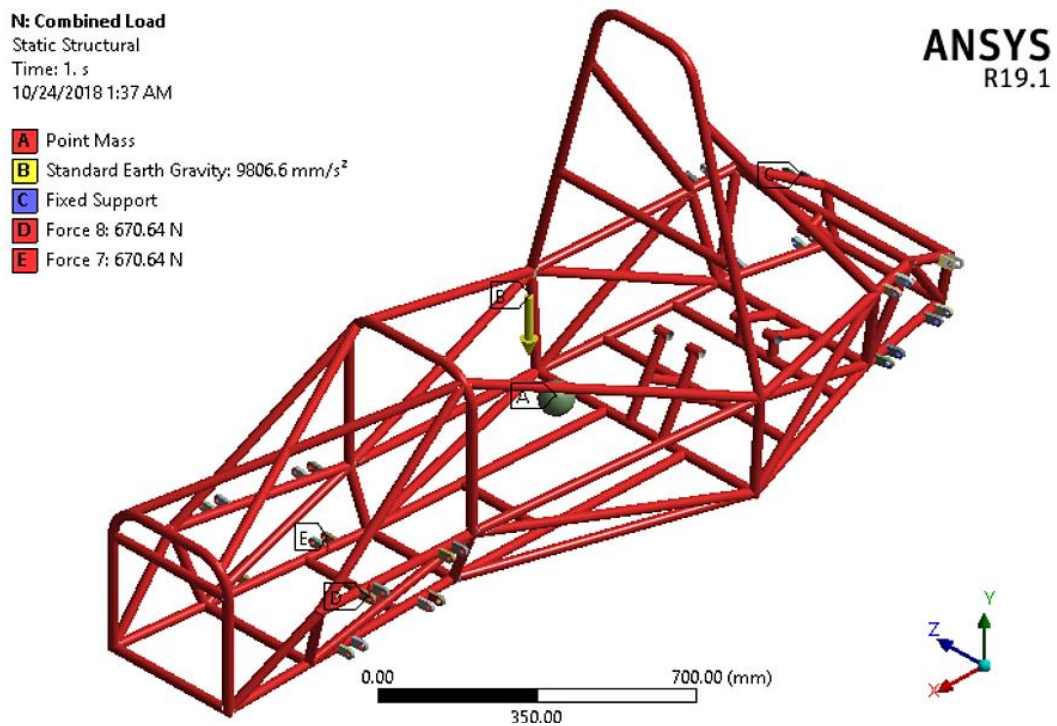


Figure 3.29 Combination of the load applied on the Formula SAE M1 Chassis

### 3.4.1.1.7 Horizontal Lozenging Analysis

The total mass of the Formula SAE is 278.243Kg and position at the center of the vehicle with a gravity acceleration of 9.81m/s<sup>2</sup>. These forces tend to distort the frame into a parallelogram shape [13] with a magnitude of 3.5g [12], [17] and fixed in three points of the steering system joint place and one is free.

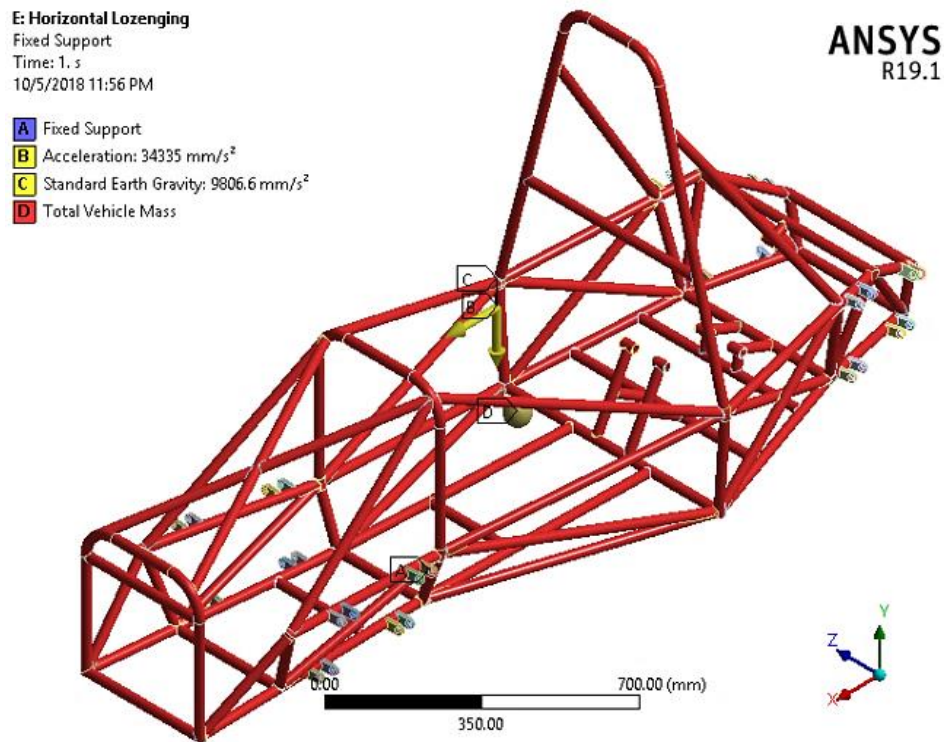


Figure 3.30 Horizontal lozenge load applied on the Formula SAE M1 Chassis

### 3.4.1.2 Formula SAE M1 and M2 with New Boundary Condition

#### 3.4.1.2.1 Vertical Symmetric or Vertical Bending (‘pure bending’) Load Analysis

This occurs when both wheels on one axle of the vehicle encounter a symmetrical bump simultaneously see Figure 1.9 [3]. This applies a bending moment to the vehicle about a lateral axis. The weight of the driver and other components mounted to the frame, such as the engine, drive train, steering and battery carried by the Chassis frame structure which will create a bending through the car frame. The reactions took up at the axles [23].

Table 12 Approximate masses of main components for Formula SAE M1 Chassis [2], [7], [12], [17].

No.	Components	Mass (kg)	Location
1	Driver + Seat	(75+15) 90	Between the front and main hoops at C
2	Engine + fuel tank + fuel	(70 + 5 + 4.62) 79.62	Engine mount at D
3	Driver-train	20	At G
4	Steering	10	At E
5	Battery	4	At G
6	Chassis	36.628	At c.g of Chassis
7	M1 Crash Box mass	3	In front of the front bulkhead at B
8	Body cover with airfoil	35	Cover the Chassis at H
	Total	278.248	---

For the vertical bending load analysis, all the components weight including the driver, engine, and Chassis sit specified at their own specific points on the Chassis. Simply supported constraints will be on the front and rear wheelbase points as seen in Figure 3.31 and Figure 3.32.

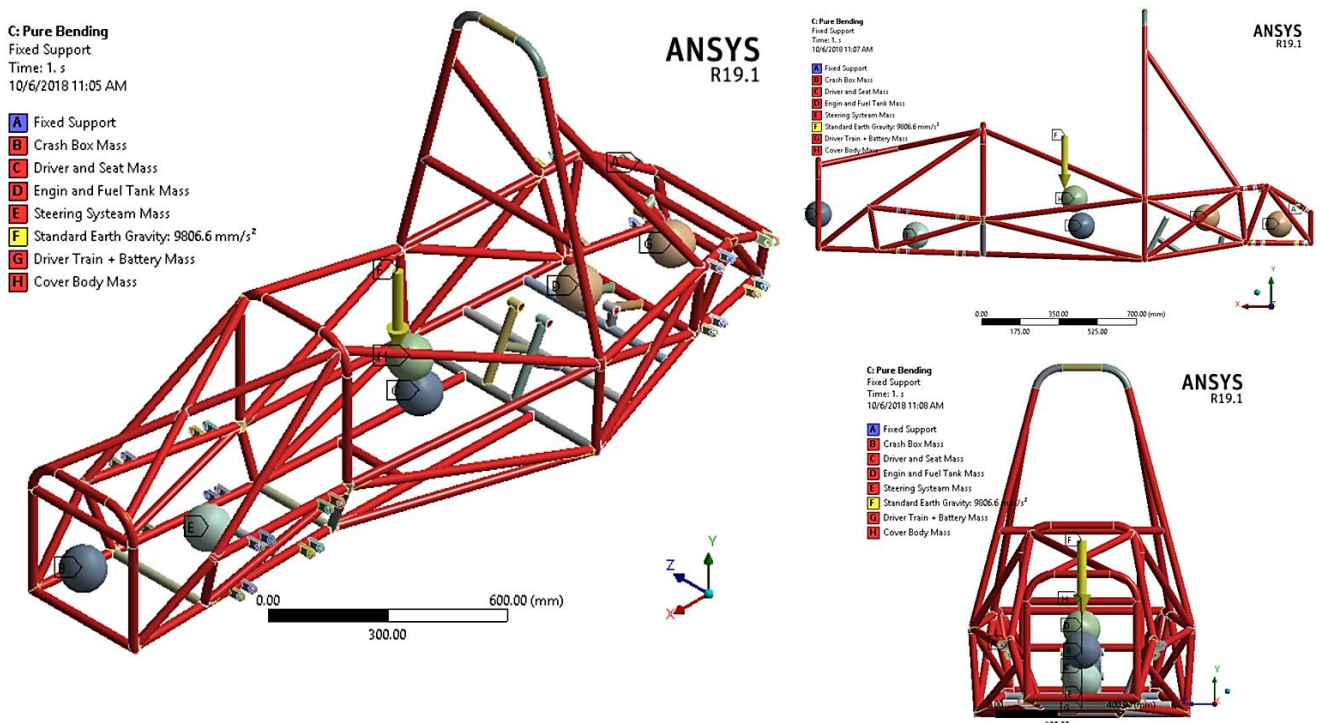


Figure 3.31 Pure bending load applied on the Formula SAE M1 Chassis (front, side, and isometric view)

Table 13 Approximate masses of main components for Formula SAE M2 Chassis [2], [7], [12], [17].

No.	Components	Mass (kg)	Location
1	Driver + Seat	(75+15) 90	Between the front and main hoops at C
2	Engine + fuel tank + fuel	(70 + 5 + 4.62) 79.62	Engine mount at D
3	Driver-train	20	At G
4	Steering	10	At E
5	Battery	4	At G
6	Chassis	29.00211	At c.g of Chassis
7	M1 Crash Box mass	3	In front of the front bulkhead at B
8	Body cover with airfoil	35	Cover the Chassis at H
	Total	270.61711	---

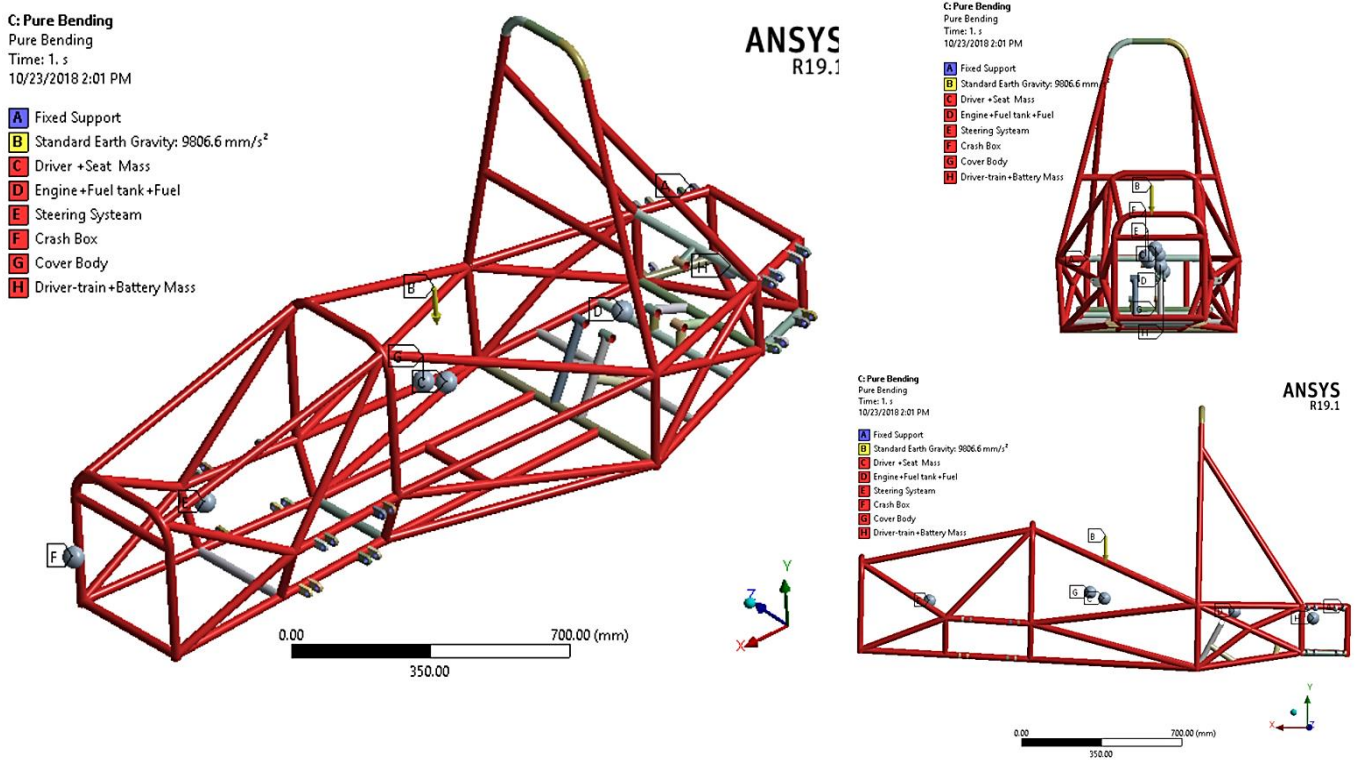


Figure 3.32 Pure bending load applied on the Formula SAE M2 Chassis (front, side, and isometric view)

### 3.4.1.2.2 Vertical Asymmetric or Longitudinal Torsion (Pure Torsion Analysis Case)

The total mass of the vehicle is 278.243Kg (which is the mass of the Chassis, engine, fuel, fuel tank, battery, steering system, driver and drivetrain, and other parts). Therefore, the total mass of the vehicle distributed equally to four points on the steering system hinge, based on that 69.562 68.3625Kg (278.243Kg/4) for Formula SAE M1 and 67.6542775Kg (270.61711Kg/4) for Formula SAE M2 applied to each point, each steering system hinge have four hinges used to connect the steering system to the Formula SAE M1 Chassis, Therefore the load applied at the hinges is:

$$F = 68.3625\text{Kg} * 9.81\text{m} = 670.636125\text{N}$$

Therefore, the moment created on the hinges is the force multiplied by the perpendicular distance (521.98mm/2 = 260.99mm=0.26) from the center of the lateral axis of the Formula SAE Chassis.

$$M = 670.636125 * 0.26\text{m} = 174.3653925\text{Nm}$$

The moment created on the FSAE Chassis act in the two sides of the front steering system like a couple Therefore the total moment becomes:

$$2 * M = 174.3653925\text{Nm} * 2 = 348.730785\text{Nm}$$

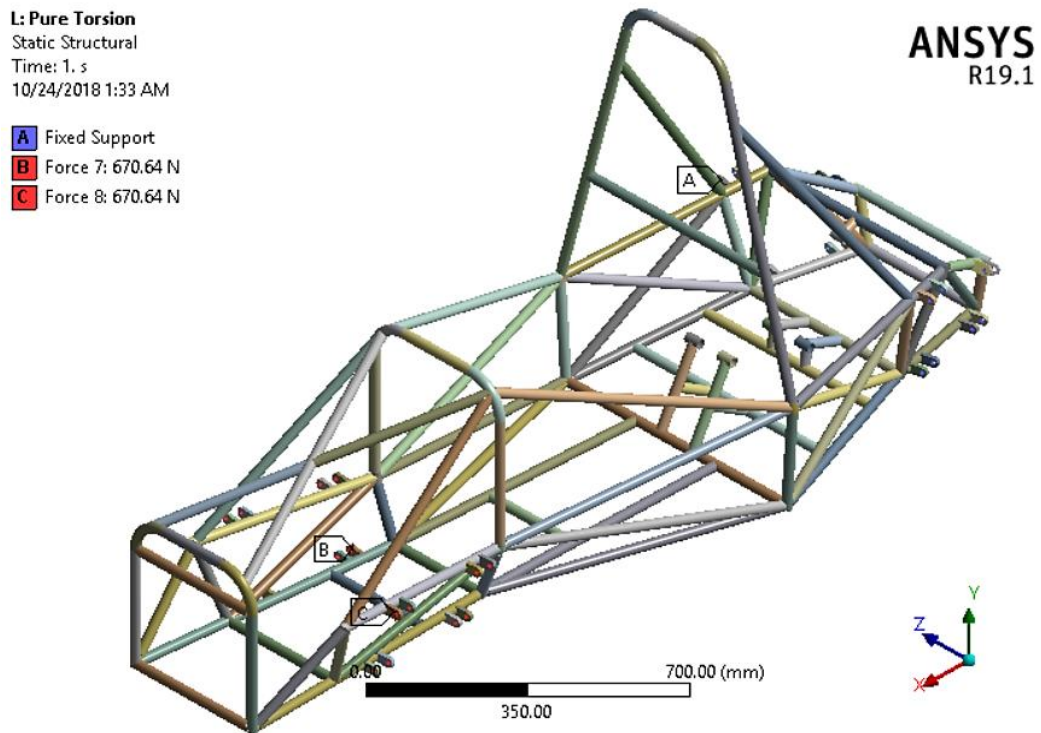


Figure 3.33 Pure torsional load applied on the Formula SAE M1 Chassis (front, side, and isometric view)

Formula SAE M2 Chassis, Therefore the load applied at the hinges is:

$$F = 67.6542775\text{Kg} \cdot 9.81\text{m} = 663.688462275\text{N}$$

Therefore, the moment created on the hinges is the force multiplied by the perpendicular distance ( $521.98\text{mm}/2 = 260.99\text{mm} = 0.26$ ) from the center of the lateral axis of the Formula SAE Chassis.

$$M = 663.688462275\text{N} \cdot 0.26\text{m} = 172.559\text{ Nm}$$

The moment created on the FSAE Chassis act in the two sides of the front steering system as a couple Therefore the total moment becomes:

$$2 \cdot M = 172.559\text{ Nm} \cdot 2 = 345.118\text{Nm}$$

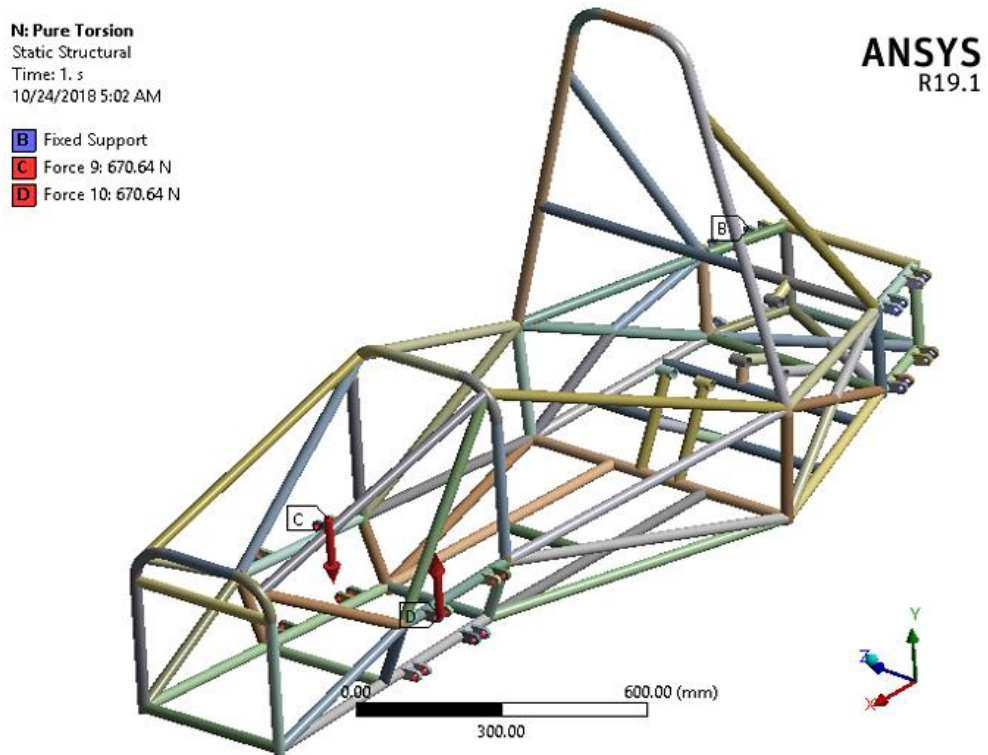


Figure 3.34 Pure torsional load applied on the Formula SAE M2 Chassis (front, side, and isometric view)

To calculate the torsional rigidity or stiffness of the chasses:

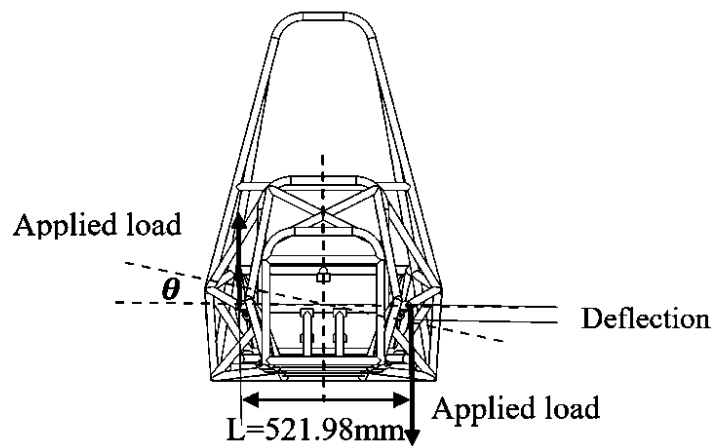


Figure 3.35 Torsional load applied on Formula SAE Chassis

For Formula SAE Chassis the torsional stiffness range is between 1000-5000Nm/deg [41] and is equal to:

$$K = T/\theta \tag{50}$$

Where: L is the distance between the two wheel supports, the angle of rotation as shown in Figure 3.35 can calculate from:

$$\theta = \tan^{-1} \left( \frac{\text{Deflection}}{(L/2)} \right) \tag{51}$$

and the torque or moment created on the Chassis:

$$T = \text{applied load} \times L \quad (52)$$

### 3.4.1.2.3 Longitudinal loads (Braking) Analysis

The total mass of the Formula SAE is 278.243Kg for M1 and 270.61711Kg for M2 distributed in the vehicle according to their approximated real position, with a gravity acceleration of  $9.81\text{m/s}^2$  and a braking load of  $1.5g$  ( $14.715\text{m/s}^2$ ) induced in the frame structure. The firm-fixed in four sides of the steering points [12], [17].

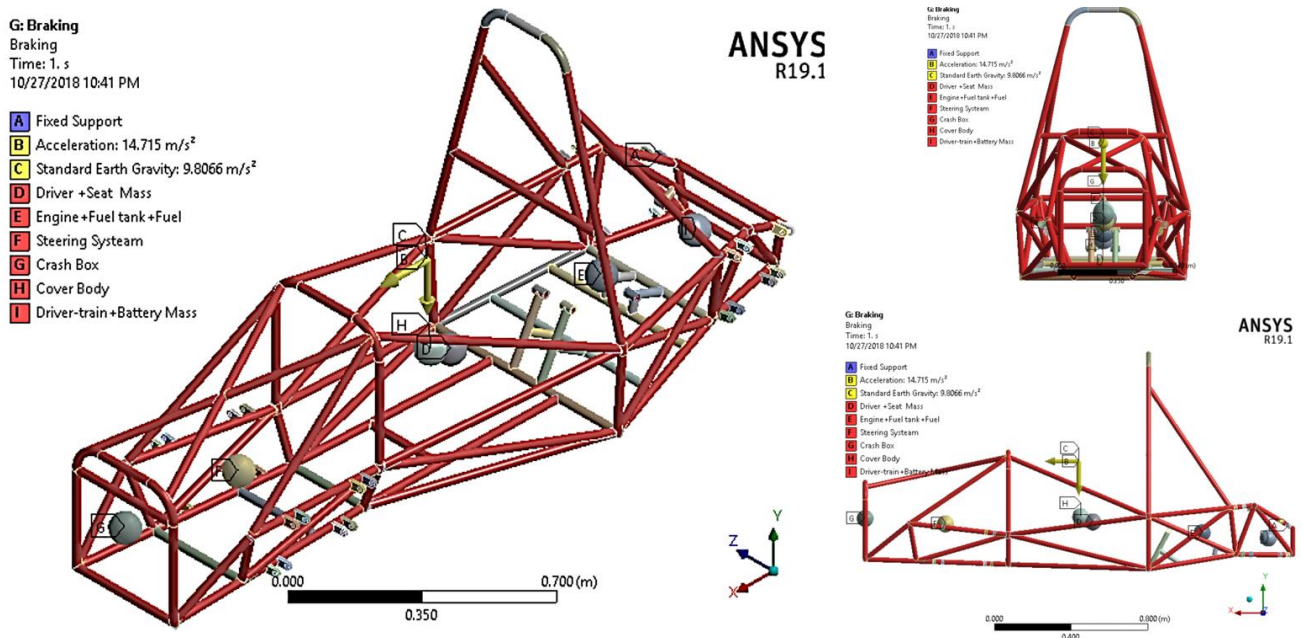


Figure 3.36 Longitudinal (braking) load applied on the Formula SAE M1 Chassis (front, side, and isometric view)

### 3.4.1.2.4 Lateral Bending (Cornering) Analysis

The mass of the Formula SAE components distributed to their respective point and subjected to a gravity acceleration of  $9.81\text{m/s}^2$ . Induced in the frame structure due to sliding of tires (cornering) and the sideways forces will act along the length of the car Chassis, will be resisted at the tires with a magnitude of  $1.5g$  ( $14.715\text{m/s}^2$ ), this causes a lateral load and resultant bending [3].

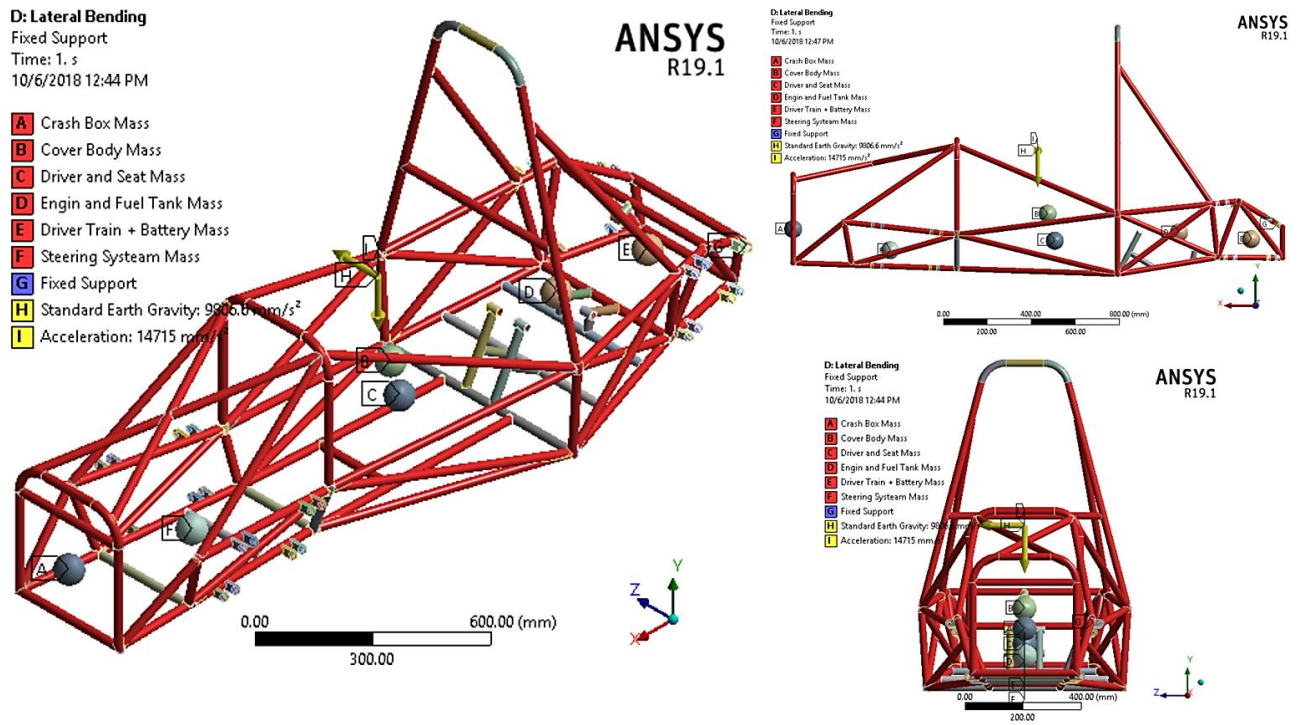


Figure 3.37 Lateral bending (cornering) load applied on the Formula SAE M1 Chassis (front, side, and isometric view)

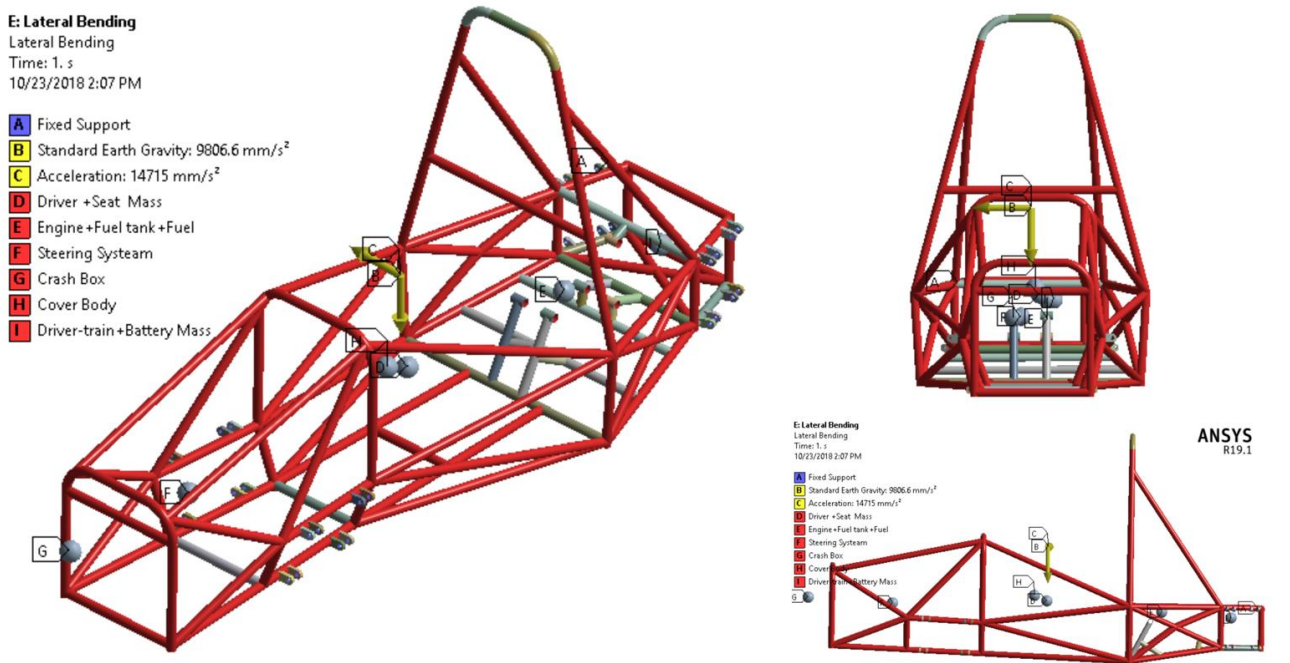


Figure 3.38 Lateral bending (cornering) load applied on the Formula SAE M2 Chassis (front, side, and isometric view)

### 3.4.1.2.5 Crash or Impact cases (Front, Side and Rollover Crash) Analysis

#### a. Front Analysis

In the front impact scenario the following load (120kN, 0N, 0N) applied in the actual attachment points between the impact attenuator and the front bulkhead, with a fixed displacement (x, y, z) but not rotation of the bottom nodes of both sides of the main roll hoop and both locations where the main hoop and shoulder harness tube connect [2], [16].

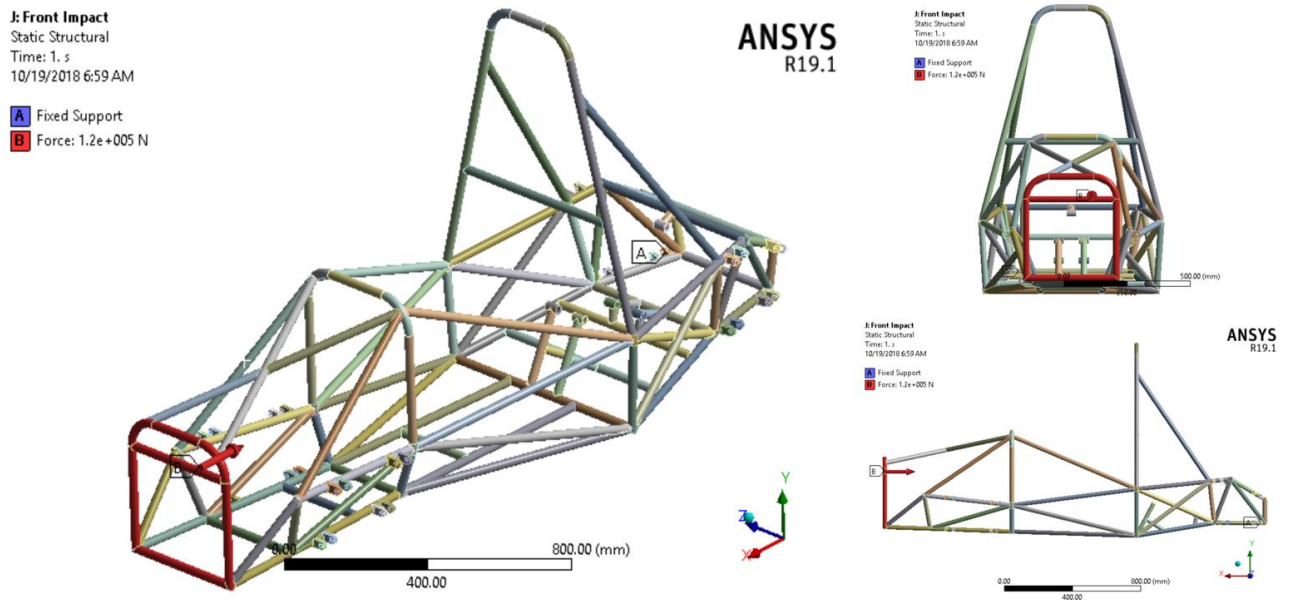


Figure 3.39 Front impact load applied on the Formula SAE M1 Chassis (front, side, and isometric view)

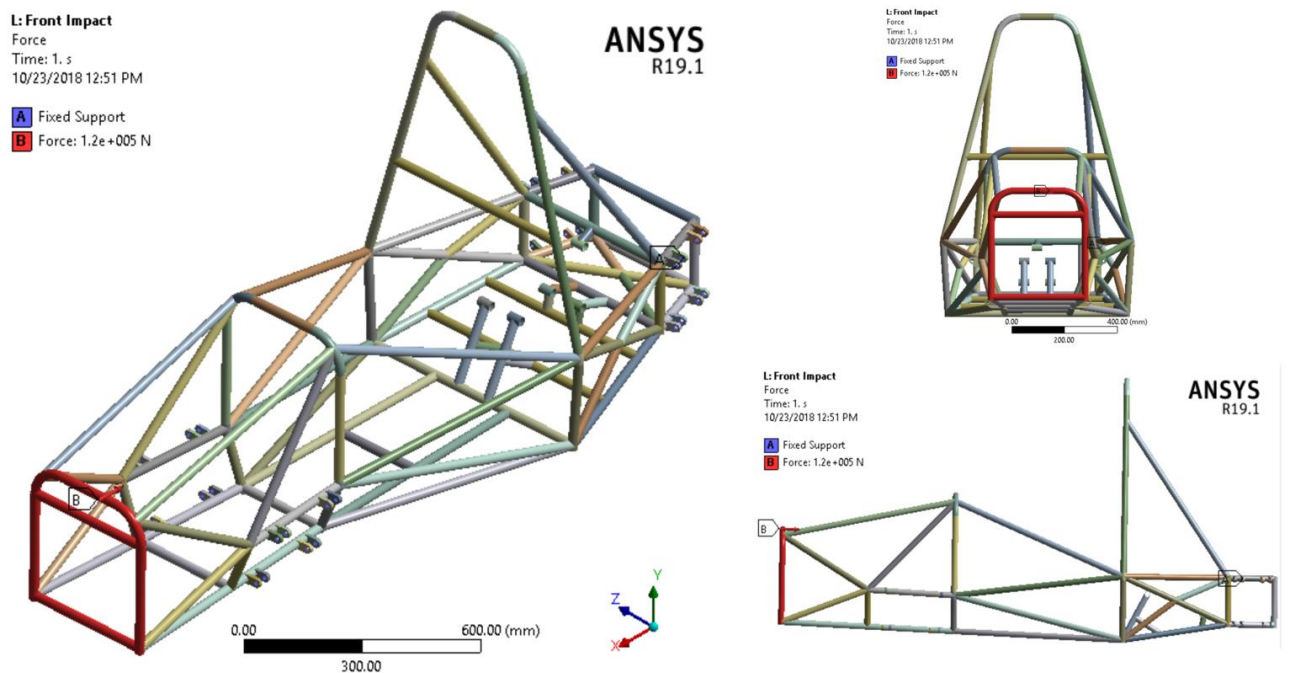


Figure 3.40 Front impact load applied on the Formula SAE M2 Chassis (front, side, and isometric view)

### b. Side Analysis

Side impact: the load applied is (0N, 0kN, 7.0N) with the following application point in the actual attachment points between the front roll and main roll hoops. Fixed displacement (x, y, z) but not the rotation of the bottom nodes of both sides of the front and main roll hoops [2], [16].

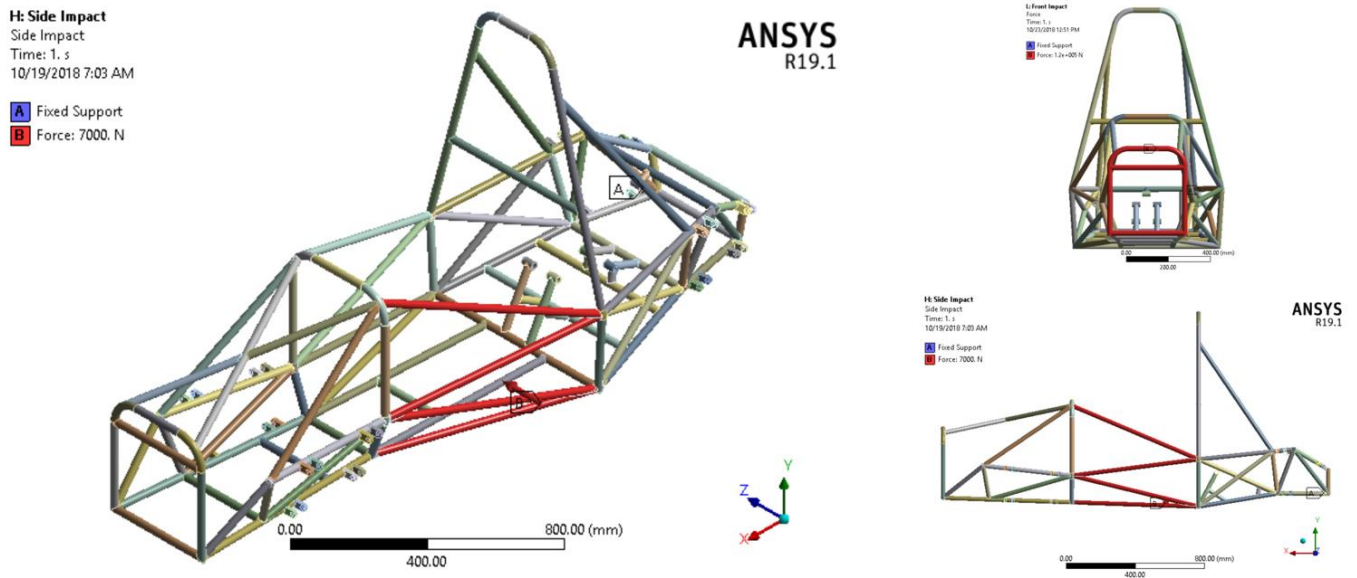


Figure 3.41 Side impact load applied on the Formula SAE M1 Chassis (front, side, and isometric view)

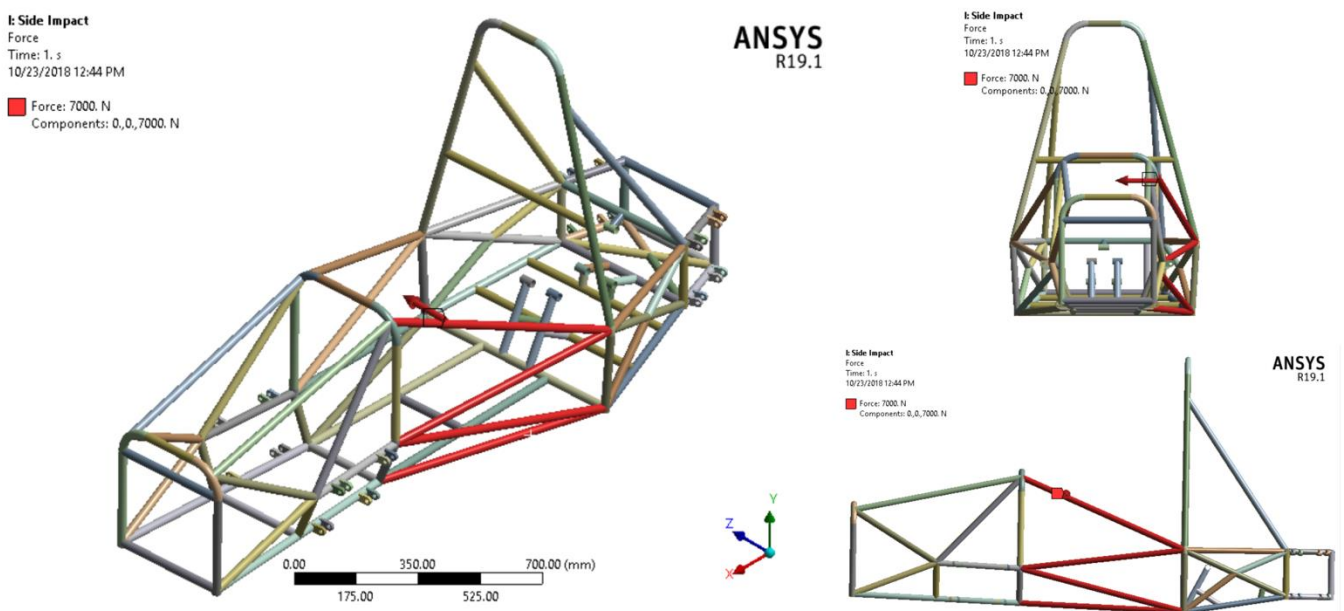


Figure 3.42 Side impact load applied on the Formula SAE M2 Chassis (front, side, and isometric view)

### c. Rollover Crash Analysis

In the main roll hoop, bracing and bracing support the following load applied (6.0kN, -9.0kN, 5.0kN) on top of main roll hoop and fixed displacement (x, y, z) but not rotation of the bottom nodes of both sides of the front and main roll hoops, with maximum allowable deflection of 25mm and no failure must occur anywhere in structure [2], [16] in the front roll hoops, the following load applied is (6.0kN, -9.0kN, 9.0kN) on the top of front roll hoop and fixed displacement (x, y, z) but not rotation of the bottom nodes of both sides of the front and main roll hoops, with a maximum allowable deflection of 25mm and no failure must occur anywhere in structure [2], [16].

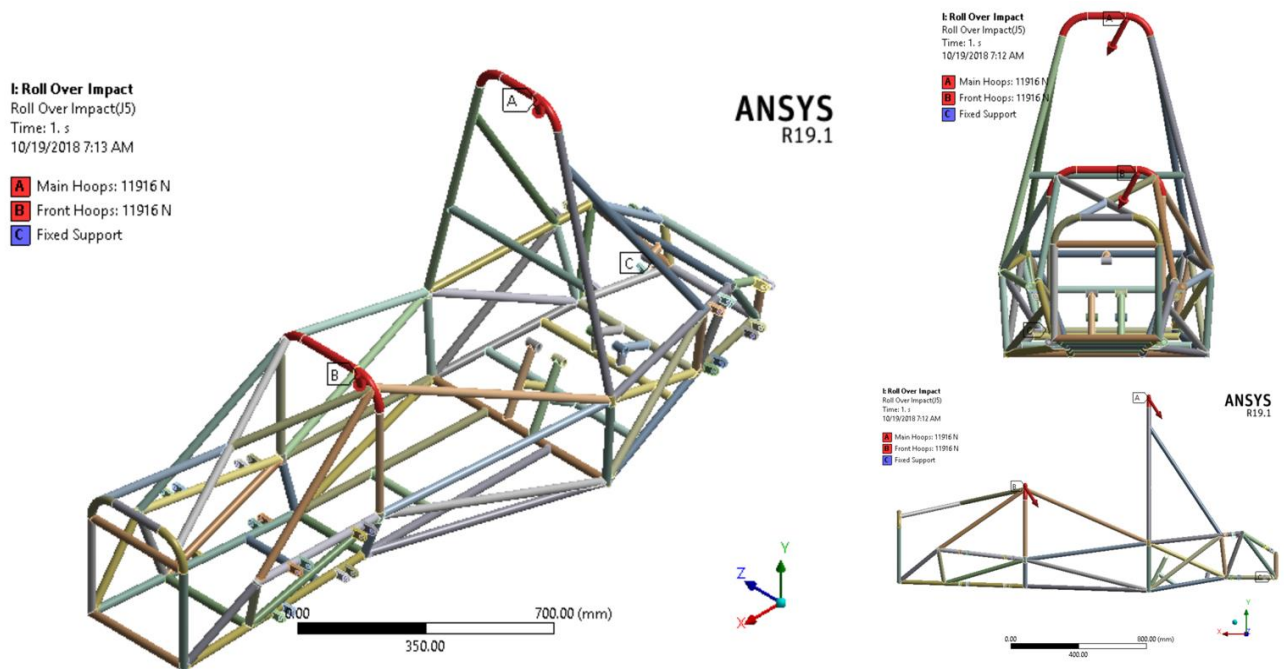


Figure 3.43 Rollover load applied on the Formula SAE M1 Chassis (front, side, and isometric view)

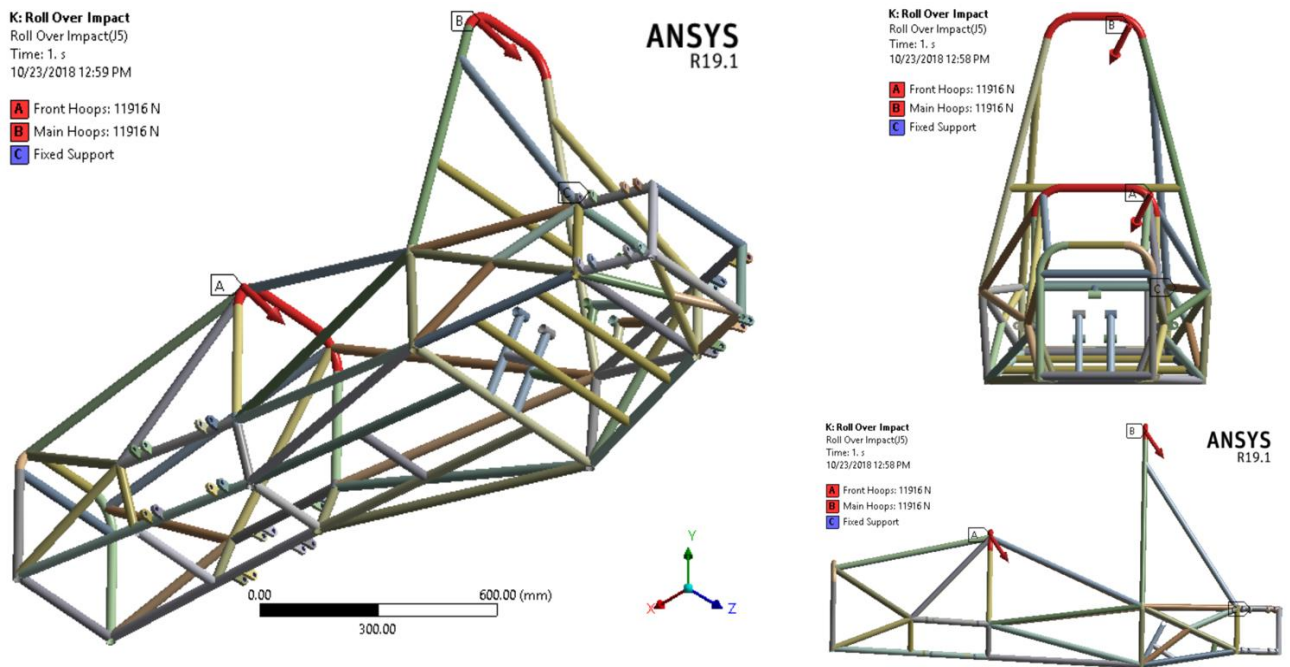


Figure 3.44 Rollover impact load applied on the Formula SAE M2 Chassis (front, side, and isometric view)

### 3.4.1.2.6 Horizontal Lozenging Analysis

Forward and backward forces applied at opposite wheels cause this deformation. These forces caused by vertical variations in the pavement or the reaction from the road driving the car forward. These forces tend to distort the frame into a parallelogram shape [13] with a magnitude of 3.5g [12], [17].

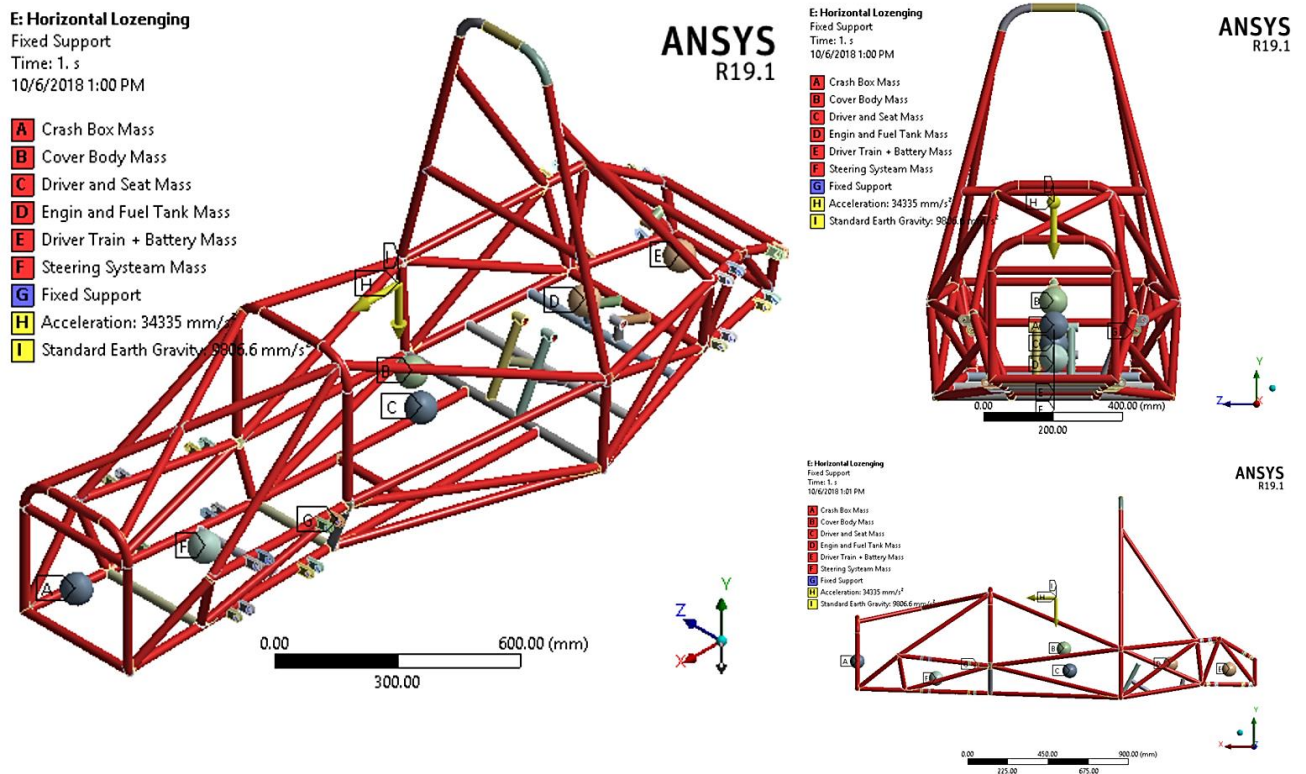


Figure 3.45 Horizontal lozenge load applied on the Formula SAE M1 Chassis (front, side, and isometric view)

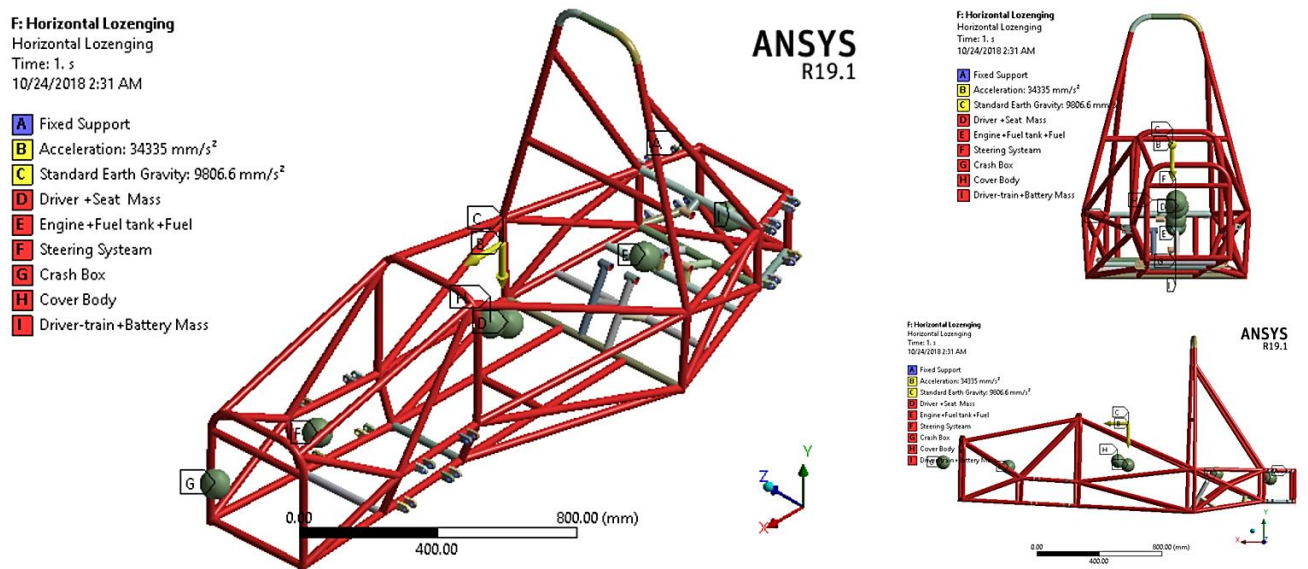


Figure 3.46 Horizontal lozenge load applied on the Formula SAE M2 Chassis (front, side, and isometric view)

### 3.4.1.2.7 Combinations of Load Analysis

This occurred due to the combination of pure bending and pure torsional load case [2].

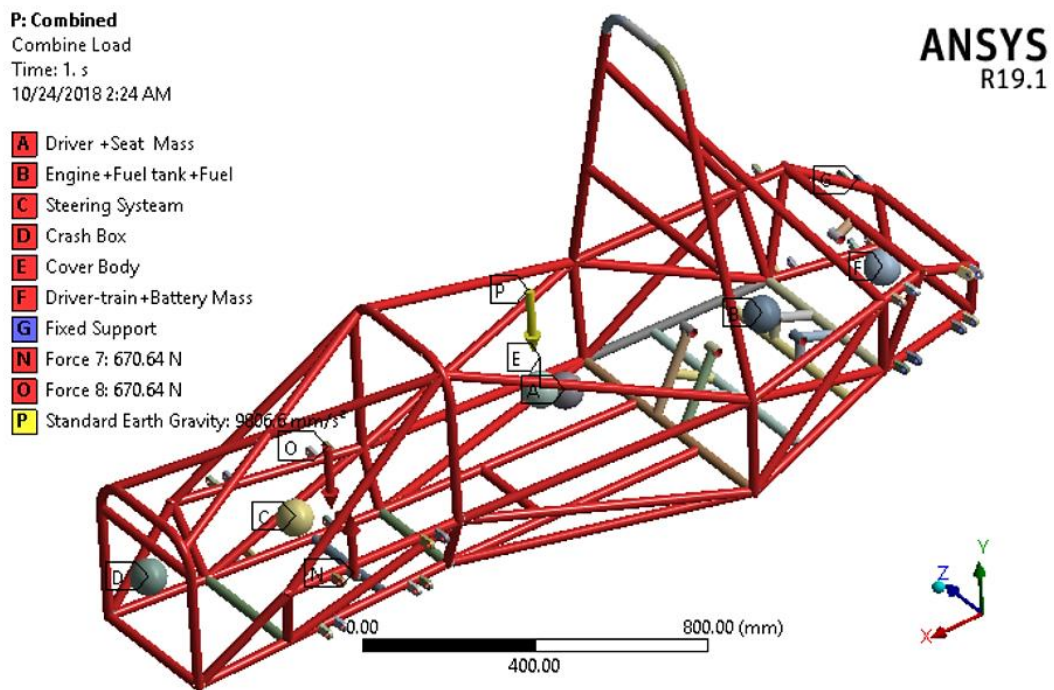


Figure 3.47 Combination of the load applied on the Formula SAE M1 Chassis (Isometric view)

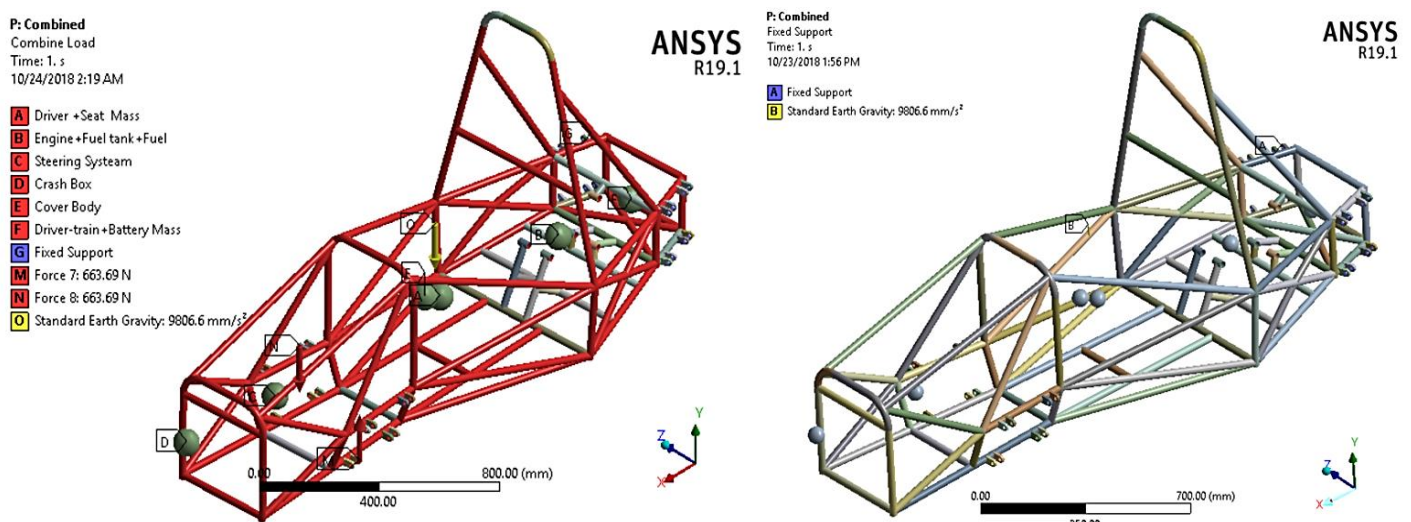


Figure 3.48 Combination of the load applied on the Formula SAE M2 Chassis (front, side, and isometric view)

### 3.4.1.3 Topological optimization of Formula SAE M1 Chassis

To apply the topological optimization on the frame Chassis the following constrained considered with the objectives of volume reduction of 10 to 15%. The constrained variable is the equivalent Von-Messes stress and the total deformation of the frame structure by using ANSYS Workbench topological optimization tool and divided into two parts design and exclusion region. The design region is where the optimization takes place and the exclusion

region are a non-optimized area, where engine mounting and suspension joining members as seen in Table 14.

Table 14 Optimization constrained and non-constrained region

Optimization constrained and non-constrained region		
Loading type	Total deformation (mm)	Equivalent Stress (MPa)
Pure Bending	0.5939	226.97
Pure Torsion	0.73674	220.82
Braking	0.84209	311
Lateral Bending	0.72157	145.46
Font Impact	0.40708	285.59
Side Impact	0.33245	112.61
Rollover Impact	1.6198	120.5
Horizontal Lozenging	1.4454	146.57
Combined	2.1557	338.8

### 3.4.2 Finite Element Modeling and Analysis for Crash Box or Impact Attenuator

In an ANSYS Explicit Dynamics solution started with a discretized domain (mesh) with assigned material properties, loads, constraints, initial conditions and this initial state integrated with time, will produce motion at the node points in the mesh seen in Figure 3.49 [40].

- ✓ The motion of the node points produces deformation in the elements of the mesh, and cause a change in volume of the material of each element,
- ✓ The rate of deformation used to derive material strain rates using Johnson-Cook Strength,
- ✓ Constitutive laws take the material strain rates and derive resultant material stresses and material stresses transformed back into nodal forces using various element formulations,

- ✓ External nodal forces computed from boundary conditions, loads, contact (body interaction) which will produce nodal accelerations and integrated explicitly in time to produce new nodal velocities,
- ✓ The nodal velocities integrated explicitly in time to produce new nodal positions,
- ✓ The solution process (Cycle) repeated until a user-defined time reached.

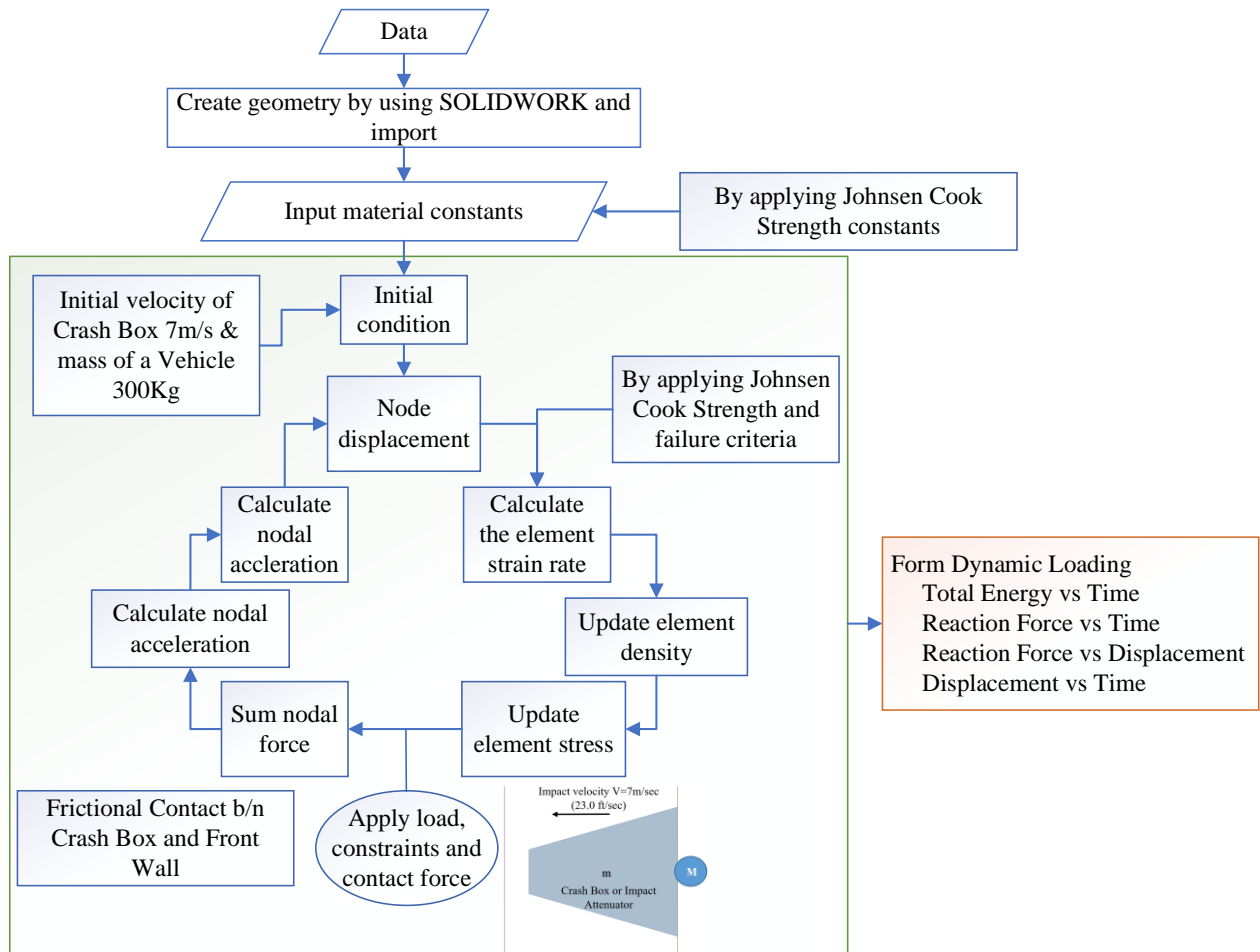


Figure 3.49 ANSYS Explicit Dynamics system for Crash Box

The ANSYS Explicit Dynamics system is designed to simulate nonlinear structural mechanics applications involving impact (from low 1m/s to very high velocity 5000m/s), rigid and flexible bodies, large deformations, complex contact conditions and also, most suited to events which take place over short periods of time, a few milliseconds or less therefore this impact takes place in low deformation/velocity (<100m/s) analysis by using a rigid boundary condition to prevent flow of material through cell faces for the front wall or barrier and front bulkhead have the following rigid stiffness behavior of [40]. This condition makes the external boundaries of the domain act as a rigid wall with a Stiffness behavior of rigid.

The material type for the impact attenuator was chosen Aluminum 7075-T651 plate and the mechanical prosperity which is stated in the above in material selection of Crash Box section, considering the Johnson-Cook strength and failure models criteria which states that when the impact scenario take place is beyond the elastic limit, different and have a high amount of kinetic energy will be generated, Therefore the energy will be converted to another form of Energy's (deformation, sound, heat and friction energy) [26].

The contact between the Crash Box or Impact Attenuator and the barrier was defined as surface-to-surface as a frictional contact in ANSYS 19.1 Explicitly Dynamics with the static and kinematic coefficient of friction selected as 0.3 and 0.2 respectively [18].

The following boundary conditions are considered on the Crash Box or Impact Attenuator: the mass of the total vehicle with its driver 300Kg and in any case, it should not penetrate the front bulkhead and the front wall these two barriers considered as a rigid, and the Crash Box moved with 7m/s (23.0 ft/sec) in the z-direction a non-yielding impact barrier in back with front Bulkhead and decelerates the vehicle at a rate not exceeding 20 g's average and 40 g's peak [2].

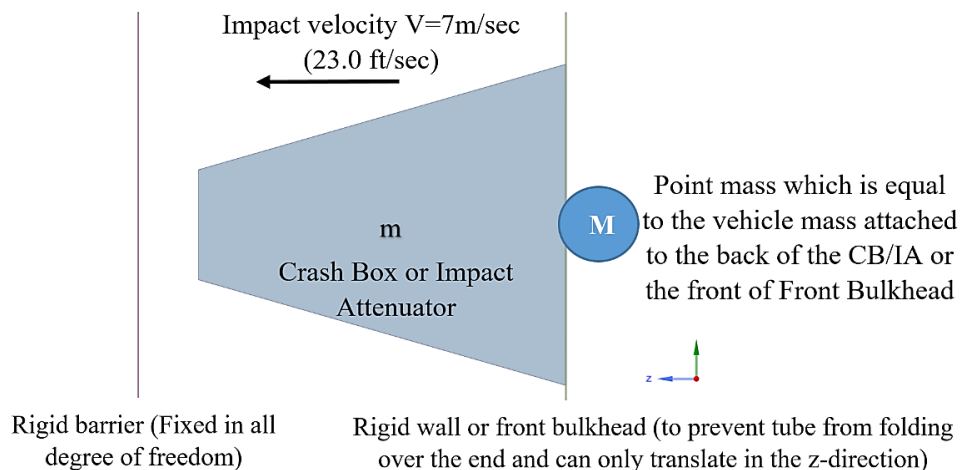


Figure 3.50 Description of load and boundary condition for Crash Box or Impact Attenuator  
The initial kinetic energy generated is:

$$KE = \frac{1}{2}(m + M)V^2 \quad (53)$$

Where  $M$  is mass of the racing car and  $m$  is mass of the Crash Box, therefore it becomes  $M = 300\text{kg}$ ,  $m_{M1} = 1.5844\text{kg}$ ,  $m_{M2} = 2.4999212\text{kg}$ , and  $m_{M1} = 5.64\text{kg}$  are the masses of the vehicle and impact attenuator respectively,

$V = 7 \text{ m/s}$  is the initial velocity.

$$K.E = KE = \frac{1}{2}(m + M)V^2 = \frac{1}{2}(1.5844 \text{ kg} + 300\text{kg})(7\text{m/s})^2$$

$$= 7388.8178 \text{ J for Crash Box M1}$$

$$K.E = KE = \frac{1}{2}(m + M)V^2 = \frac{1}{2}(2.4999212\text{kg} + 300\text{kg})(7\text{m/s})^2$$

$$= 7403.8980694 \text{ J for Crash Box M2}$$

$$K.E = KE = \frac{1}{2}(m + M)V^2 = \frac{1}{2}(5.64\text{kg} + 300\text{kg})(7\text{m/s})^2$$

$$= 7488.18 \text{ J for Crash Box M3}$$

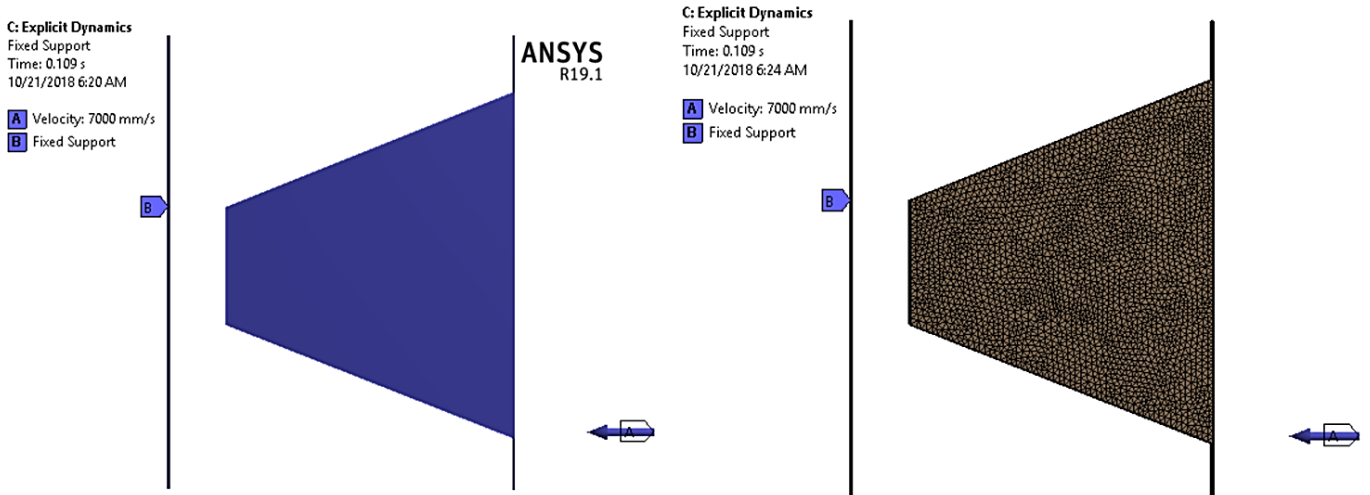


Figure 3.51 Boundary condition on Crash Box or Impact Attenuator in ANSYS Explicit Dynamics for M1, M2, and M3

The mesh size for each size, order, element number and node number for FSAE Crash Box Models is shown in Table 15.

Table 15 Mesh property used for the Formula SAE Crash Box Models

FSAE Crash Box Model	Element size	Order and Type	Element number	Node number
M1	10mm	Liner triangulated	7478	4770
M2			16915	9093
M3			80835	44538

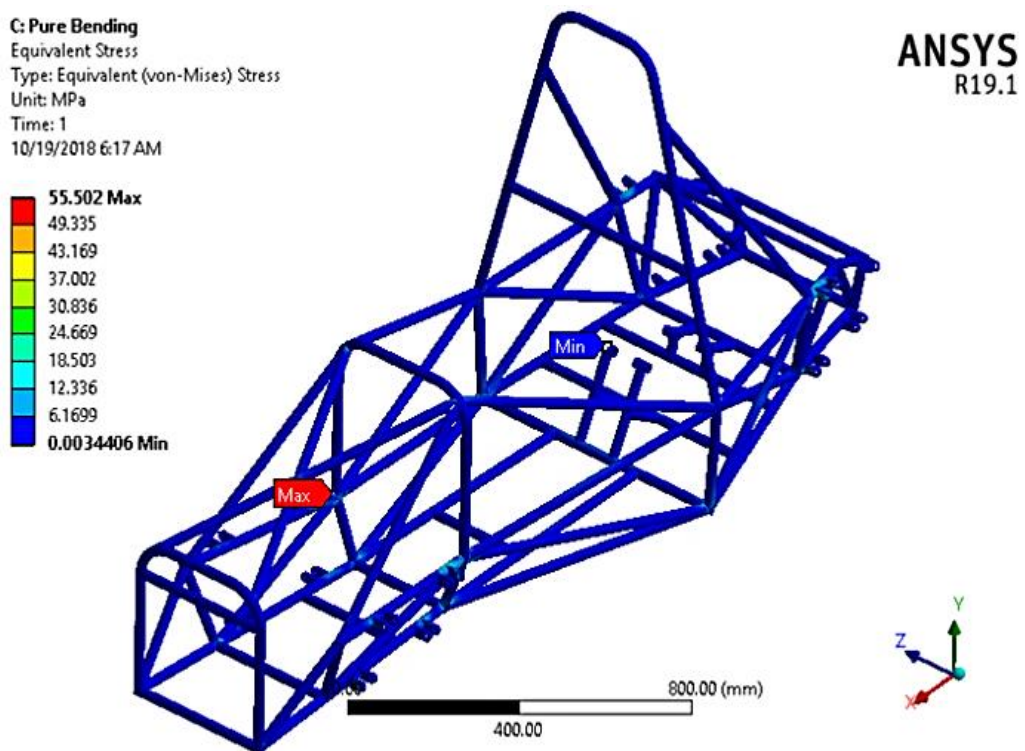
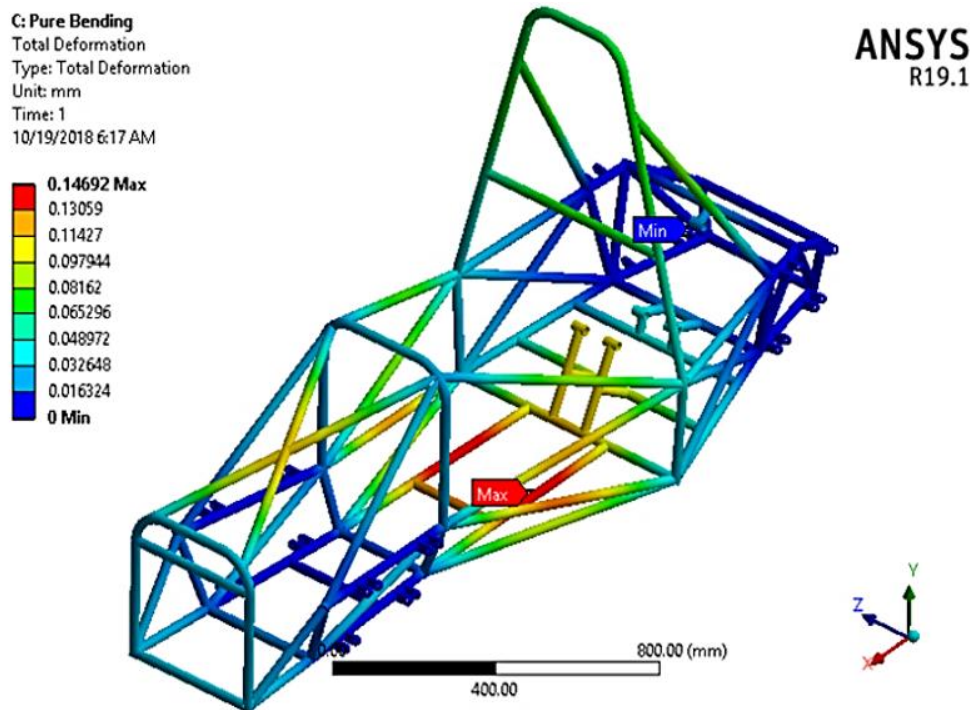
## CHAPTER 4

### RESULTS AND DISCUSSION

#### 4.1 Results

##### 4.1.1 Formula SAE M1 with Old Boundary Condition Result (Quai-Static Simulation)

##### 4.1.1.1 Vertical Symmetric or Vertical Bending ('pure bending') Load Analysis



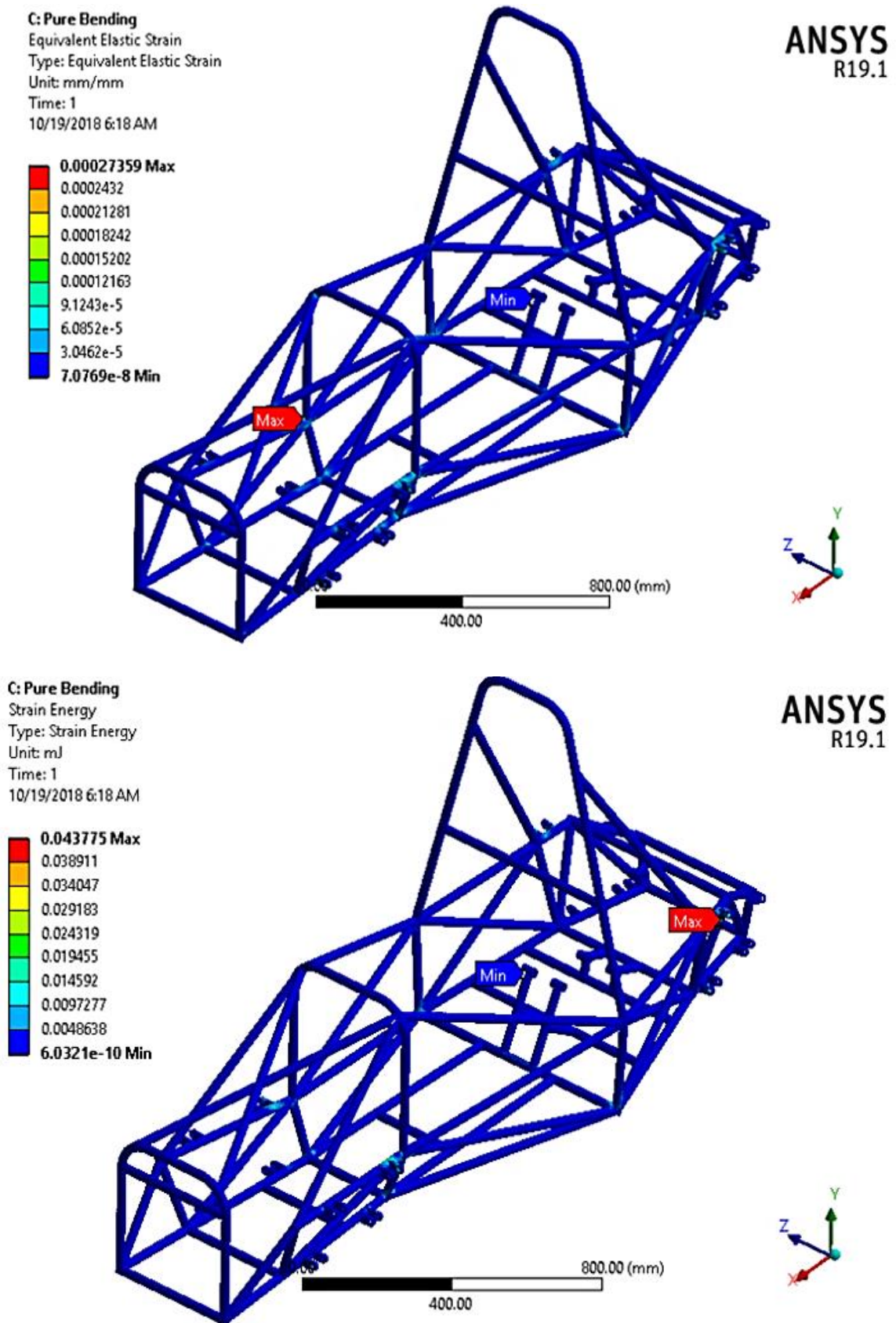


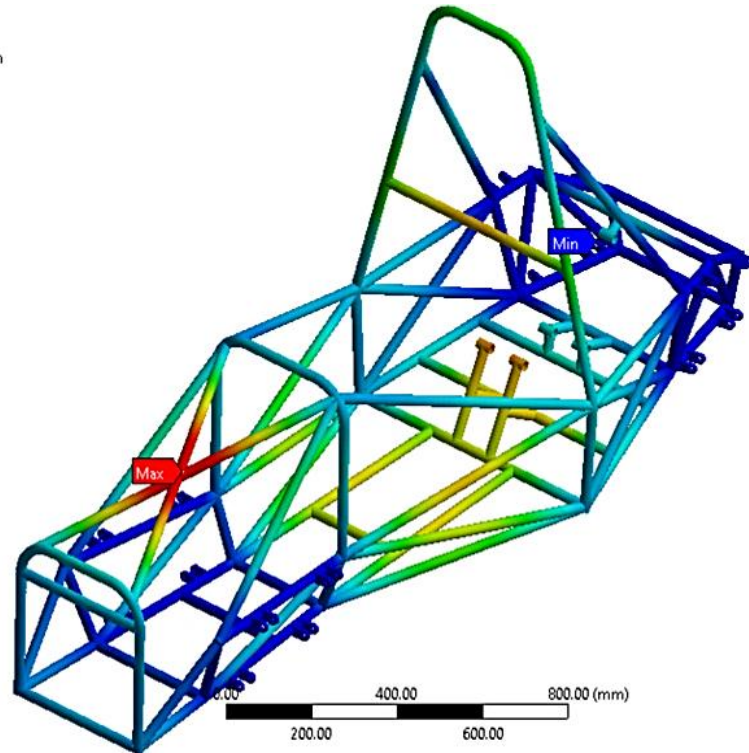
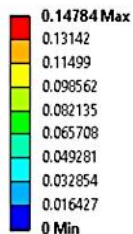
Figure 4.1 Formula SAE M1 Chassis pure bending results

#### 4.1.1.2 Vertical Asymmetric or Longitudinal Torsion (Pure Torsion Analysis Case)

The same as section 4.1.2.2 because, the total mass of the vehicle distributed equally to four points on the steering system hinge, based on that 68.3625Kg (278.243Kg/4) applied to each point, each steering system hinge have four hinges used to connect the steering system to the Formula SAE M1 Chassis.

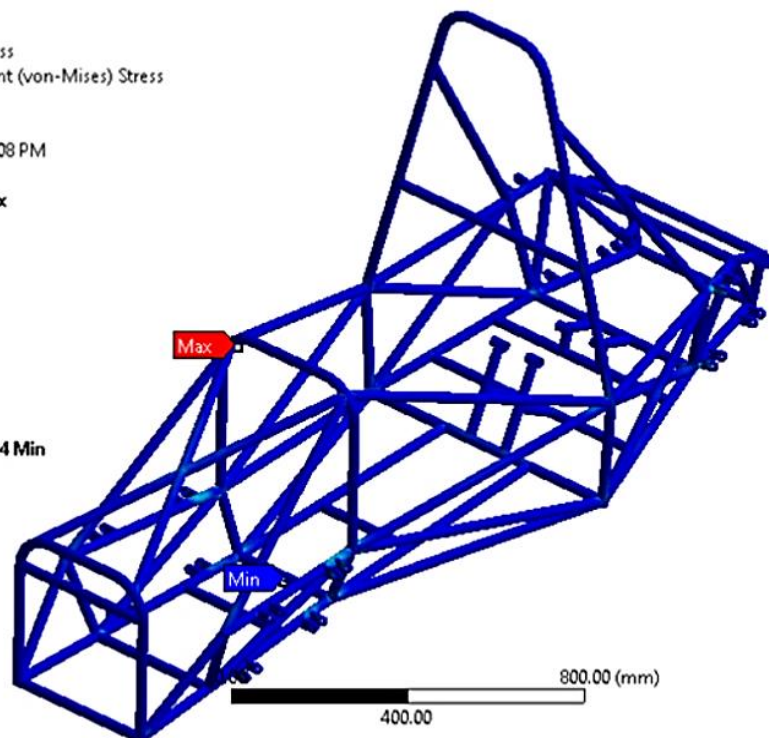
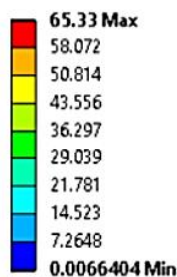
#### 4.1.1.3 Longitudinal loads (Braking) Analysis

F: Braking  
 Total Deformation  
 Type: Total Deformation  
 Unit: mm  
 Time: 1  
 11/6/2018 1:27 AM



ANSYS  
R19.1

F: Braking  
 Equivalent Stress  
 Type: Equivalent (von-Mises) Stress  
 Unit: MPa  
 Time: 1  
 10/27/2018 11:08 PM



ANSYS  
R19.1

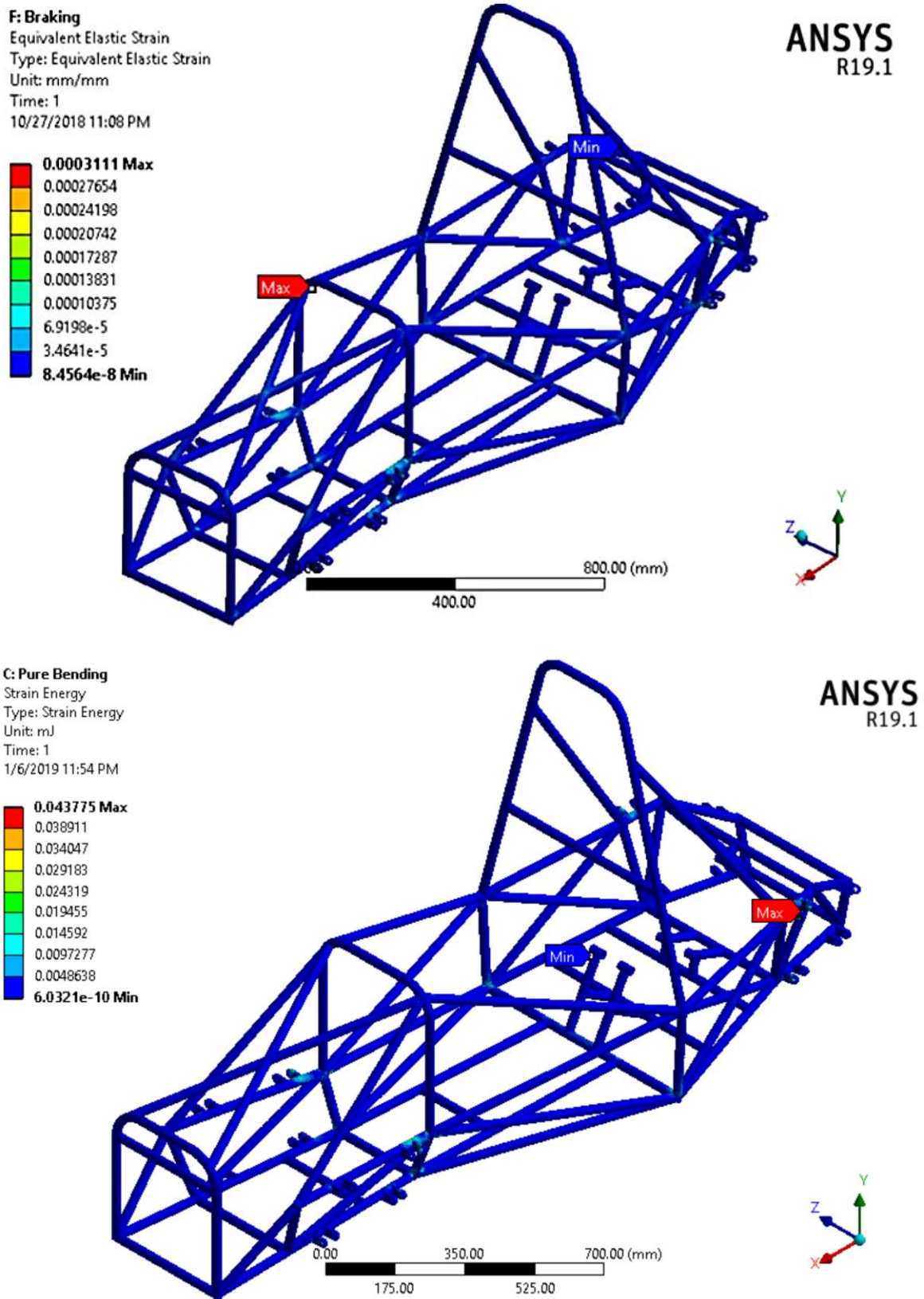
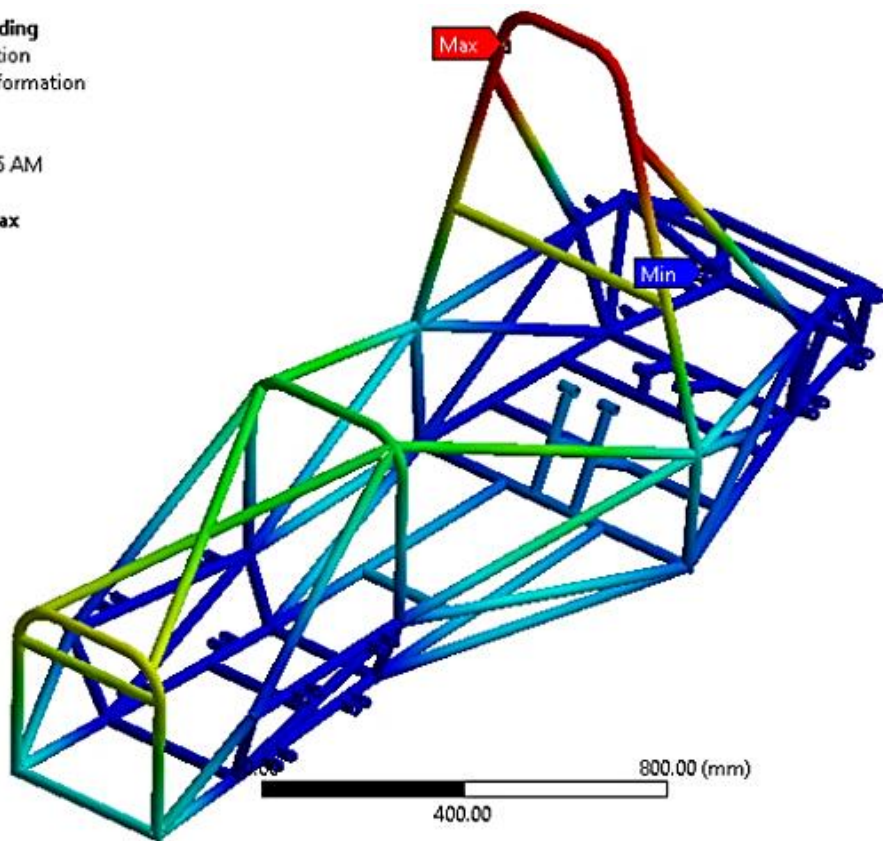
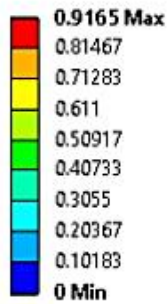


Figure 4.2 Formula SAE M1 Chassis longitudinal load results

#### 4.1.1.4 Lateral Bending (Cornering) Analysis

**D: Lateral Bending**

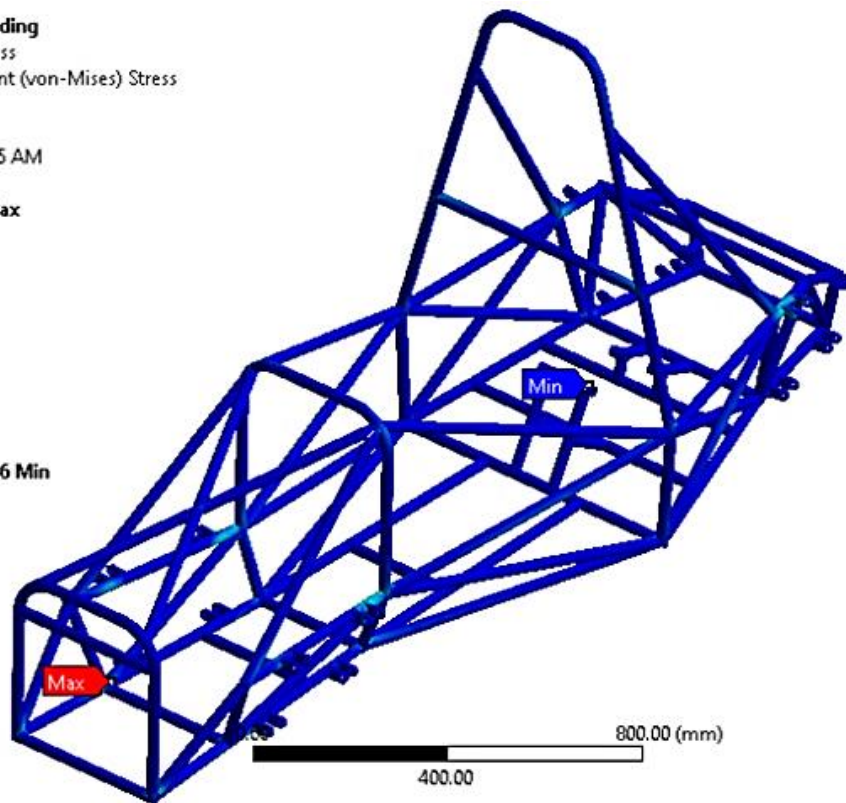
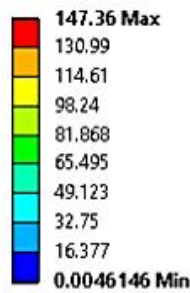
Total Deformation  
 Type: Total Deformation  
 Unit: mm  
 Time: 1  
 10/19/2018 6:15 AM



**ANSYS**  
R19.1

**D: Lateral Bending**

Equivalent Stress  
 Type: Equivalent (von-Mises) Stress  
 Unit: MPa  
 Time: 1  
 10/19/2018 6:15 AM



**ANSYS**  
R19.1

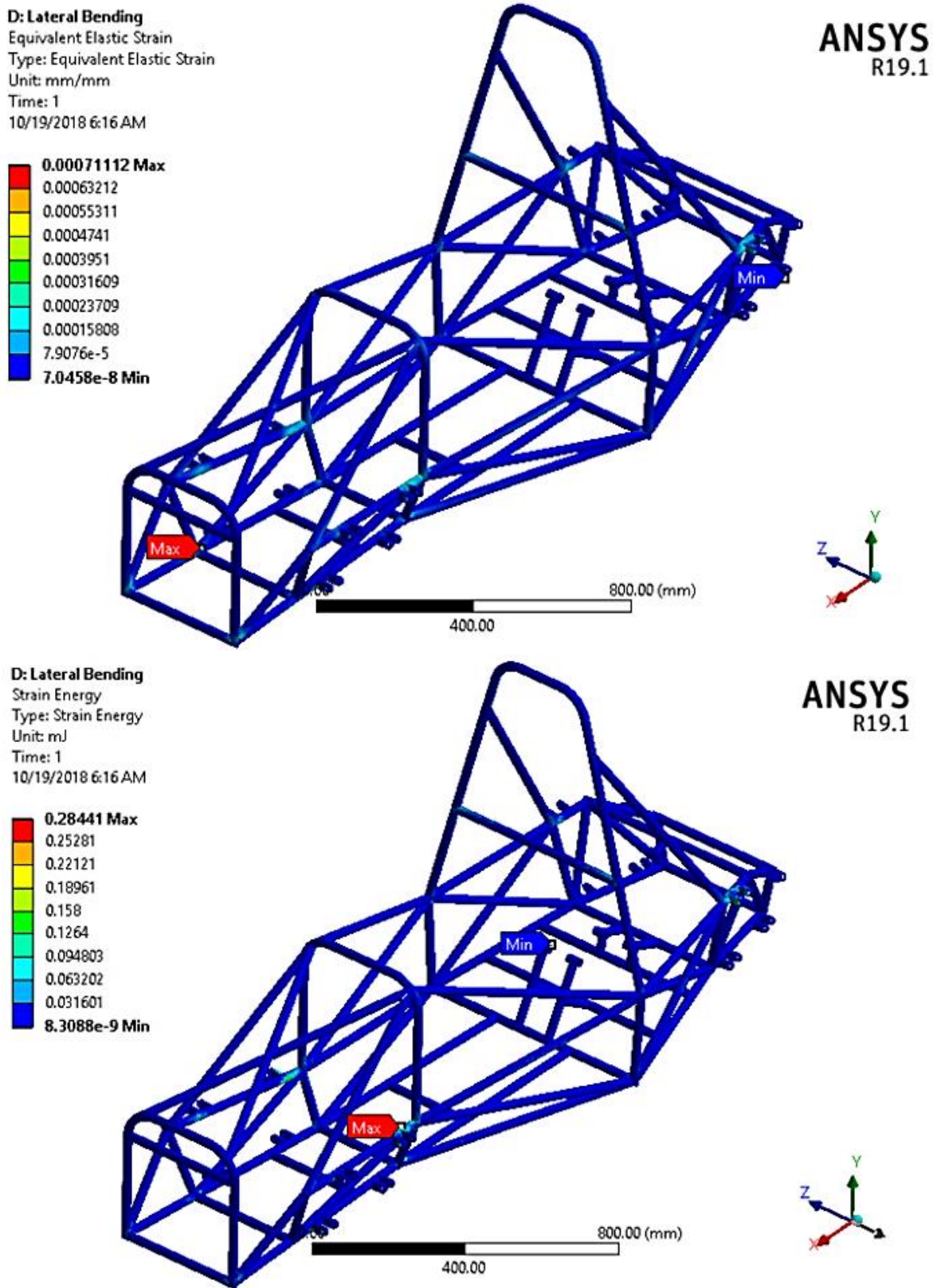
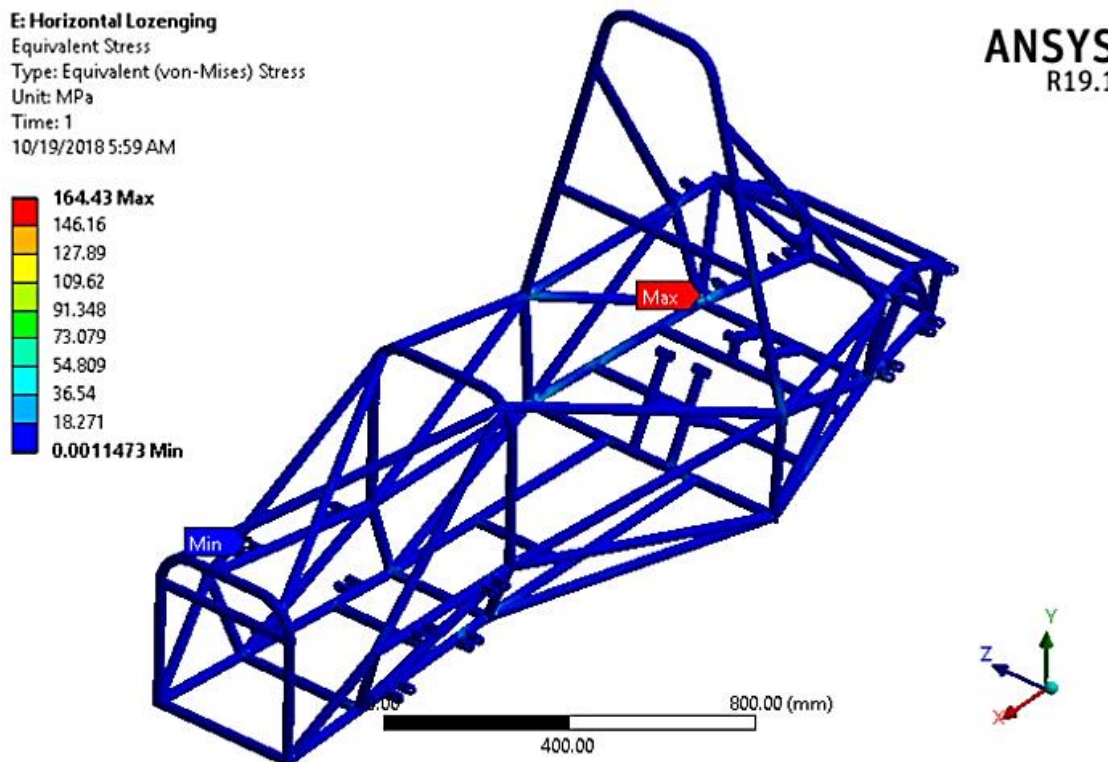
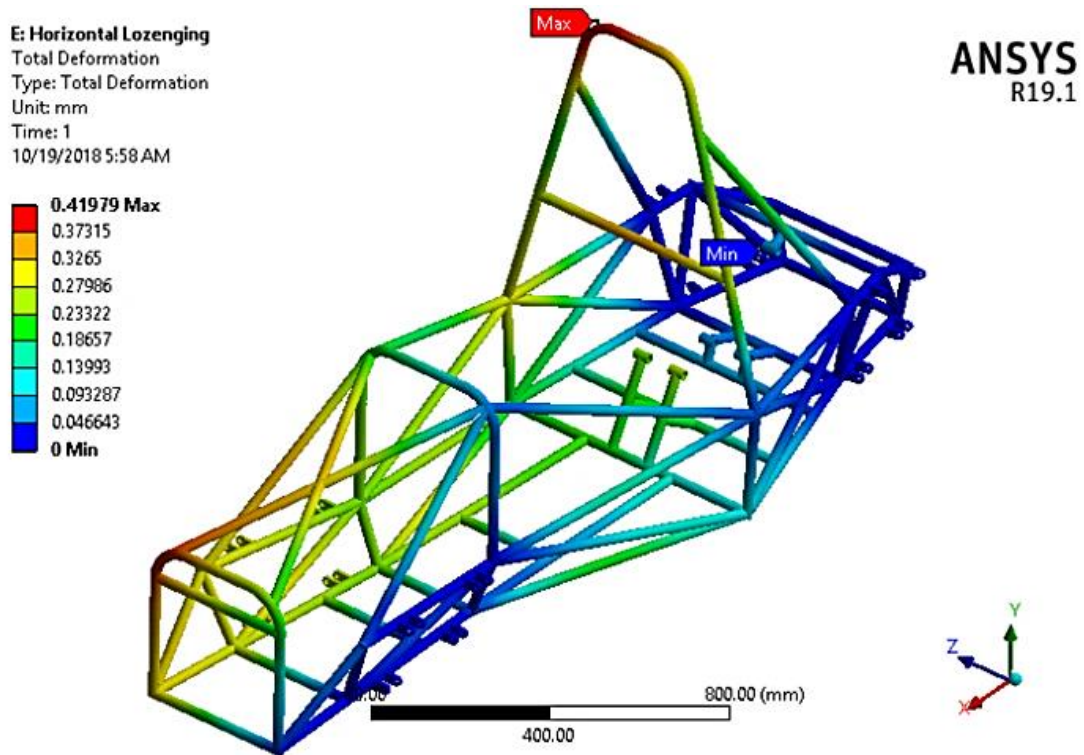


Figure 4.3 Formula SAE M1 Chassis lateral bending results

#### 4.1.1.5 Crash or Impact cases (Front, Side and Rollover Crash) Analysis

The same as section 4.1.2.5 because, the same amount of load applied in the main hoops, front hoops, and front bulkhead in Formula SAE M1 Chassis because the same type of load applied on the Chassis structure.

#### 4.1.1.6 Horizontal Lozenging Analysis



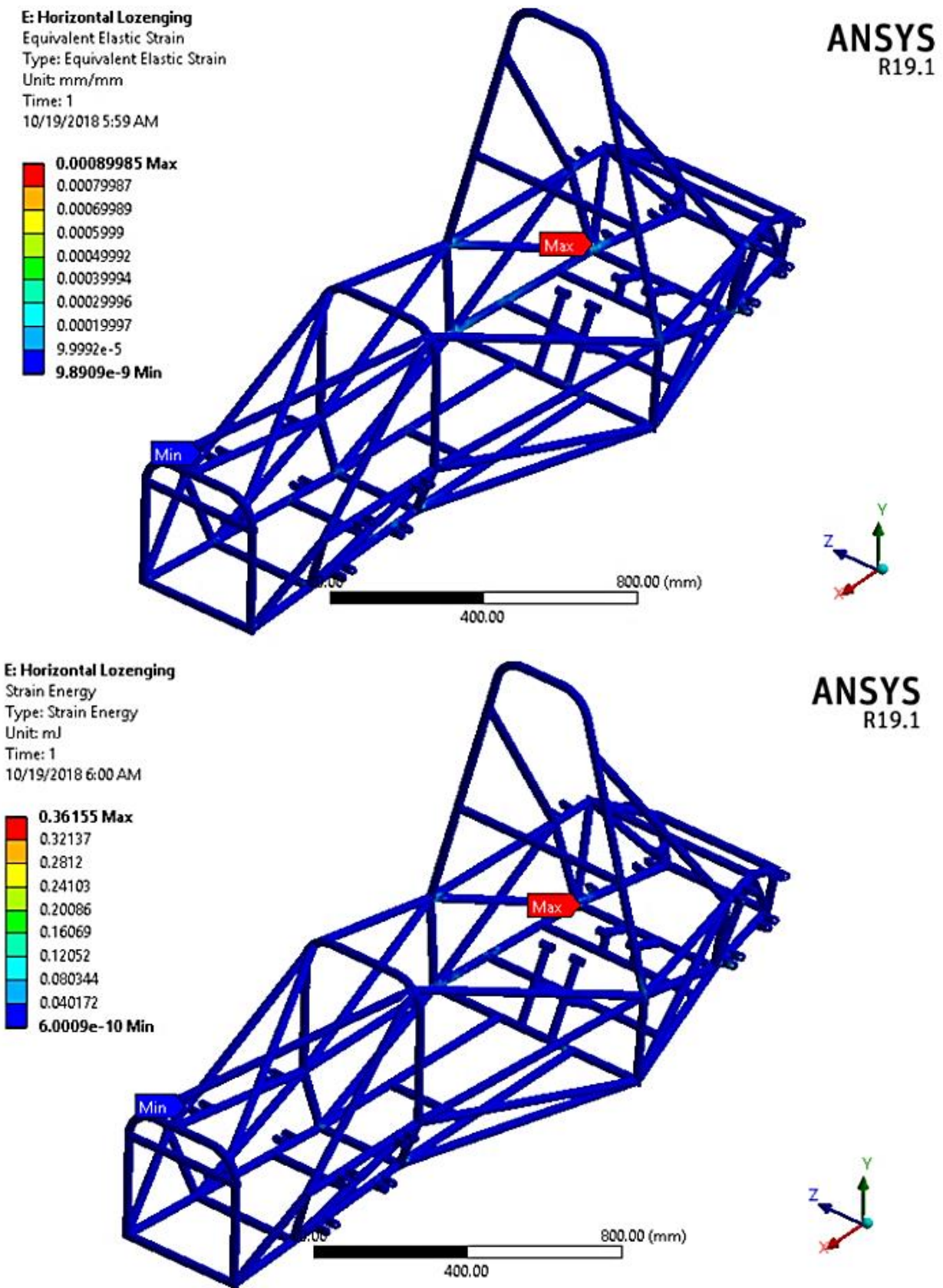


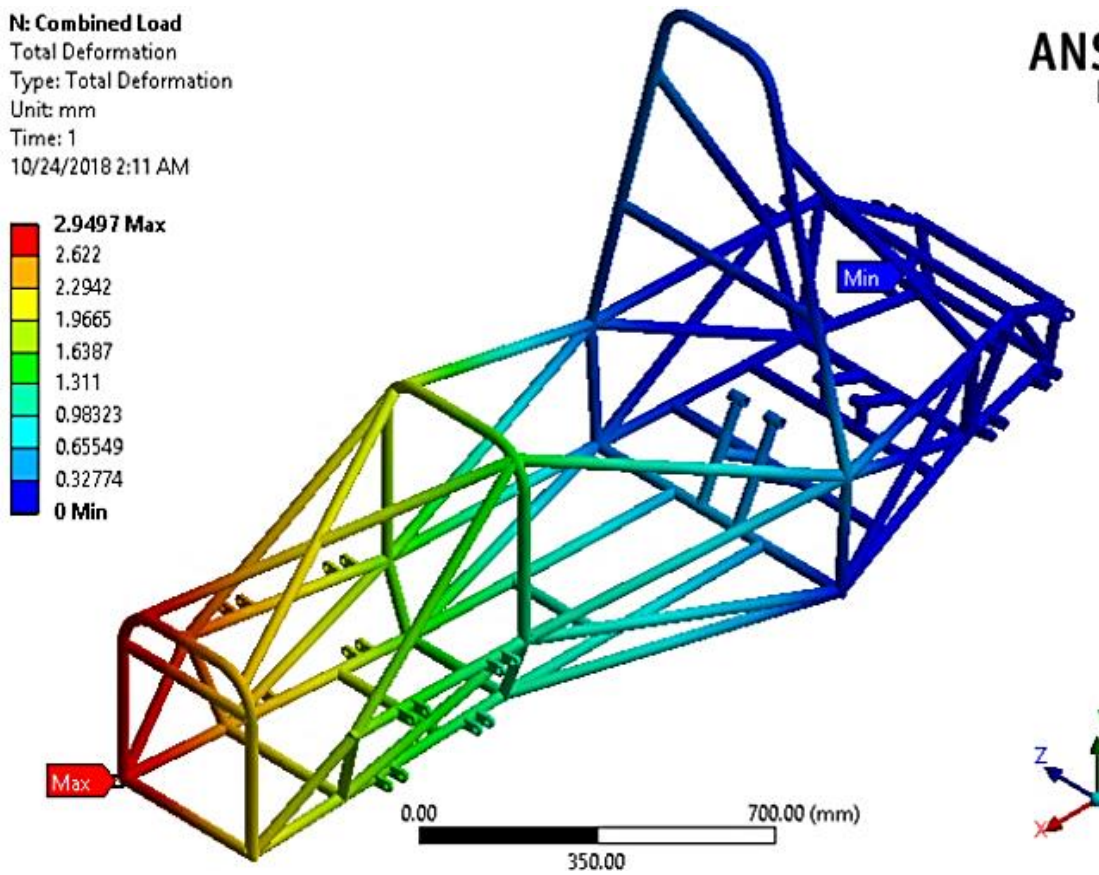
Figure 4.4 Formula SAE M1 Chassis lateral bending results

#### 4.1.1.7 Combinations of Load Analysis

**N: Combined Load**  
 Total Deformation  
 Type: Total Deformation  
 Unit: mm  
 Time: 1  
 10/24/2018 2:11 AM

**ANSYS**  
 R19.1

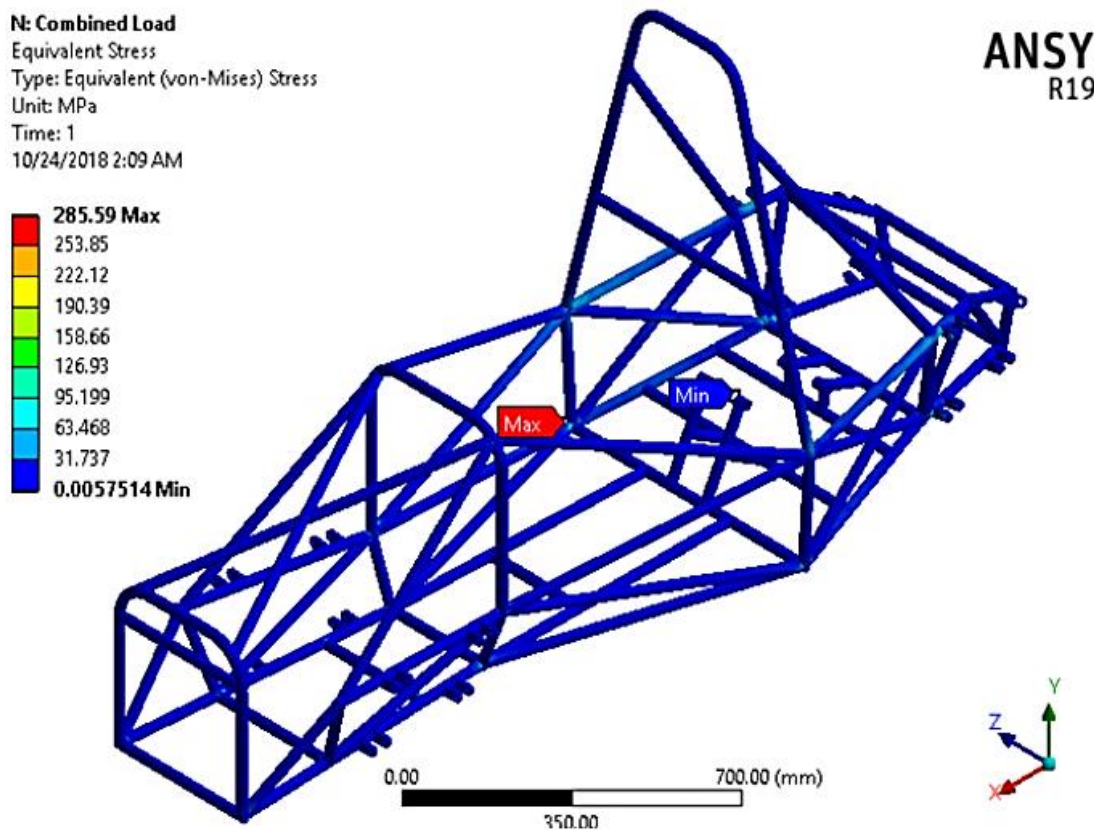
2.9497 Max  
 2.622  
 2.2942  
 1.9665  
 1.6387  
 1.311  
 0.98323  
 0.65549  
 0.32774  
 0 Min



**N: Combined Load**  
 Equivalent Stress  
 Type: Equivalent (von-Mises) Stress  
 Unit: MPa  
 Time: 1  
 10/24/2018 2:09 AM

**ANSYS**  
 R19.1

285.59 Max  
 253.85  
 222.12  
 190.39  
 158.66  
 126.93  
 95.199  
 63.468  
 31.737  
 0.0057514 Min



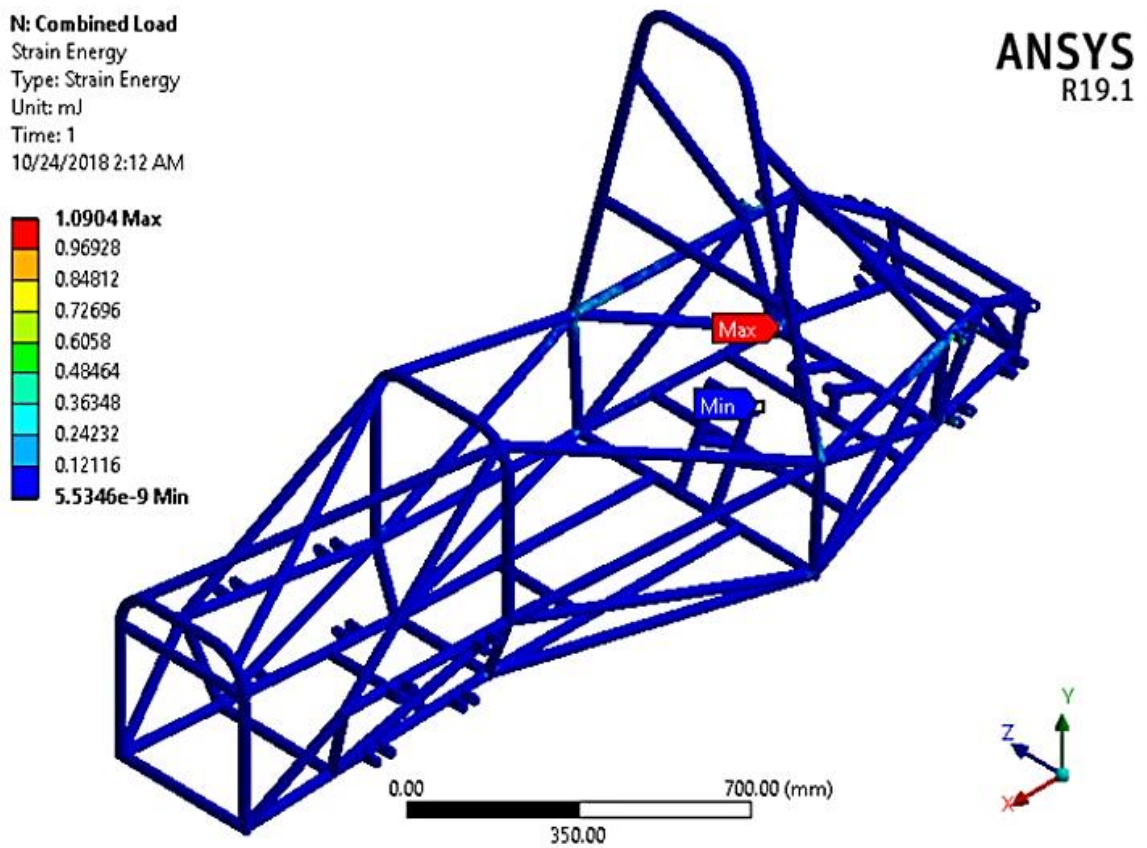
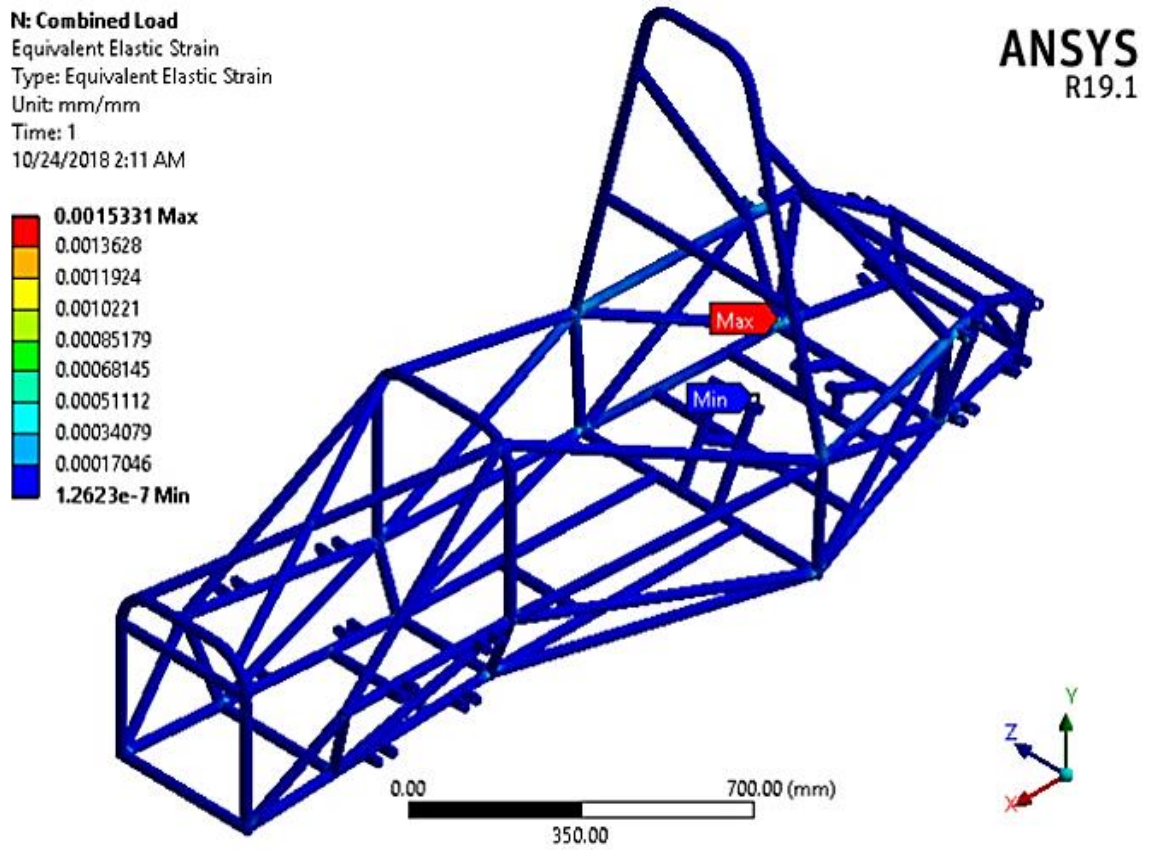
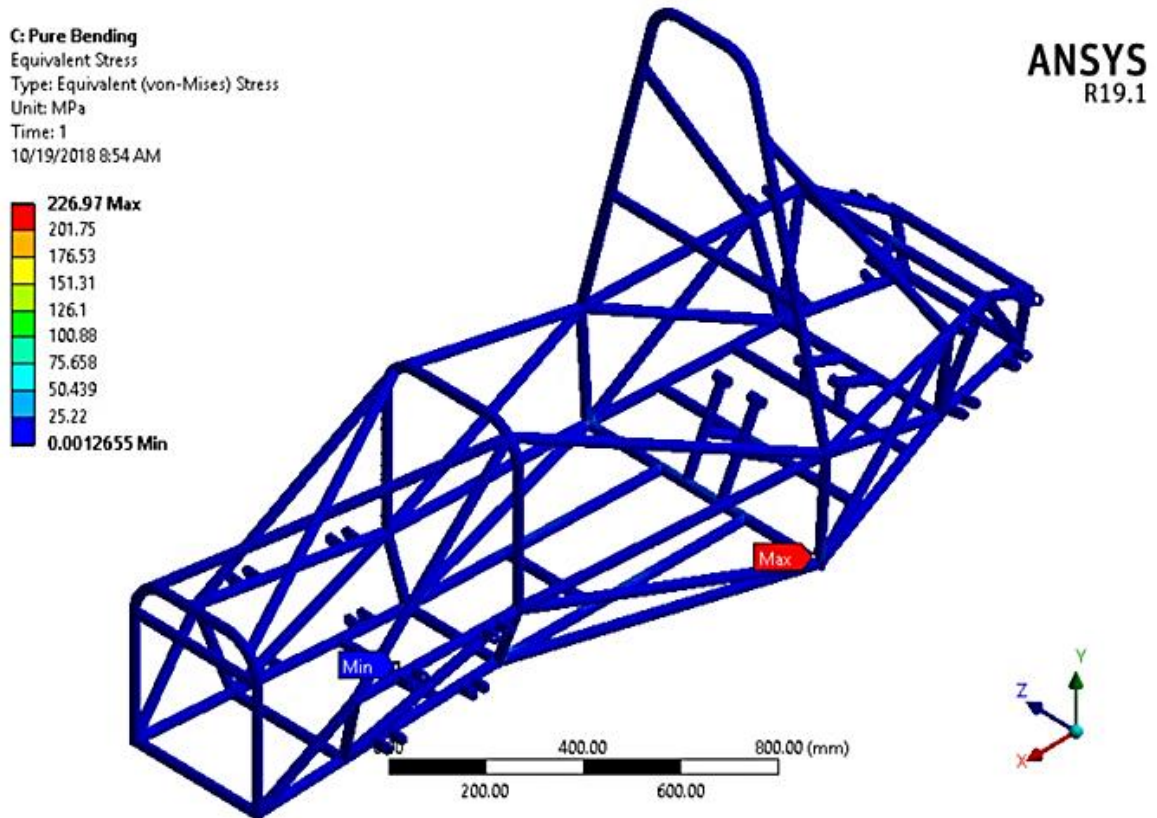
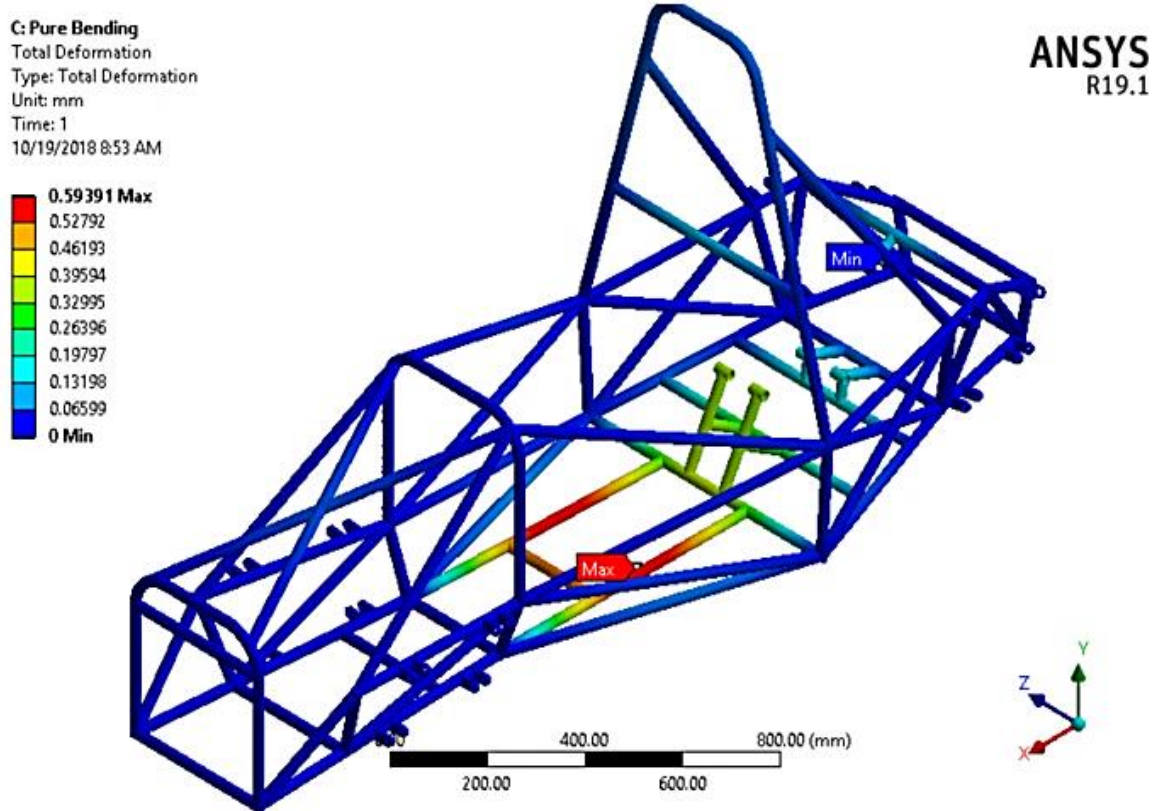


Figure 4.5 Formula SAE M1 Chassis combined load results

### 4.1.2 Formula SAE M1 with New Boundary Condition Result (Quai-Static Simulation)

#### 4.1.2.1 Vertical Symmetric or Vertical Bending ('pure bending') Load Analysis



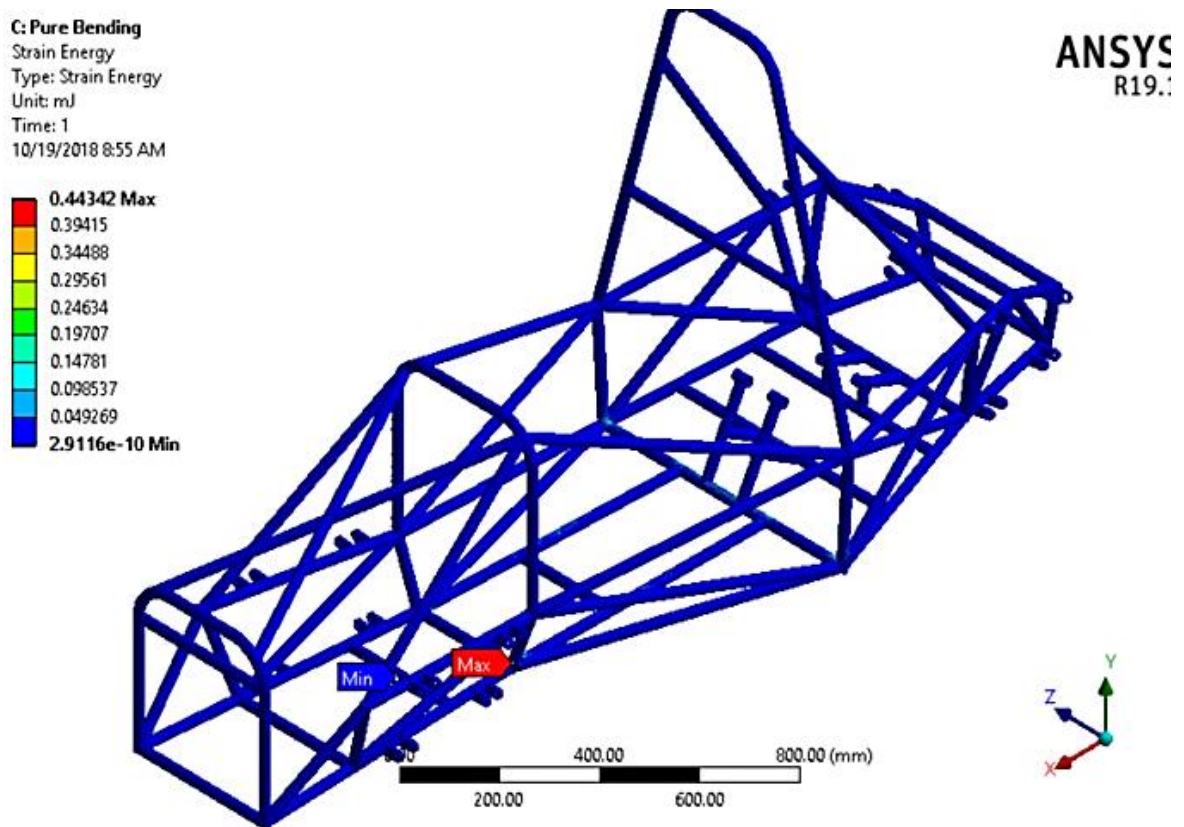
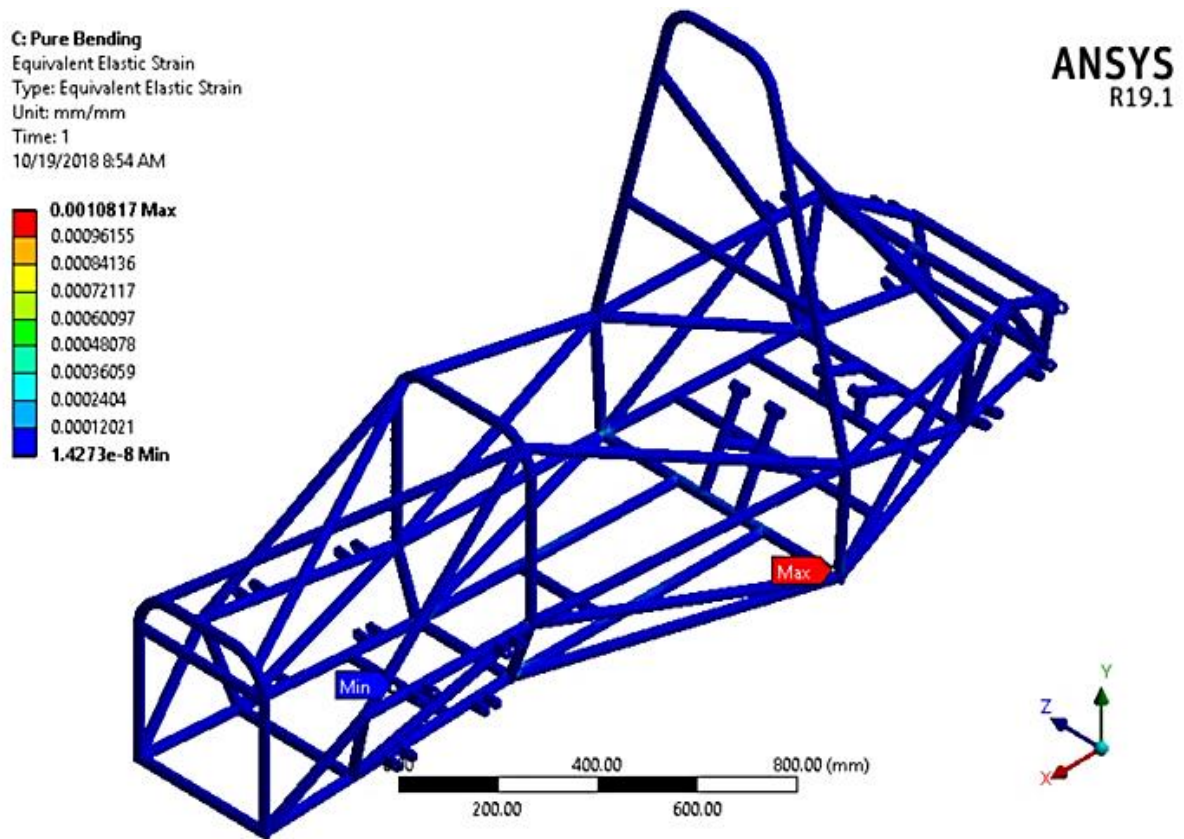
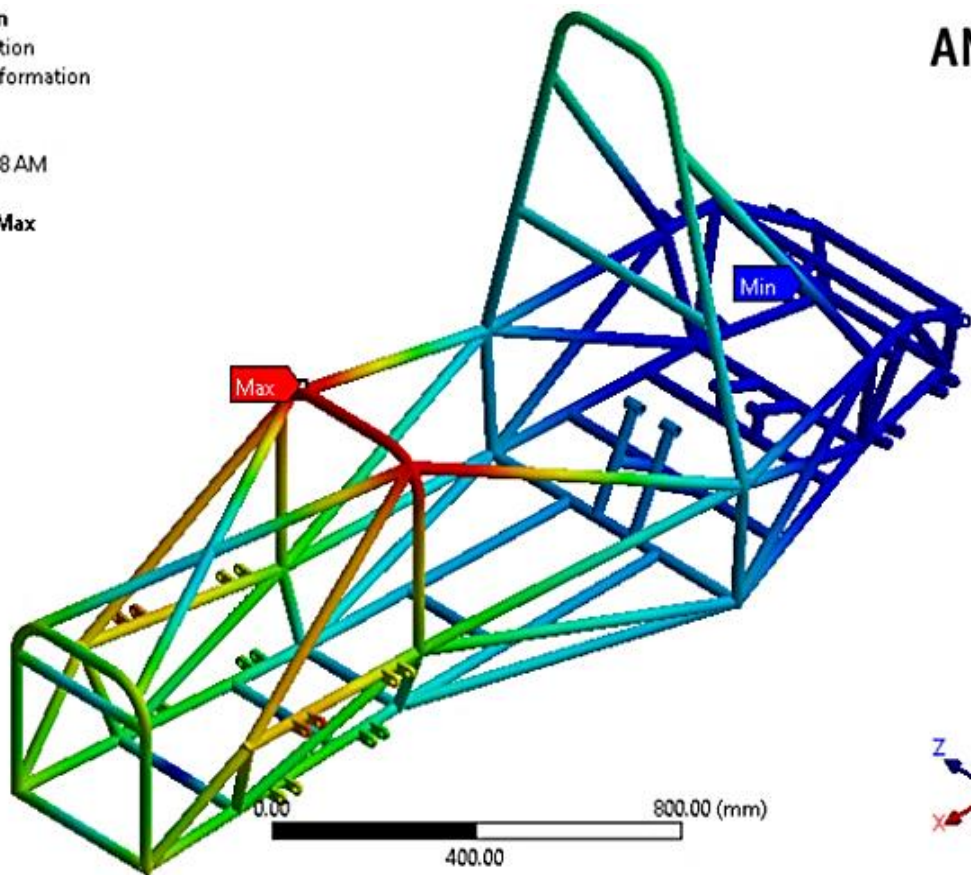
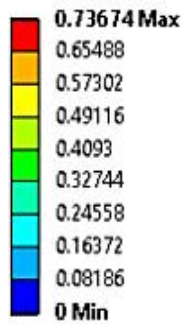


Figure 4.6 Formula SAE M1 Chassis pure bending results

### 4.1.2.2 Vertical Asymmetric or Longitudinal Torsion (Pure Torsion Analysis Case)

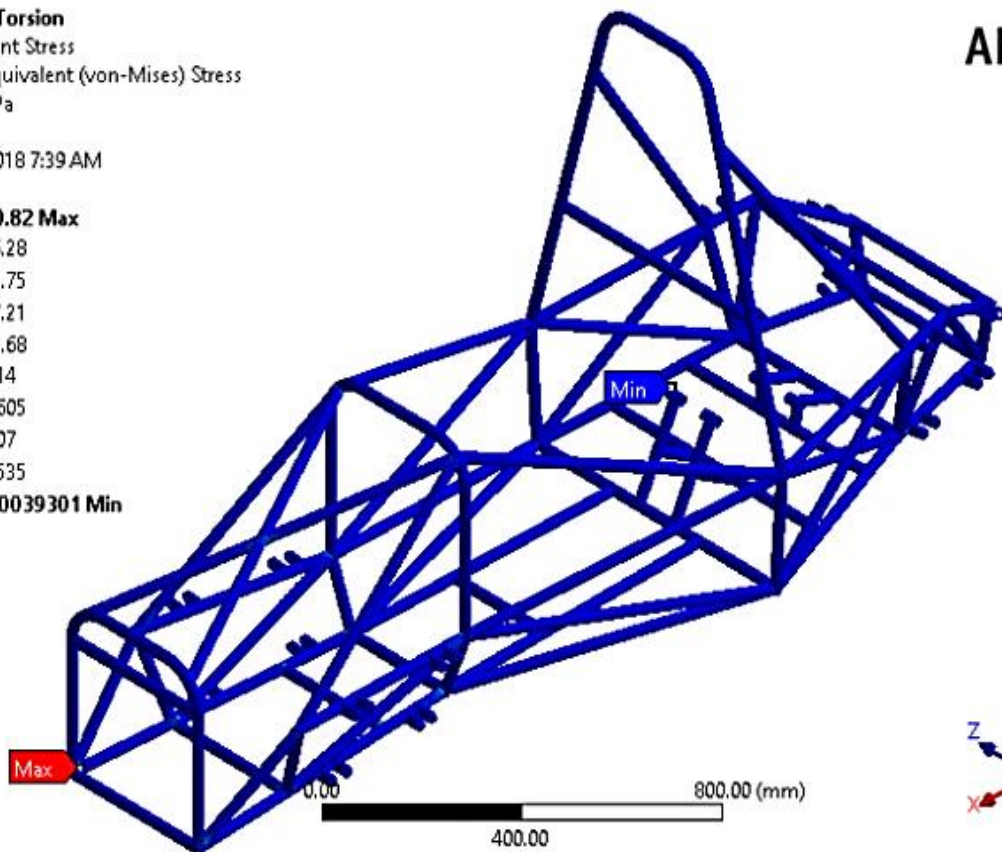
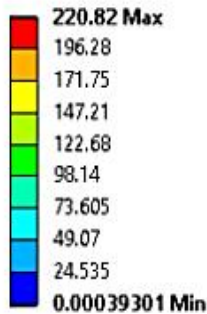
L: Pure Torsion  
 Total Deformation  
 Type: Total Deformation  
 Unit: mm  
 Time: 1  
 10/19/2018 7:38 AM

ANSYS  
 R19.1



L: Pure Torsion  
 Equivalent Stress  
 Type: Equivalent (von-Mises) Stress  
 Unit: MPa  
 Time: 1  
 10/19/2018 7:39 AM

ANSYS  
 R19.1



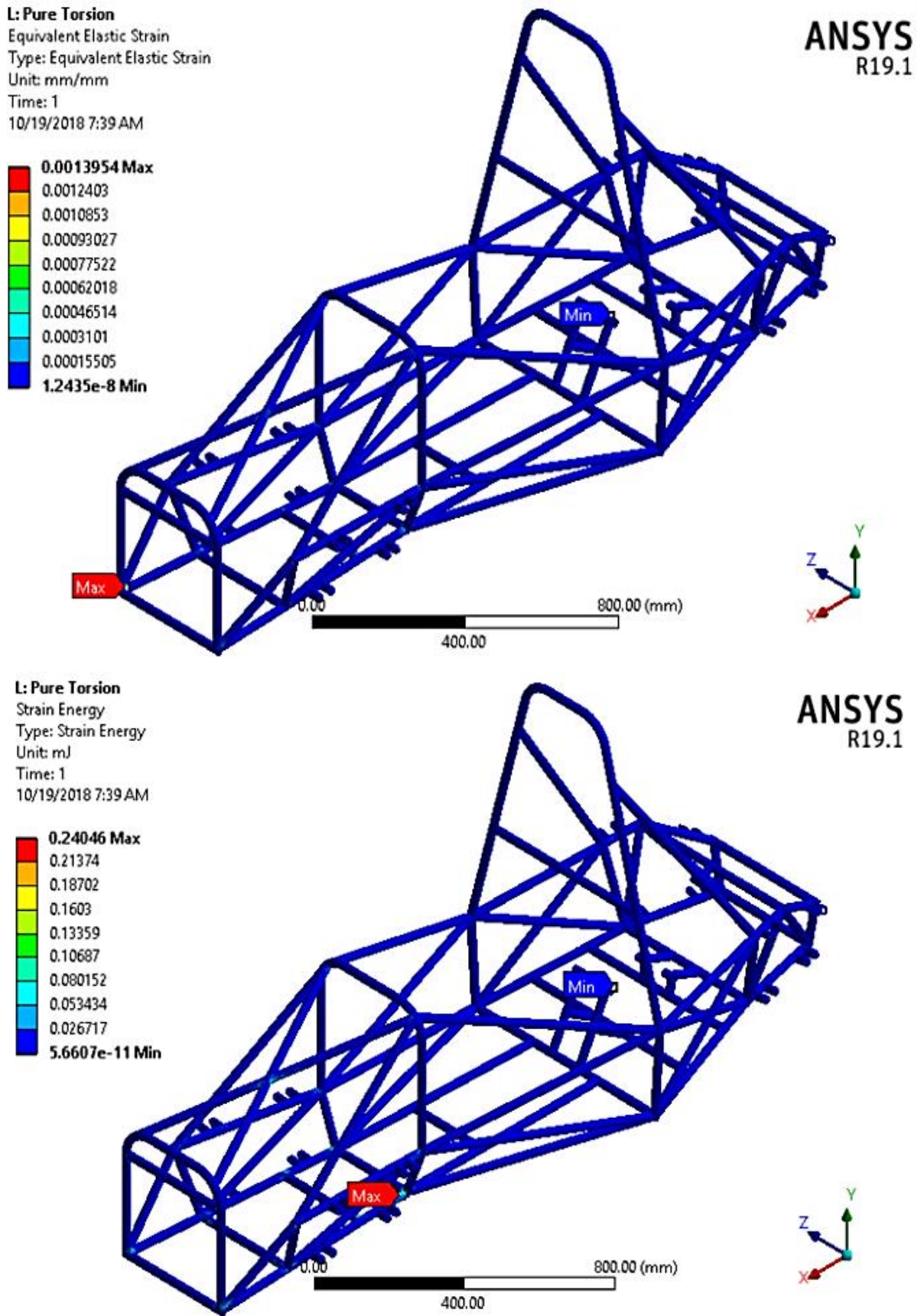


Figure 4.7 Formula SAE M1 Chassis pure torsional load results

### 4.1.2.3 Longitudinal loads (Braking) Analysis

G: Braking

Total Deformation

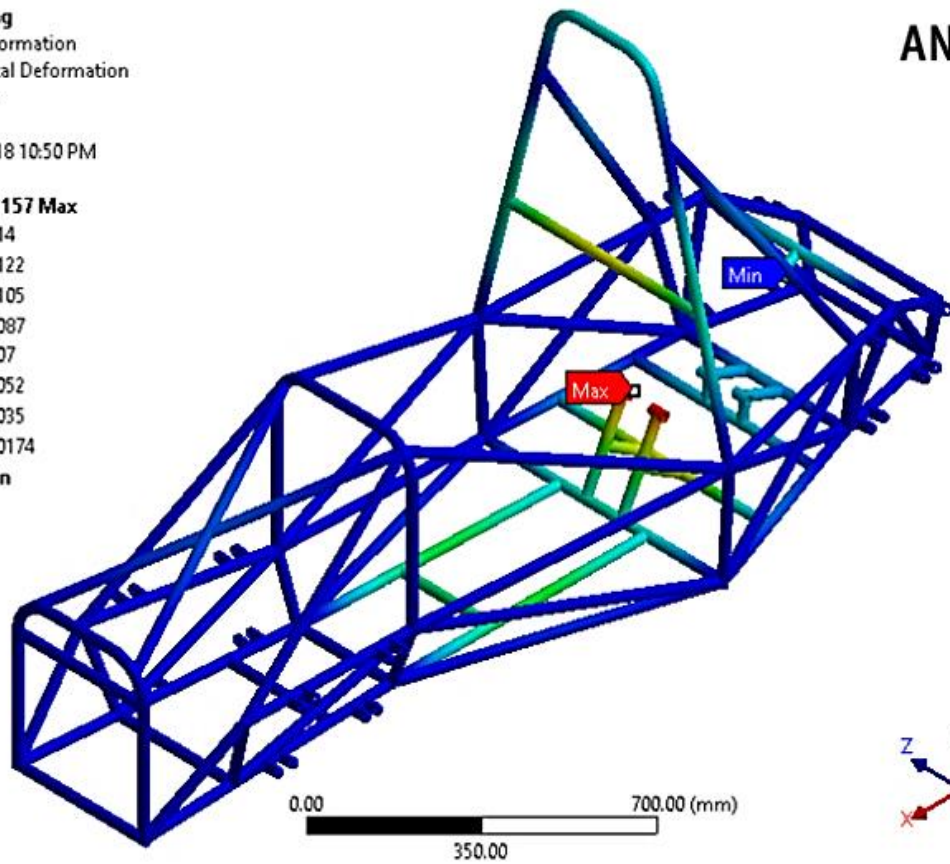
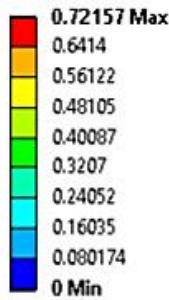
Type: Total Deformation

Unit: mm

Time: 1

10/27/2018 10:50 PM

ANSYS  
R19.1



G: Braking

Equivalent Stress

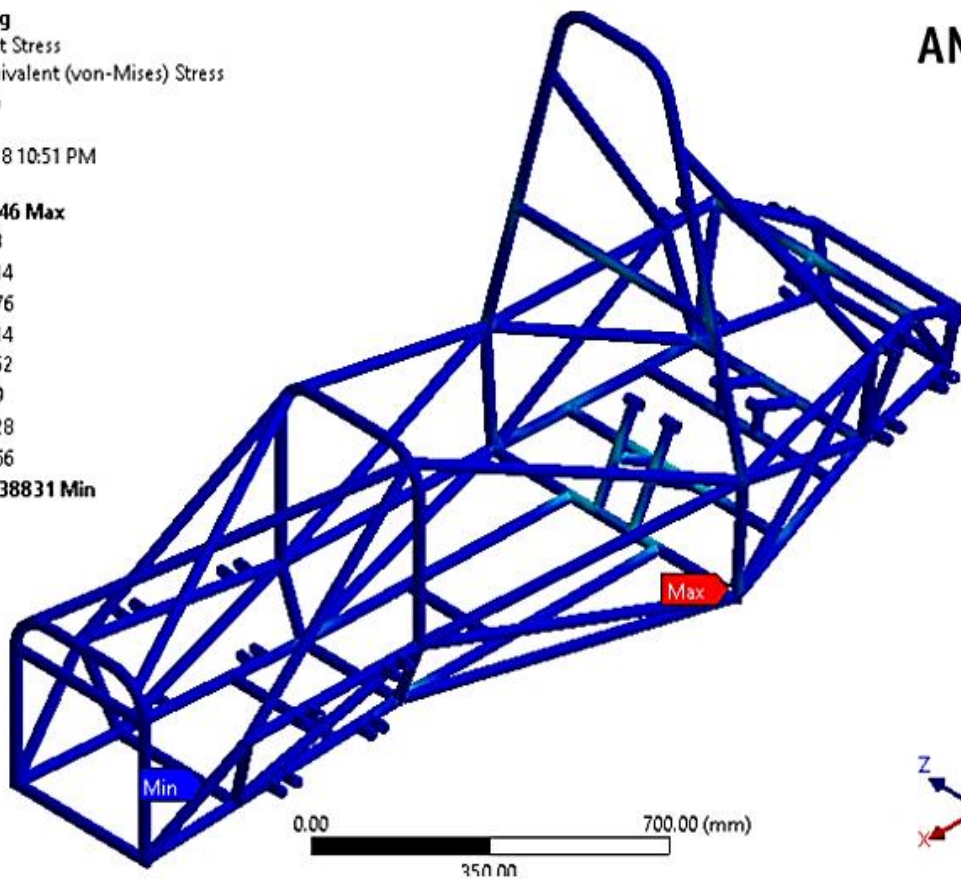
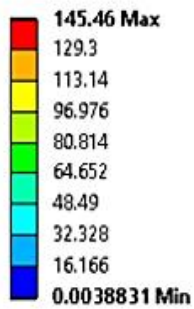
Type: Equivalent (von-Mises) Stress

Unit: MPa

Time: 1

10/27/2018 10:51 PM

ANSYS  
R19.1



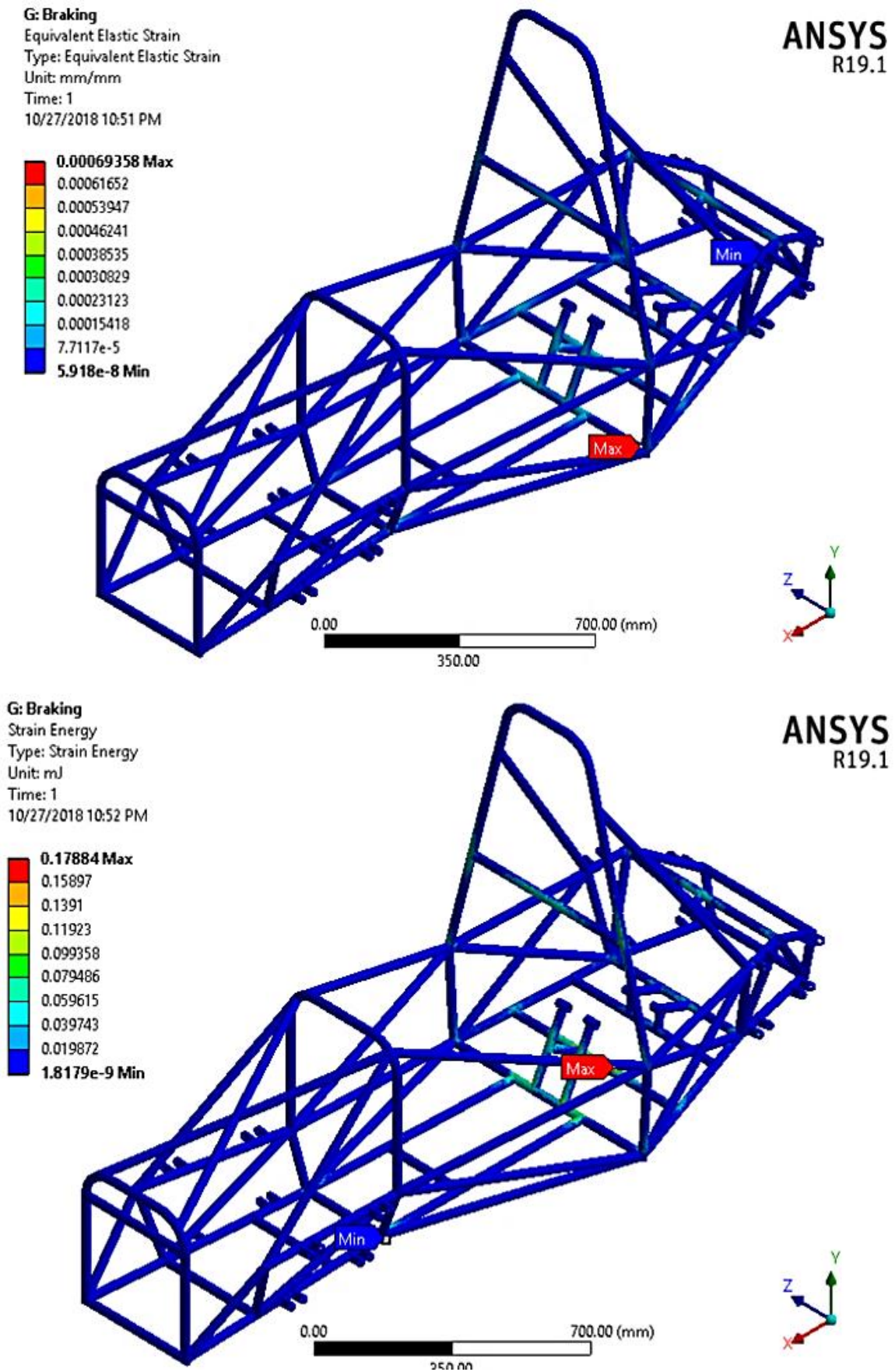
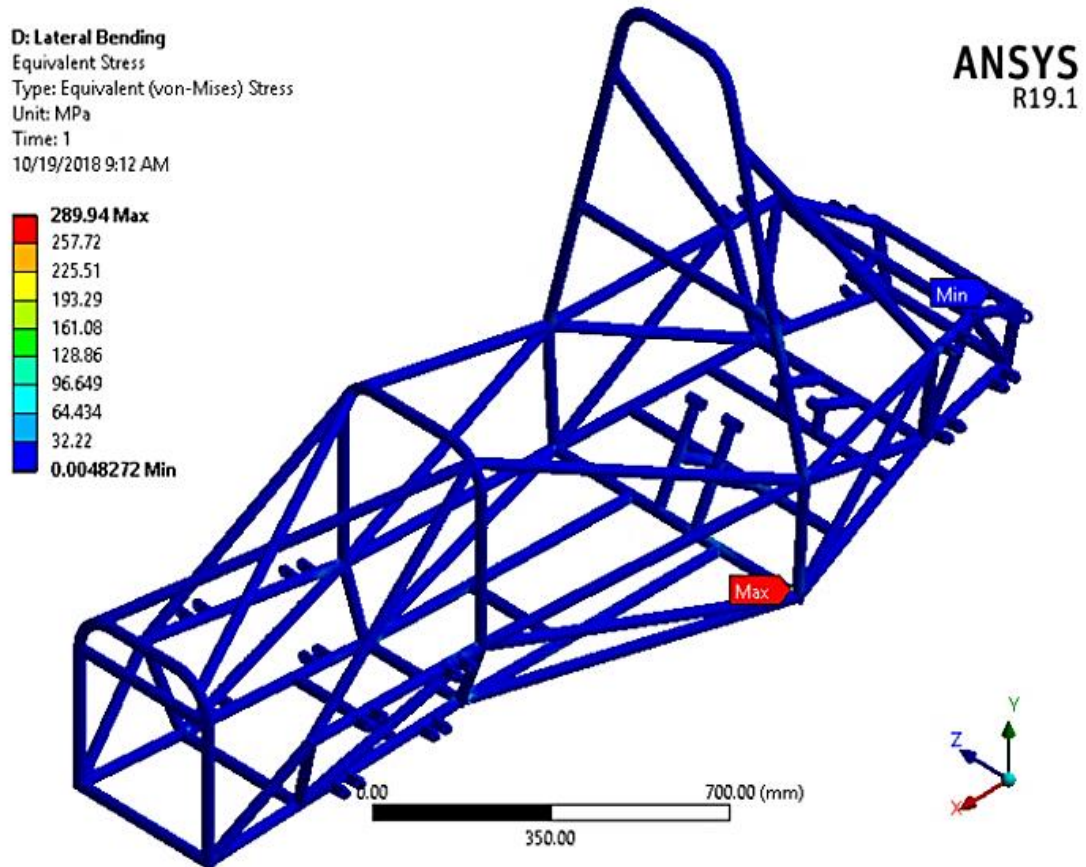
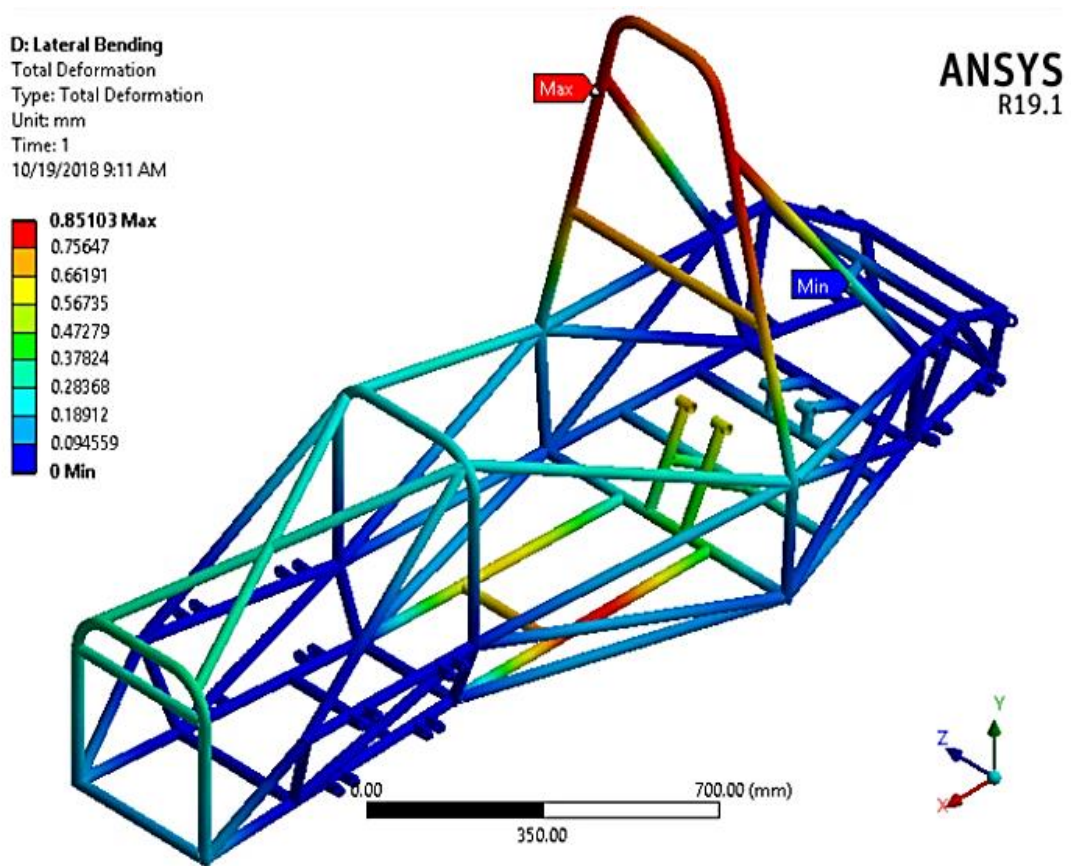


Figure 4.8 Formula SAE M1 Chassis longitudinal load results

#### 4.1.2.4 Lateral Bending (Cornering) Analysis



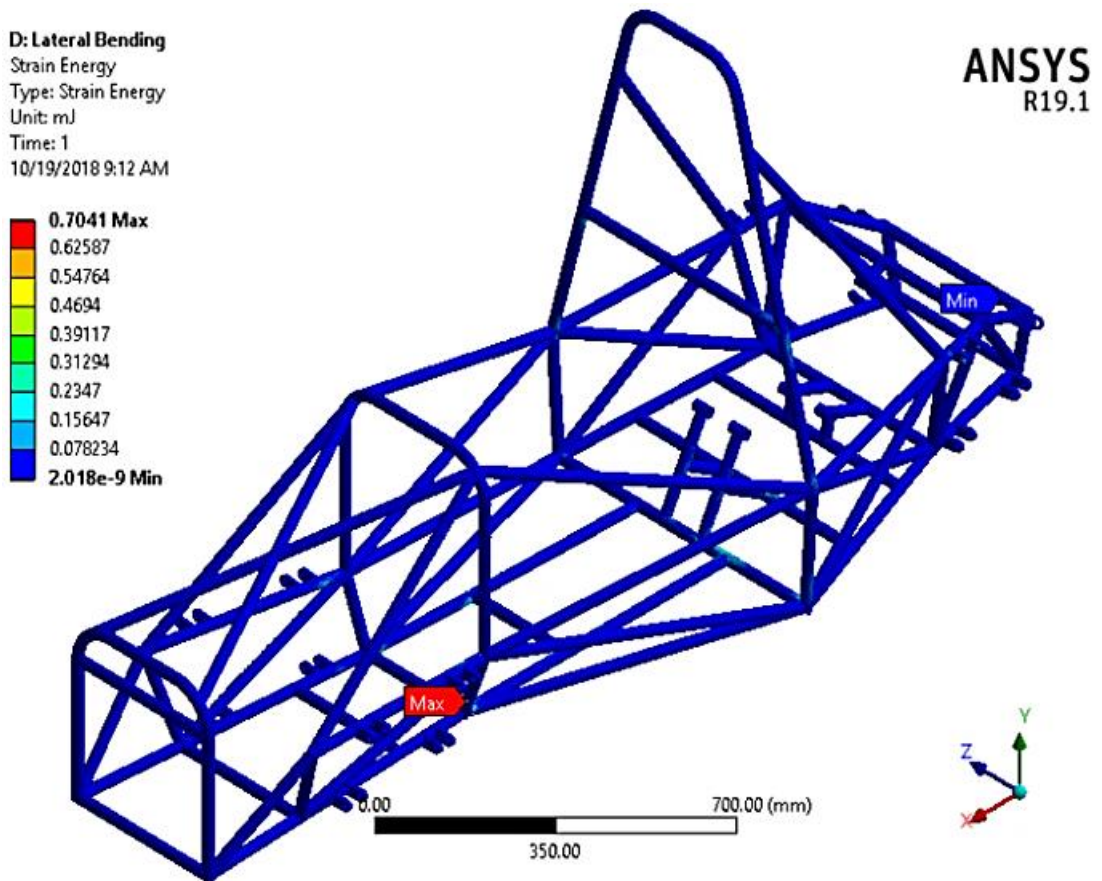
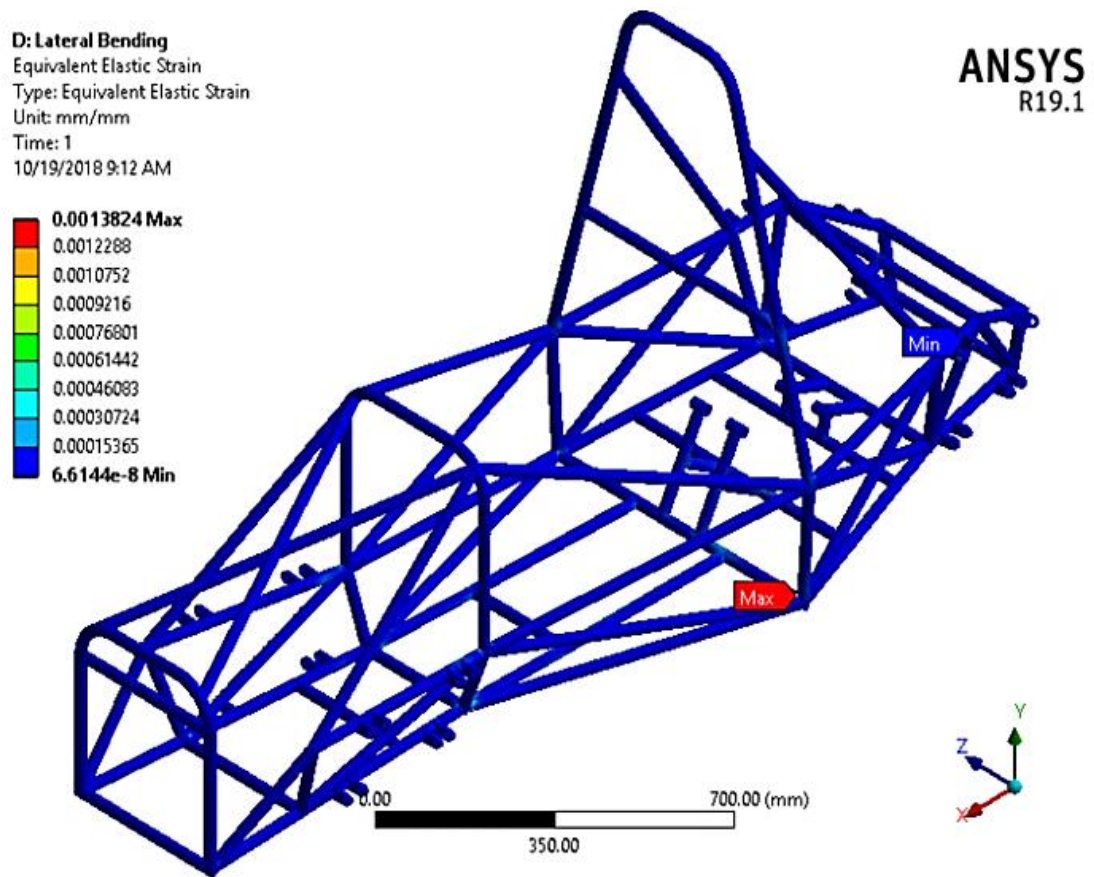
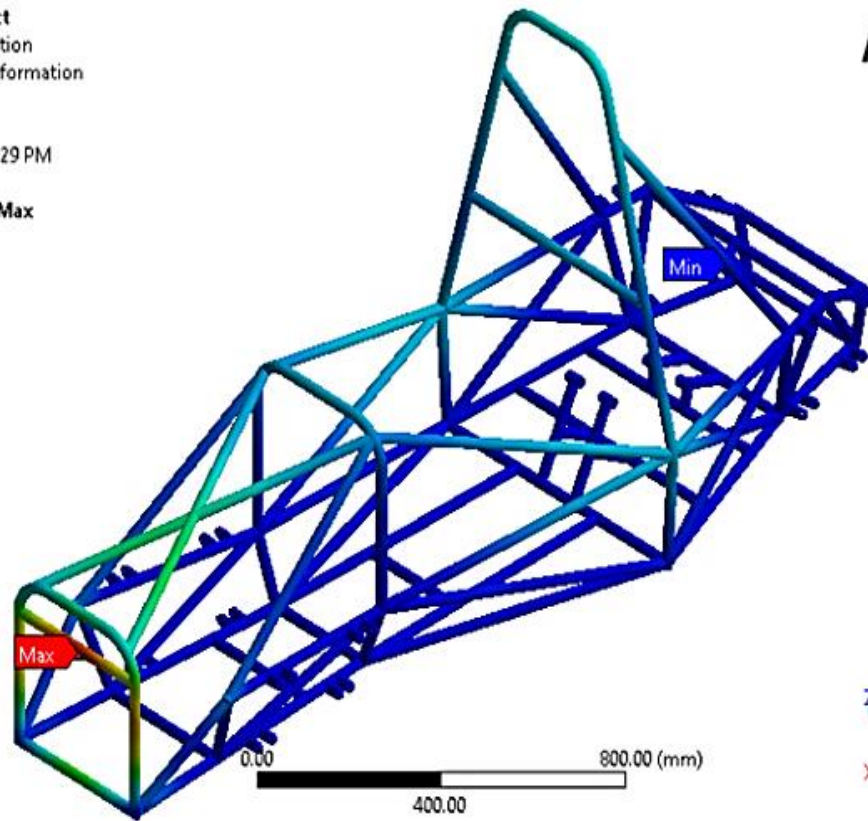
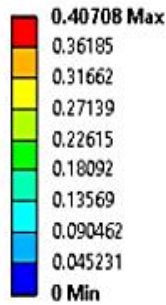


Figure 4.9 Formula SAE M1 Chassis lateral bending results

### 4.1.2.5 Crash or Impact cases (Front, Side and Rollover Crash) Analysis

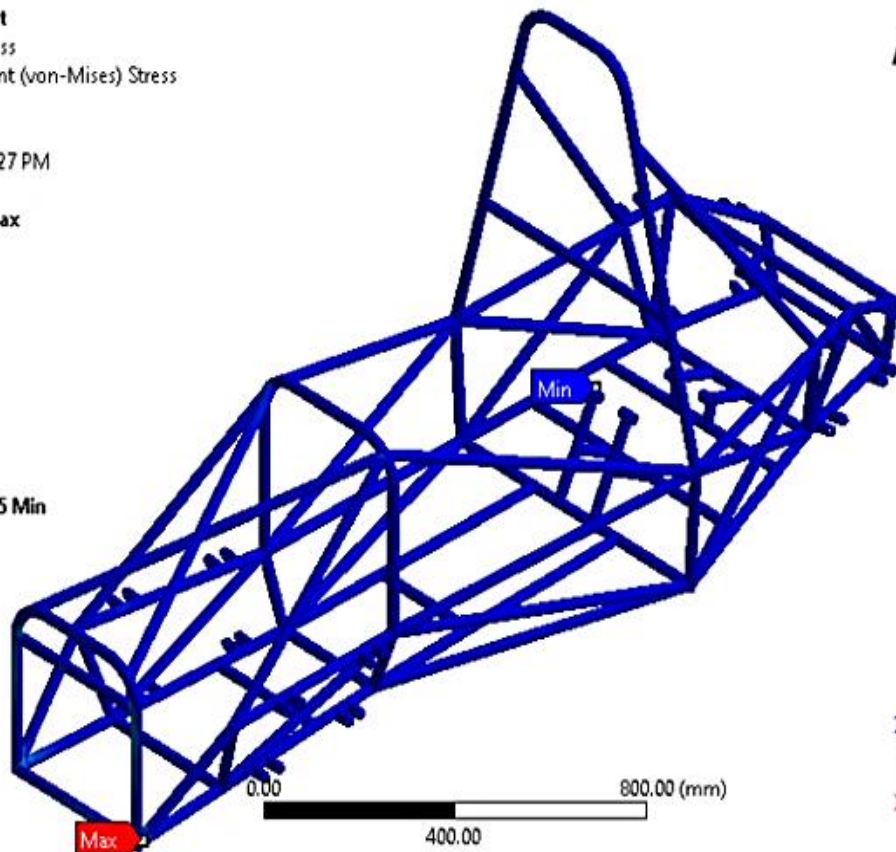
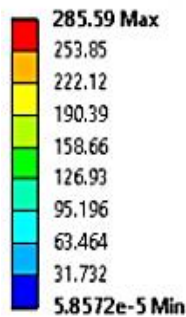
#### a. Front impact

**J: Front Impact**  
 Total Deformation  
 Type: Total Deformation  
 Unit: mm  
 Time: 1  
 10/19/2018 12:29 PM



**ANSYS**  
R19.1

**J: Front Impact**  
 Equivalent Stress  
 Type: Equivalent (von-Mises) Stress  
 Unit: MPa  
 Time: 1  
 10/19/2018 12:27 PM



**ANSYS**  
R19.1

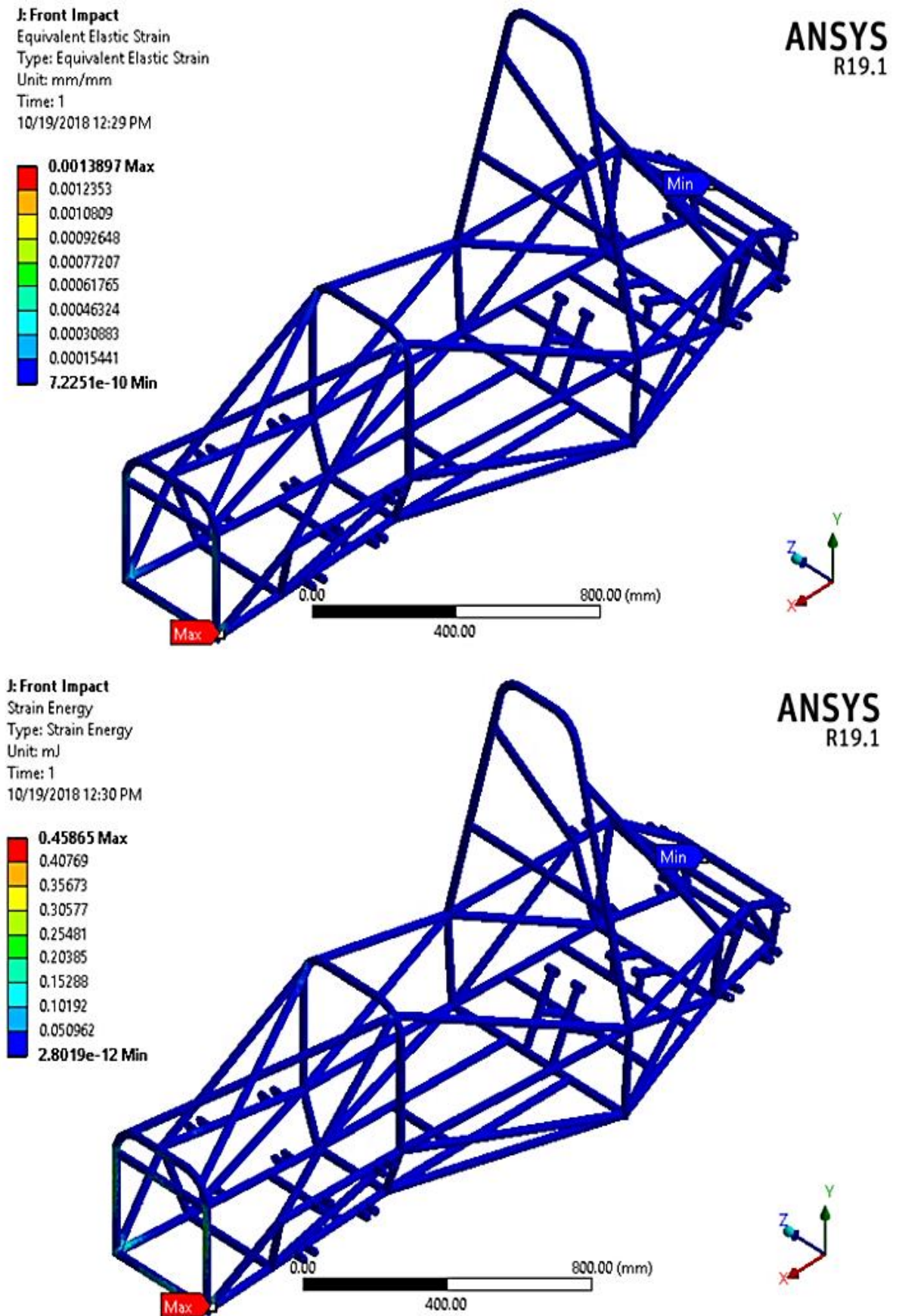


Figure 4.10 Formula SAE M1 Chassis lateral bending results

### b. Side Impact

H: Side Impact

Total Deformation

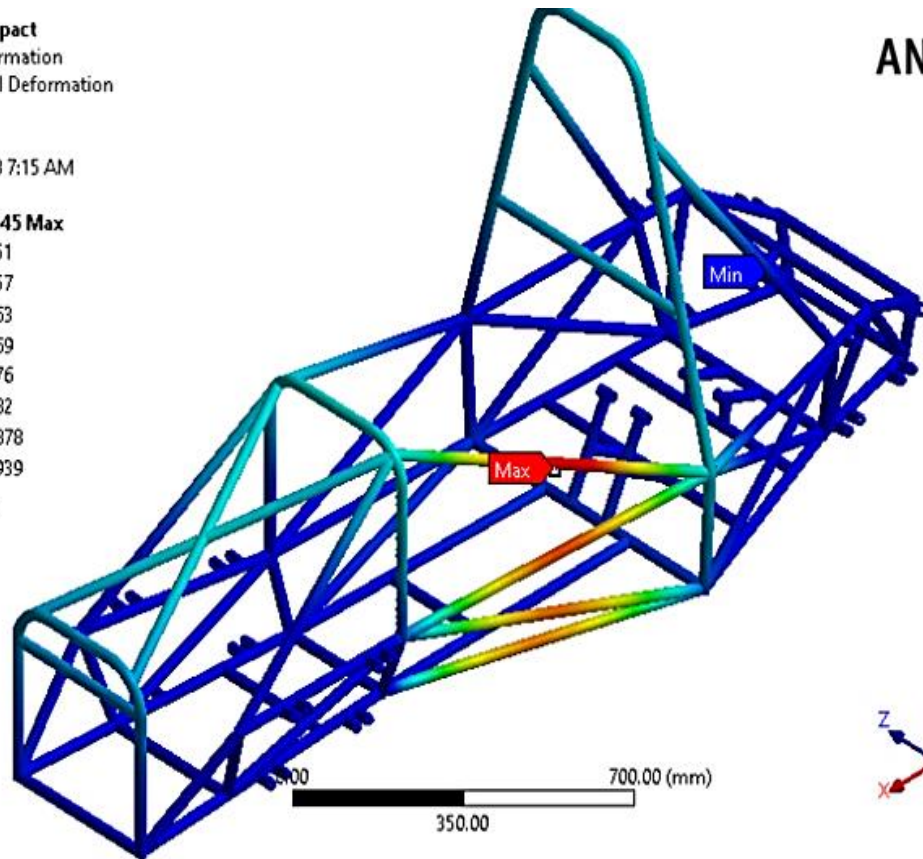
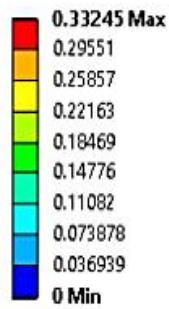
Type: Total Deformation

Unit: mm

Time: 1

10/19/2018 7:15 AM

ANSYS  
R19.1



H: Side Impact

Equivalent Stress

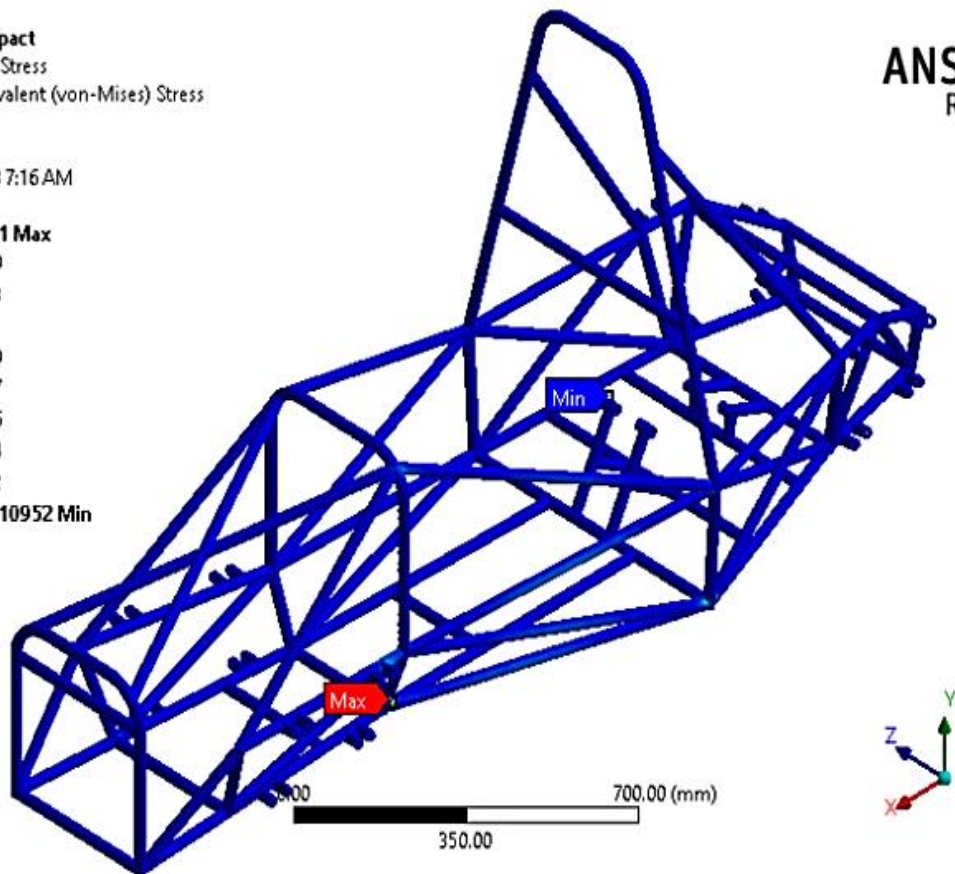
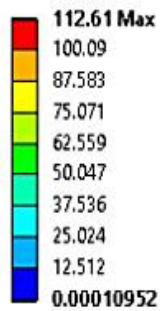
Type: Equivalent (von-Mises) Stress

Unit: MPa

Time: 1

10/19/2018 7:16 AM

ANSYS  
R19.1



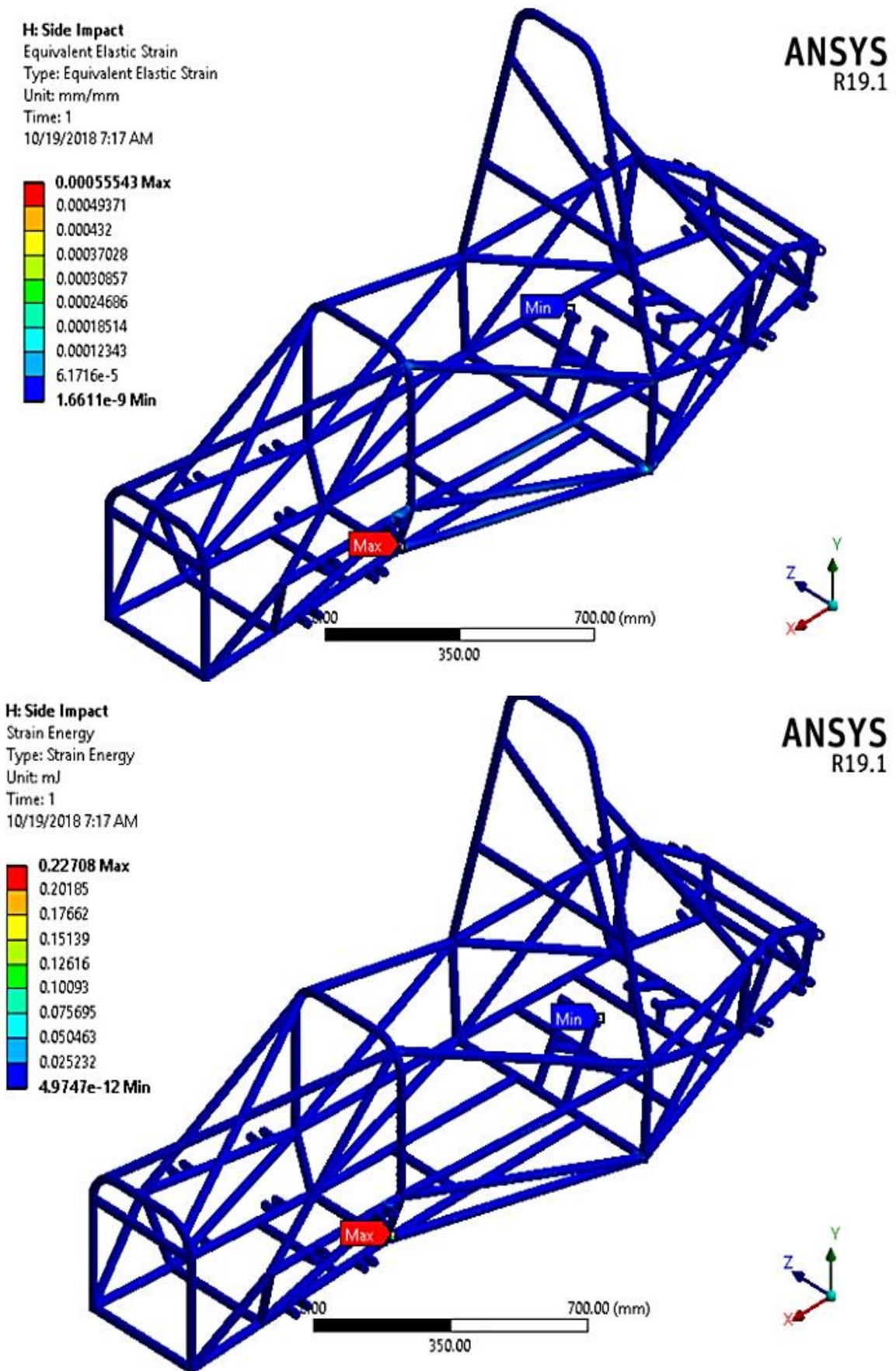


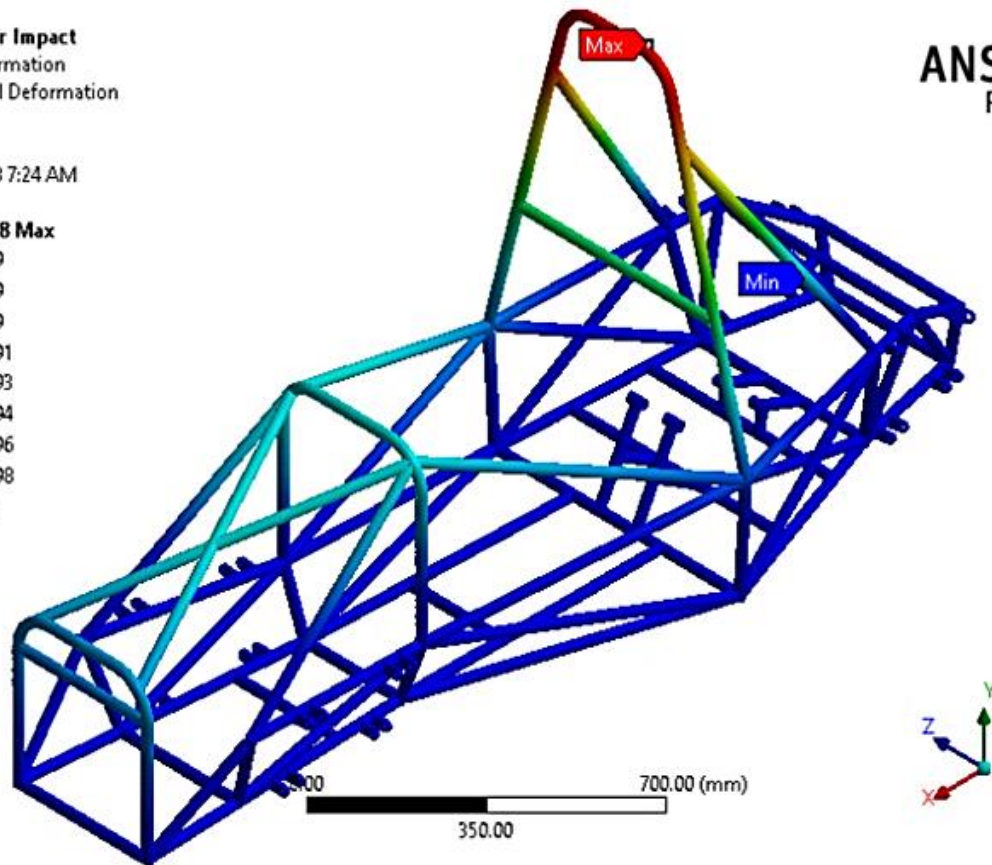
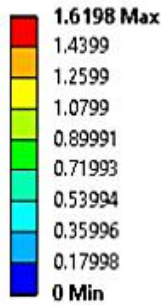
Figure 4.11 Formula SAE M1 Chassis lateral bending results

### c. Rollover Impact

**I: Roll Over Impact**

Total Deformation  
 Type: Total Deformation  
 Unit: mm  
 Time: 1  
 10/19/2018 7:24 AM

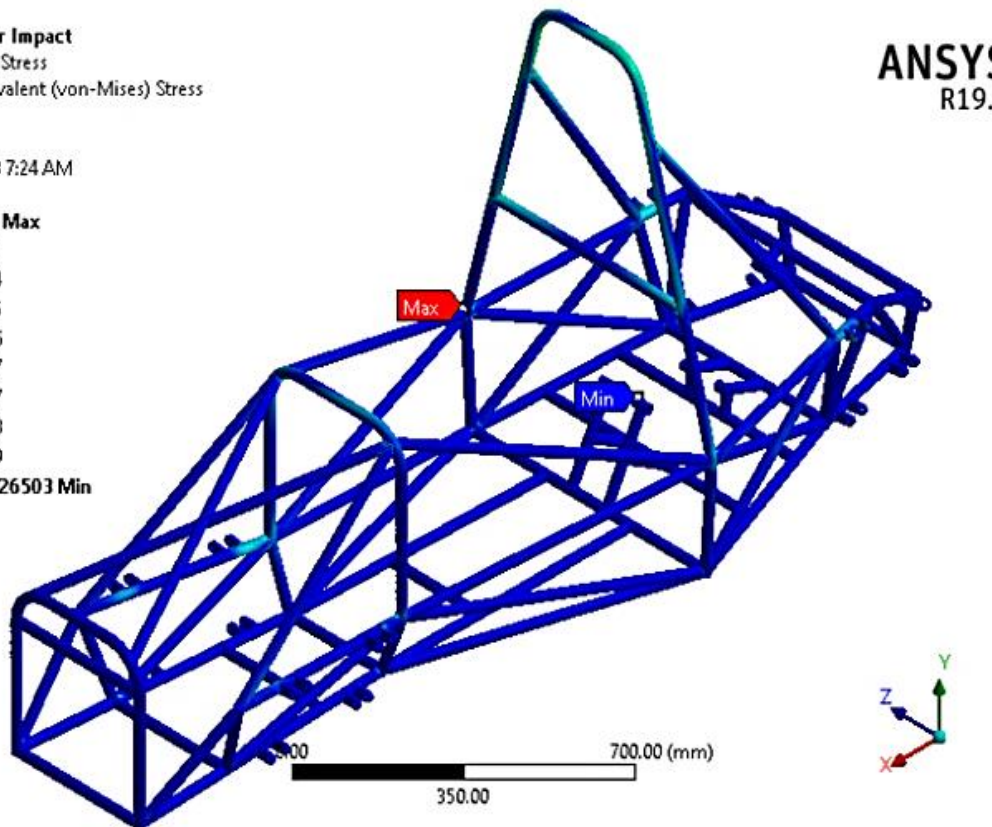
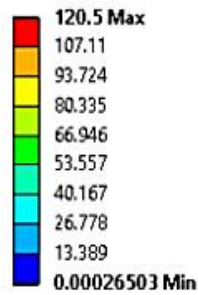
**ANSYS**  
R19.1



**I: Roll Over Impact**

Equivalent Stress  
 Type: Equivalent (von-Mises) Stress  
 Unit: MPa  
 Time: 1  
 10/19/2018 7:24 AM

**ANSYS**  
R19.1



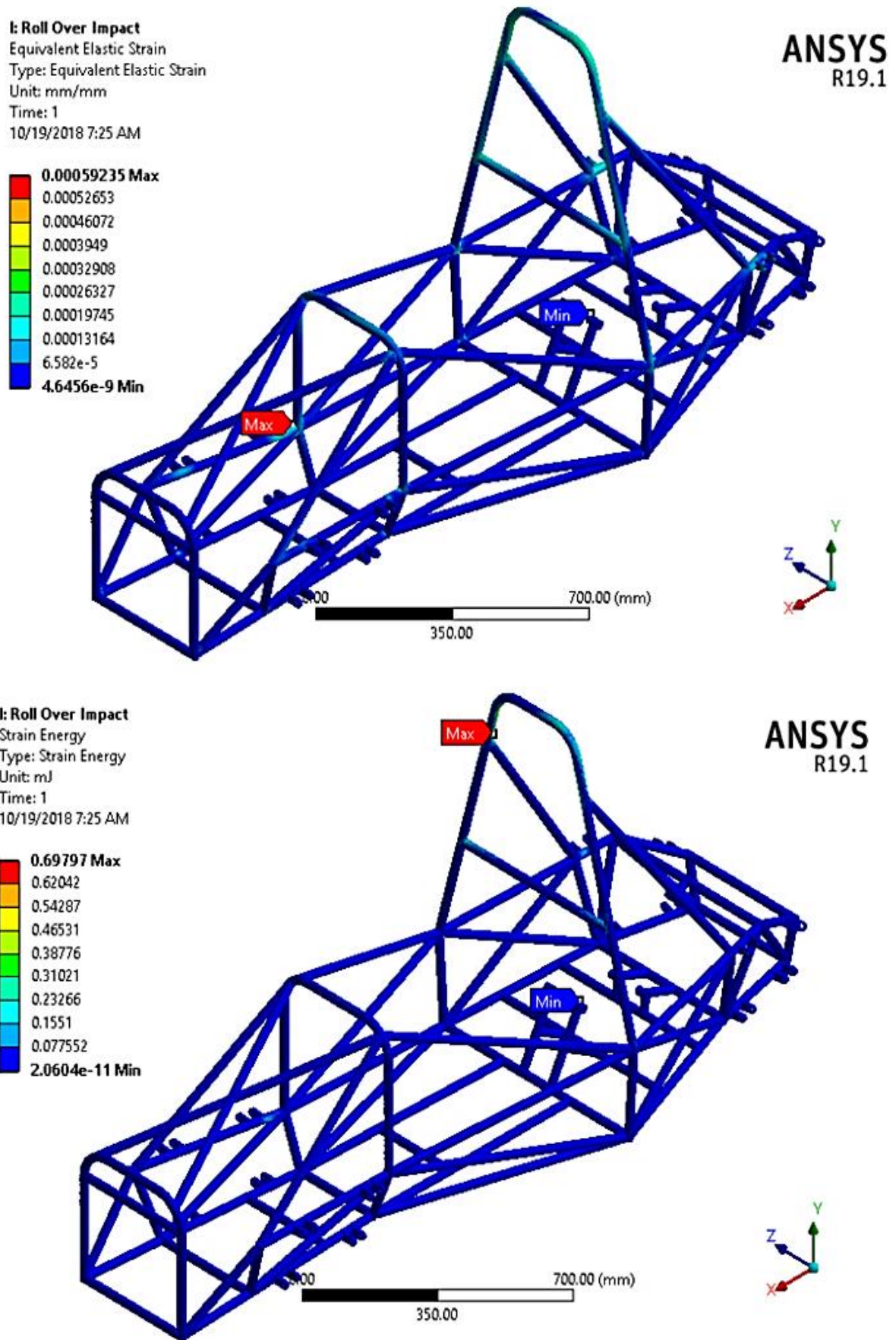
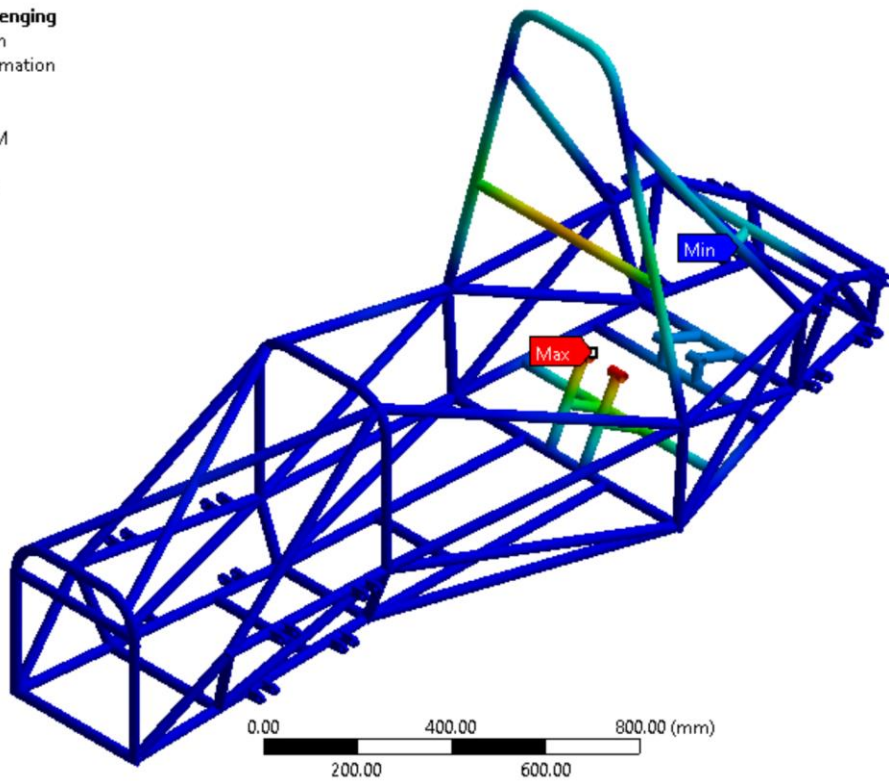
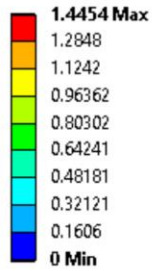


Figure 4.12 Formula SAE M1 Chassis lateral bending results

### 4.1.2.6 Horizontal Lozenging Analysis

**F: Horizontal Lozenging**

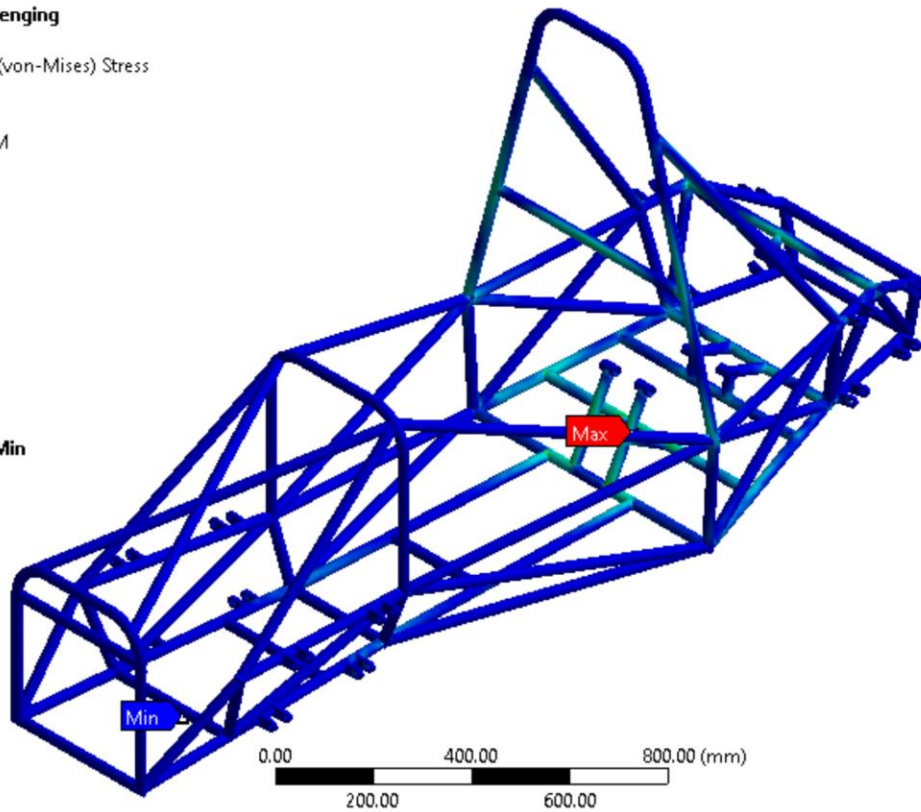
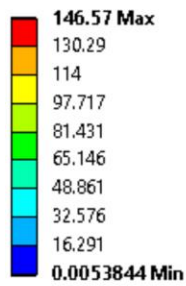
Total Deformation  
 Type: Total Deformation  
 Unit: mm  
 Time: 1  
 1/7/2019 12:16 AM



ANSYS  
R19.1

**F: Horizontal Lozenging**

Equivalent Stress  
 Type: Equivalent (von-Mises) Stress  
 Unit: MPa  
 Time: 1  
 1/7/2019 12:18 AM



ANSYS  
R19.1

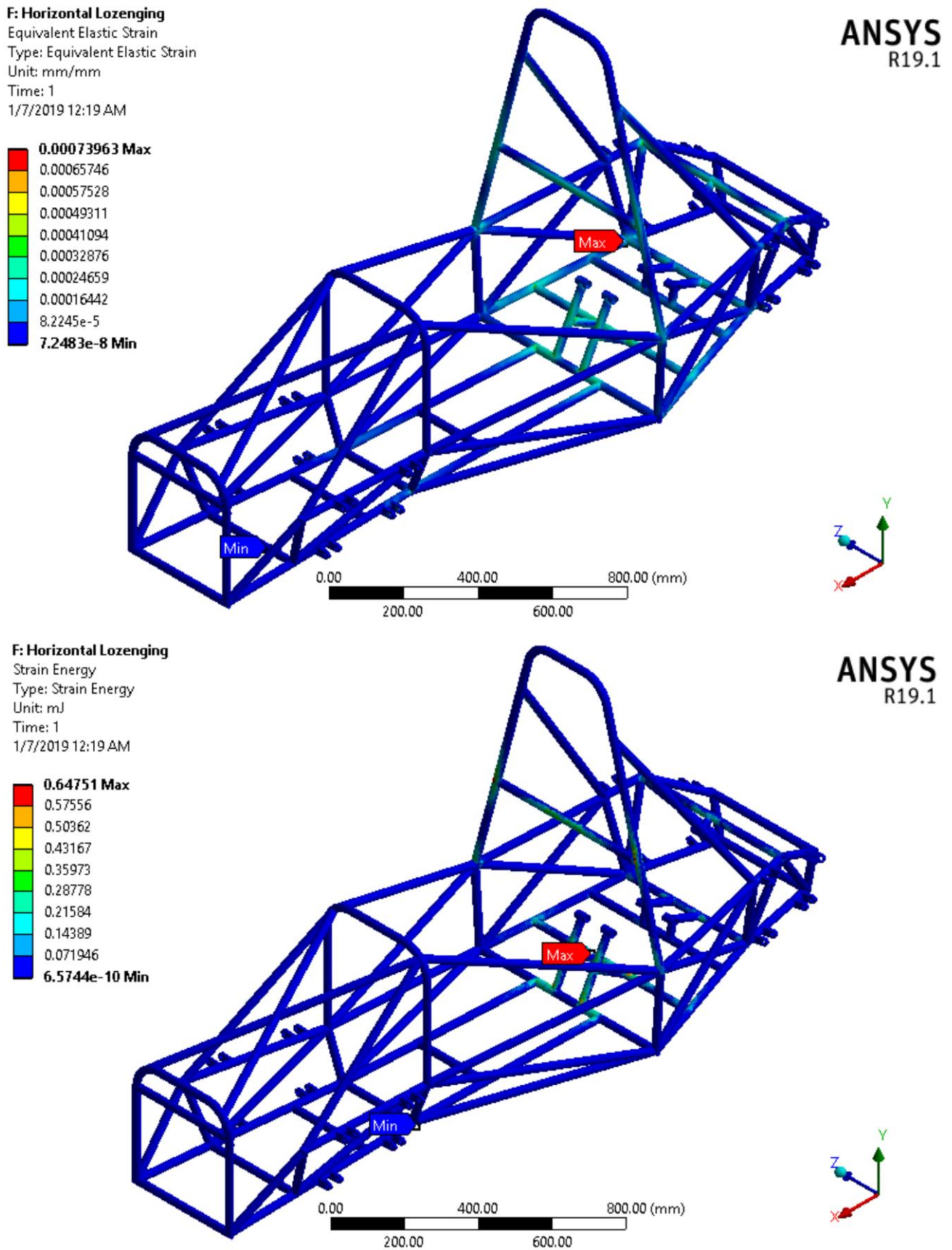
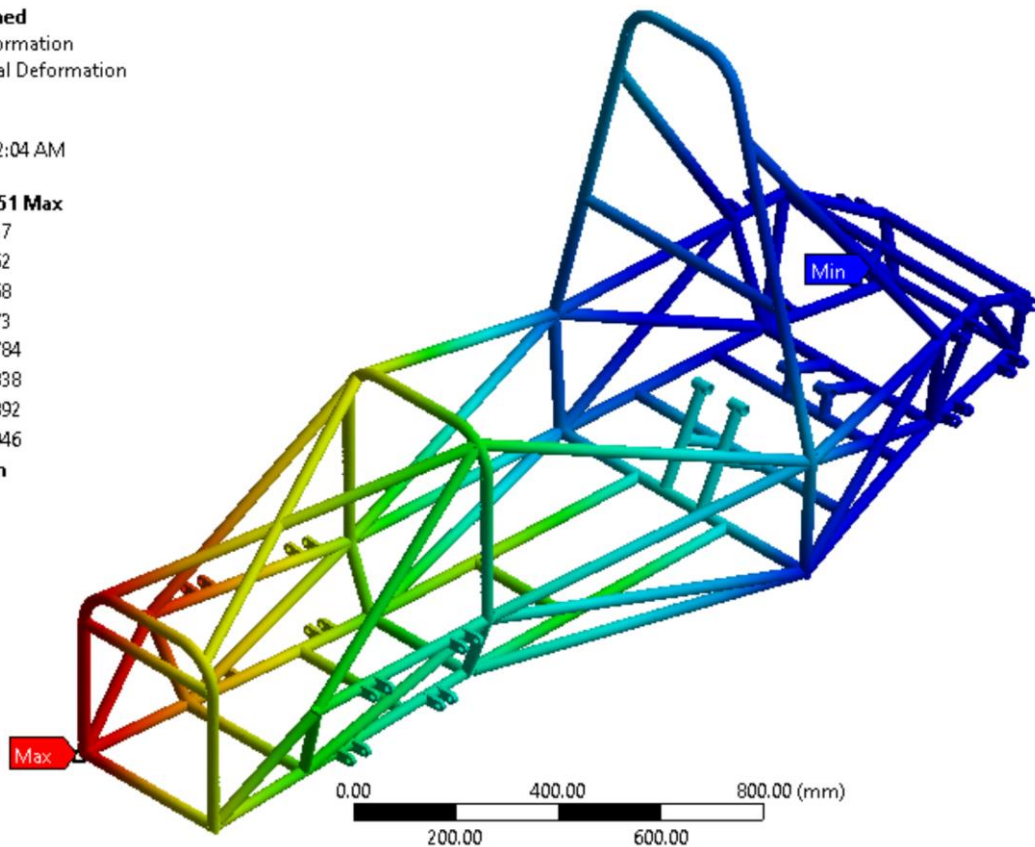
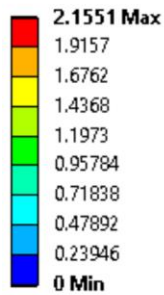


Figure 4.13 Formula SAE M1 Chassis lateral bending results

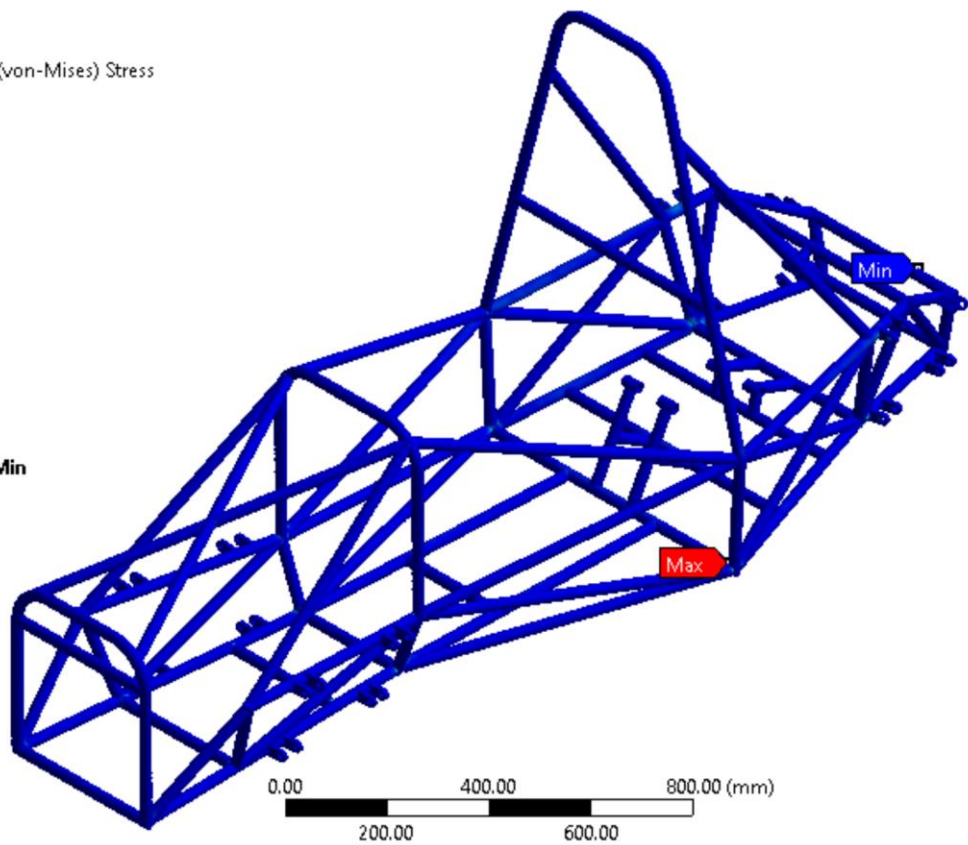
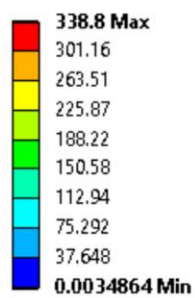
### 4.1.2.7 Combinations of Load Analysis

**P: Combined**  
 Total Deformation  
 Type: Total Deformation  
 Unit: mm  
 Time: 1  
 1/7/2019 2:04 AM



**ANSYS**  
R19.1

**P: Combined**  
 Equivalent Stress  
 Type: Equivalent (von-Mises) Stress  
 Unit: MPa  
 Time: 1  
 1/7/2019 2:04 AM

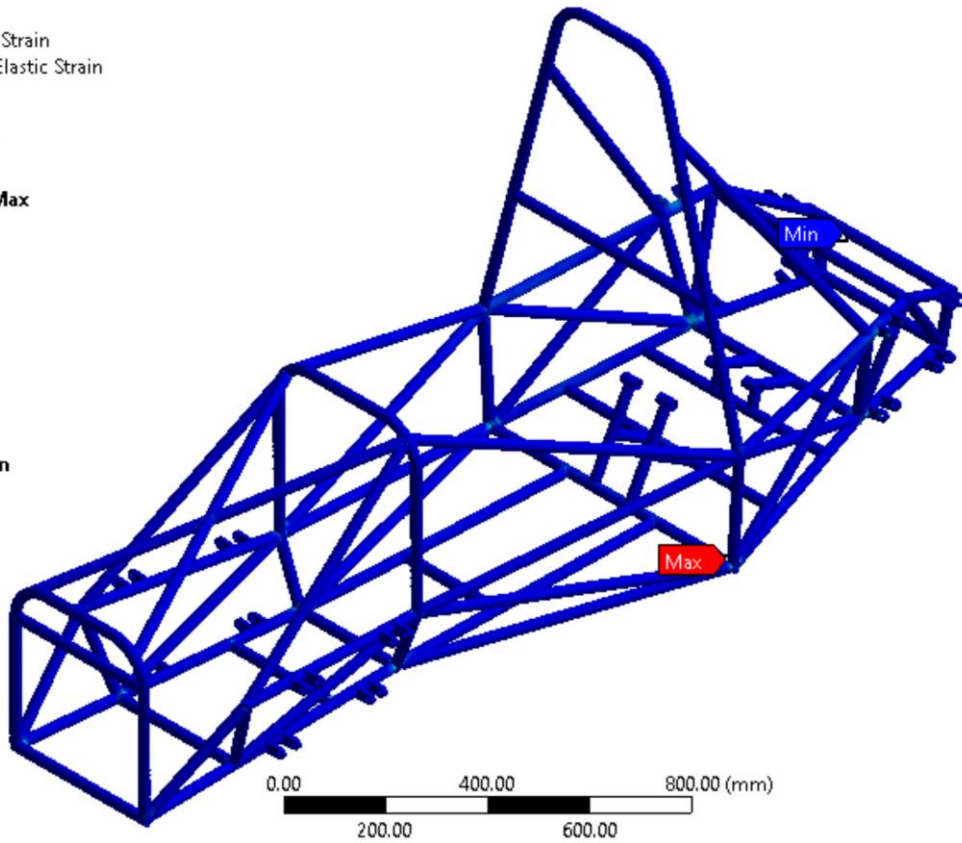


**ANSYS**  
R19.1

**P: Combined**  
 Equivalent Elastic Strain  
 Type: Equivalent Elastic Strain  
 Unit: mm/mm  
 Time: 1  
 1/7/2019 2:05 AM

**ANSYS**  
 R19.1

0.0016179 Max  
 0.0014381  
 0.0012584  
 0.0010786  
 0.00089886  
 0.00071909  
 0.00053933  
 0.00035957  
 0.00017981  
 4.774e-8 Min



**P: Combined**  
 Strain Energy  
 Type: Strain Energy  
 Unit: mJ  
 Time: 1  
 1/7/2019 2:06 AM

**ANSYS**  
 R19.1

0.85595 Max  
 0.76084  
 0.66574  
 0.57063  
 0.47553  
 0.38042  
 0.28532  
 0.19021  
 0.095105  
 1.3747e-9 Min

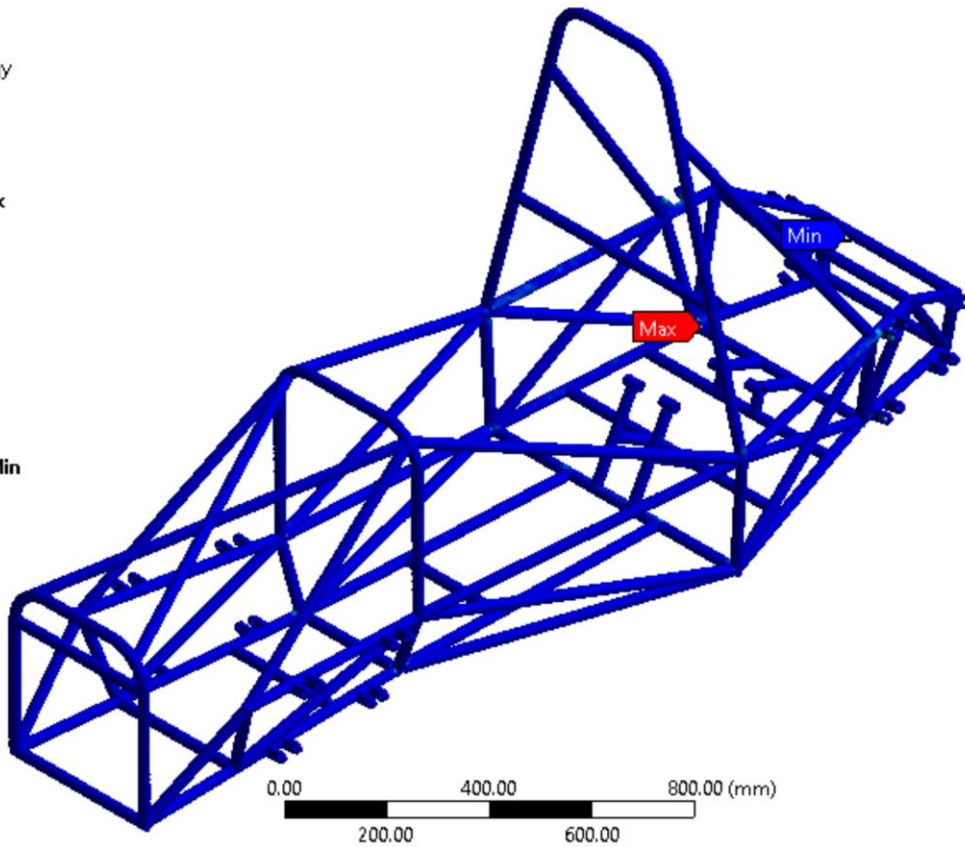


Figure 4.14 Formula SAE M1 Chassis combined load results

### 4.1.3 Formula SAE M1 Topological Optimization with New Boundary Condition Result

From the Formula SAE M1 Chassis with new boundary condition found the equivalent Von-Mess stress less than the material yield tensile strength and total deformation of the material is less than 25mm as recommended by Formula SAE rule. By using these results, the topological optimization of the frame takes place and divided it into three parts:

**Topological Optimization 1:** the optimization of Formula SAE M1 Chassis base on the pure bending, braking, horizontal lozenging and combine loading condition using the new boundary type (see Figure 4.15).

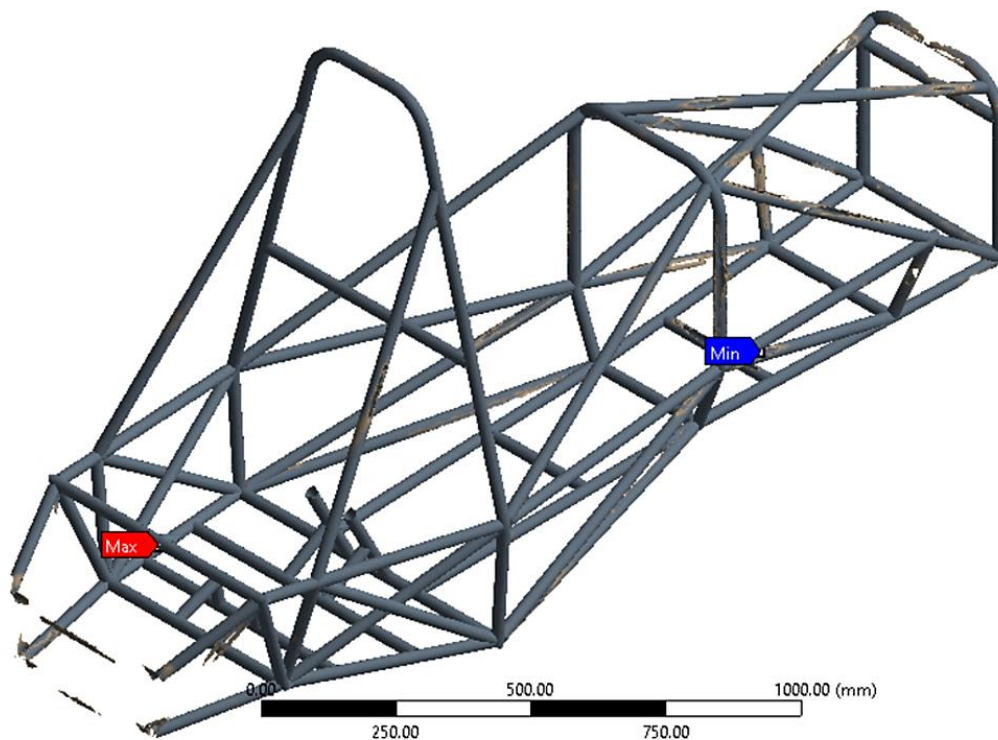


Figure 4.15 Optimization 1 base on the following loading types

**Topological Optimization 2:** the optimization of Formula SAE M1 Chassis base on the pure torsion loading condition using the new boundary type (see Figure 4.16).

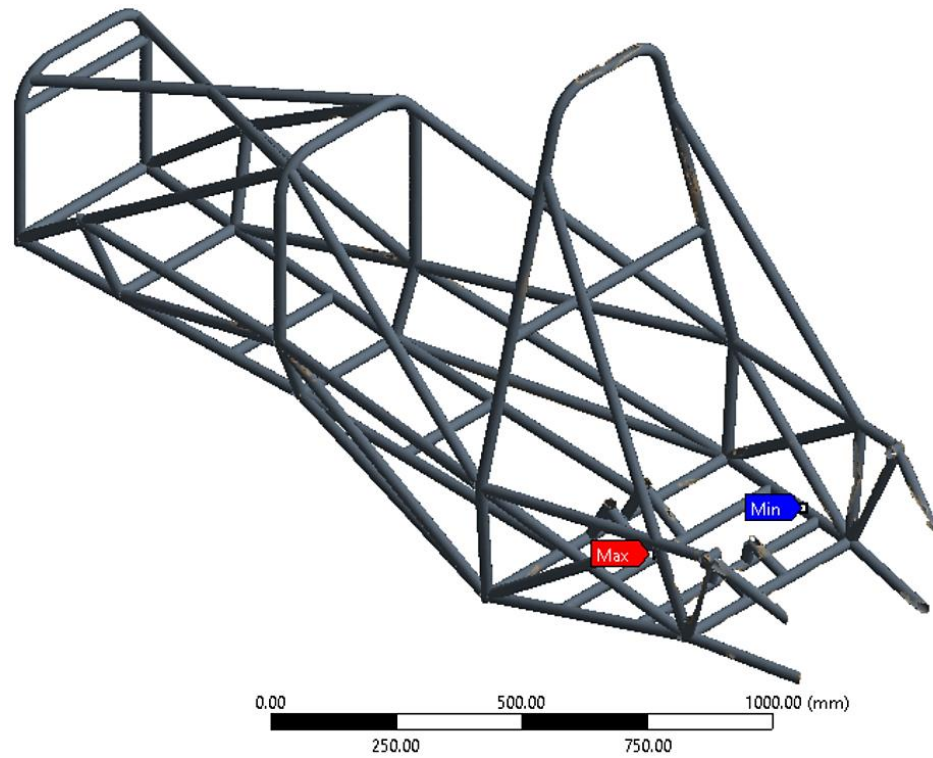


Figure 4.16 Optimization 2 based on Pure Torsion analysis

**Topological Optimization 3:** the optimization of Formula SAE M1 Chassis base on the front, side and rollover impact condition using the new boundary type (see Figure 4.17).

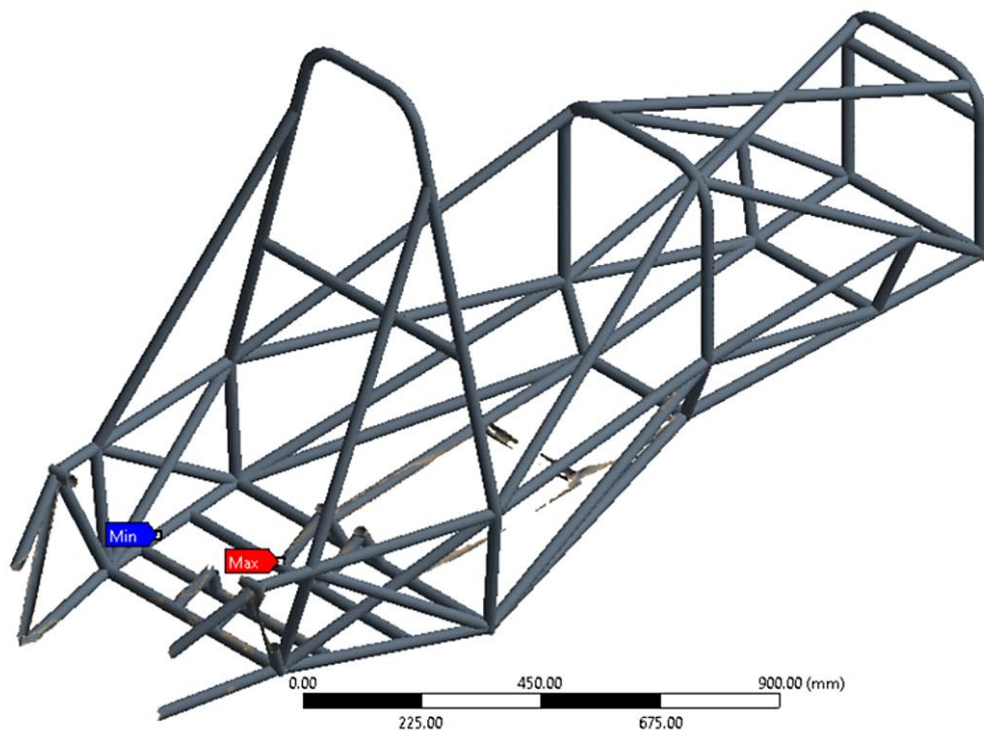
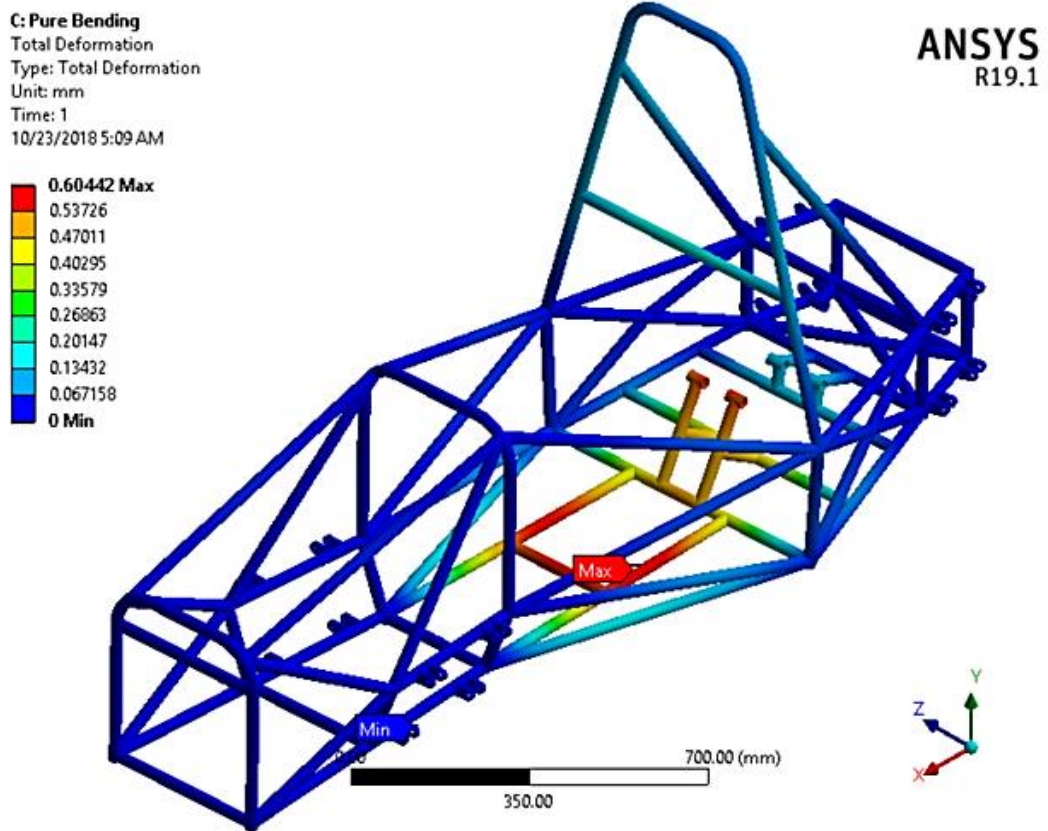


Figure 4.17 Optimization results from the impact analysis

#### 4.1.4 Formula SAE M2 with New Boundary Condition Result (Quai-Static Simulation)

##### 4.1.4.1 Vertical Symmetric or Vertical Bending ('pure bending') Load Analysis



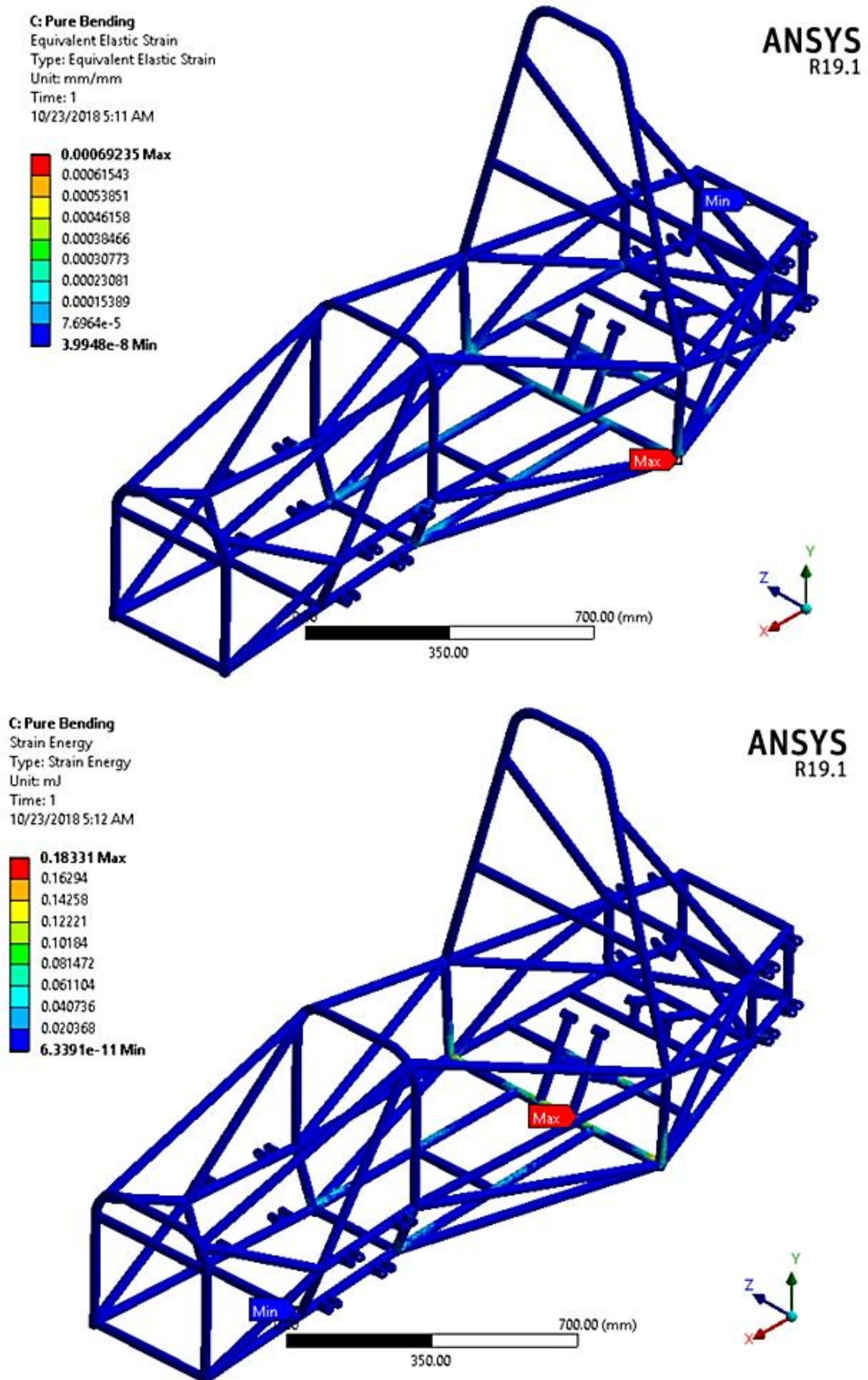
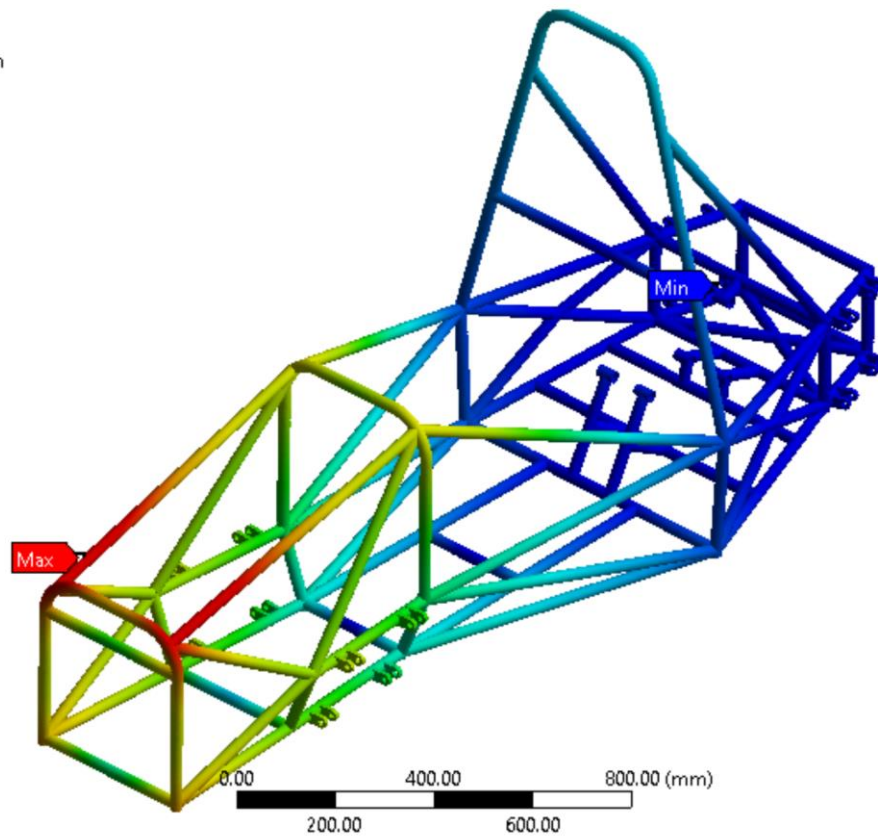
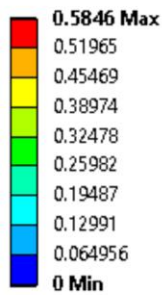


Figure 4.18 Formula SAE M1 Chassis pure bending results

#### 4.1.4.2 Vertical Asymmetric or Longitudinal Torsion (Pure Torsion Analysis Case)

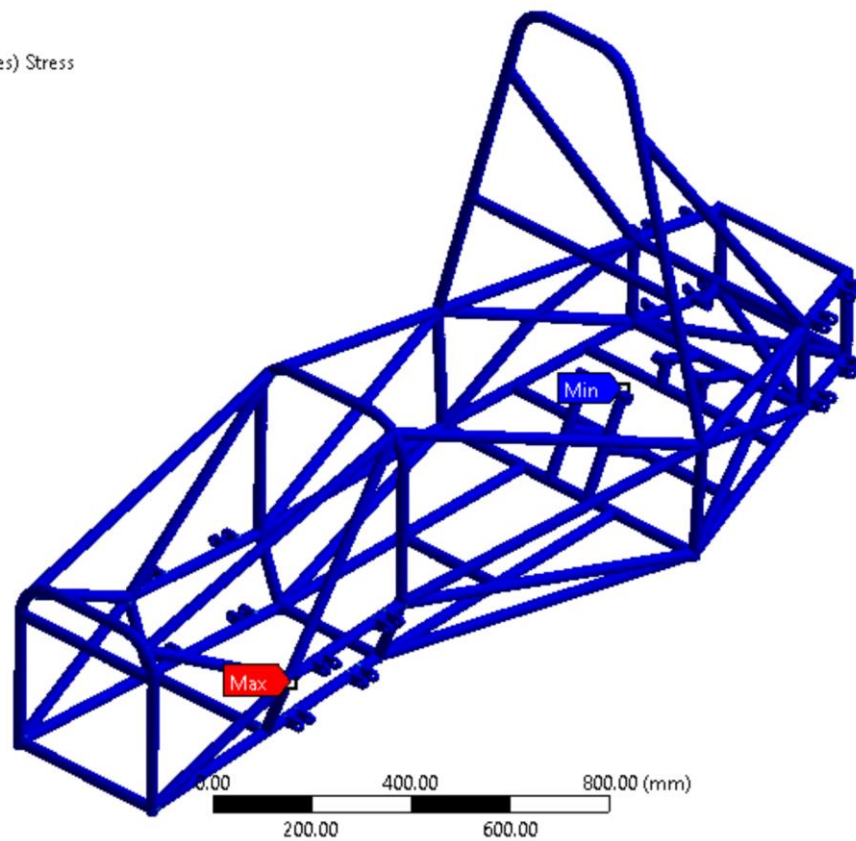
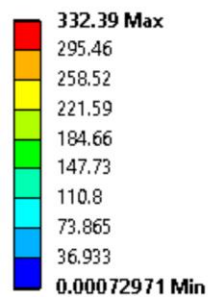
**N: Pure Torsion**  
 Total Deformation  
 Type: Total Deformation  
 Unit: mm  
 Time: 1  
 1/7/2019 2:15 AM

**ANSYS**  
 R19.1



**N: Pure Torsion**  
 Equivalent Stress  
 Type: Equivalent (von-Mises) Stress  
 Unit: MPa  
 Time: 1  
 1/7/2019 2:16 AM

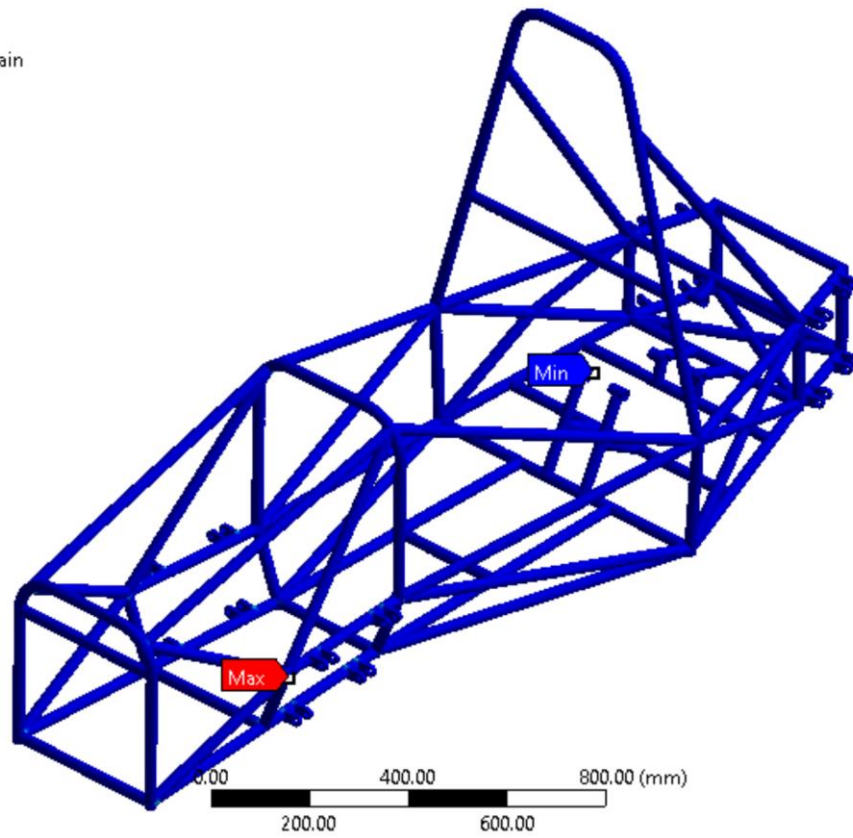
**ANSYS**  
 R19.1



**N: Pure Torsion**  
 Equivalent Elastic Strain  
 Type: Equivalent Elastic Strain  
 Unit: mm/mm  
 Time: 1  
 1/7/2019 2:16 AM

**ANSYS**  
 R19.1

0.0016024 Max  
 0.0014243  
 0.0012463  
 0.0010682  
 0.0008902  
 0.00071216  
 0.00053413  
 0.00035609  
 0.00017805  
 1.2228e-8 Min



**N: Pure Torsion**  
 Strain Energy  
 Type: Strain Energy  
 Unit: mJ  
 Time: 1  
 1/7/2019 2:17 AM

**ANSYS**  
 R19.1

0.45139 Max  
 0.40124  
 0.35108  
 0.30093  
 0.25077  
 0.20062  
 0.15046  
 0.10031  
 0.050155  
 1.571e-12 Min

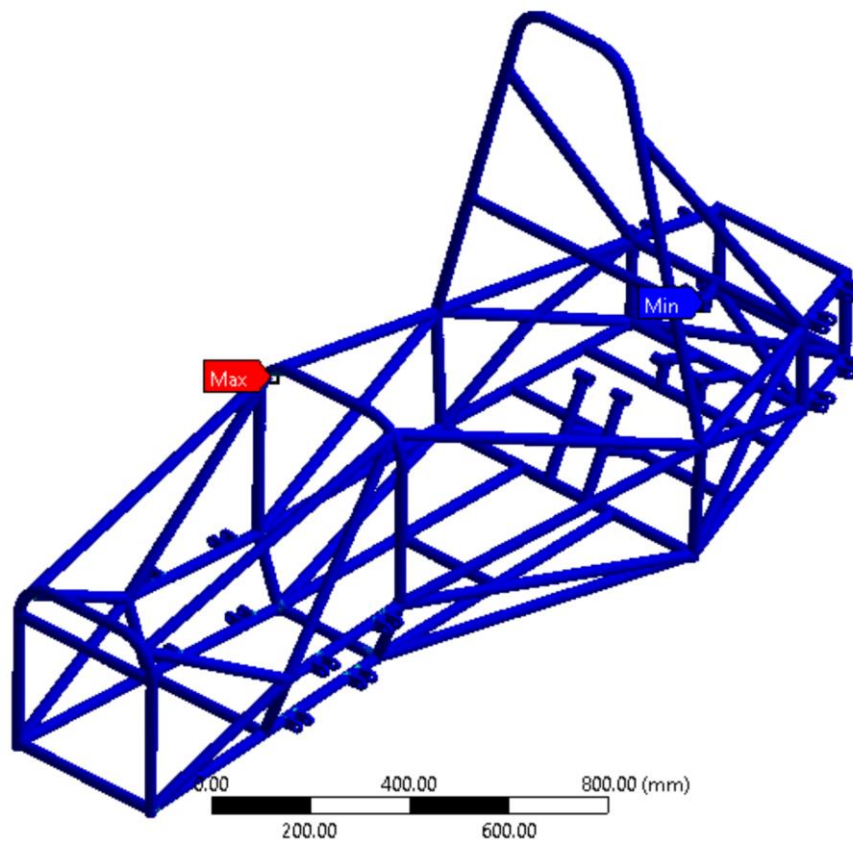
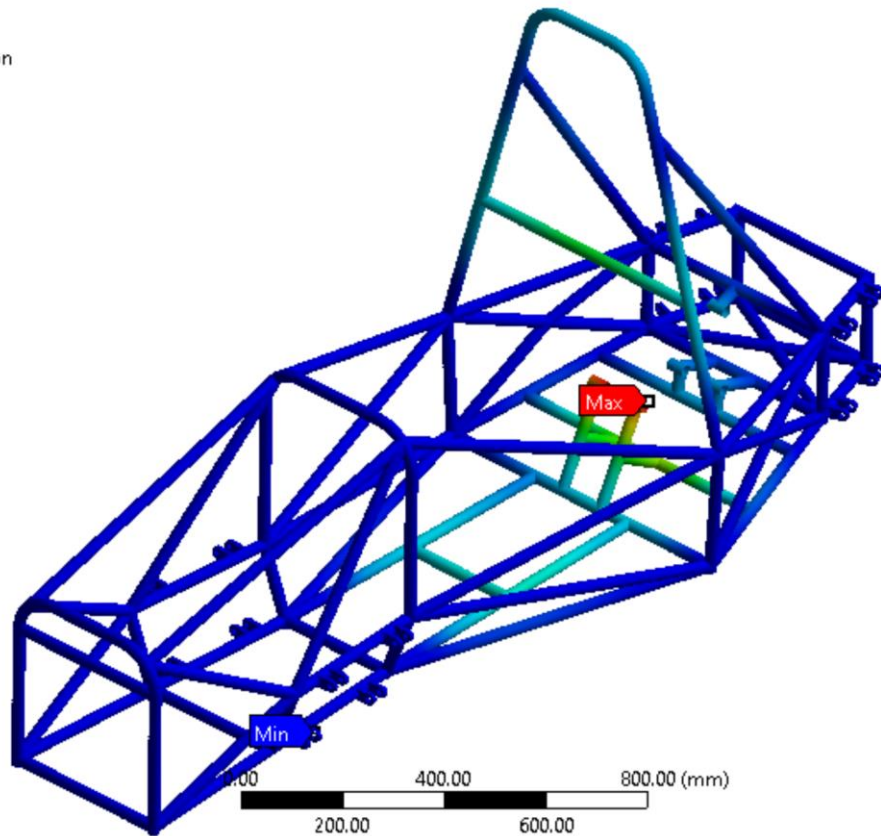
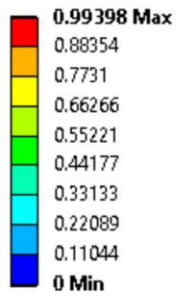


Figure 4.19 Formula SAE M1 Chassis pure torsion results

### 4.1.4.3 Longitudinal loads (Braking) Analysis

**G: Braking**

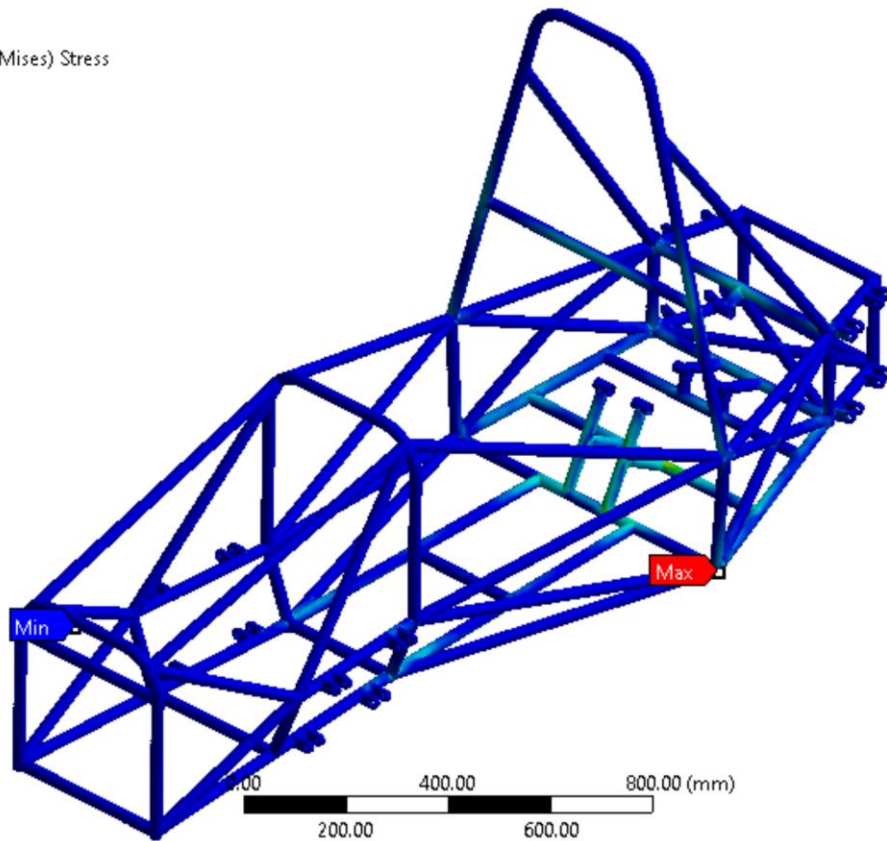
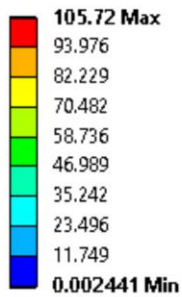
Total Deformation  
 Type: Total Deformation  
 Unit: mm  
 Time: 1  
 1/7/2019 2:19 AM



**ANSYS**  
R19.1

**G: Braking**

Equivalent Stress  
 Type: Equivalent (von-Mises) Stress  
 Unit: MPa  
 Time: 1  
 1/7/2019 2:19 AM



**ANSYS**  
R19.1

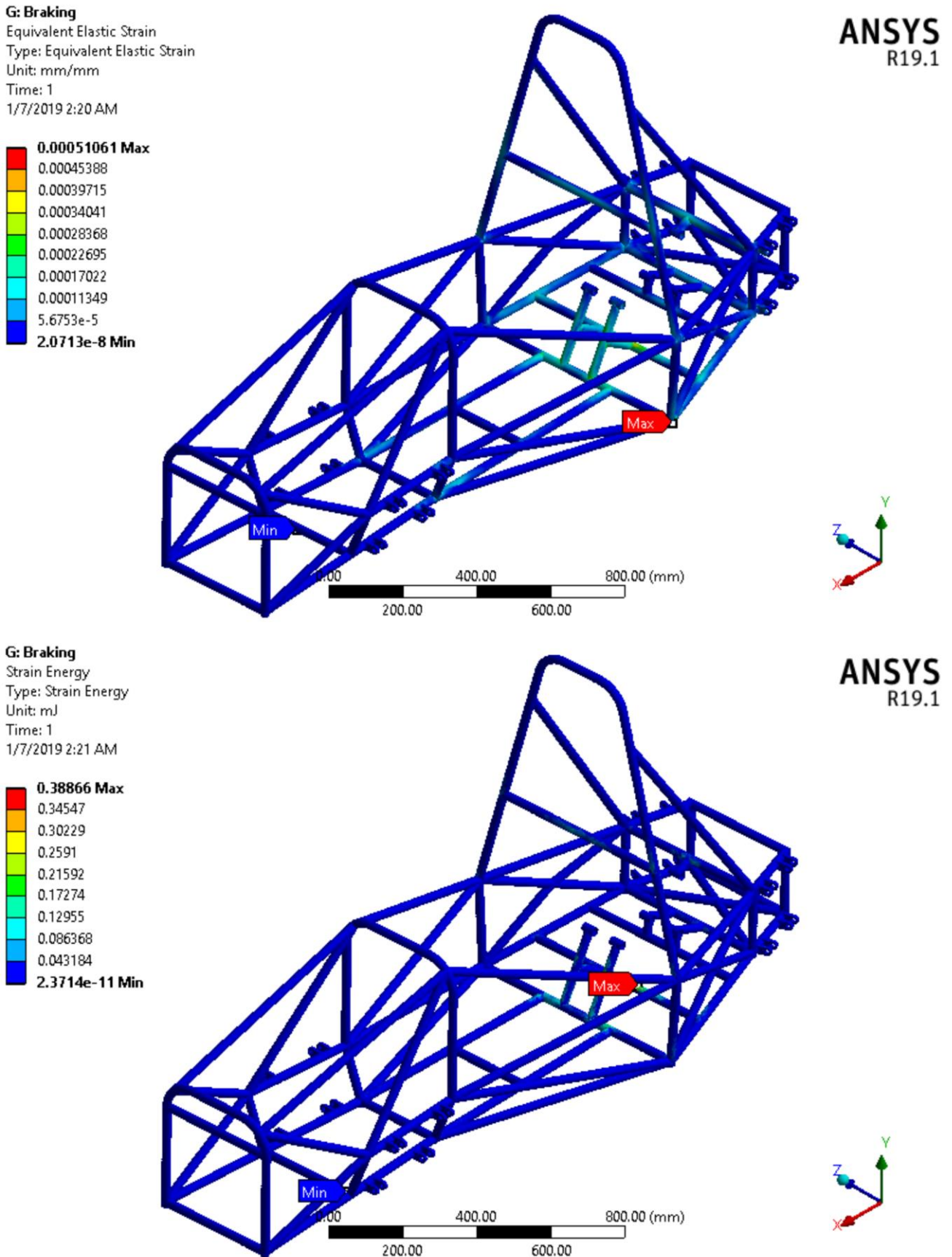
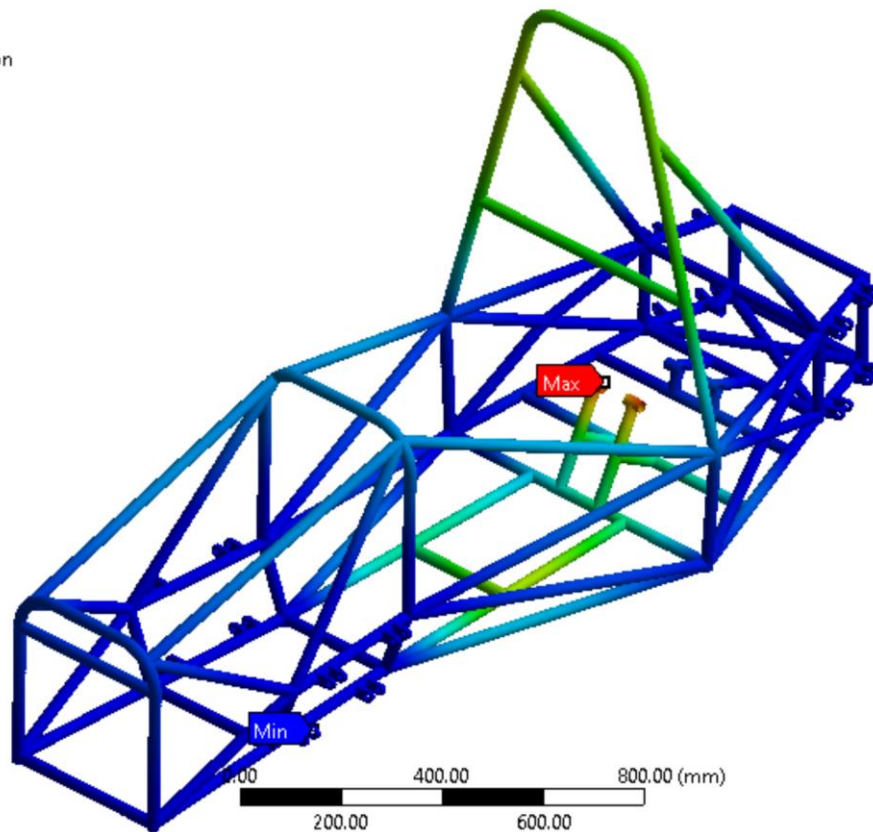
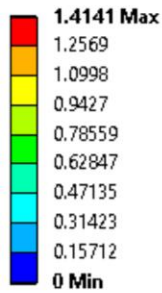


Figure 4.20 Formula SAE M1 Chassis longitudinal load results

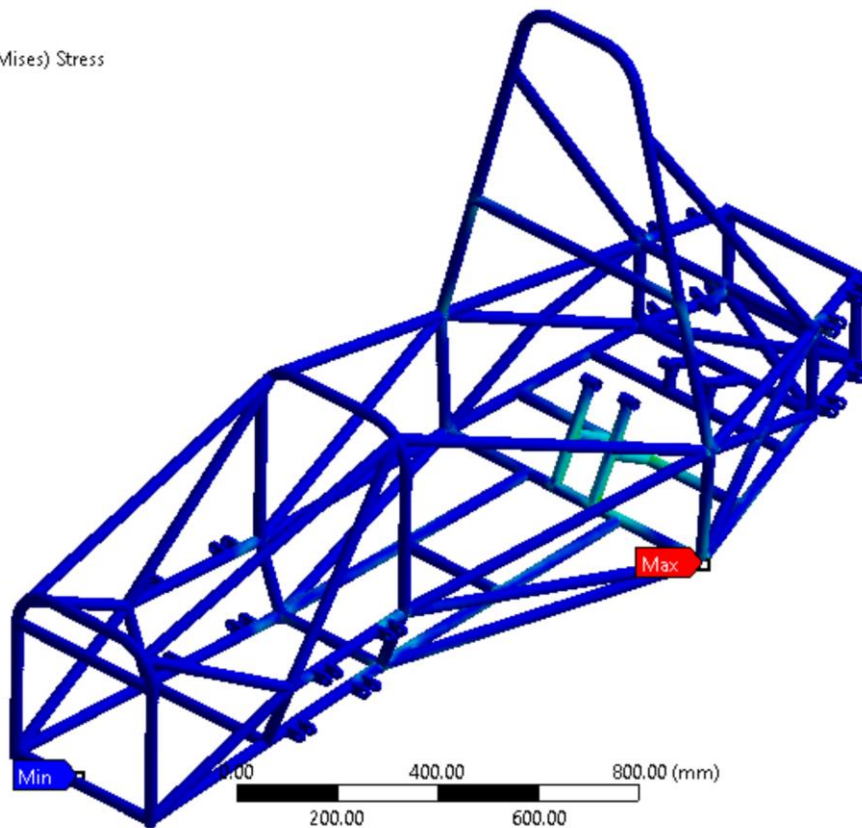
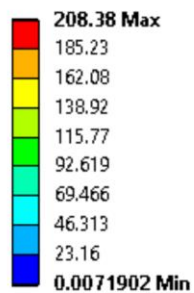
#### 4.1.4.4 Lateral Bending (Cornering) Analysis

**E: Lateral Bending**  
 Total Deformation  
 Type: Total Deformation  
 Unit: mm  
 Time: 1  
 1/7/2019 2:23 AM



**ANSYS**  
R19.1

**E: Lateral Bending**  
 Equivalent Stress  
 Type: Equivalent (von-Mises) Stress  
 Unit: MPa  
 Time: 1  
 1/7/2019 2:26 AM



**ANSYS**  
R19.1

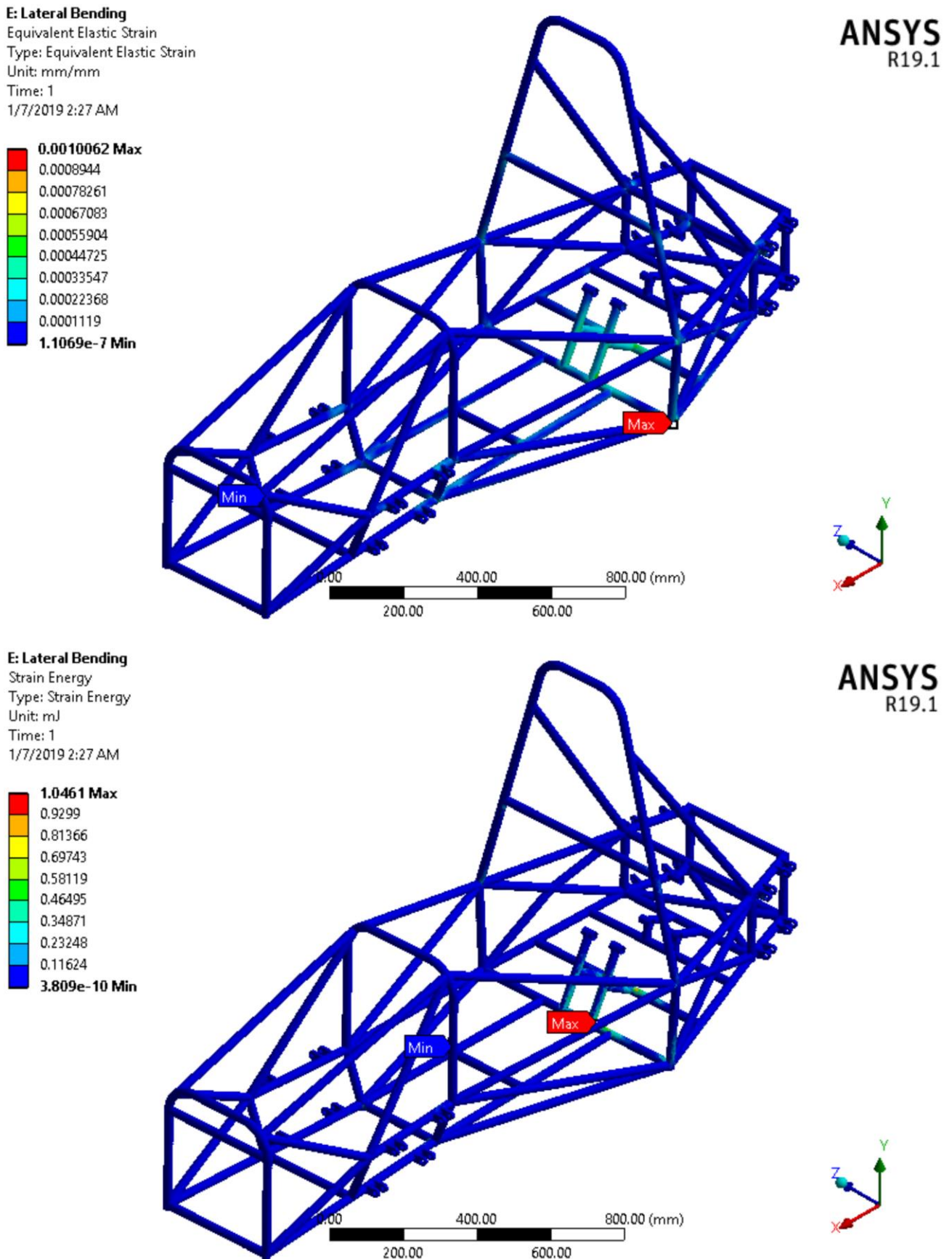


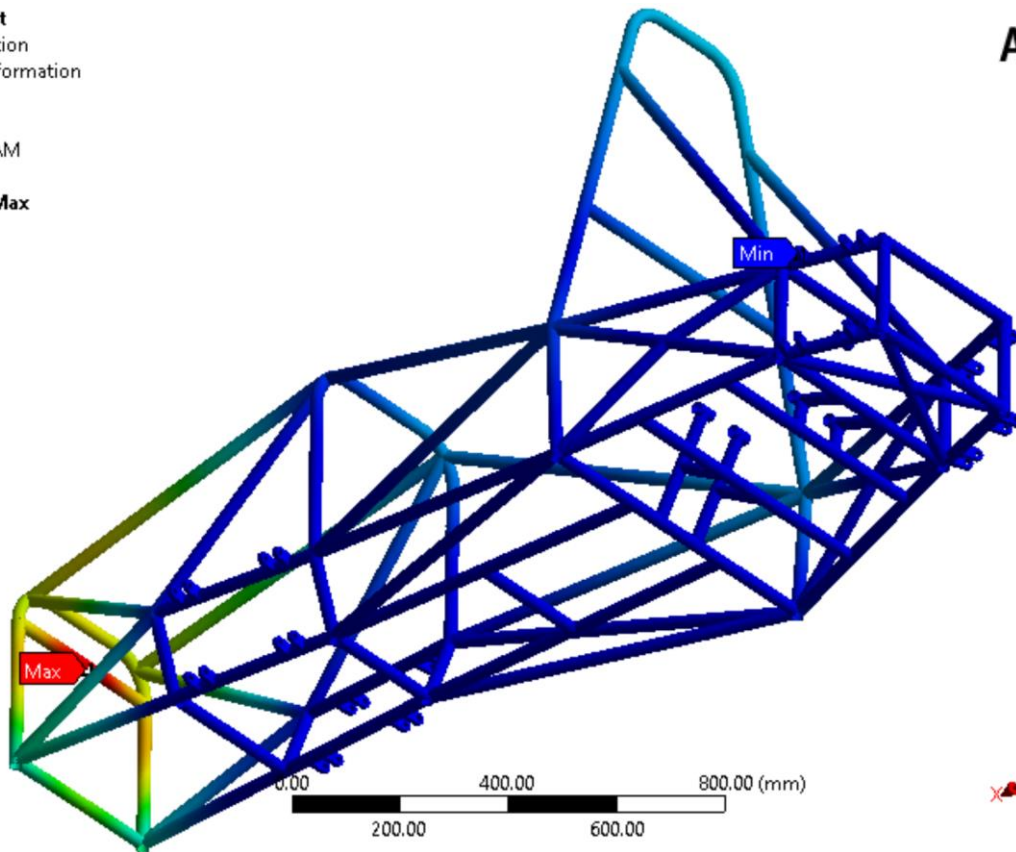
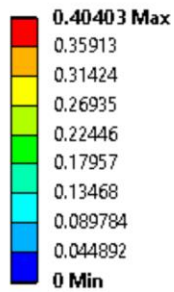
Figure 4.21 Formula SAE M2 Chassis lateral bending results

#### 4.1.4.5 Crash or Impact cases (Front, Side and Rollover Crash) Analysis

##### a. Front Impact

**L: Front Impact**

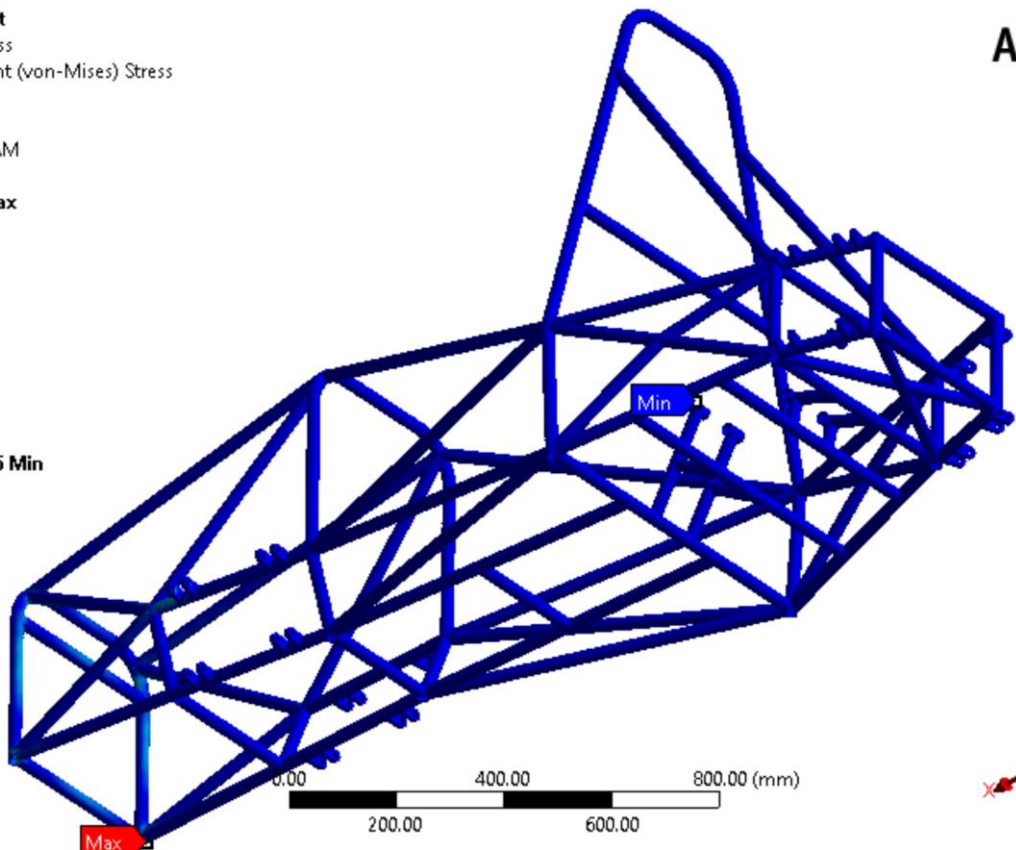
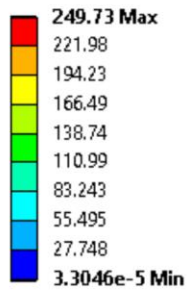
Total Deformation  
 Type: Total Deformation  
 Unit: mm  
 Time: 1  
 1/7/2019 2:36 AM



**ANSYS**  
R19.1

**L: Front Impact**

Equivalent Stress  
 Type: Equivalent (von-Mises) Stress  
 Unit: MPa  
 Time: 1  
 1/7/2019 2:36 AM



**ANSYS**  
R19.1

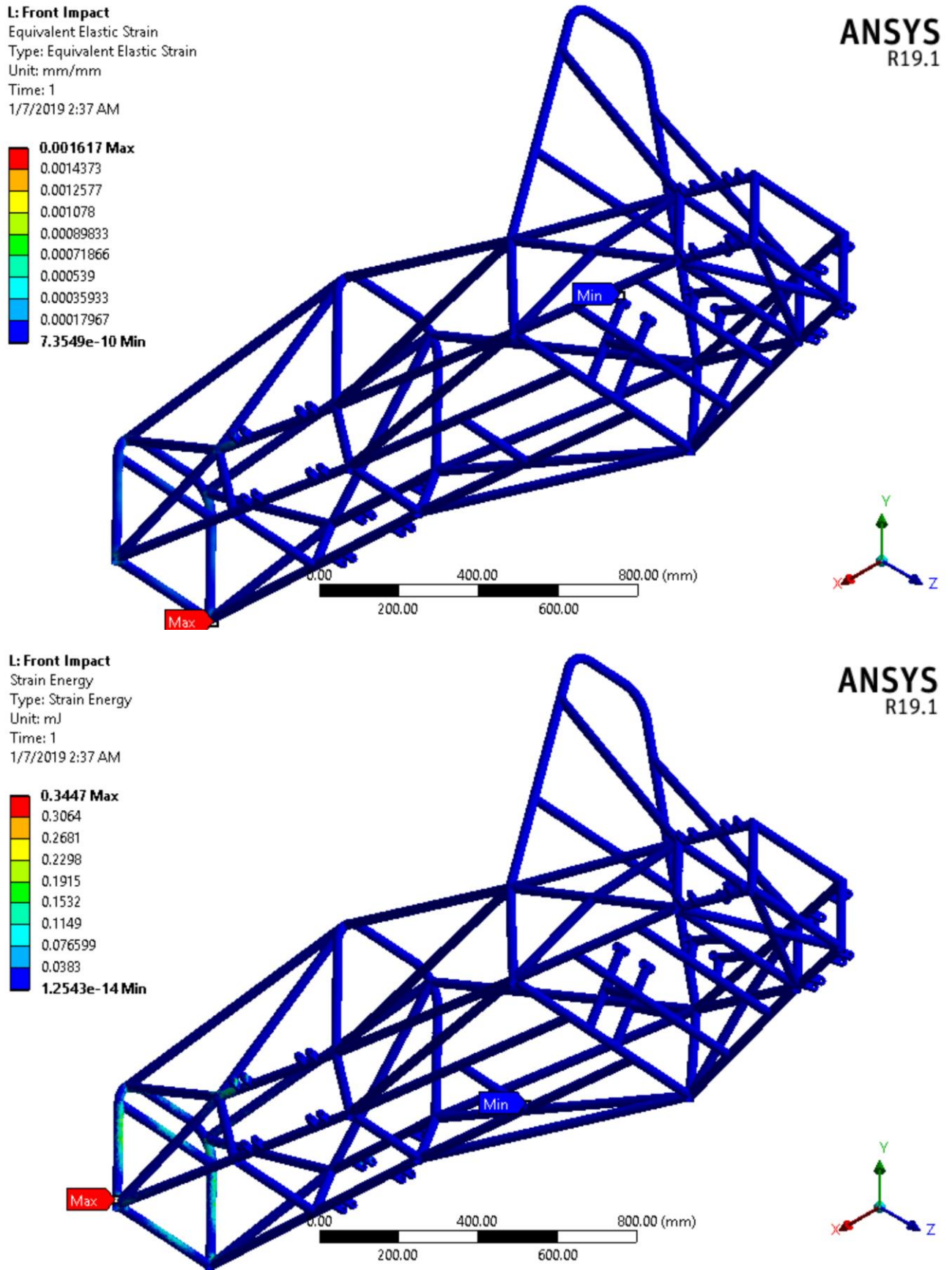
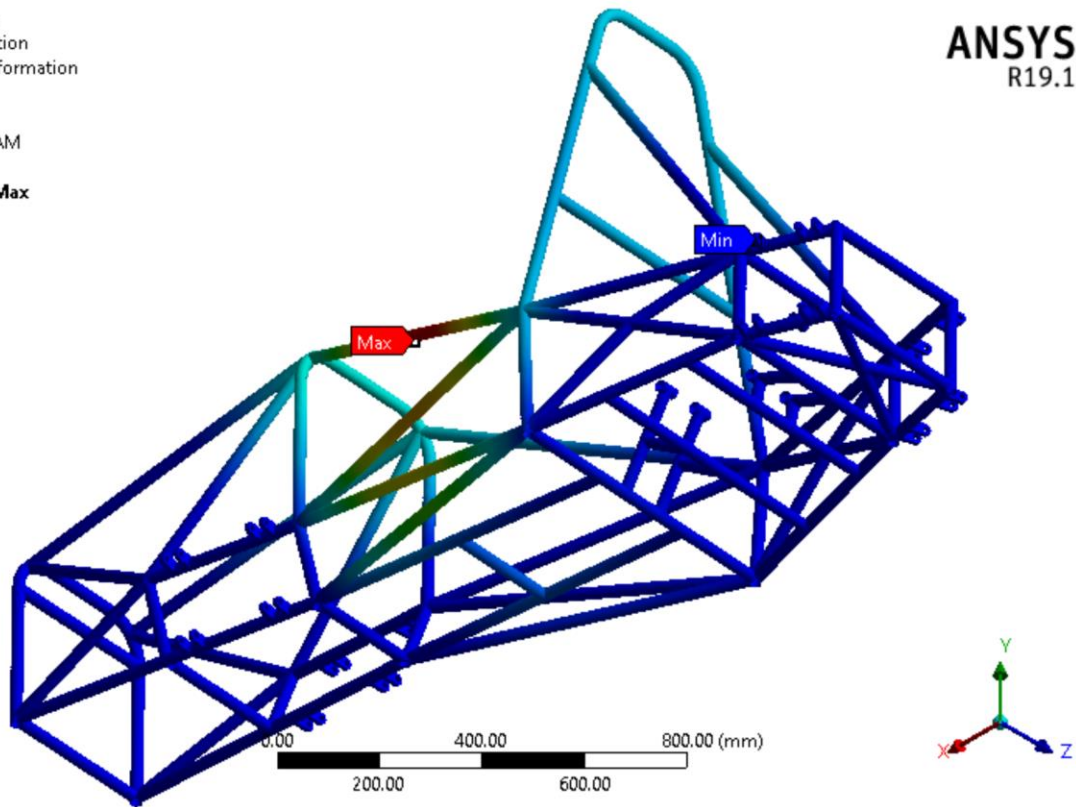
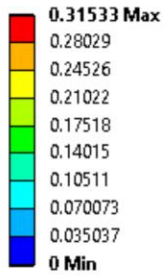


Figure 4.22 Formula SAE M2 Chassis front impact results

### b. Side Impact

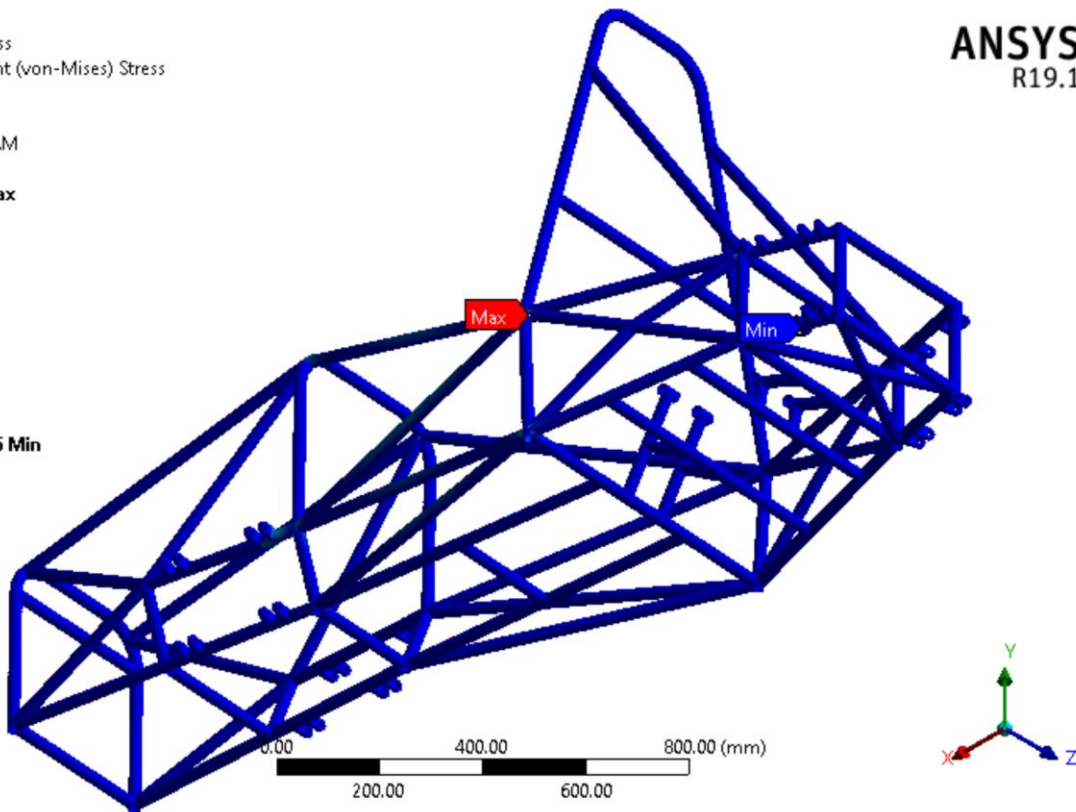
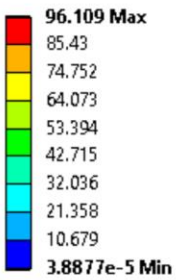
**I: Side Impact**  
 Total Deformation  
 Type: Total Deformation  
 Unit: mm  
 Time: 1  
 1/7/2019 2:31 AM

**ANSYS**  
 R19.1



**I: Side Impact**  
 Equivalent Stress  
 Type: Equivalent (von-Mises) Stress  
 Unit: MPa  
 Time: 1  
 1/7/2019 2:31 AM

**ANSYS**  
 R19.1



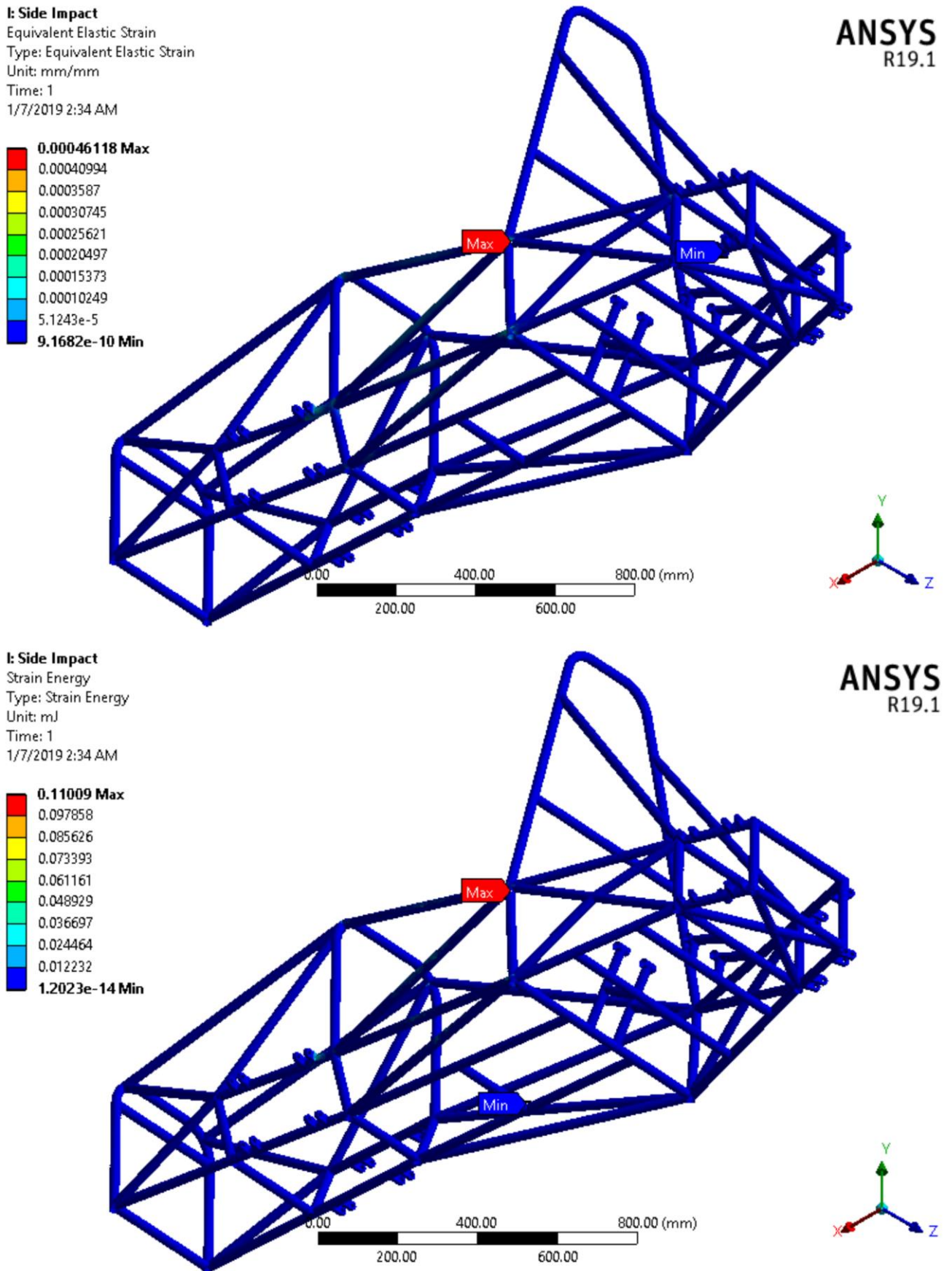
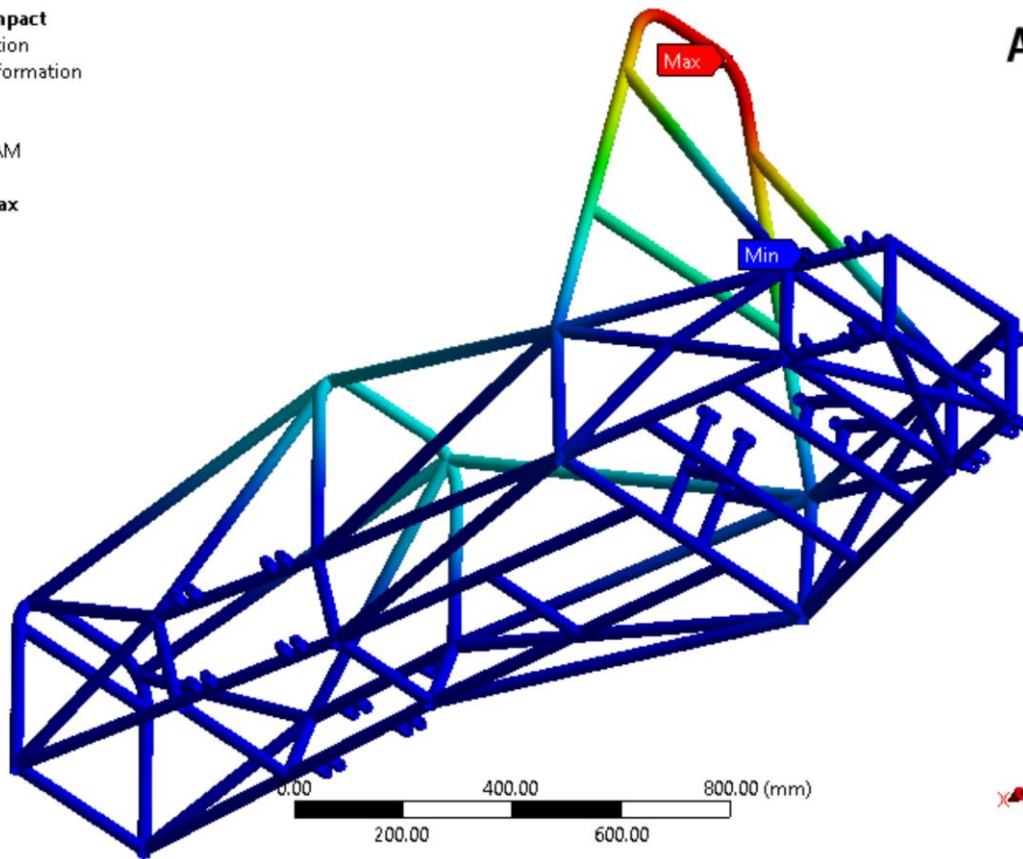
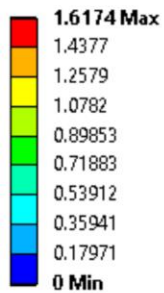


Figure 4.23 Formula SAE M2 Chassis side impact results

### c. Rollover Impact

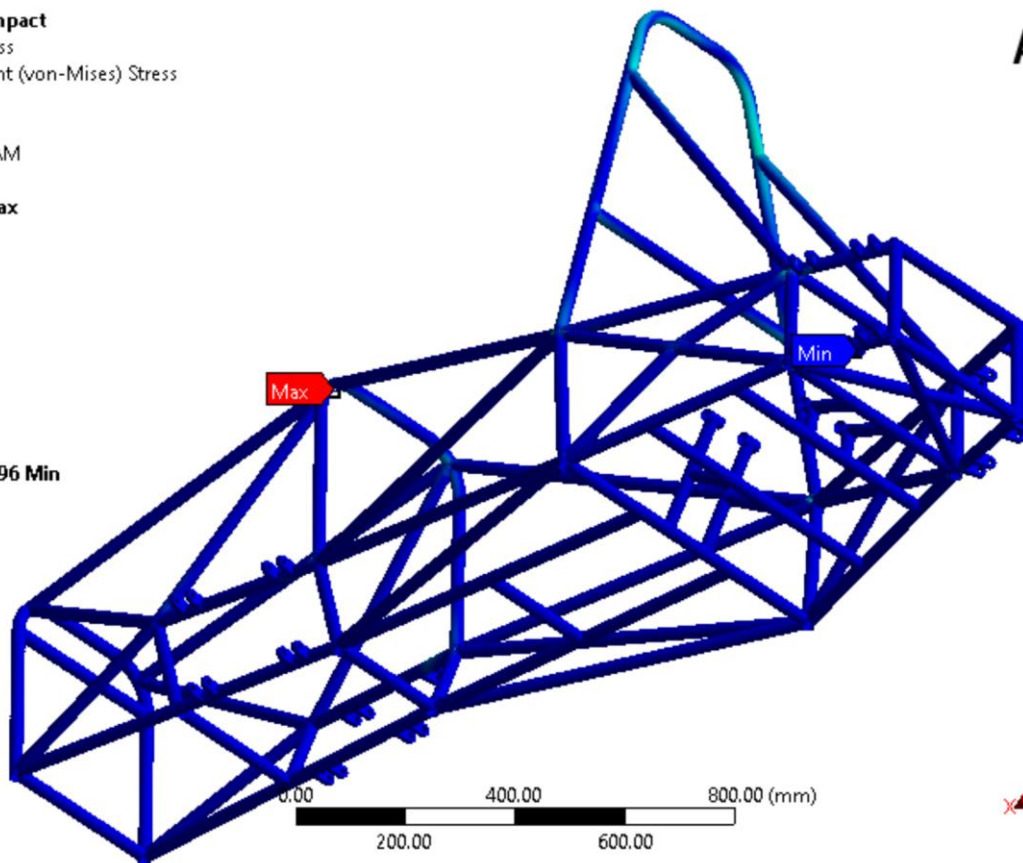
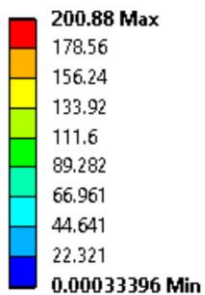
**K: Roll Over Impact**  
 Total Deformation  
 Type: Total Deformation  
 Unit: mm  
 Time: 1  
 1/7/2019 2:38 AM

**ANSYS**  
 R19.1



**K: Roll Over Impact**  
 Equivalent Stress  
 Type: Equivalent (von-Mises) Stress  
 Unit: MPa  
 Time: 1  
 1/7/2019 2:39 AM

**ANSYS**  
 R19.1



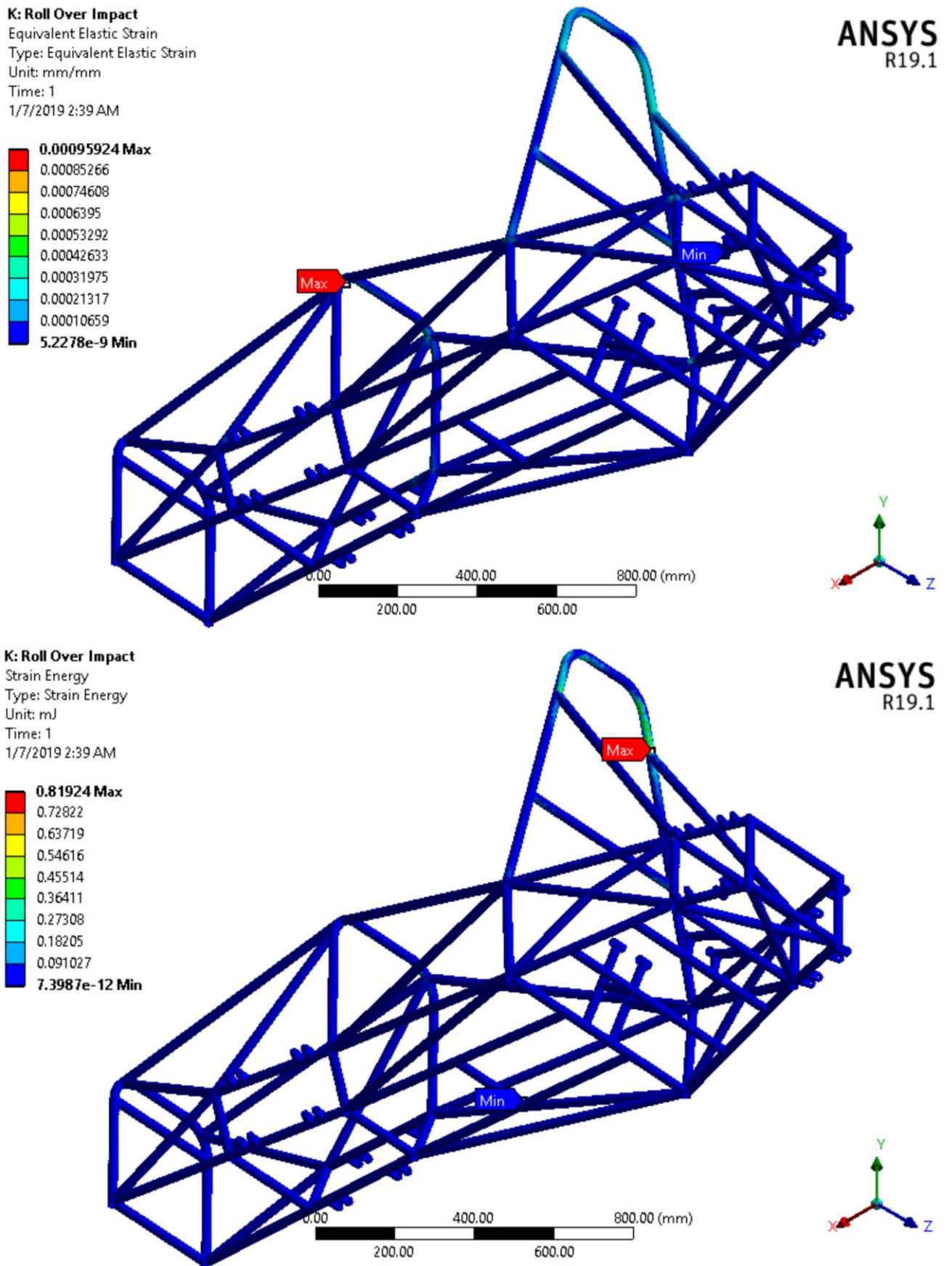
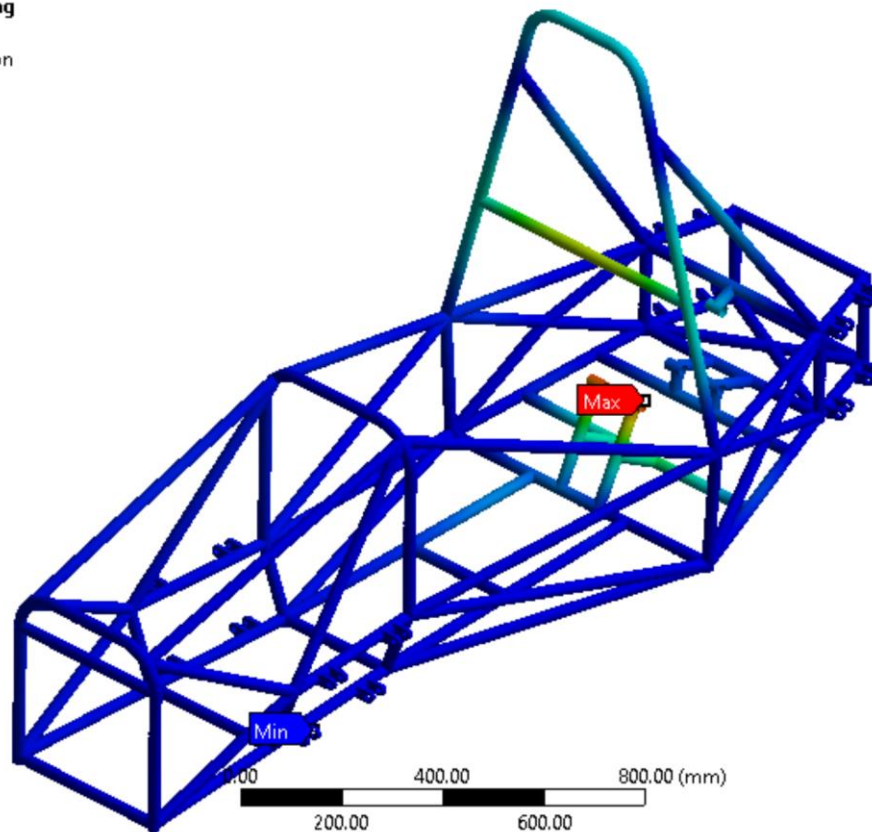
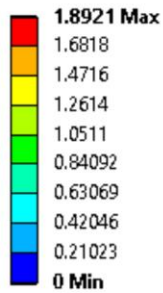


Figure 4.24 Formula SAE M2 Chassis rollover impact results

#### 4.1.4.6 Horizontal Lozenging Analysis

##### F: Horizontal Lozenging

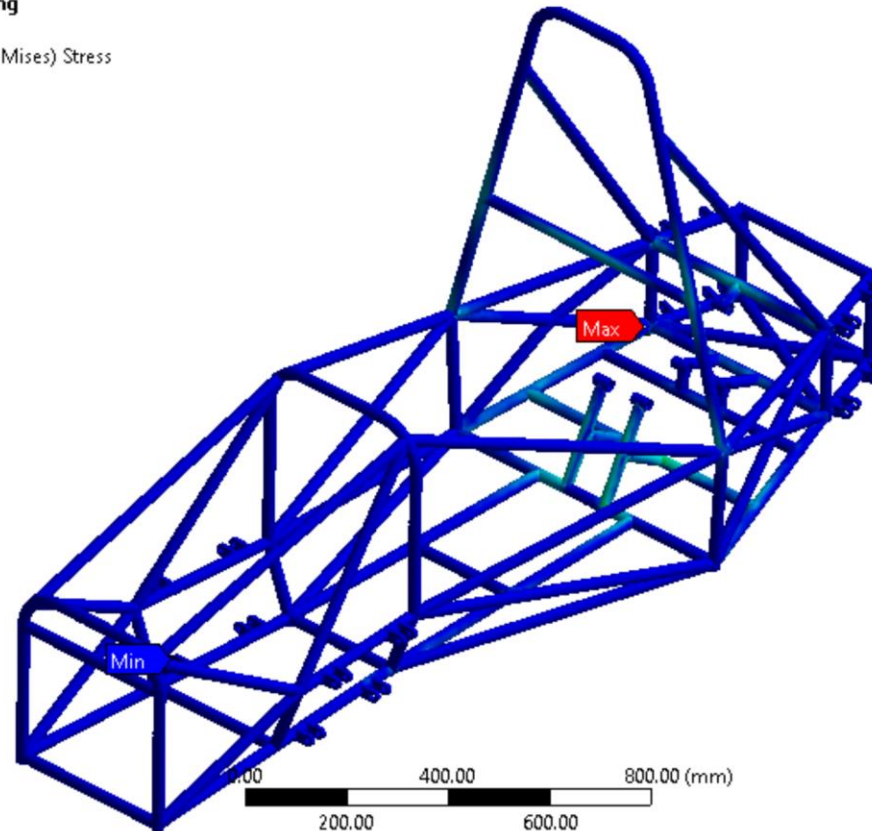
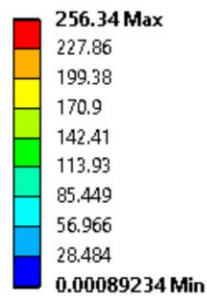
Total Deformation  
 Type: Total Deformation  
 Unit: mm  
 Time: 1  
 1/7/2019 2:44 AM



ANSYS  
R19.1

##### F: Horizontal Lozenging

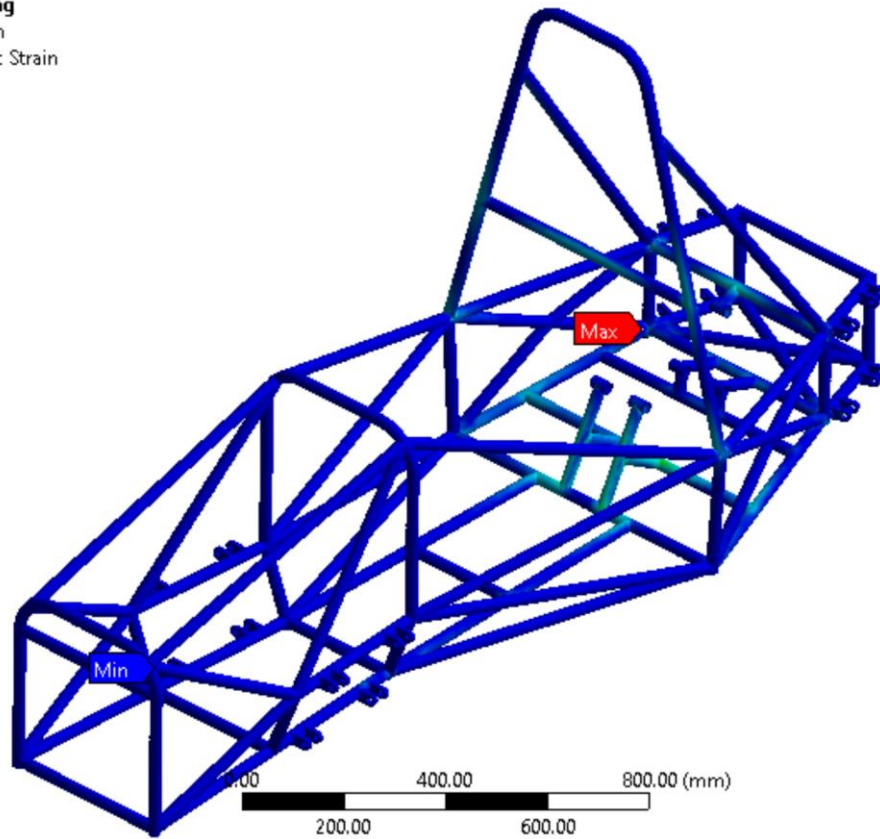
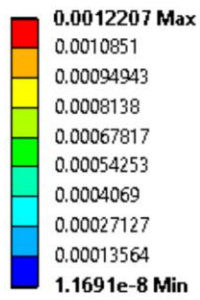
Equivalent Stress  
 Type: Equivalent (von-Mises) Stress  
 Unit: MPa  
 Time: 1  
 1/7/2019 2:45 AM



ANSYS  
R19.1

**F: Horizontal Lozenging**

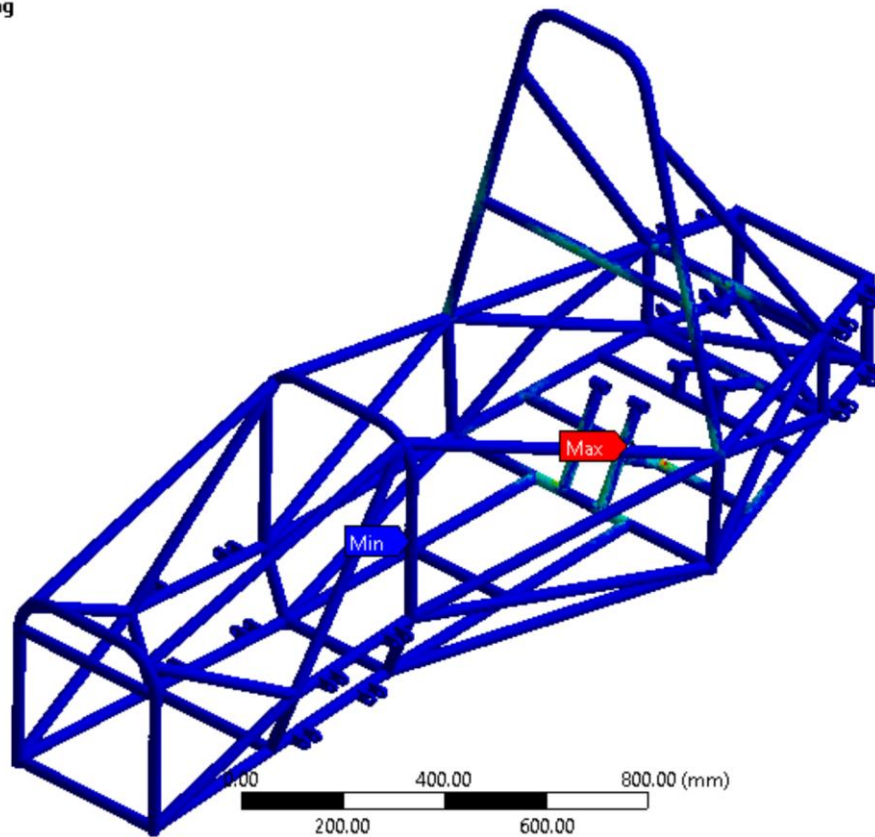
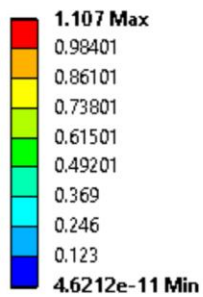
Equivalent Elastic Strain  
 Type: Equivalent Elastic Strain  
 Unit: mm/mm  
 Time: 1  
 1/7/2019 2:45 AM



**ANSYS**  
R19.1

**F: Horizontal Lozenging**

Strain Energy  
 Type: Strain Energy  
 Unit: mJ  
 Time: 1  
 1/7/2019 2:45 AM

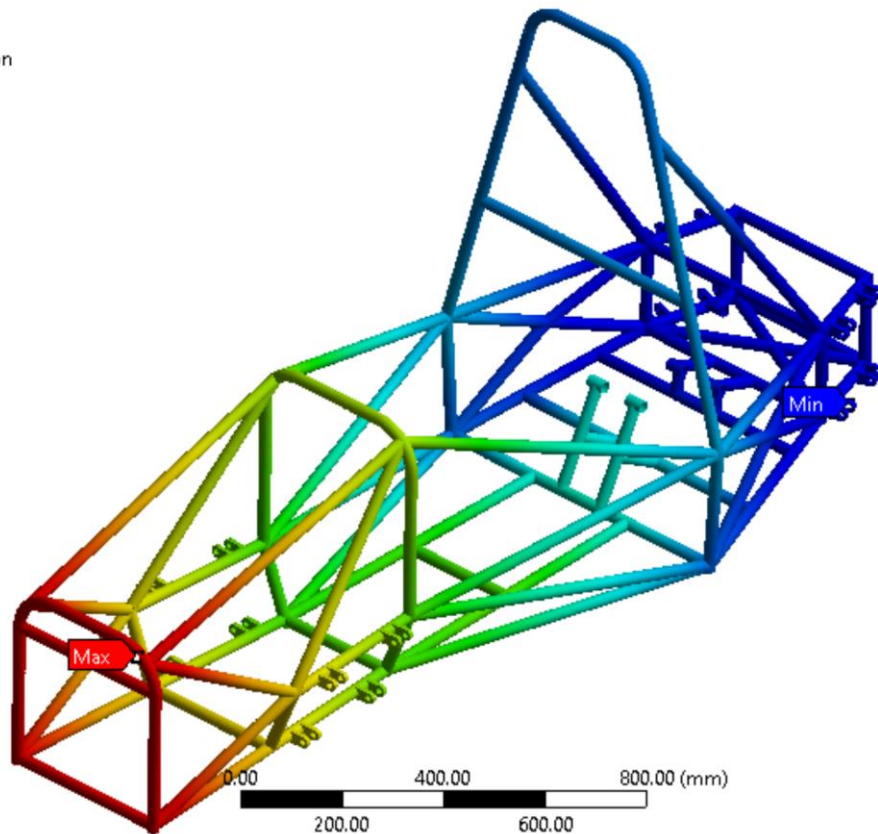
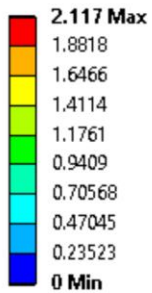


**ANSYS**  
R19.1

Figure 4.25 Formula SAE M1 Chassis lateral bending results

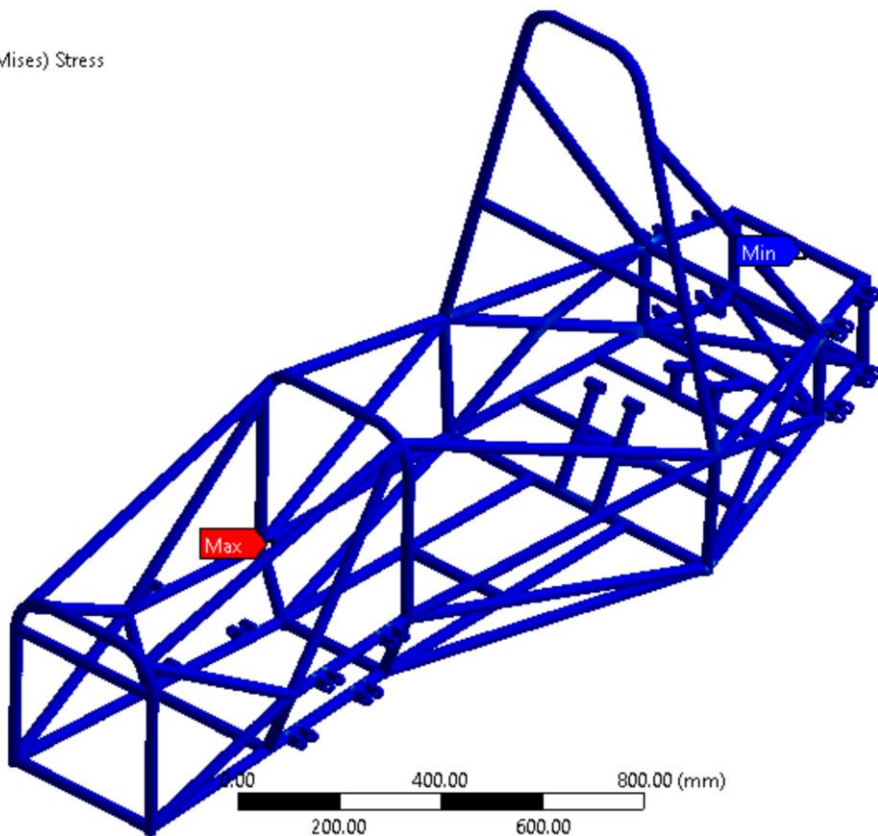
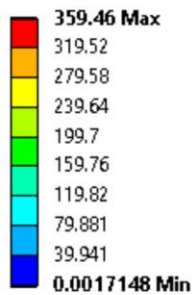
#### 4.1.4.7 Combinations of Load Analysis

**P: Combined**  
 Total Deformation  
 Type: Total Deformation  
 Unit: mm  
 Time: 1  
 1/7/2019 2:46 AM



**ANSYS**  
R19.1

**P: Combined**  
 Equivalent Stress  
 Type: Equivalent (von-Mises) Stress  
 Unit: MPa  
 Time: 1  
 1/7/2019 2:47 AM



**ANSYS**  
R19.1

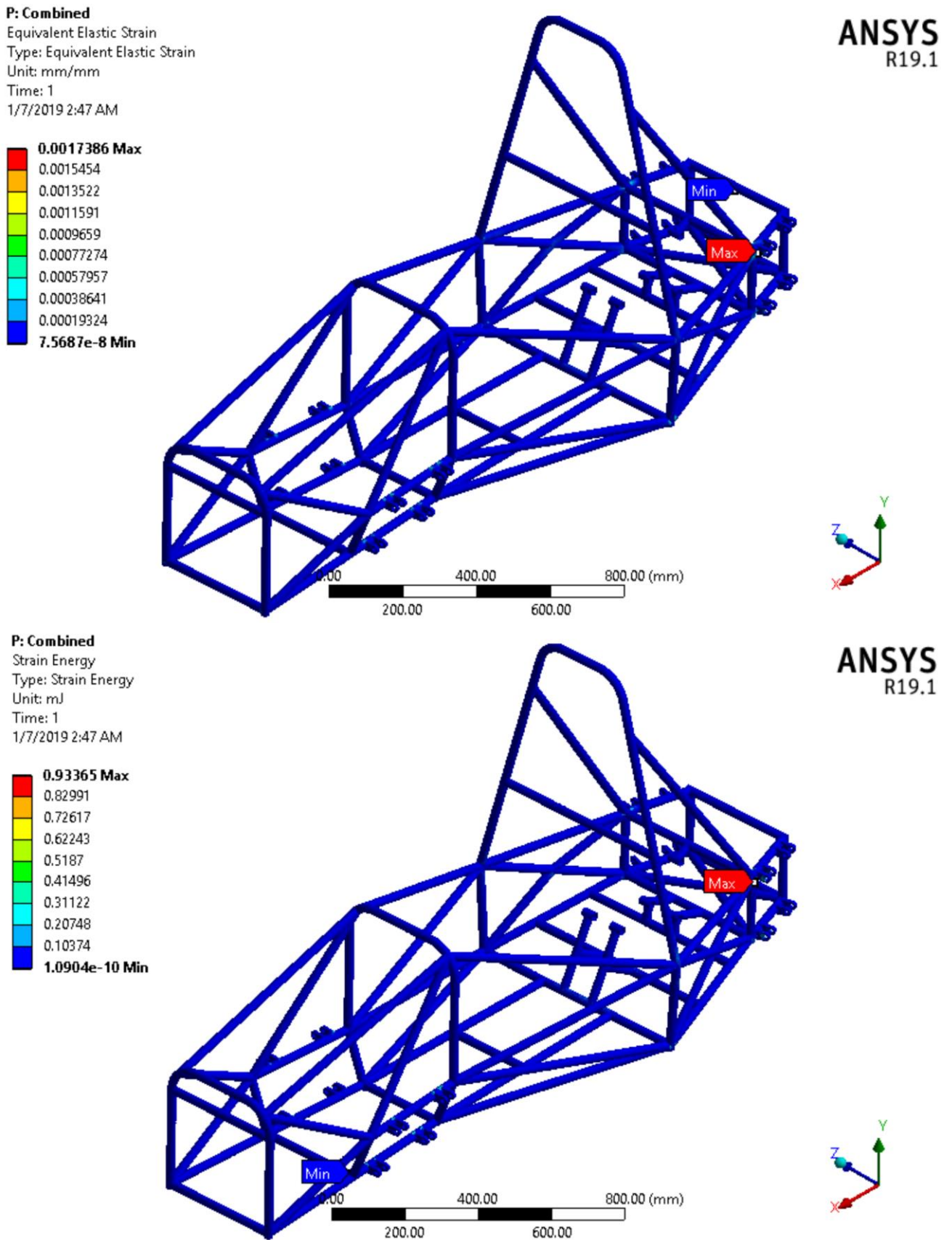
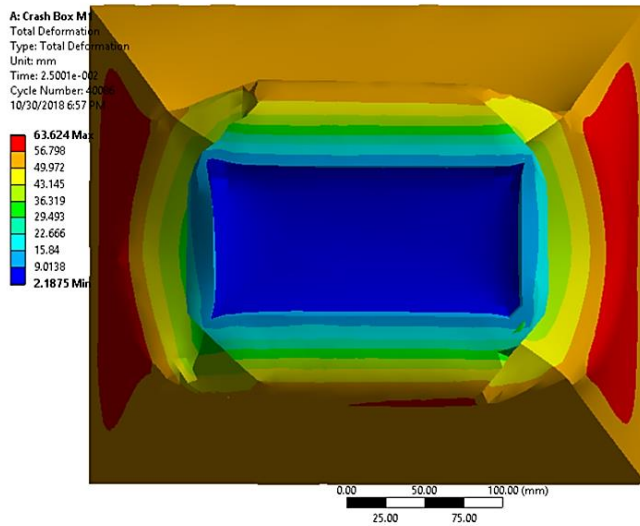


Figure 4.26 Formula SAE M1 Chassis combined load results

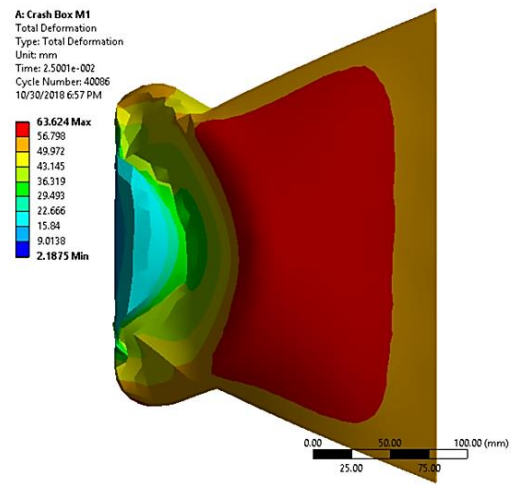
### 4.1.5 Formula SAE Crash Box results (Dynamic Simulation)

#### 4.1.5.1 Formula SAE Crash Box M1 or Impact Attenuator

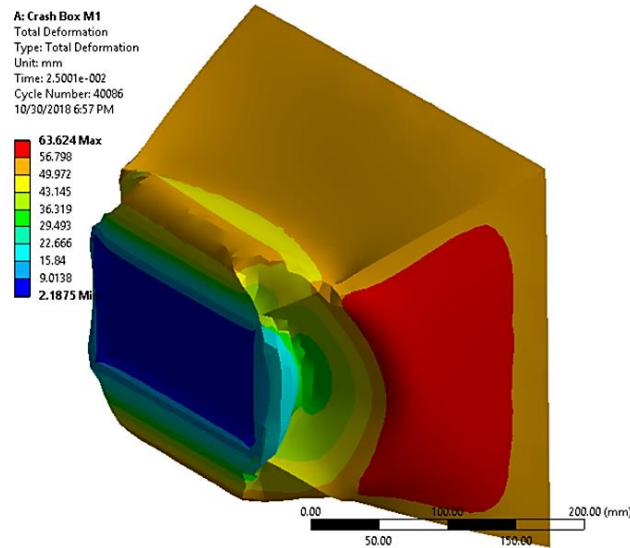
Front View



Side View



Isometric View



Top View

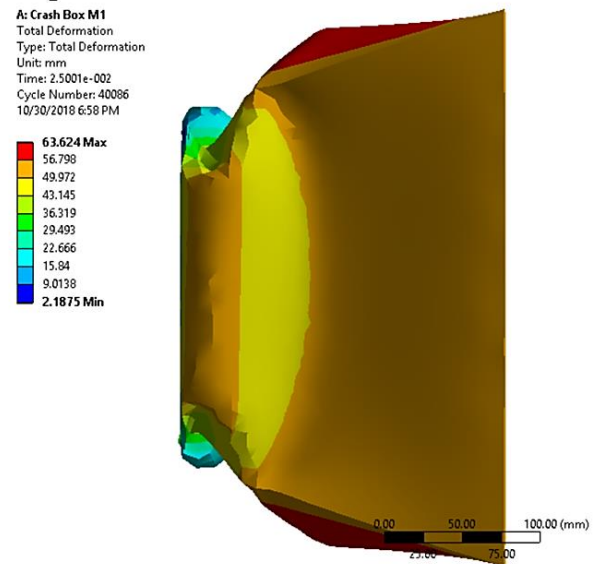
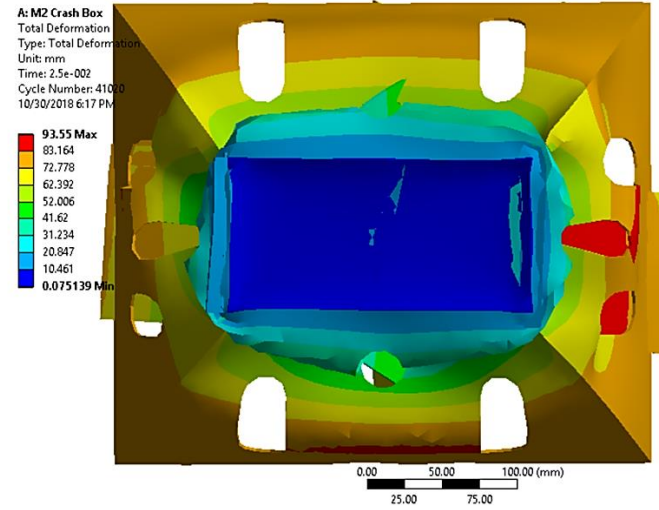


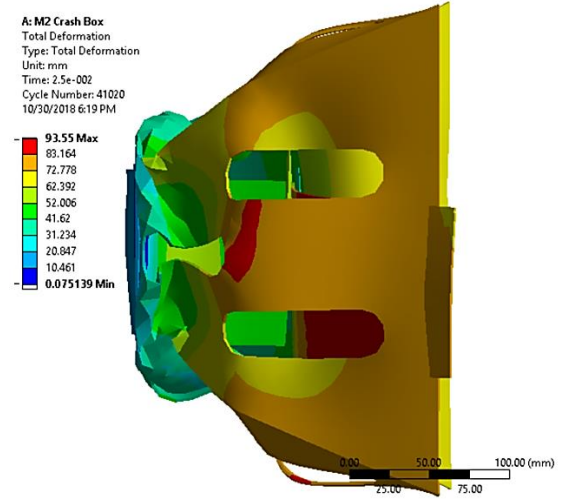
Figure 4.27 Total deformation of FSAE Crash Box (Side and Top View)

### 4.1.5.2 Formula SAE Crash Box M2 or Impact Attenuator with Holes

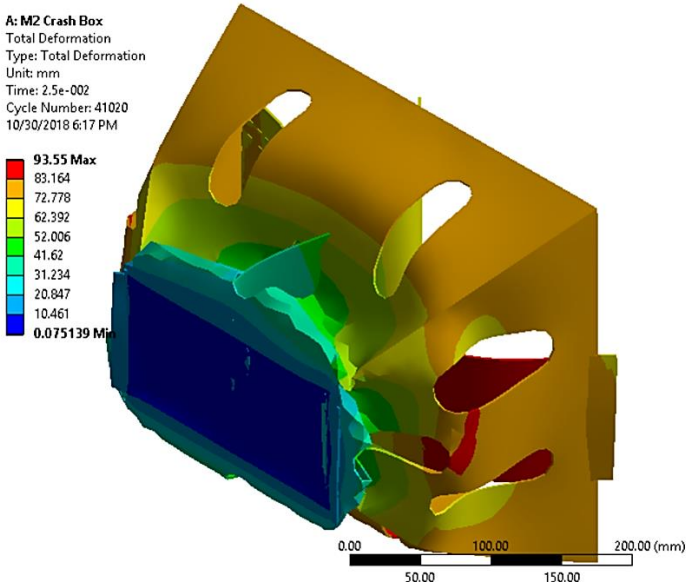
Font View



Side View



Isometric View



Top View

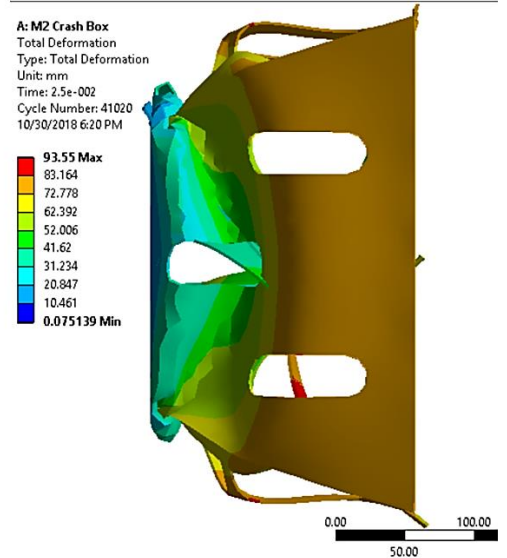
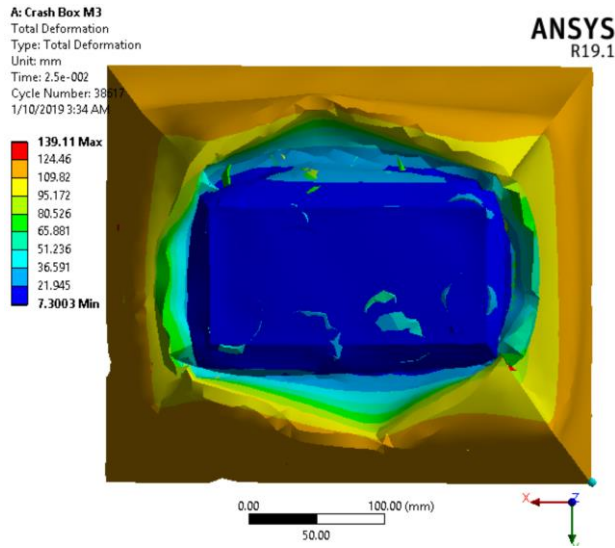


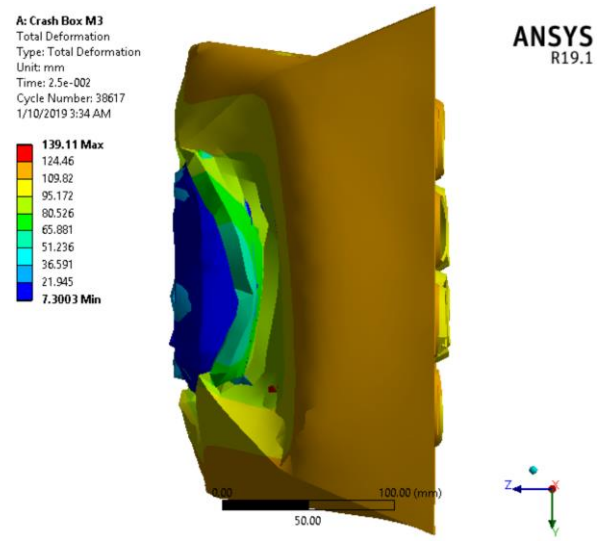
Figure 4.28 Total deformation of FSAE Crash Box M2 model

### 4.1.5.3 Formula SAE Crash Box M3 or Impact Attenuator with Caterpillar Model

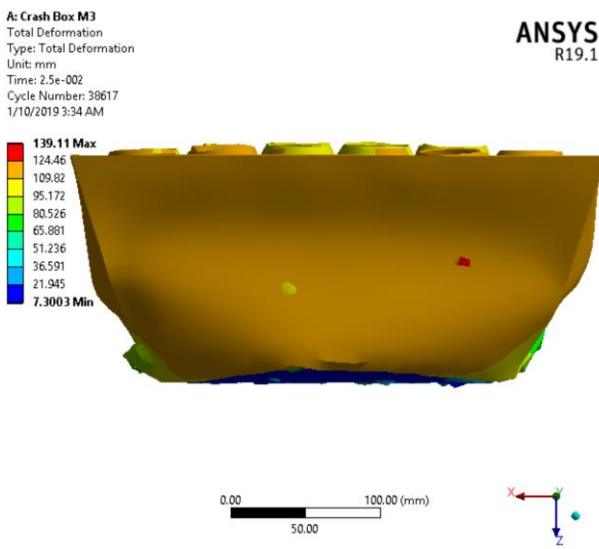
Front view



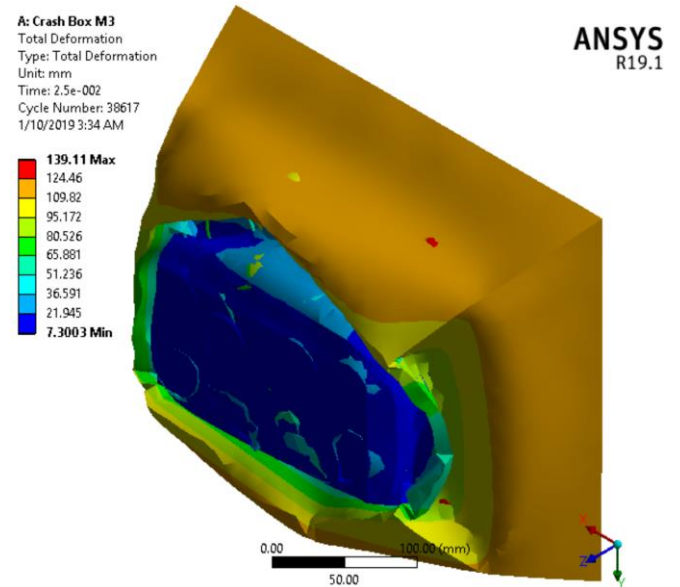
Side view



Top view



Isometric view



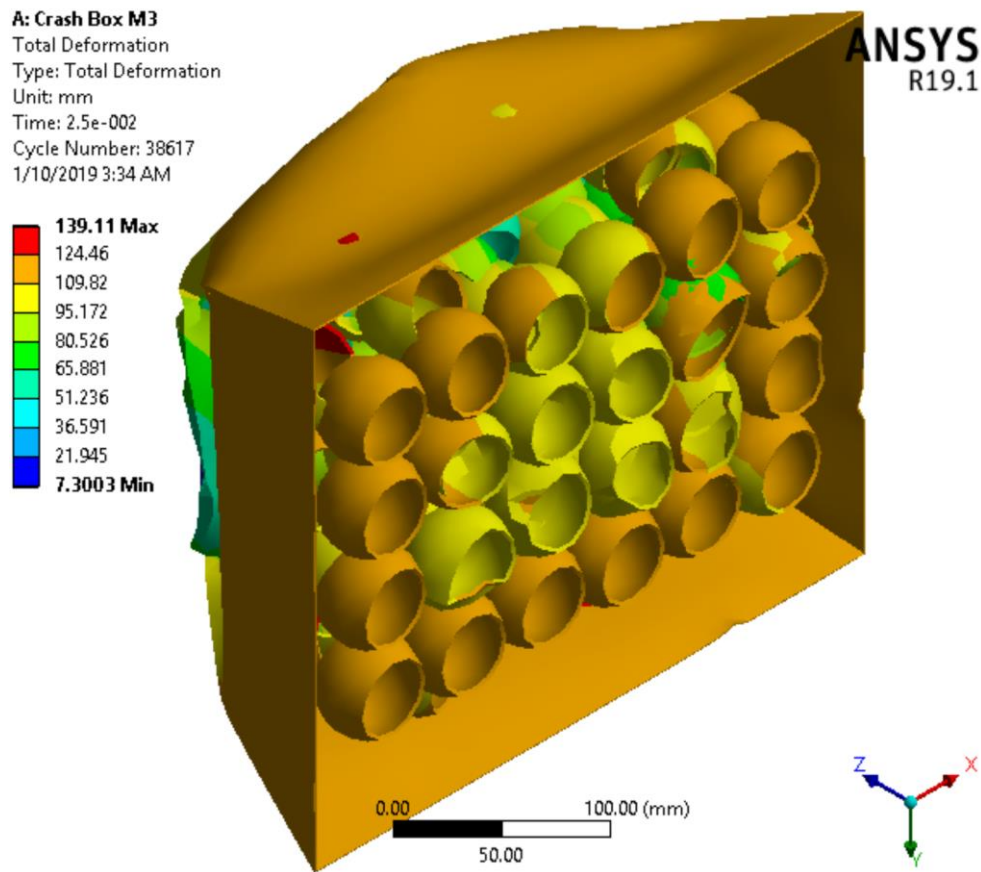


Figure 4.29 Total deformation of internal Caterpillar model Crash Box (different view)

## 4.2 Discussion

### 4.2.1 Discussion on Formula SAE M1, M2 with Old and New Boundary Condition Results

Selecting realistic boundary conditions for any simulation is critical and for Formula SAE Chassis Model is one of the most important parts. This research considers two types of boundary conditions the old and new one, considering the basic component of Formula SAE vehicle. The basic components are attached to the vehicle Chassis and cause a different kind of loading condition in their respect center of mass according to section 3.2.1.1.

**The old boundary condition for Formula SAE M1 Chassis:** the following assumption take place from the preceding researches and journal papers with a result of all mass (278.248Kg) of the vehicle component including the Chassis weight applied at the center of mass of the vehicle case different kind of loading condition.

**New boundary condition for SAE M1 Chassis:** all accessory parts are applied to the Formula SAE M1 Chassis in their perspective center of mass such as driver + seat 75Kg, Engine 70Kg, fuel + fuel tank 9.62Kg, driver train 20Kg, Chassis 36.628Kg, Battery 4Kg,

Steering 10kg, FSAE Crash Box M1 3Kg and body cover including airfoil 35Kg, then the weight of the car become 278.248Kg.

**New boundary condition for SAE M2 Chassis:** after completing the topological optimization based on the reduction of volume of the Formula SAE M1 Chassis by 15%, and geometrical improvement the following loads applied in their perspective center of mass, such as driver + seat 75Kg, Engine 70Kg, fuel + fuel tank 9.62Kg, driver train 20Kg, Chassis 29.00211Kg, Battery 4Kg, Steering 10kg, FSAE Crash Box M2 3Kg and body cover including airfoil 35Kg, then the weight of the racing car become 270.61711Kg.

Table 16 below shows the total deformation and equivalent (Von-Mises) stress occurred in Formula SAE Chassis from the finite element simulation in ANSYS19.1. The two results which are the equivalent elastic strain and strain energy, shown in the above section 4.1 are nearly to zero, therefore they did not consider for topological optimization design purpose of Formula SAE M1 Chassis.

From Table 16 the equivalent Von-Mises stress and total deformation generated for Formula SAE Chassis M1 with old and new boundary condition seen that for the crash and pure torsion load results are equal on account of the boundary condition similarity.

Applying the topological optimization in the Formula SAE M1 Chassis with a concept of removal or inefficient material regions without affecting the structural performance. The applied load's types, maximum Von-Mises stress generated, maximum total deformation and support conditions used for optimization of the Chassis structure.

Finally, the topological optimization took place by seating the design and excluded region by generating holes in the free stress members and zero total deformation areas to reduce the weight of the Chassis and generating the new Formula SAE Chassis with the following three topological optimizations:

- ✓ Optimization 1 shows that members found between the front bulkhead and front hoops, and at the back-side regions of the Chassis members the topological optimization takes place.
- ✓ Optimization 2 considers pure torsional loading. The Formula SAE Chassis M1 model at the back side above the driver train member are free stress member, therefore the topological optimization takes place.
- ✓ Optimization 3 based on the impact load type from the front, side, and rollover condition. The driver support and the back side of the drive train are free stress members and topological optimization performed.

Table 16 Overall result of Formula SAE M1 and M2 Chassis according to the different boundary condition

Loading Types	Results	Formula SAE Chassis Model Types with Different Type of Boundary Conditions		
		M1 with old BC	M1 with New BC	M2 with New BC
Pure Bending	Total deformation (mm)	0.14692	0.5939	0.60442
	Equivalent Stress (MPa)	55.502	226.97	143.12
Pure Torsion	Total deformation (mm)	0.73674		0.5846
	Equivalent Stress (MPa)	220.82		332.39
	Torsional Spiffiness (Nm/deg)	2152.6592		2675.34
	Deflection (mm)	0.73674		0.5846
	Angle of rotation (degree)	0.162		0.129
Braking	Total deformation (mm)	0.14784	0.72157	0.99398
	Equivalent Stress (MPa)	65.33	145.46	105.72
Lateral Bending	Total deformation (mm)	0.9165	0.85103	1.4141
	Equivalent Stress (MPa)	147.36	289.94	208.38
Font Impact	Total deformation (mm)	0.40708		0.40403
	Equivalent Stress (MPa)	285.59		249.73
Side Impact	Total deformation (mm)	0.33245		0.31533
	Equivalent Stress (MPa)	112.61		96.109
Rollover Impact	Total deformation (mm)	1.6198		1.6174
	Equivalent Stress (MPa)	120.5		208.88
Horizontal Lozenging	Total deformation (mm)	0.41979	1.4454	1.8921
	Equivalent Stress (MPa)	164.43	146.57	256.28
Combined	Total deformation (mm)	2.9497	2.1557	2.117
	Equivalent Stress (MPa)	285.59	338.8	359.46
Mass of Chassis	Kg	36.628		29.00211

From Table 16, Figure 3.30 and Figure 4.31 the weight of the Formula SAE Chassis reduced from 36.628Kg to 29.00211Kg by 20.81%, and improves the torsional rigidity or

stiffness of the Formula SAE Chassis from 2152.6592Nm/deg to 2675.34Nm/deg, which means the torsional stiffness of then new model Formula SAE M2 Chassis increased by 19.53%.

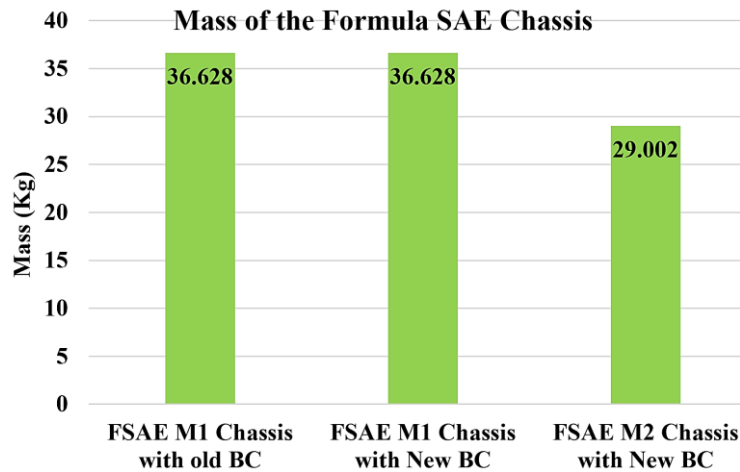


Figure 4.30 Mass of the Formula SAE Chassis vs Chassis type

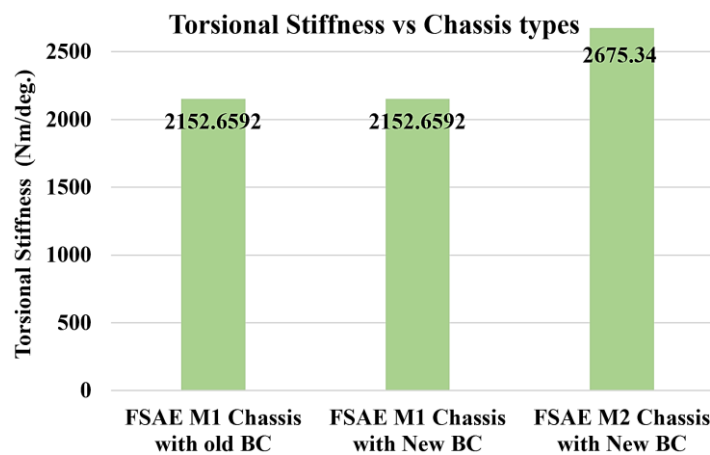


Figure 4.31 Torsional stiffness vs Chassis type

The new material selected by using digital logic method for the Formula SAE Chassis is SAE 1018 Steel which has a tensile yielding strength of 360MPa, therefore the Von-Messes stress induced in the frame Chassis from a different kind of loading condition is less than the yield strength (360MPa) of the material see Figure 4.32.

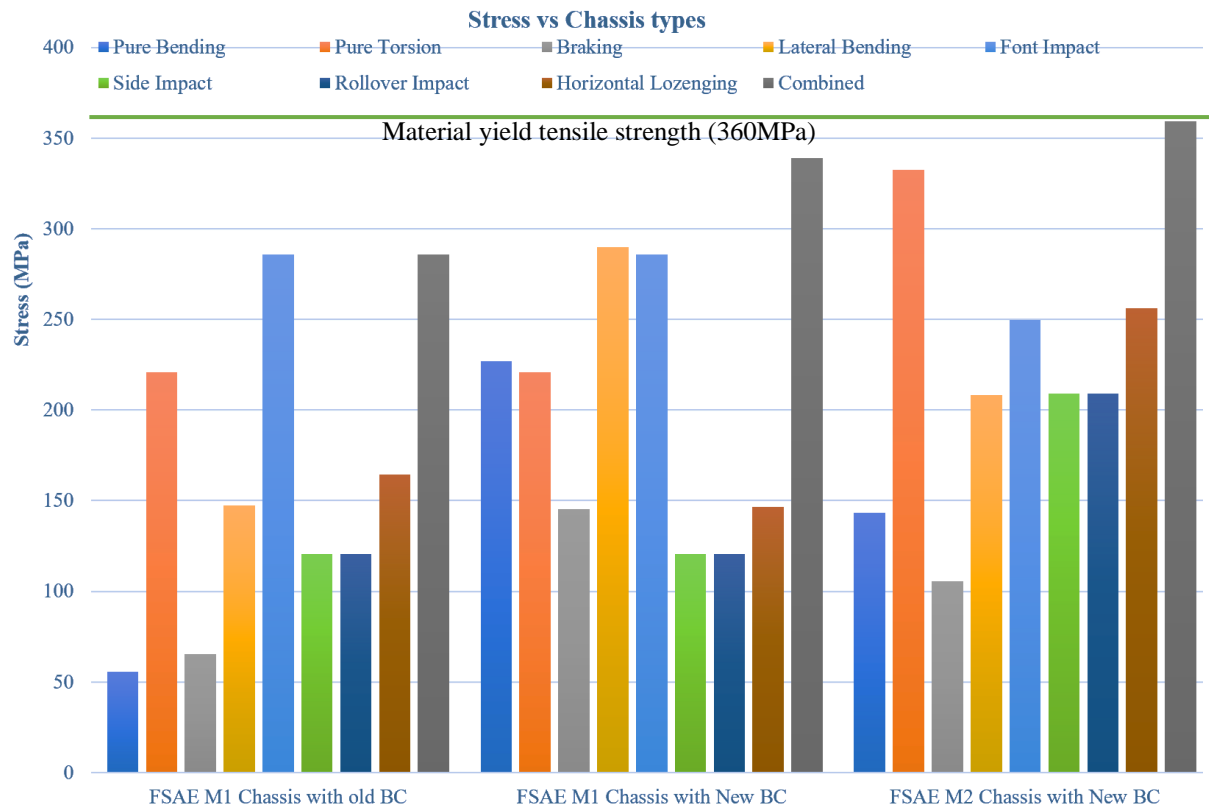


Figure 4.32 Maximum Von-Miss Stress vs Formula SAE Chassis type

From Figure 4.33 and finite element simulation of Formula SAE Chassis, the total deformation according to different types of loading condition is less than 25mm as recommended by Formula SAE rule.

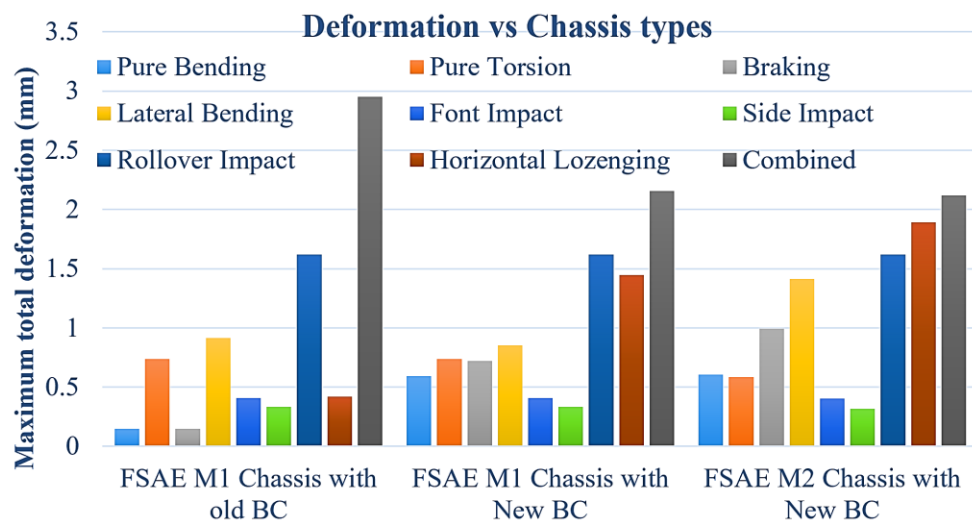


Figure 4.33 Maximum total deformation vs Formula SAE Chassis type

#### 4.2.2 Discussion on Formula SAE M1, M2 and M3 Crash Box or Impact Attenuator Results

To evaluate the crashworthiness performance of the Formula SAE Crash Box thin-wall structures, several crashworthiness indicators are used, these indicators are energy

absorption, Mean Crashing Force (MCF), Pick Crash Force (PCF), and total deformation or deformation length occurred during impact.

The front impact or crash analysis takes place with an initial vehicle velocity of 7m/sec, the time range of impact is 0 to 0.025sec (25 millisecond). The gap between the Crash Box and the front rigid wall is 10mm for all three Crash Box models to keep consistency and see their results within the given time intervals. When the crash scenario takes place, it is more complex to predict the best result therefore Johnson-Cook strength and failure model considered for the material modeling of Formula SAE Crash Box, which states that the material is loaded with impact environment in the form of the plastic range including large strains, large strain rates, high pressures, and high temperatures for Aluminum 7075-T651 plate for Formula SAE Crash Boxes.

Table 17 Summary results of Formula SAE Crash Box models

Crash Box Model	M1	M2	M3
Mass, Kg	1.5844	2.5849	4.87
Maximum kinetic energy, J	7388.82	7403.59	7488.18
Maximum Energy Absorption (EA), J	7319.29	7348.85	7443.44
Energy transfer to the Chassis, J	69.52376	54.74204	44.736
Maximum total deformation, mm	70.606	95.266	141.49
Peak Crash Force (PCF), KN	110.82	94.73	53.21
Peak acceleration, m/sec <sup>2</sup>	363.79 (37.08g)	313.06 (31.91g)	175.25 (17.86g)
Average acceleration, m/sec <sup>2</sup>	310.06 (31.6g)	255.47 (26g)	115.6 (11.78g)

The models used are the same shape as Formula SAE stated; their difference is adding holes and caterpillar geometry inside the Crash Box. Model M1 is based on formula SAE rule, model M2 adds holes in the outer part with aluminum sheet members inside the Crash Box and in model M3 a caterpillar geometry is added to the Crash Box without any holes in the outer part of the Crash Box. Hence, the masses increased from 1.5844Kg, 2.5849Kg, and 4.87Kg for Formula SAE Crash Box M1, M2, and M3 respectively seen in Table 17.

From Figure 4.34 and Table 17 the total deformation increased with a value of 70.606mm, 95.266mm, 141.49mm for Formula SAE Crash Box M1, M2 and M3 respectively.

Hence, adding holes and using caterpillar geometry cause the pathway for the stress and make the Crash Box to deform up to halfway, comparing M3 to M1 model as see Figure 4.34.

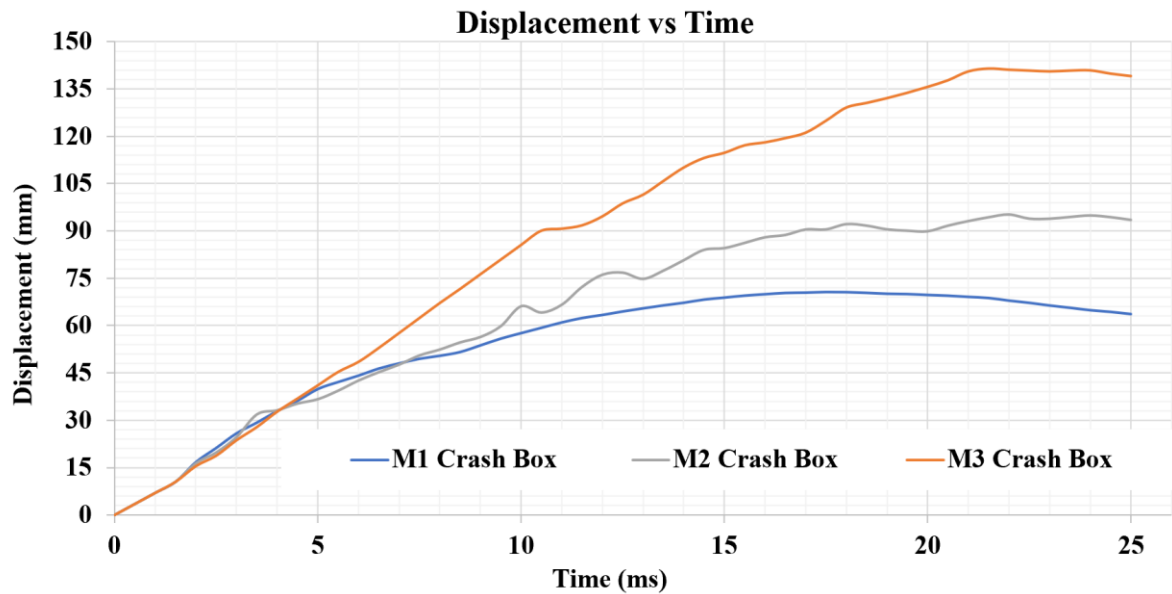


Figure 4.34 Total deformation Vs Time for Formula SAE Crash Box's

And from Figure 4.34 can see that the maximum deformation rate generated during impact for the three Crash Box models is:

$$\text{Deformation Rate for the Crash Box} = \frac{\text{Maximum displacement or deformation}}{\text{Time of maximum displacement}}$$

For Crash Box M1,

$$\text{Deformation Rate of M1} = \frac{70.606\text{mm}}{17.5\text{msec}} = 4.03\text{m/sec}$$

For Crash Box M2,

$$\text{Deformation Rate of M2} = \frac{95.266\text{mm}}{22\text{msec}} = 4.33\text{m/sec}$$

For Crash Box M3,

$$\text{Deformation Rate of M3} = \frac{141.49\text{mm}}{21.5\text{msec}} = 6.58\text{m/sec}$$

The deformation rate generated at the peak deformation result shows the deformation rate generated during impact is increased from 4.03m/s to 6.58m/s, which means that less reaction force generated by the Crash Box M3 as seen in Figure 4.35.

From Figure 4.35, shows the peak crash force created on M1, M2 and M3 are 110.82kN at 25msec, 94.73kN at 7msec and 53.21kN at 25msec respectively. The peak crash force indicates survival rate of the driver of Formula SAE race car. Figure 3.35 shows that the Crash Box M3 have a less, smooth, and steady reaction, which means when the impact tack places

the material deformed more and smoothly this cause less force and energy transmitted to the Chassis structure and driver as seen Figure 4.39.

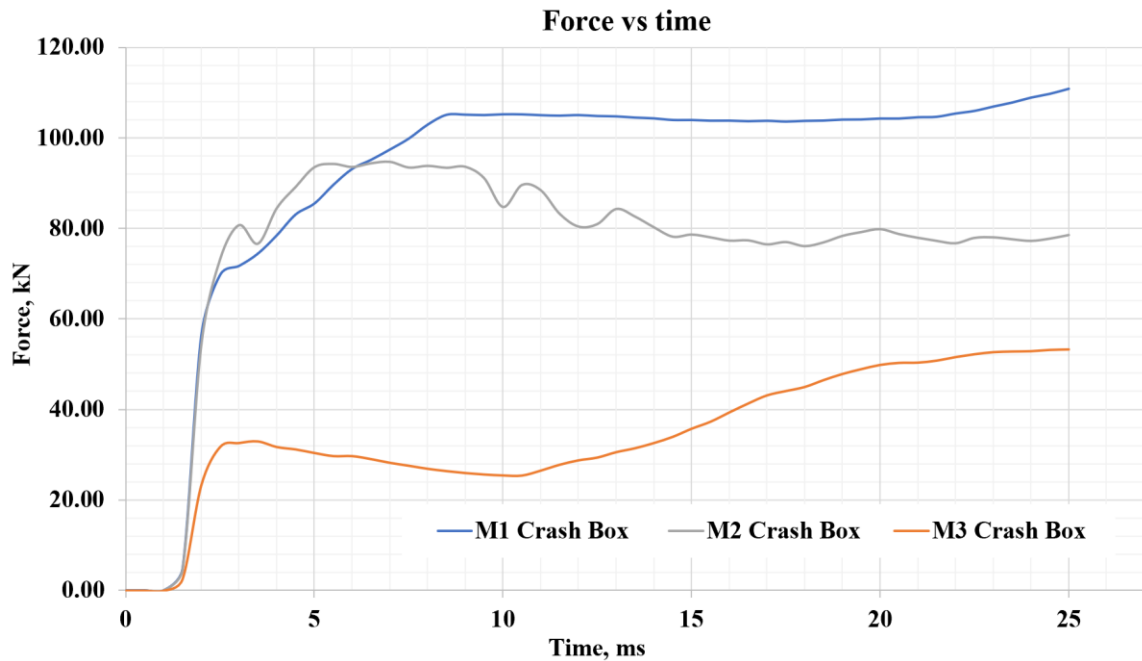


Figure 4.35 Mean Reaction Force Vs Time for Formula SAE Crash Box's

As seen in the above Figure 4.35 and Figure 4.36 initially the Crash Box move with a constant velocity of 7m/s for 1.0ms, then impact tack place between the Crash Box and the rigid barrier. Causing for Formula SAE M1 Crash Box to create more resistant to the impact force that is why a high reaction force generated and it is dangerous to the driver and the Chassis structure.

From Figure 4.36 and Figure 4.37, shows that the peak and average acceleration generated on the Crash Box's structure and the recommended maximum value by the Formula SAE rules. Therefore, the peak acceleration induced in the Crash Box M1, M2, and M3 model is 37.08g, 31.91g and 17.86g respectively and it satisfies the Formula SAE requirement because it is less than 40g. But the average acceleration generated is 31.61g, 26.04g and 11.78g for Crash Box model M1, M2 and M3 and only Crash Box M3 model is less than the recommended value and satisfy Formula SAE rule.

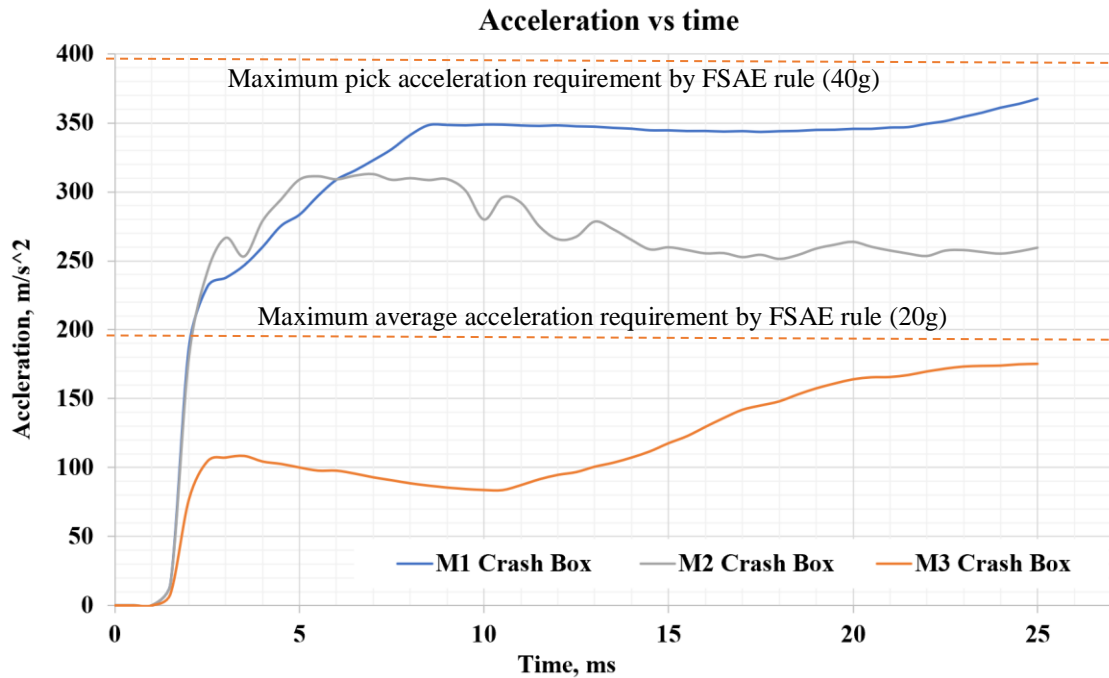


Figure 4.36 Acceleration Vs time of Formula SAE Crash Box's

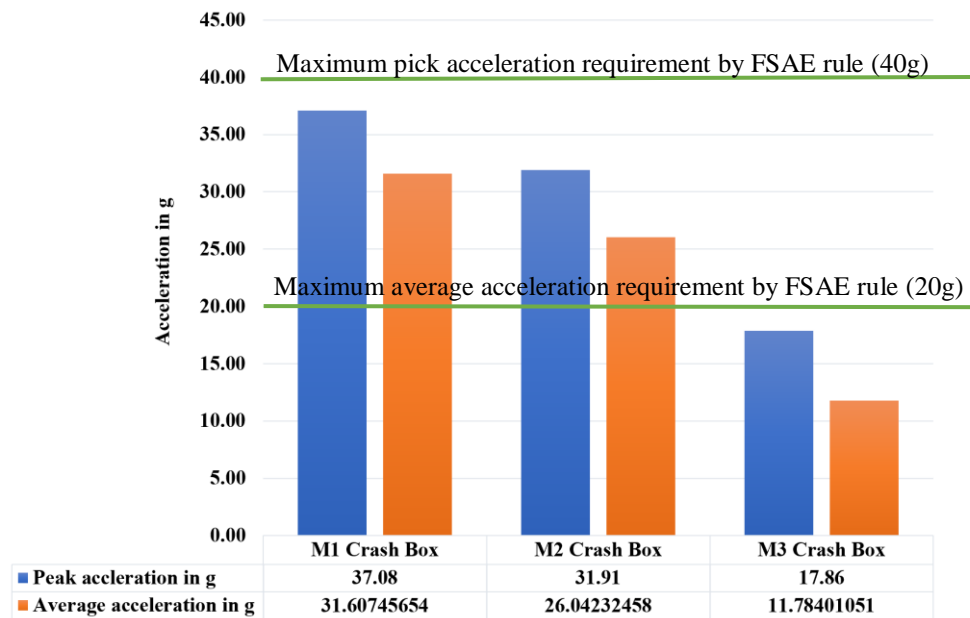


Figure 4.37 Formula SAE Crash Box maximum peak and average acceleration results

After encountering Figure 4.38 and Figure 4.39, the maximum kinetic energy generated by the Crash Box model M1, M2 and M3 are 7388.818J, 7403.59J and 7488.18J respectively this is due to the variation of the Crash Box masses. The energy absorbed by each Crash Box model M1, M2 and M3 is 7319.29J, 7348.84J and 7443.44J respectively, shows that the energy transfer to the Crash Box model reduced from 69.52J to 44.736J which means the that the adding holes and caterpillar geometry in the Formula SAE Crash Box M1 model

improve the energy absorption, deformation pattern and less load transfer to the Chassis structure and driver as seen Figure 4.39.

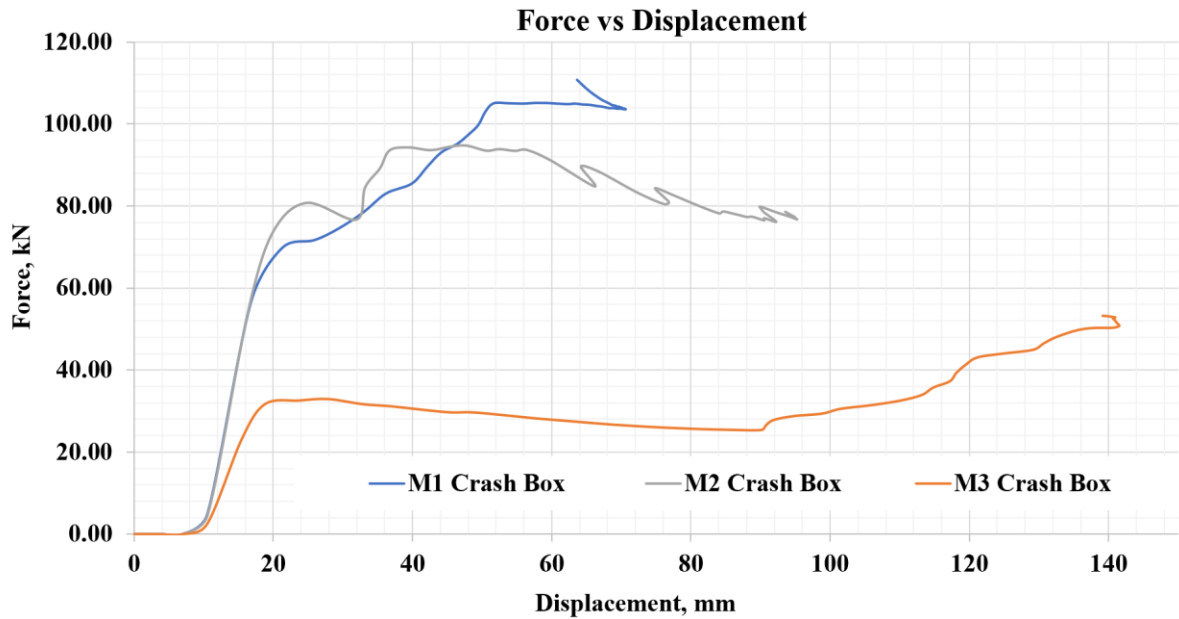


Figure 4.38 Crash force vs displacement for Formula SAE Crash Box's

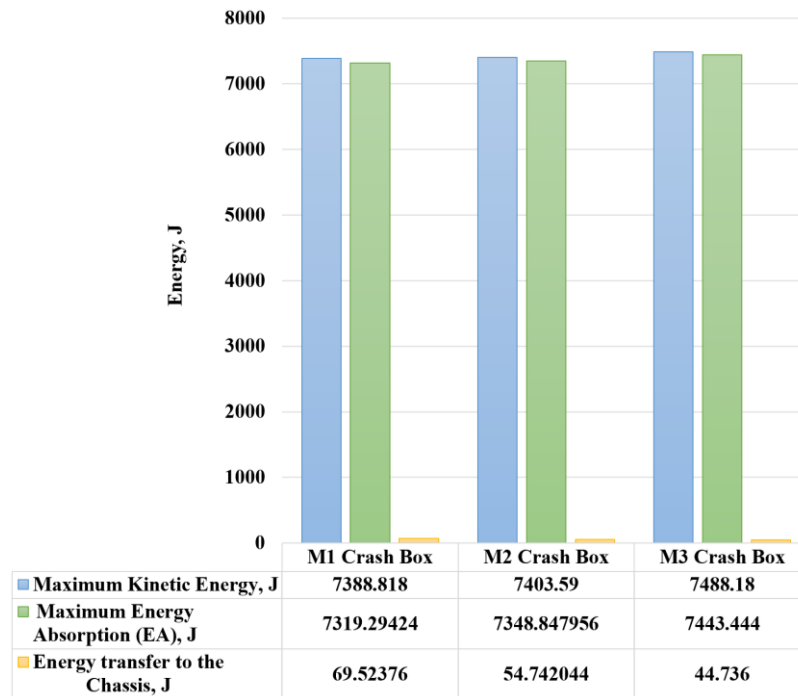


Figure 4.39 Different energy forms vs Crash Box type

## CHAPTER 5

### CONCLUSION AND RECOMMENDATION

#### 5.1 Conclusion

##### 5.1.1 Conclusion on Formula SAE Chassis

In this research paper seven types of load condition considered to design and analysis the Formula SAE Chassis. These loading conditions are static (pure bending, pure torsion, braking, lateral cornering, horizontal lozenging and combination) and crash (front, side, and rollover) to make it as much as possible to the real-world scenario. Improving the boundary condition improve the simulation result there for a new type of boundary condition used by specifying each vehicle component to their respect center of mass and the structural simulation tack place. After performing the structural simulation by using topological optimization analysis to identify free stress and less deformed members, using the maximum stress and deformation as a design parameter to design the new Formula SAE M2 Chassis model.

Based on improved boundary condition, loading types, and material selection (using digital logic method) the Formula SAE Chassis design and simulation tack place with a result of a Von-Mess stress and total deformation generated less than the material (SAE 1018 Steel) tensile yield strength (360MPa) and the total deformation less than 25mm accepted by Formula SAE rule.

The torsional stiffens of the new model Formula SAE M2 Chassis after performing topological optimization and geometrical design on the Formula SAE M1 Chassis based on the new and improved boundary condition with a result of increased from 2152.6592Nm/deg to 2675.34Nm/deg by 19.53% without compromising the weight of the Chassis and reduced from 36.628Kg to 29.00211Kg by 20.81%. Therefore, the new Chassis design M2 is satisfactory because the torsional stiffness generated by the Chassis between the range of Formula SAE rule stated (1000-5000Nm/deg) and no structural member fails from the generated stress due to different loading condition.

##### 5.1.2 Conclusion on Crash Box or Impact Attenuator

One of the main reasons for adding the Crash Box in any vehicle is to absorb more energy. In this research paper, three types of Crash Box models are used based on the Formula SAE rule with additional geometric futures by using Aluminum 7075-T651 plate and material modeling tack place according to Johnson-Cook strength and failure models.

The displacement or deformation took place during impact increased from a value of 70.606mm to 141.49mm, which means adding holes and caterpillar geometry in the Crash Box structure cause the pathway for the stress and make the Crash Box to deform up to halfway, comparing M3 to M1 model as seen in Figure 4.34 and Table 17.

The deformation rate generated at the peak deformation result shows the deformation rate generated during impact is increased with a value of 4.03m/s, 4.33m/s and 6.58m/s for Crash Box M1, M2 and M3 model respectively, which means that less reaction force generated as shown in Figure 4.35, and more energy absorbed as seen in Table 17 by the Crash Box M3.

The variation of the geometry, adding holes, and caterpillar geometry in the Crash Box cause the variation of reaction force and time to reach the PCF (see Figure 4.35), therefore Crash Box M1 and M2 model has more eminent amount of peak reaction force 110.82kN, 94.73kN with more time 25msec, 7msec to reach, comparing to Formula SAE Crash Box M3 Model with a value of 53.21kN, 25msec respectively. The reaction force generated is smooth and steady in Crash Box M3 with a caterpillar geometry causing the deformation to become smoother, steady, a larger time to reach the peak reaction force, an advantage of creating a less PCF and more deformation comparing it with the other two Crash Box models (M1 and M2) as seen in Figure 4.34 and Figure 4.35.

The average and peak acceleration generated on the Crash Box according to Formula SAE rule and regulation ordered that it should not exceed 20g (196.2 m/sec<sup>2</sup>) and 40g's (392.4m/sec<sup>2</sup>) respectively, therefore Crash Box M3 model satisfy and reduced the average acceleration from 31.61g to 11.78g by 62.78% and peak acceleration from 37.08g to 17.86g by 51.83%. Hence the average and peak acceleration generated in the Crash Box M1 and M2 model is more than the recommended and cause energy transfer to the Chassis structure in the form of a jerk (high rate of acceleration) especially by making it dangerous to the driver.

The work done or energy absorption by the Crash Box is a product of force and displacement and directly proportional to both, which means force and displacement are inversely proportional to each other. The work done on the Crash Box structure is seen in Figure 4.38, there is a high reaction force (109.71kN) in Formula SAE M1 Crash Box with less displacement or deformation (70.606mm) comparing to others. The reaction force generated in Crash Box M2 and M3 is less with higher displacement comparing to Crash box M1 model as seen in Table 17.

The energy absorbed by each Crash Box model M1, M2 and M3 is 7319.29J, 7348.84J and 7443.44J respectively, shows that the energy transfer to the Crash Box model reduced from 69.52J to 44.736J which means that the adding holes and caterpillar geometry in

the Formula SAE Crash Box M1 model improve the energy absorption, deformation pattern and less load transfer to the Chassis structure and driver.

Finally, the Formula SAE M3 Crash Box model is selected for the Formula SAE racing car because of less reaction force, beneficial energy absorption, higher velocity generation, satisfactory average acceleration, peak acceleration, smooth, steady and large total deformation due to the adding of the caterpillar geometry in the Formula SAE Crash Box.

## **5.2 Recommendation**

### **5.2.1 Recommendation on Formula SAE Chassis**

Adding the Chassis to the crash box and checking the senior will improve the result for Formula SAE Crash Box's and predicate the energy transfer from the Crash Box to the Chassis and to the driver. More optimization for Formula SAE M2 model, by varying thickness, geometry and using new kind of material improve the result.

### **5.2.2 Recommendation on Crash Box or Impact Attenuator**

Adding the Chassis to the Crash Box and checking the crash senior improve the result of Formula SAE Crash Box's analysis and predicate the energy transfer from the Crash Box to the Chassis to the driver.

More optimization by varying the hole size and plate thickness for Crash Box M2 model, by varying a caterpillar geometry with respect to the size of the hollow sphere, diameter, and thickness for Crash Box M3 model and using a new type of material (like composite) improve the result.

## **5.3 Future Work on Formula SAE Chassis and Crash Box or Impact Attenuator**

The future works other than on the research performed in the Formula SAE Chassis and Crash Box structure as follows:

Future work for Formula SAE Chassis:

- ✓ Structure design and modeling of FSAE Chassis which can stand vibration load (improve the first vibration mode and frequency).
- ✓ Stability of the Formula SAE M2 Chassis.
- ✓ Experimental evaluation of all the above seven types of loading condition.
- ✓ Test like the computational fluid dynamics (CFD), Chassis Balancing, Thermal Heating, Heat Treatment etc. carried out on various manufacturing and stimulation software's that can result in a more specific, sophisticated, and detailed inquiry or analysis of the created Formula SAE Module.

- ✓ The energy created on the front part of the Chassis with and without a Crash Box.
- ✓ Design, analysis, and simulation of accessory parts like a wheel, steering, brake system, electrical control system and aerodynamic system of Formula SAE.

Future work for Formula SAE Crash Box or Impact Attenuator:

- ✓ The Crash Box design needs additional filler materials to increase energy absorption by stabilizing the crush pattern and bettering the collapse of the tube.
- ✓ Types of connection used between the Crash Box and Chassis in the Front Bulk Head.
- ✓ Different type of geometrical optimization of the Crash Box (Formula SAE M1, Formula SAE with holes and Formula SAE with Caterpillar Geometry inside) by varying the geometrical shape, thickness, holes profile, caterpillar internal and external diameter variation.
- ✓ Using composite material with appropriate structural geometry and arrangement of layer material that has a better crashworthiness property.
- ✓ Reduced the mass of Crash Box M3 by using proper optimization method.

## REFERENCE

- [1] J. Happian-Smith, “An Introduction to Modern Vehicle Design,” 2001.
- [2] F. Sae and R. Table, “2017-18 Formula SAE ® Rules,” 2017.
- [3] A. J. R. and S. T. S. Jason C. Brown, *Motor Vehicle Structure: Concepts and Fundamentals*, Jason C. B. UK and USA: Butterworth Heinemann, 2002.
- [4] N. G. Jogi, P. R. Shahade, and A. K. Kaware, “1Analysis of Formula Racing Car Frame Using Ansys,” vol. 3, no. 6, pp. 22–33, 2014.
- [5] T. Limwathanagura, C. Sithananun, T. Limchamroon, and T. Singhanart, “The-Frame-Analysis-and-Testing-for-Student-Formula,” vol. 6, no. 5, pp. 998–1002, 2012.
- [6] P. Du Bois, C. C. Chou, B. B. Fileta, A. I. King, and H. F. Mahmood, “VEHICLE CRASHWORTHINESS AND VEHICLE AND OCCUPANT PROTECTION.”
- [7] R. P. Singh, “Structural Performance Analysis of Formula Sae Car,” *J. Mek.*, no. 31, pp. 46–61, 2010.
- [8] A. Oshinibosi, “Chassis and Impact Attenuator Design for Formula,” no. August 2012.
- [9] R. Abrams, “Formula SAE Race Car Analysis: Simulation & Testing of the Engine as a Structural Member,” *FISITA 2008 World Automotive. Congr. Munich, ...*, 2008.
- [10] U. S. Outside, “SAE ® Design and Analysis Project with SolidWorks ® Software Put Picture Here Dassault Systèmes.”
- [11] M. Costin and D. Phipps, “Racing and Sports Car Chassis Design,” *B. T. Batsford LTD, Bentley Pub.* p. 147, 1966.
- [12] H. M. Mahendra, B. S. P. Kumar, S. Puttaswamaiah, and G. S. Prakash, “Design and Crash Analysis Of A Rollcage For Formula Sae Race Car,” *Int. J. Res. Eng. Technol.*, pp. 126–130, 2014.
- [13] N. Y. Reddy and V. S. Kumar, “Study of Different Parameters on the Chassis Space Frame For the Sports Car by Using Fea,” *IOSR J. Mech. Civ. Eng.*, vol. 9, no. 1, pp. 2320–334, 2013.
- [14] David V.Hutton, *Fundamentals of Finite Element Analysis*. NY, USA, 2004.
- [15] D. C. Y. D.LAVANYA, G.GURU MAHESH, V.AJAY, “Design and Analysis of a Single-Seater Race Car Chassis Frame,” vol. 2, no. 8, pp. 1–13, 2015.
- [16] Y. S. Rajput, V. Sharma, S. Sharma, and G. Saxena, “A Vibration Analysis Of Vehicle Frame,” vol. 3, no. 2, pp. 348–350, 2013.
- [17] A. B. et al. Ajay Bangar et al., “Design and Analysis of Car Chassis,” *Int. J. Mech. Prod. Eng. Res. Dev.*, vol. 7, no. 4, pp. 119–126, 2017.

- [18] S. Heimbs and F. Strobl, "Crash Simulation of an F1 Racing Car Front Impact Structure," *7th Eur. LS-DYNA Conf.*, no. MAY, pp. 1–8, 2009.
- [19] C. Abrahamson, B. Bruns, J. Hammond, J. Lutter, and S. Duan, "Formula SAE Impact Attenuator Testing," pp. 35–46.
- [20] S. P. Venkatesh, M. D. Pawar, and B. H. Maruthi, "Design, Optimisation and Impact Analysis of a Chassis System of Race Car," vol. 3, no. 7, pp. 377–386, 2014.
- [21] Surya Patnaik and Dale Hopkins, *Strength of Materials*. 2004.
- [22] M. H. Mat and A. R. A. Ghani, "Design and analysis of 'eco' car chassis," *Procedia Eng.*, vol. 41, no. Iris, pp. 1756–1760, 2012.
- [23] Ansel C. Ugural and Saul K. Fenster, *Advanced Strength and Applied Elasticity*. .
- [24] I. Journal and M. Engineering, "Materials selection of a bicycle frame using cost per unit property and digital logic methods MATERIALS SELECTION OF A BICYCLE FRAME USING COST PER UNIT," no. March 2014, 2010.
- [25] D. D. Desai, "ANALYSIS AND DEVELOPMENT OF ENERGY ABSORBING CRASH BOX," no. 3, pp. 3776–3782, 2016.
- [26] E. Corona and G. E. Orient, "An Evaluation of the Johnson-Cook Model to Simulate Puncture of 7075 Aluminum Plates," 2014.
- [27] S. Dyuti and M. M. R. Member, "Material Selection Method in Design of Automotive Brake Disc," vol. III, 2010.
- [28] P. R. Shahade and A. K. Kaware, "Structural Performance Analysis of Formula SAE Car.," vol. 2, no. 8, pp. 191–200, 2014.
- [29] R. Nain, "Design and Analysis of Space Frame Tubular Chassis to be used in Formula SAE," vol. 2, no. 6, pp. 22–25, 2015.
- [30] V. Muralidharan and G. Madhusudhana, "Design and Analysis of a Tubular Space Frame Chassis of a High-Performance Race Car," pp. 497–501, 2014.
- [31] K. Wang, *Johnson-cook failure parameters*. 2016.
- [32] D. Skibicki, "Determination of Johnson-Cook Model Constants by Measurement of Strain Rate by Optical Method," vol. 060003, 2016.
- [33] M. Beusink, "Measurements and simulations on the ( dynamic ) properties of aluminum alloy," 2011.
- [34] J. Hart, C. Kennedy, T. Leclerc, and J. Pollard, "FSAE Impact Attenuator 2009-2010," p. 59, 2010.
- [35] H. Rhee, M. T. Tucker, W. R. Whittington, and M. F. Horstemeyer, "Structure-property responses of bio-inspired synthetic foams at low and high strain rates," no.

- March 2017, 2014.
- [36] *Animals 2 (insects and spider)*. 2009.
- [37] I. A. rights reserved. U. © 2009 SAS IP, *Theory Reference for the Mechanical APDL and Mechanical Applications*, vol. 3304, no. April. 2009.
- [38] G. R. Liu S. S. Quek, *The Finite Element Method: A Practical Course*. 2003.
- [39] J. P. Leiva, “Structural Optimization Methods and Techniques to Design Efficient Car Bodies.”
- [40] A. D. Canonsburg, “ANSYS Explicit Dynamics Analysis Guide,” vol. 15317, no. January, pp. 724–746, 2016.
- [41] P. K. A. Babu and M. R. Saraf, “Design, Analysis, and Testing of the Primary Structure of a Race Car for Supra SAEINDIA Competition,” no. January 2012, 2015.